The characterization of pharmacokinetic properties and evaluation of *in vitro* drug combination efficacies of novel antimalarial compounds.

LIZAHN LAING

Thesis presented for the degree of
DOCTOR OF PHILOSOPHY
In the Division of Clinical Pharmacology
UNIVERISTY OF CAPE TOWN

March 2020

Supervisor: Assoc. Prof. Lubbe Wiesner
Co-supervisors: Dr. Liezl Gibhard
Prof. Richard Haynes (North-West University)

Plagiarism Declaration

This thesis, "The characterization of pharmacokinetic properties and evaluation of in vitro drug combination efficacies of novel antimalarial compounds" has been submitted to the Turnitin module and I confirm that my supervisor has seen my report and any concerns revealed by such have been resolved with my supervisor.

Name: Lizahn Laing

Student number: LNGLIZ003

Signature:

Signed by candidate

Date: 29 March 2020

Acknowledgements

This PhD would not have been possible on my own and I would like to convey my sincere gratitude to those who assisted and supported me throughout this journey:

Assoc Professor Lubbe Wiesner, as supervisor, thank you for your expert guidance throughout every aspect of my PhD journey. I greatly appreciate the time and resources you have invested into my work, as well as the motivation and faith you had in me – without it, this thesis would not have materialised.

To Dr Liezl Gibhard as co-supervisor who from my first day at Pharmacology made the transition into the lab much easier. I am grateful for the knowledge you shared and always being available to discuss data and being a sounding board for my thoughts. Thank you for your constant support, advice and encouragement during the writing phase.

Prof Richard Haynes as second co-supervisor who was always available to provide support and offer valuable insights on results as well as the reading and editing of this thesis. Thank you for the opportunity to be a part of the MRC Flagship project.

My colleagues from the Division of Pharmacology: Sumaya Salie and Virgil Verhoog, for the initial activity and toxicity screening of the compounds, as well as always being available to assist with anything TC related. Mr Trevor Finch, for his assistance with every early-morning mouse experiment. Dr Jill Combrinck, for her support, motivation and the time spent reading and editing chapters of my thesis. Alicia Evans, for her encouragement and interesting toxicology talks. You were always available to assist with instrument issues and share your knowledge and experience, thank you. My cheerleaders Devasha and Daniel, for their genuine friendship and with whom I am grateful to have shared in the daily struggles of this PhD experience.

Most of all, I would like to thank **my family** for their unconditional love and support throughout this process, and constantly reminding me of God's love, grace and faithfulness to His children. To my parents, Johann and Elizna, and my sister Richelle, thank you for always believing in me and providing everything I needed to pursue my ambitions. To my husband, Marco, for the love and patience you have shown every step of the way throughout this challenging time. The late-night pep talks meant more than you'll ever know. I am deeply grateful to have you.

Lastly, I am very grateful for the **financial support received** from the following organisations: National Research Foundation for providing scholarship support through the NRF-DAAD Scholarship (Grant number 101613), as well as the University of Cape Town and Department of Clinical Pharmacology for additional scholarship funding.

Soli Deo gloria

Conference Proceedings

2016 The H3D Symposium 2016 held at Goudini, Cape Town on 23–26 November 2016. Poster: Evaluation of Efficacies and Pharmacokinetics of Novel Antimalarial Compounds

2017 The South African Society for Basic and Clinical Pharmacology Conference held at the University of the Free State (Department of Pharmacology), Bloemfontein on 1–4 October 2017. Poster: Evaluation of Efficacies and Pharmacokinetics of Novel Antimalarial Compounds

2018 Keystone Symposia: The 21st Century Drug Discovery and Development for Global Health held at the Hotel Palace Berlin, Berlin, Germany on 17–20 October 2018. Poster: Evaluation of Efficacies of Novel Antimalarial Combinations

Abstract

Relief of the global malaria burden relies on the management and application of effective therapies. Unfortunately, the continuous development of resistance to therapies by the deadliest parasite strain, *Plasmodium falciparum*, has made the treatment and control of malaria much more difficult. Derivatives of the Chinese peroxidic antimalarial drug artemisinin primarily used in first-line combination therapy for treatment of *P. falciparum* malaria have proved to be highly effective. However, their use also is now compromised by the development of resistance by the parasite to the artemisinin derivative in the drug combination. This event emphasizes the need for ongoing development of new and effective drug combinations.

This research aimed to identify efficacious combinations selected from a group of compounds known to induce oxidative stress by redox cycling combined with an artemisinin, which as an oxidant drug also induces oxidative stress but is unable to undergo redox cycling. Combination of the artemisinin with a redox-active compound is expected to both enhance and maintain oxidative stress within the parasite's proliferative environment. These combinations should be used together with a third drug with a completely different mode of action, such as a quinolone.

Selected amino artemisinins and redox active phenothiazines, phenoxazines, thiosemicarbazones, and quinolone derivatives were screened for antimalarial activity and mammalian toxicity. These were found to be potently active (<100 nM) against NF54 chloroquine-sensitive (CQS) and Dd2 chloroquine-resistant (CQR) parasite strains, and relatively non-toxic (>11 μM) to Chinese Hamster ovarian (CHO) cells. The compounds are thus highly selective for *P. falciparum*, as revealed by the selectivity indices (SI) of >270.

The *in vitro* absorption, distribution, metabolism, and elimination (ADME) properties of the compounds were also determined through the application of specific assays.

In vivo pharmacokinetic (PK) profiling was also carried out by intravenous and oral administration of the individual compounds to healthy C57BL/6 mice. Biological samples were analysed via liquid chromatography-tandem mass spectrometry (LC-MS/MS) bioanalytical methods, which were validated according to the fit-for purpose

recommendations by the FDA. Evaluation of the *in vitro* and *in vivo* profiles thereby facilitated the identification of suitable combination candidates.

The phenoxazine and phenothiazine derivatives were identified as the best potential redox partners and were each investigated in combination with the amino-artemisinin artemisone through fixed ratio isobole analysis. A substantial synergistic interaction was observed.

Overall, the investigation enabled the identification of drug combinations that are potently active *in vitro*. This synergistic interaction strongly supports the redox cycling rationale for identifying new antimalarial therapies and further suggests that such combinations in chemotherapy may delay the onset of resistance to the new agents. The results strongly encourage further investigation of the *in vivo* pharmacokinetic and pharmacodynamic (PK/PD) relationships of these combinations in the humanized murine model of *P. falciparum*.

List of Abbreviations

·OH	hydroxyl radical
AAG	α1-acid glycoprotein
ACN	acetonitrile
ACT	artemisinin-based combination therapy
ADME	absorption, distribution, metabolism and excretion
AMS	artemisone
ANOVA	analysis of variance
APAD	3-acetylpyridine adenine dinucleotide
AS	artesunate
ATP	adenosine triphosphate
AUC	area under the curve
$AUC_{0-\infty}$	area under the concentration-time curve from zero to infinity
BA	bioavailability
BCRP	breast cancer resistance protein
BCS	bio classification system
CHO	Chinese hamster ovarian (cells)
CI	confidence interval
CL	clearance
CL_H	hepatic clearance
CL_{int}	intrinsic clearance
$CL_{int,u}$	unbound intrinsic clearance
CM	complete medium
C_{max}	maximum concentration
CQ	chloroquine
CQR	chloroquine resistant
CQS	chloroquine sensitive
CV	coefficient of variation
CYP	cytochrome P450
DHA	dihydroartemisinin
DHFR	dihydrofolate reductase
DHPS	dihydropteroate synthase
DMA	*N,N*-dimethylacetamide
DMSO	dimethyl sulfoxide
DQ	decoquinate
DV	digestive vacuole

ED_{50}	50% of the effective dose
EMA	European Medicines Agency
FAD	flavin adenine dinucleotide
FDA	The Food and Drug Administration
Fe(II)	ferrous iron
Fe(II)PPIX	haem
Fe(III)PPIX	haematin
FFP	fit for purpose
FIC	fractional inhibitory concentration
FMN	flavin mononucleotide
f_u	fraction unbound
G6PD	glucose-6-phosphate dehydrogenase
GIT	gastrointestinal tract
GR	glutathione reductase
GSH	glutathione
GSSG	oxidised glutathione
H_2O_2	hydrogen peroxide
Hb	haemoglobin
HPLC	high-performance liquid chromatography
HPMC	hydroxypropyl methylcellulose
HSA	human serum albumin
HTS	high-throughput screening
IC_{50}	50% inhibitory concentration
IV	intravenous
ISTD	internal standard
LC-MS/MS	liquid chromatography-mass spectrometry
LLE	liquid-liquid extraction
LLOQ	lower limit of quantitation
LogD	logarithm of distribution coefficient
LMB	leucomethylene blue
MB	methylene blue
MeOH	methanol
MMV	Medicines for Malaria Venture
MR4	Malaria Research and Reference Reagent Resource Centre
MRP	multidrug resistance protein
MTT	3-(4,5-dimethylthiazol-2-yl)-2,5-diphenyl tetrazolium bromide
NADPH	nicotinamide adenine dinucleotide phosphate
NBT	nitroblue tetrazolium

NCA	non-compartmental analysis
$O_2^{\cdot-}$	superoxide anion
PAMPA	parallel artificial membrane permeability assay
P_{app}	Apparent permeability
PBS	phosphate buffered saline
PC	parasite cytosol
PEG	polyethylene glycol
P-gp	P-glycoprotein
PK	pharmacokinetics
PK/PD	pharmacokinetic–pharmacodynamic
PPB	plasma protein binding
PPE	protein precipitation extraction
PPG	polypropylene glycol
PO	oral
QC	quality control
RBC	red blood cell (RBCs as plural–red blood cells)
Redox	reduction/oxidation
RF	riboflavin
RI	resistance index
RNS	reactive nitrogen species
ROS	reactive oxygen species
SEM	standard error of the mean
SG	SYBR Green
SI	selectivity index
STD	standard
TACT	triple artemisinin-based combination therapy
TCP	target candidate profile
TCS	total concentration samples
T_{max}	time to reach C_{max}
Trx	thioredoxin
TrxR	thioredoxin reductase
Vd	volume of distribution
WHO	World Health Organisation

Table of Contents

1Literature Review

1.1 Project Introduction

The high global prevalence of malaria infection remains problematic and highlights the persistent need for improved control and treatment measures, especially in endemic countries. Unfortunately, the effective control of malaria is hampered by increasing tolerance to first-line artemisinin-based combination therapies. Continuing efforts are underway at both academic institutions and industries to find new and effective compounds in the hope of slowing the progression of drug resistance and to maintain the progress which has already been made in the fight against the elimination of malaria.

In this project, it is proposed that newer, more stable, artemisinin derivatives should be combined with a redox-active compound to counter the progression of the parasite's tolerance towards artemisinin therapies. This proposal is based on evidence that suggests artemisinins function as intracellular oxidants. Amplification of this action by a redox partner can overwhelm intrinsic parasite mechanisms that maintain redox homeostasis.

The effect of redox cycling may be assessed by the known redox drug methylene blue (MB). The rapid oxidation by intracellular oxygen of the reduced, colourless form leucomethylene blue (LMB) back to MB provides a mechanism to preserve oxidative stress in the presence of an artemisinin derivative. In this project, new compounds are identified as potential redox-combination partners with an artemisinin derivative using biological screening methods. Their ADME properties are predicted from *in vitro* assays and then evaluated in a murine model.

1.2 Background of the disease

1.2.1 The global malaria burden in 2019

Malaria is caused by the protozoan *Plasmodium* parasite and is responsible for millions of infections occurring predominantly in tropical and sub-tropical regions of the globe. Five different species of *Plasmodium* can infect humans, namely *P. falciparum*, *P. vivax*, *P. malariae*, *P. ovale* and *P. knowlesi*. The highest prevalence of malaria infections outside of Africa arise from *P. vivax*, occurring mainly in South-East Asia, the Western Pacific and some parts of the Americas.[1] However, *falciparum* malaria has the widest global distribution. It is most prevalent in Africa and results in the highest mortality rates.[2,3]

According to the World Health Organisation (WHO) 2019 World Malaria Report, an estimated 228 million cases (95% CI: 206–258 million) of malaria occurred in 2018 (Figure 1-1), compared to 231 million cases (95% CI: 211–260 million) in 2017.[1] Of these, an estimated 213 million (93%) occurred in the WHO African region. The remainder was made up of cases in the WHO South-East Asia Region (3.4%), WHO Eastern Mediterranean Region (2.1%), Western Pacific region (0.8%), and the Americas (0.4%). Encouragingly, the global estimated deaths from malaria per year was reported to have decreased considerably from 585 000 in 2010 to 405 000 in 2018. Children under the age of 5 are particularly susceptible to the disease and constituted 272 000 deaths in 2018. Unfortunately, there are still many challenges to overcome in accomplishing the goals that the WHO has set out in their Global Technical Strategy for Malaria for 2016–2030, for achieving malaria elimination. Of these, the goals to eliminate malaria transmission within countries and the prevention of re-establishment of malaria from malaria-free countries are important focus points of research in drug discovery and development.[1] In order to preserve sustainable drug discovery and development of antimalarial drugs, new alternative therapies with the best prospects for being developed should be prioritised.[4]

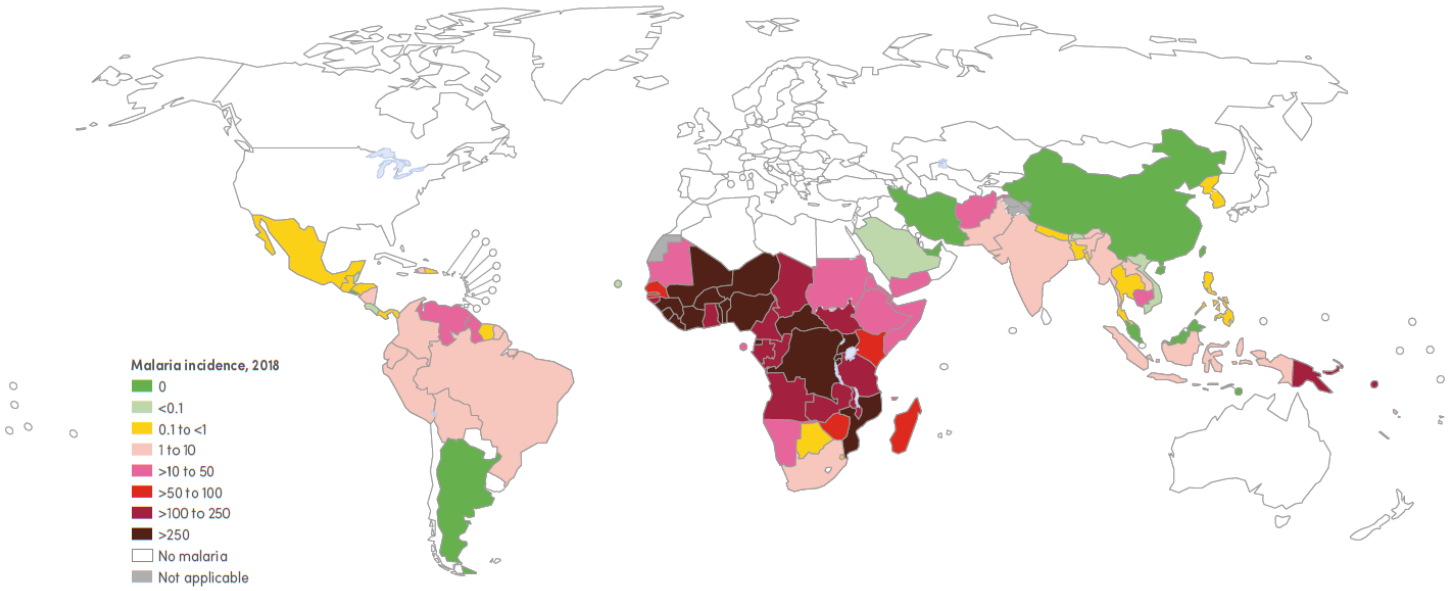

Figure 1-1: Map of malaria cases per 1000 population at risk by country in 2018. Image reproduced from the WHO World Malaria Report 2019.[1]

1.2.2 Biology and clinical features of *Plasmodium falciparum*

The prokaryotic parasite *P. falciparum* is transmitted by the female mosquito of the species complex *Anopheles* and causes the vector borne disease malaria.[5] The lifecycle of *P. falciparum* requires two hosts and encompasses three major developmental stages - the mosquito, liver, and blood stages.[6] The lifecycle begins when sporozoites from an infected mosquito are injected into the human host during a blood meal (Figure 1-2a). Development and replication within the human can be divided into the liver stage and blood stage cycles (Figure 1-2b). The blood stage parasites are responsible for disease manifestation and the production of gametocytes. The lifecycle continues in the mosquito vector once a mosquito takes a blood meal from an infected human, which initiates gamete maturation during the sporogonic cycle. Mature oocysts rupture and release sporozoites which initiate a new proliferation cycle.[7,8]

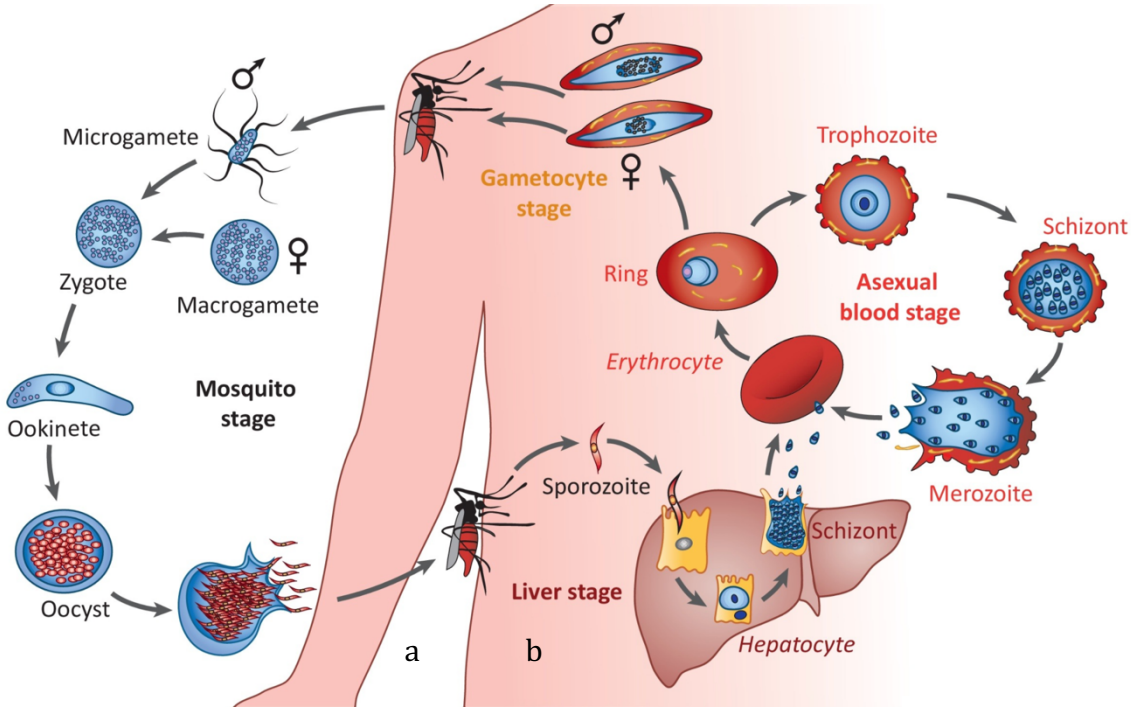

Figure 1-2: The two-phase parasitic lifecycle of *Plasmodium* in a) the *Anopheles* vector and b) the human host. Reprinted from Trends in Parasitology, 35(6), Maier A.G, Matuschewski K., Zhang M. and Rug M., Plasmodium falciparum, 1-2, Copyright (2019), with permission from Elsevier.[9]

Clinical manifestation of malaria infection occurs during the blood stage and is categorized as either uncomplicated or severe malaria. The general symptoms of malaria infection are described as nonspecific and flu-like, and may include fever, headache, fatigue, jaundice and gastrointestinal disturbances.[10] As result of this, diagnosis of the malaria infection is sometimes overlooked, which causes a delay in treatment and escalation of the severity of the infection. Fatal complications my arise in the case where the diagnosis and treatment are not promptly initiated. This is referred to as severe malaria in which *P. falciparum* can cause obstruction and eventual rupture of the small capillaries of the brain by sequestered parasites.[7] Severe malaria is frequently found in young children and presents more serious symptoms such as multiple convulsions, impaired consciousness, respiratory distress, spontaneous bleeding and pulmonary oedema.[10] A patient is diagnosed with malaria if positive parasitological diagnostic tests confirm the symptoms of malaria. The traditional method of diagnosis is by observation of Giemsa-stained infected erythrocytes under light microscopy (Figure 1-3).[11]

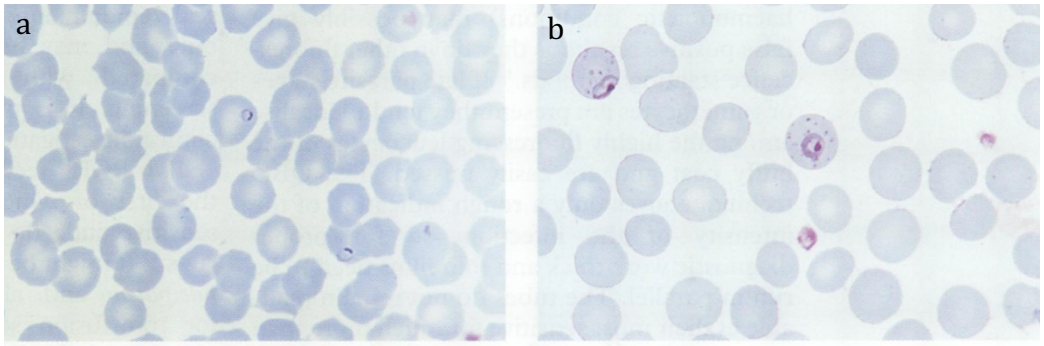

Figure 1-3: Thin blood smears of *Plasmodium falciparum* infected erythrocytes stained with Giemsa; a) small ring stage trophozoites and b) mature trophozoites. Reproduced from [ACP Broadsheet no 148. July 1996. Laboratory diagnosis of malaria, Warhurst D.C, Williams J.E., 49(7):533-8, 1996] with permission from BMJ Publishing Group Ltd.[11]

1.2.2.1 Life cycle in the mosquito

Mature male and female gametocytes are taken up by the mosquito during a blood meal.[12] *Plasmodium* parasites within the mosquito vector (Figure 1-2a) undergo maturation and DNA replication to form microgametes (male) and macrogametes (female).[13,14] Gametes travel to the midgut of the mosquito and fuse to form a zygotes which mature into ookinetes. Ookinetes cross the epithelial cell wall of the mid-gut and become oocysts, containing sporozoites.[15] The mosquito life cycle is complete when the oocysts rupture, releasing sporozoites after which they migrate to the salivary glands of the mosquito. Transmission of the parasite can occur at the next blood meal.[16]

1.2.2.2 Life cycle in humans

Sporozoites contained in the salivary glands of mosquitoes are injected into the circulatory system of a human host during a blood meal. This initiates the exoerythrocytic stage whereby the uninucleate sporozoites invade the liver parenchymal cells 5–21 days after the bite from an infected mosquito (Figure 1-2b). During its time in the liver, sporozoites develop into spherical multinucleate schizonts, each containing thousands of merozoites. The merozoites are released into the bloodstream upon rupture of schizonts and enter the red blood cells (RBCs). This marks the start of the blood stage where the cyclical production of merozoites is followed (asexual development), or the formation of

gametocytes (sexual development) takes place.[17] Upon entry of merozoites into the RBC, small ring-stage parasites develop to trophozoites through DNA replication and mature into schizonts (Figure 1-4). These schizonts rupture from the RBC and can release 8–36 merozoites which may then infect new RBCs and start the blood stage-schizogony again.[6,17] This recurring cycle of invasion and rupture manifests as the clinical presentation of the disease, which results in intervals of fever. Merozoites that do not go on to form trophozoites and schizonts become uninucleate gametocytes, the sexual stage of the blood stage that forms male and female gametocytes. A certain portion of asexual blood stage parasites circulating in the human peripheral blood develop into male and female gametocytes which are then transmitted to the mosquito during a blood meal.[14,8,18]

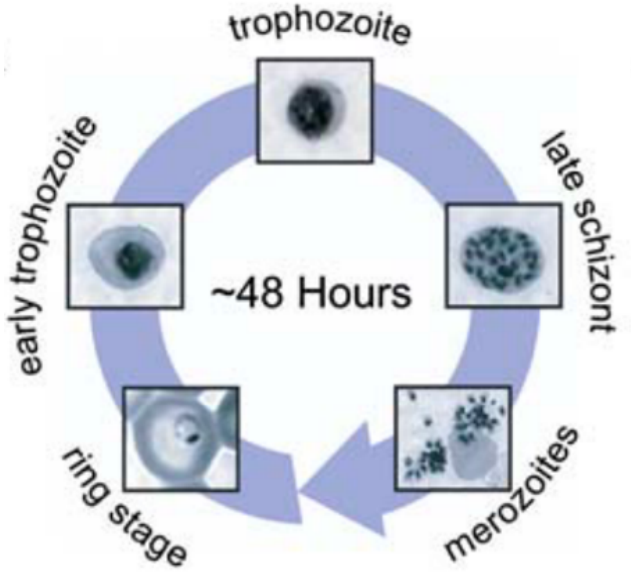

Figure 1-4: Giemsa stains of the major morphological stages throughout the intraerythrocytic developmental cycle.[6]

1.2.3 Antimalarial therapy today

Malaria prevention and control relies greatly on collective efforts which according to the WHO, should include better diagnostic tools for early detection and prompt treatment with effective drug combinations. The risk of infection is reduced by indoor residual spraying, long-lasting insecticide-treated mosquito nets and intermittent preventive therapy for pregnant women.[1,19] Development of vaccines against malaria have also featured in malaria-control interventions and recently the vaccine candidate RTS,S/AS01

has been developed. However, Phase III clinical trials showed only modest protection against infections.[20] Although the need is urgent for a vaccine that can provide long-lasting sterile protection, the RTS,S/AS01 vaccine candidate may still offer valuable protection in conjunction with current therapies.[21] Thus, the search continues for new drugs that can be used to treat and effectively prevent the spread of malaria infections.

A review by Hooft Van Huijsduijnen and Wells in 2018 highlighted antimalarial drugs in early and clinical development that are mainly active against blood stage schizonts.[22] The blood stage parasites are the primary target for drug development, because this is the stage of the disease responsible for symptoms and patient death. In the last decade, the generation of new compounds targeting previously overlooked molecular targets at the blood stage has benefitted from collaboration between academic institutions and industry. These efforts have delivered leading compounds that are currently being evaluated in clinical trials. Examples include the spiroindolone KAE609 developed by Novartis which targets the sodium channel PfATP4,[23,24] the imidazolopiperazine KAF156 developed by Novartis[25] and MMV390048 developed by the University of Cape Town which targets PfPI4-kinase.[26]

1.2.3.1 Treatment and control efforts

Clinical treatment of malaria infections depend on several different classes of drugs designed to target specific phases of the malaria life cycle.[8] As previously mentioned, blood stage parasites are the most common drug target and the focus of current therapies. The most common classes used for antimalarial treatment include quinoline derivatives, antifolates, artemisinins, arylamino alcohol derivatives and some antimicrobials (Table 1-1).[27,28] Some tetracycline and erythromycin antibiotics, like doxycycline and azithromycin, are considered useful against malaria and are mainly used for chemoprophylactic therapy.[29] Although slow acting, they can be clinically useful when combined with artemisinin derivatives or quinolones for the follow-up treatment of severe malaria.[30,31] Many of these compounds have been used in combination therapy. For example, the arylamino alcohol derivative lumefantrine is co-formulated with artemether as Coartem® and administered in current first-line artemisinin-based combination therapy (ACT) regimens. Figure 1-5 summarises the chemical structures of commonly used drugs.

Table 1-1: Examples of available antimalarial drugs used today.

Class	Category	Drug
Quinoline derivatives	4-amino quinoline	Chloroquine
		Amodiaquine
		Piperaquine
	8-amino quinoline	Primaquine
	Quinoline methanol	Quinine
		Quinidine
		Mefloquine
	Arylamino alcohol derivatives	Lumefantrine
Antifolates	Folate antagonists; sulfadoxine combination	Pyrimethamine/ Sulfadoxine
	Naphthoquinone; folate antagonist combinations	Atovaquone/ Proguanil
Artemisinin and derivatives	Sesquiterpene endoperoxides	Artesunate
		Artemether
		Dihydroartemisinin
Antimicrobials		Tetracycline
		Doxycycline
		Clindamycin
		Azithromycin

Table adapted from Mishra *et al*.[28]

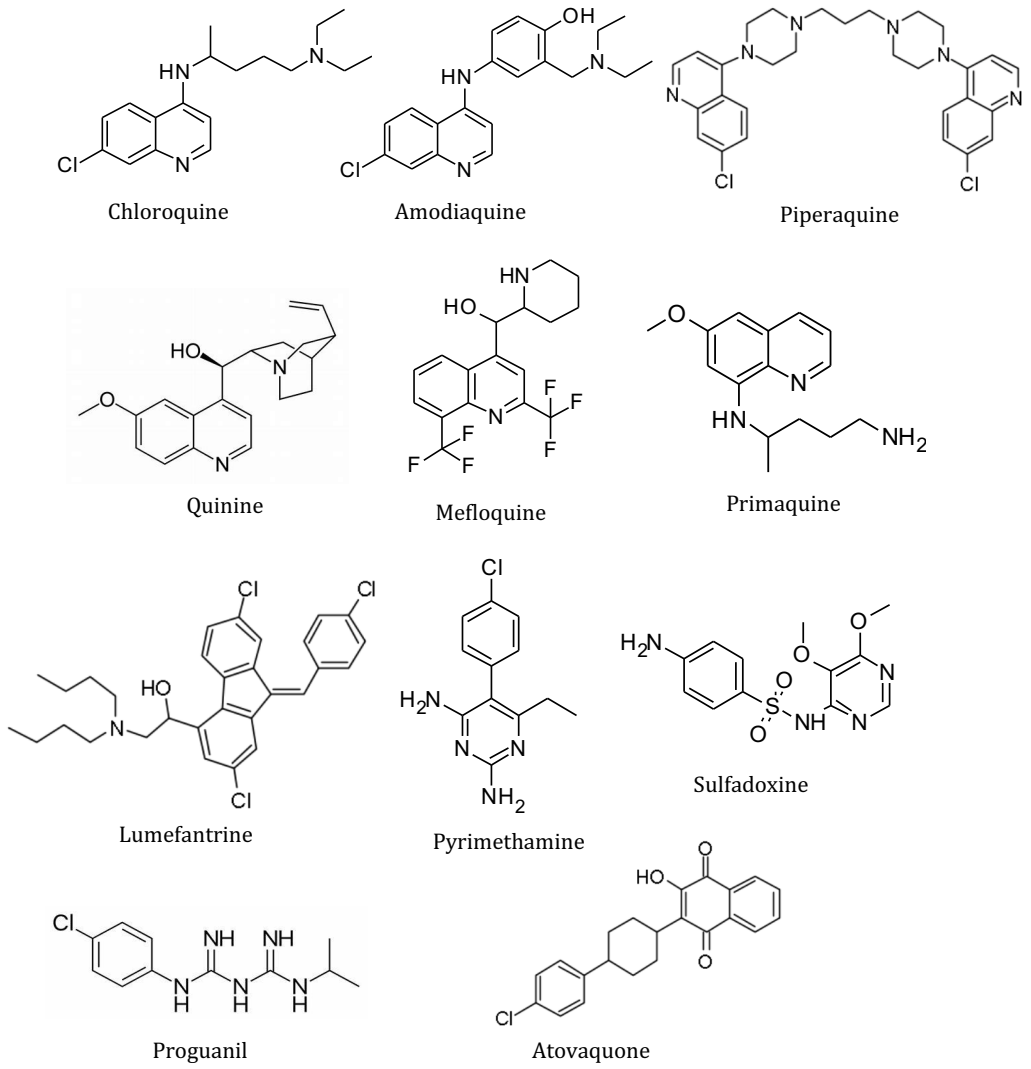

Figure 1-5: Structural representation of clinically applied antimalarial drugs.

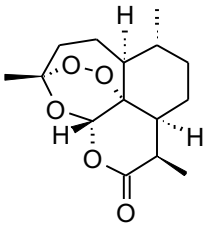

Artemisinin

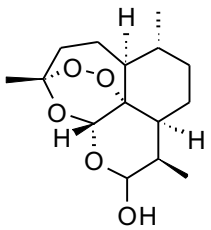

Dihydroartemisinin

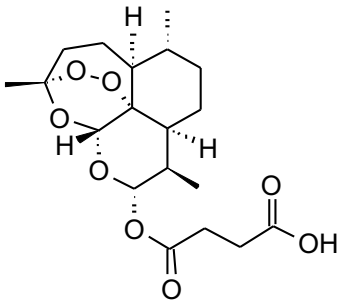

Artesunate

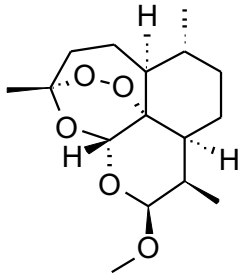

Artemether

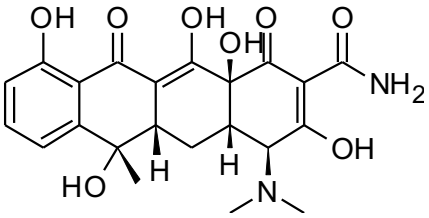

Tetracycline

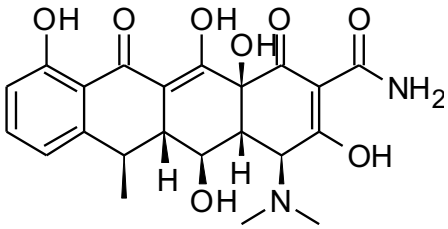

Doxycycline

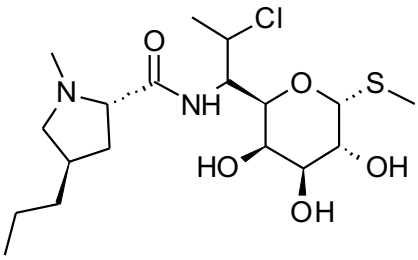

Clindamycin

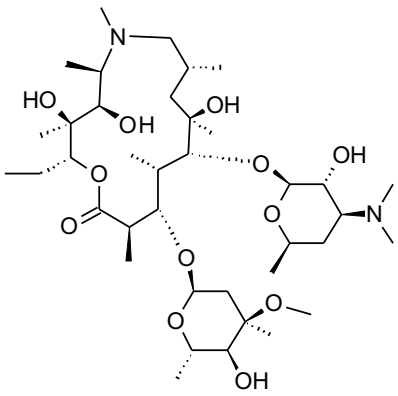

Azithromycin

Figure 1-5: (Continued)

Quinoline derivatives

The quinoline derivative chloroquine (CQ) was once the most widely used of all antimalarial drugs. However, due to widespread resistance to CQ, treatment shifted to other drugs.[32,33] The 4-aminoquinolines are highly active against the blood stage of the malaria parasite lifecycle and their mechanism of action is proposed to selectively inhibit haemoglobin (Hb) degradation by the parasite and thereby interfering with haem detoxification (Figure 1-6).[34,35]

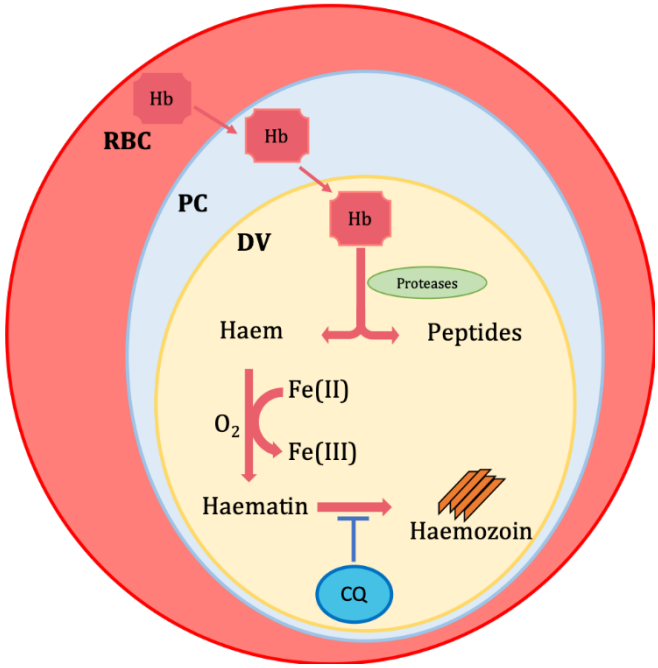

Figure 1-6: Haemozoin formation and inhibition by CQ.

Hb is transported from the RBC, though the parasite cytosol (PC) and into the digestive vacuole (DV). Hb is digested to haem and peptides by proteases. Fe(II) haem is auto-oxidised to toxic Fe(III) haematin. Haematin is sequestered to inert haemozoin crystals. The dimerization process of haematin is inhibited by quinoline drugs such as CQ.

Another quinoline derivative that has been used with considerable success is the 8-aminoquinoline primaquine. Currently, it is used mainly as prophylactic treatment and for the radical cure of *P. ovale* and *P. vivax* infections, or as a single dose gametocytocide.[36–38] The addition of primaquine to an ACT has been shown to shorten estimated gametocyte circulation times and thus hinder malaria transmission.[39,40] Tafenoquine, a newer 8-aminoquinoline, has greatly improved *in vitro* activity and *in vivo* half-life over primaquine. Concerns exist regarding the use of high doses of primaquine and tafenoquine in populations with glucose-6-phosphate dehydrogenase (G6PD) deficiency, as the high dosages of these drugs may cause haemolytic toxicity in these deficient individuals.[38,41] Further demonstration of haemolytic toxicity was found in a study completed by Chu *et al.,* where the standard high dose of piperaquine (0.5 mg/kg or 1.0 mg/kg per day for 14 or 7 days, respectively)[42,43] was administered to investigate the radical cure efficacy of *P. vivax* malaria on the Thai-Myanmar border.[42] However, Bancone *et al*. recently reported the gametocytocidal potency of low dose (0.25 mg base/kg) primaquine without clinically relevant haemolysis in G6PD deficient populations.[44,45]

The mechanism of action of 8-aminoquinolines was poorly understood, but very recently it has been shown in the case of primaquine that gametocytocidal efficacy is explicitly due to the generation of reactive oxygen species (ROS) formed by redox cycling of a quinone-imine metabolite generated from the primaquine *in vivo*.[46,47] Camarda *et al.* demonstrated that primaquine exhibits a two-step biochemical pathway through CYP2D6 and CYP450 nicotinamide adenine dinucleotide phosphate (NADPH) oxidoreductase, which is essential for its gametocytocidal efficacy. This process allows oxidation of primaquine by CYP2D6 to hydroxy-primaquine. Subsequent oxidation results in quinone-imine and the generation of hydrogen peroxide (H_2O_2). Quinone-imine, in turn is a substrate for the reducing activity by CYP450 NADPH oxidoreductase and results in H_2O_2 build-up.[46] In this sense, the conversion of primaquine into the quinone-imine metabolite that undergoes redox cycling, in fact mimics the behaviour of the redox-active drugs indicated above.

Antifolates

Antifolates are made up of two classes of drugs: dihydropteroate synthase (DHPS) inhibitors (Class I) and dihydrofolate reductase (DHFR) inhibitors (Class II). Sulfa drugs are inhibitors of DHPS which inhibit *de novo* folate synthesis in the parasite, whereas DHFR inhibitors affect activity of the parasite's bifunctional DHFR-thymidylate

synthetase protein. Drugs of these two classes interact synergistically and are co-formulated.[48] Examples of co-formulations include Fansidar® (sulfadoxine + pyrimethamine) or Malarone® (atovaquone + proguanil), among others. Sulfadoxine + pyrimethamine are often used in combination with other drugs. In Uganda, triple combinations of sulfadoxine + pyrimethamine with CQ showed improved efficacy outcomes.[49] Combinations with amodiaquine or mefloquine was used as low-cost alternative and effective treatment in African regions of high CQ resistance. However, widespread resistant mutations in parasites from eastern and southern Africa have since led to the efficacy surveillance of populations receiving those combinations and the implementation of ACT.[50] Today, the WHO recommends that sulfadoxine + pyrimethamine be mainly used as intermittent preventative malaria treatment during pregnancy. It is also provided for infants in moderate-to-high transmission areas in Africa. Sulfadoxine + pyrimethamine combinations with amodiaquine are prescribed for seasonal malaria chemoprevention in children aged 3 – 59 months.[51]

1.2.3.2 Artemisinins: background and resistance

The most effective drug class is based on the peroxidic compound artemisinin. These have been shown to be fast acting and are currently the most potent antimalarial drugs against *P. falciparum* malaria.[52] Because of their short half-lives, their use as monotherapy for uncomplicated malaria is prohibited by the WHO, as it may jeopardize their efficacy by increasing the potential for emergence of resistance.[53]

Background

Traditional Chinese medical literature describes various applications of the traditional Chinese medicinal herb qinghao (*Artemisia annua*) that included treatment of fevers, jaundice, itching, and usage for detoxifying blood.[54] In the late 1960's qinghao and other traditional herbal medicines were selected for examination against malaria by Chinese scientists. The extracts of qinghao were found to possess antimalarial activity.[55,56] The active principle was then isolated and purified in 1972 and named 'qinghaosu', the 'active principle of qinghao'.[54] Clinical trials were launched as early as 1974 and the pharmacology of artemisinin as an antimalarial drug was published by 1979 in the Chinese Medical Journal.[57] As resistance against previously effective drugs such as CQ had

begun to spread, the introduction of artemisinin was particularly timely, and by the 1990's it was widely used in Thailand, Burma, and Vietnam. Many derivatives of artemisinin have been developed over the years in order to optimise and maintain therapeutic efficacy.[55]

Mechanism of action

Forty years after publication of its use as an antimalarial drug, the exact mechanism of how artemisinin elicits its antimalarial effect is yet to be defined. However, many different theories have been proposed.[58,59] According to a review by Edikpo *et al*., theories on the antimalarial activity of artemisinin fall in two categories: radical-dependent toxic and inhibitory effects of artemisinin on vital parasite macromolecules, and interference with the parasite Hb degradation and haem detoxification pathways.[60] Despite the different theories, one fact is clear: the peroxide in the 1,2,4-trioxane (Figure 1-7) in the artemisinins is essential for antimalarial activity,[61–63] and, therefore, artemisinins may be classed as antimalarial peroxide drugs.

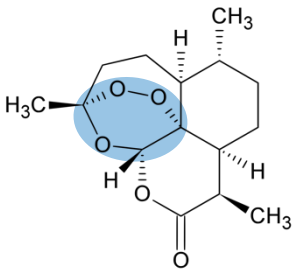

Figure 1-7: The structure of artemisinin where the 1,2,4-trioxane is indicated by the shaded area.

Increased levels of ROS occur once the parasite enters the host RBC. Oxidative damage to the RBC, resulting from the increased generation of lipid peroxides, leads to an unfavourable environment for parasite proliferation.[64] The parasite is presumably able to withstand these severe conditions during its intra-erythrocytic proliferation by utilizing two inherent, highly-elaborate redox (reduction/oxidation) systems. The thioredoxin

(Trx) and glutathione (GSH) redox systems, among other additional mechanisms, are thought to play a pivotal role in active redox defence.[65]

These redox systems are dependent on a constant supply of NADPH. In *P. falciparum* parasites, NADPH is supplied by G6PD and 6-phosphogluconolactonase for downstream redox reactions.[66–69] As shown in Figure 1-8a, the presence of NADPH allows GSH reductase (GR), Trx reductase (TrxR), and other flavin disulfide reductases[70] to reduce flavin cofactors such as flavin adenine dinucleotide (FAD) and flavin mononucleotide (FMN).[70–72] The reduced FAD and FMN are then able to provide electrons for the reduction of oxidised GSH (GSSG) and Trx-disulfide ($TrxS_2$) to GSH and reduced Trx ($Trx(SH)_2$), respectively. This step essentially intercepts ROS and thereby maintains intracellular redox homeostasis.[73–75]

Artemisinins have been shown to rapidly oxidise $FADH_2$, $FMNH_2$, and other reduced flavin cofactors (Figure 1-9). As further illustrated in Figure 1-8b, this action will prevent downstream reduction of GSSG and $TrxS_2$, interrupts the parasite's cycle of redox homeostasis, and leads to potentiation of ROS. It is this production of ROS that is believed to be responsible for parasite death. Therefore, artemisinins can act as exogenous peroxides enhancing the generation of ROS, which overwhelms the delicately-balanced parasite antioxidant defence system.[76] Additionally, supply of NADPH via the G6PD-catalyzed step has to be enhanced in the infected erythrocyte. This however is a rate-limiting step, and the supply is unable to meet the demand for additional reducing equivalents required to control the increased oxidative stress.[72]

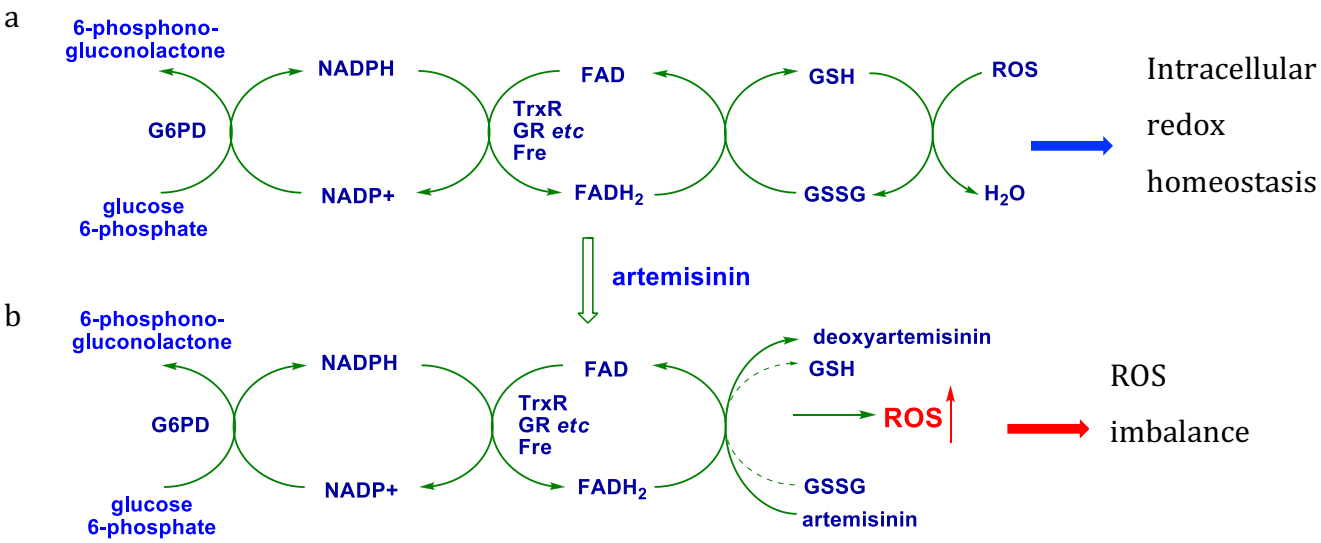

Figure 1-8: Management of redox homeostasis within the parasite. a) The mechanism of NADPH-modulated active redox defence in the *Plasmodium* parasite, which results in intracellular redox homeostasis. b) The addition of artemisinin disrupts efficient redox homeostasis and results in oxidative stress. Upon exhaustion of artemisinin, the redox homeostasis is re-established and maintained by the parasite. Fre, Flavin reductase. (Adapted from Haynes *et al.*, 2012)[77]

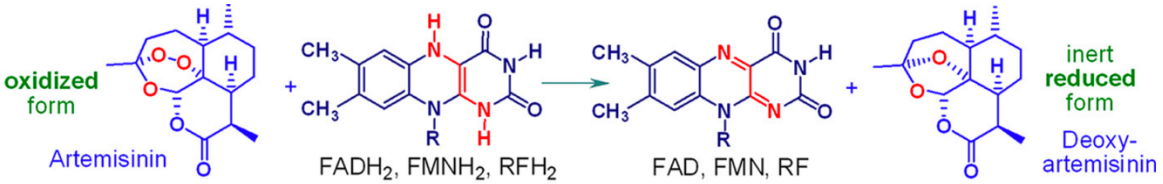

Figure 1-9: Artemisinin is irreversibly reduced by reduced conjugates of flavin cofactors FAD, FMN, and other reduced flavins, e.g., riboflavin (RF), to the inert deoxyartemisinin.[77,78]

Artemisinin-based combination therapy

Currently, the WHO recommends that artemisinins only be used in ACT for uncomplicated malaria.[79] ACTs combinations became the first-line treatment regimens for uncomplicated malaria due to high resistance in endemic countries. Since the first ACT (artesunate + mefloquine) was released in Thai-Myanmar in 1994, there have been multiple other combination regimens explored which include an artemisinin.[80] According

to the WHO Guidelines there are five main combinations currently in use. These include: artemether + lumefantrine, artesunate + amodiaquine, artesunate + mefloquine, dihydroartemisinin (DHA) + piperaquine, and the triple combination of artesunate with sulfadoxine-pyremethamine.[30] ACT combinations offer the advantage of a highly potent artemisinin component with a short plasma half-life which is able to rapidly reduce the parasite burden, while a more slowly eliminated drug protects formation of resistance to the artemisinin and clears remaining parasites after the initial drug action.[81] While this approach has been effective, there has been increasing evidence of resistance being formed against the partner drug, as in the case with DHA + piperaquine or artesunate + mefloquine combinations.[82,83] It has been suggested that triple ACT (TACT) therapies may offer effective treatment and preserve artemisinin efficacy in efforts to mitigate the spread of resistance.[84] According to a review recently published by Rosenthal, this strategy presents two main advantages: resistant parasites are still killed by artemisinins and ACT partner drugs have opposing resistance mechanisms.[85] Van der Pluijm and colleagues demonstrated the efficacy of DHA + piperaquine + mefloquine and artemether + lumefantrine + amodiaquine TACT in a multicentre study in areas which had established ACT resistance or a high threat thereof. The researchers concluded that these combinations are safe and efficacious in areas with artemisinin and partner drug resistance and that TACTs have the potential to delay the emergence and spread of resistance.[84]

Artemisinin resistance

Artemisinins are notably effective and from 2000–2015 had a significant impact on malaria prevalence and control.[19] In the early 2000's, ACTs started to become readily available in the highest-burden countries, after resistance to the then first line therapies such as CQ and sulfadoxine-pyrimethamine became a major issue.[86] From 2006 onwards, the ACTs were deployed as first-line therapy.[87] However, there is increasing evidence which shows that the *Plasmodium* parasites are becoming resistant to ACTs. Declining clinical efficacy of DHA-piperaquine first-line treatment was recently reported in southeast Asia. Furthermore, rapid regional spread of parasite mutations was observed for genes associated with decreased artemisinin efficacy.[88] This emergence of resistance to ACTs highlights the ever-evolving nature of the parasite to generate resistance to

therapies, and the pressing need for new therapies which may overcome the problem of artemisinin resistance.

Resistance to artemisinins is clinically defined as a delay in the time within which *P. falciparum* parasites are cleared from the blood of a malaria patient treated with an ACT or artesunate monotherapy.[89] The first evidence of ACT resistance was reported in 2009 in Pailin, western Cambodia as a 100-fold reduction in parasite clearance rate.[87] Since then, artemisinin resistance has been defined as a parasite clearance half-life ≥5 hours following treatment with artesunate monotherapy or an ACT.[90] In 2012, Phyo *et al.* examined the spread of resistance from Cambodia to the Thailand-Myanmar border. The researchers found that a geometric mean of parasite clearance times increased from 2.6 hours in 2001 to 3.7 hours in 2010, in comparison to a mean of 5.5 hours in western Cambodia measured between 2007 and 2010.[91] Data from a study completed in 2013 by Ashley *et al.* shows that artemisinin resistance was already then firmly established in parts of Myanmar, Cambodia, Thailand, and Vietnam which manifested as increased parasite-clearance times as a result of reduced susceptibility of ring-stage parasites. Despite the spread of resistance, the researchers found that ACTs remained highly efficacious.[92] Importantly, this suggests that as parasite clearance times have increased, greater dependence is placed on the partner compounds in the combinations for therapy to maintain efficacy. The authors correctly argue that one option to delay progression of artemisinin resistant malaria, is to prolong the course of treatment with ACT from the standard 3-day regimen. By extending the regimen, in which a 3-day artesunate course was followed with the standard 3-day ACT course, the researchers found that the failure rate decreased by a factor of 10 in areas of established resistance.[92] The suggestions of extending treatment to 6-day regimens is not a long-term solution but may provide some relief and time to search for new drugs.

ACT resistance has been detected in five countries of the Greater Mekong subregion (GMS), which includes Cambodia, Myanmar, Lao, Vietnam, and Thailand.[54,79] Currently, five ACTs are recommended by the WHO in the Greater Mekong subregion: artemether + lumefantrine, artesunate + amodiaquine, artesunate + mefloquine, artesunate + sulfadoxine-pyrimethamine, and DHA-piperaquine. However, first line treatment with DHA-piperaquine in Thailand and Cambodia has since been replaced with artesunate-pyronaridine combinations, due to the increase of parasites resistant to DHA-

piperaquine.[1] Figure 1-10 shows the geographic distribution of ACT resistance to these antimalarials.[79]

Winstanley and co-workers proposed that the mechanism by which resistance develops depends on multiple factors, which include the mechanism of drug action, efficacy of parasite elimination, PK profile of the drug, and parasite transmission dynamics.[32] Researchers discovered that a single-point mutation on the parasite chromosome 13 containing a gene which codes for the Kelch13 protein is associated with longer parasite clearance times.[92,93] Furthermore, research by Ashley *et al.* in 2013 demonstrated the correlation of single-nucleotide polymorphisms in the Kelch13 propeller domain with slow parasite clearance. This finding is significant, as it can be used and developed as molecular marker for tracking and monitoring of the spread of ACT resistance.[92]

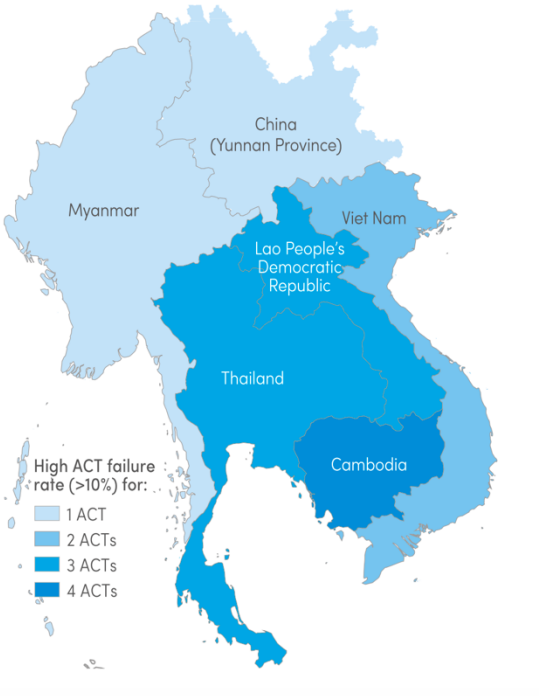

Figure 1-10: Geographic distribution of ACTs with high failure rates in the treatment of *P. falciparum* infection in the GMS. The countries are classified by the number of failing ACTs (>10% treatment failure) after 2010. Image reproduced from the WHO World Malaria Report 2018.[79]

No alternative treatment option with the efficacy and tolerability of ACTs currently exists and, therefore, the emergence of artemisinin resistance is a matter of great concern. The rational development of new antimalarial compounds should be of the highest priority if

the spread of resistance to ACT is to be controlled. The goal should be to develop compounds with longer half-lives, whilst maintaining rapid efficacy comparable to that of the current clinically used artemisinins.[94]

1.3 The search for new drug combinations

In a review by Fidock *et al.*, there is discussion over what constitutes an ideal antimalarial. According to the authors, the ideal profile for new antimalarials should encompass the following: activity against drug resistant strains, cure rates of less than three days, safety, and appropriate formulations. Most importantly, drugs should be affordable as the high-burden malaria-endemic countries often have limited resources and would not be able to afford expensive treatment.[95,96]

Guerin *et al.* discuss the growing consensus that combination therapy should be the focus if the goal is to control the spread of malaria in populations living in areas of high malaria endemicity.[97] Combination therapy offers an array of advantages over monotherapy. Firstly, drugs used in combination should be more effective than those used alone. This highlights the principle of synergy, which is a 'favourable' drug interaction and can greatly assist the potency of some drugs. Dorsey *et al.* demonstrate this principle with the improved efficacy of sulfadoxine + pyrimethamine combinations in African patients, where the use of combination therapy prolonged the lifespan of available treatment regimens in areas with drug-resistant malaria.[98]

It is important to note, as Fidock emphasised, that drug development should not solely rely on synergism to offer protection against resistance selection, because if one of the partners in the combination experiences resistance, both components may lose their efficacy.[95] In contrast, the combination of amodiaquine with sulfadoxine-pyrimethamine improved efficacy outcomes of CQ drug-resistant malaria infections in Eastern Africa.[50,98] Therefore, it is suggested that drug combinations can reduce the selection of antimalarial drug resistance and prolong the therapeutic lifespan of available treatments. Finally, if the partners in combination are effective against different stages of the parasite lifecycle, the opportunity exists to reduce treatment time, dosing concentrations, cost, and toxicity.

The use of drug combinations incorporating an artemisinin is now mandated by the WHO.[30,99] Because of their short half-lives, artemisinins are less prone to elicit formation of resistant parasites. Therefore, drugs combined with artemisinins should have longer half-lives to delay significant selection for parasites resistant to the longer-acting partner compound.[100] The need to select new compounds for combination therapy with artemisinins or derivatives is urgent, to counter the increasing prevalence of resistance.

The combination of an artemisinin with a new redox compound whose activity synergizes the action of the artemisinin should elicit potent activity against the malaria parasite. Importantly, one should also be mindful of the partner compound's half-life to avoid PK mismatch in these combinations. Half-lives should be long enough to eliminate any remaining parasites that escaped the initial rapid clearance by the artemisinin, but not extensively long as to leave the remaining partner compound susceptible to develop resistance.[101] The rational for this research project is to identify drugs which amplify oxidative stress through their action against flavoenzyme cofactors which modulate intracellular redox homeostasis utilizing NADPH.[70] These redox drugs are reduced by the same flavoenzymes responsible for maintaining homeostasis. The reduced drug in turn is oxidized back to the original redox molecule by intracellular oxygen in a reaction that generates ROS; thus, redox cycling occurs.

1.3.1 Oxidative stress and malaria

Oxidative stress is defined as the imbalance between antioxidants and pro-oxidants, whereby the latter are increased and oxygen-based damage to the host's cellular environment ensues and antioxidant activity is diminished.[102,103] ROS and reactive nitrogen species (RNS) are the most prominent agents involved in oxidative stress and are generally cytotoxic.[104] Conversely, ROS and RNS also fulfil various protective biological roles in host defence mechanisms, such as cellular signalling and apoptosis.[97] These molecules may include the free-radicals superoxide anion ($O_2^{\cdot-}$) and hydroxyl radical ($\cdot OH$), or non-radicals such as singlet oxygen and H_2O_2. ROS play an important role in many physiological processes. However, if an imbalance between damaging oxidants and protective antioxidants takes place, then the system experiences 'oxidative stress.'[104]

Oxidative stress has detrimental biochemical consequences and contributes to several human pathologies, such as cancer, vascular disease, neurodegeneration, and immunologic disorders.[104,105] Nitric oxide is another free radical species found in mammalian cells. Formed from oxidation of the amino acid L-arginine to citrulline via the action of nitric oxide synthases, it is an important mediator of blood pressure regulation, neurotransmission, and effector immune responses.[104] Secondary RNS occurring from the production of nitric oxide are highly cytotoxic. Nitric oxide is more stable than oxygen free radicals and has particular affinity for reaction with haem-containing proteins.[106]

It is proposed that during infection of the RBC by the malaria parasite, ROS production occurs via two distinct mechanisms; either by the activation of the host's immune response,[107] or via the degradation of haem within the DV of the intracellular parasite.[108]

The first mechanism involves production of inflammatory cytokines tumour necrosis factor alpha and interferon gamma in response to infection of RBCs, as these increase ROS production and phagocytosis.[107]

The second mechanism, as briefly described in Section 1.2.3.1., occurs following the metabolic breakdown of Hb to haem and globin. The rapidly growing and multiplying parasite is exposed to oxidative stress during the blood stage of the lifecycle, resulting from ROS formed as a by-product of Hb metabolism.[109] Hb is the main food source of parasites. As mentioned previously, Hb is metabolised in a stepwise manner in the parasite's acidic DV. The haem [Fe(II)PPIX] is separated from globin by proteases. The globin portion is further metabolised to peptides through various proteases that are utilized for parasite growth.[110] The resulting high amounts of haem is toxic to the parasite. Haem has been shown to cause redox damage to host proteins and membranes, inhibit parasite enzymes, and lyse erythrocytes.[111] The main pathway of detoxification of haem occurs via crystallization of hematin [Fe(III)PPIX], the oxidised form of haem, which results in the formation of hemozoin crystals (haem biomineral or malaria pigment), as described by Egan *et al.*[112] and occurs mainly in the DV of the parasite (Figure 1-11).[113]

While most of the haem is detoxified in the DV by conversion to haemozoin, some might escape into the parasite cytosol where it can cause substantial redox damage to the parasite protein and membranes.[109] Auto-oxidation of the haem to haematin results in the formation of several ROS species such as $O_2^{\cdot-}$, $\cdot OH$ and H_2O_2. The radicals are detoxified by the parasite's inherent antioxidant and redox mechanisms. The dismutation of $O_2^{\cdot-}$ to H_2O_2 and oxygen is accomplished by superoxide dismutase. Trx peroxidases then subsequently neutralises H_2O_2 to water. By interaction with transition metals such as labile ferrous iron (Fe(II)), or with haem-Fe(II), $O_2^{\cdot-}$ and H_2O_2 can generate $\cdot OH$ via the successive result of the Haber Weiss and Fenton reactions, which are known to cause lipid peroxidation (Figure 1-12).[114] Both hematin and H_2O_2 are considered toxic to the parasite and require neutralisation.[70]

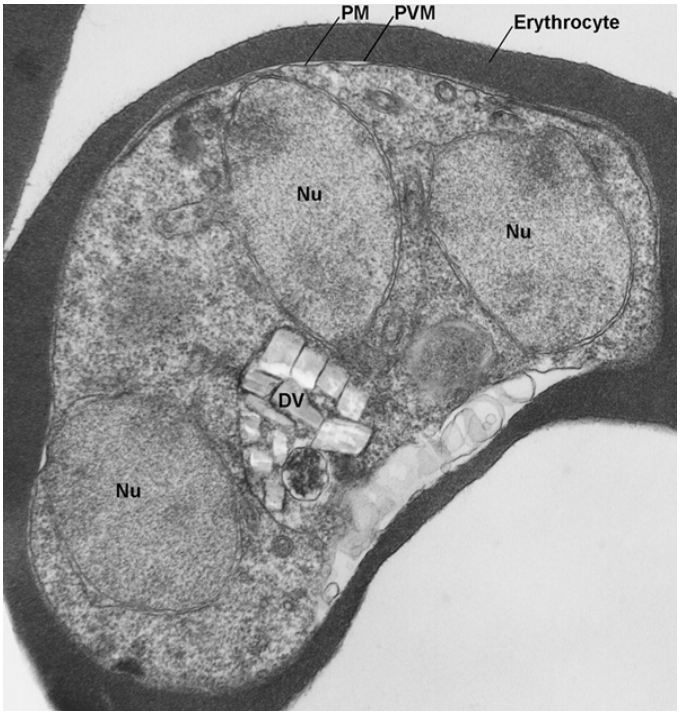

Figure 1-11: Electron microscopy image of a *P. falciparum* infected erythrocyte containing a DV with hemozoin crystals; DV, digestive vacuole; Nu, nucleus; PM, parasite plasma membrane; PVM, parasitophorous vacuole membrane.[113]

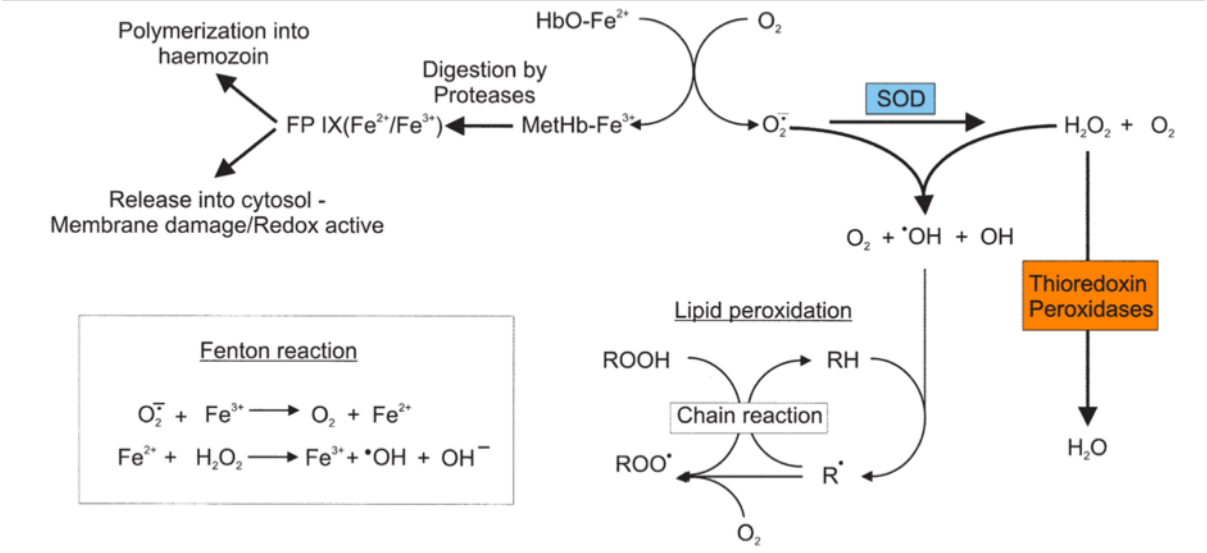

Figure 1-12: Sources of reactive oxygen species in *P. falciparum*.[70]

1.3.2 Parasite homeostasis mechanisms

Mammalian cells have innate mechanisms which are the first line of defence to protect against the cytotoxic actions of ROS. Their major antioxidant enzymes can be categorised

in three system. The first group includes superoxide dismutase, catalase and GSH peroxidase, which are responsible for the dismutation of superoxide and limits the formation of H_2O_2. The second category is the Trx-dependent system comprised of Trx and peroxiredoxins, which reduce protein disulfides and are maintained by TrxR. The third group includes GR which converts H_2O_2 to water, while reduced GSH scavenge $\cdot OH$.[104,115]

The malaria parasite is particularly sensitive to oxidative stress during its blood stage proliferation phase,[76,109,116] due to the pro-oxidant environment in the RBC that contains oxygen and iron which are key elements for the production of ROS.[70] However, malaria parasites do not have particularly sophisticated defence systems.[115]

Parasites utilize an inherent range of low molecular weight antioxidants. The most prominent antioxidant GSH, together with Trx systems, form part of thiol-redox system which are vital for parasites to maintain intracellular homeostasis (Figure 1-13).[65,72,117] These pathways require enzyme disulfide reductases such as GR or TrxR to reduce GSSG to GSH and reduce other endogenous disulfides to thiols. GSH acts as an electron donor and is oxidised to GSSG by GSH peroxidase that reduces toxic peroxides. GR reduces GSSG back to GSH using NADPH as an electron donor in the reaction. $NADP^+$ is then reduced to NADPH through the pentose phosphate pathway, G6PD or 6-phosphogluconate dehydrogenase.[109,118] *P. falciparum* also possesses a functional Trx system comprising TrxR[119,120] and Trx-dependent peroxidases[121] as well as a 1-cys-peroxiredoxin.[122] The Trx redox cycle is proposed to be essential for the biological function and survival of blood stage *P. falciparum*.[123] Other elements essential for the successful management of oxidative stress are cellular enzymes such as G6PD which can maintain a NADP, NADPH, and FADH-dependent reducing environment.[104]

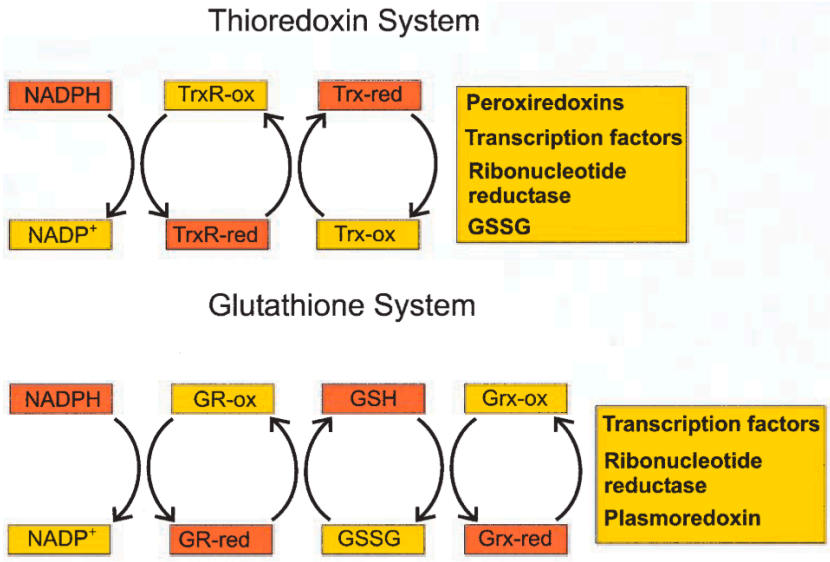

Figure 1-13: Thioredoxin and glutathione redox systems. A proposed link of the thioredoxin and GSH redox cycles in *Plasmodium* by the reduction of GSSG via thioredoxin, may be of physiological relevance under enhanced oxidative stress.[70]

CQ is an excellent example of a clinically used drug that exerts its effect, in part, by increasing oxidative stress, i.e. by preventing haem detoxification. This activity is postulated to be enhanced by depleting GSH.[109] The enzymes described in this section are, therefore, promising targets for the development of new antimalarials.[124]

1.3.3 Redox combinations

In this study, the investigated therapeutic approach consisted of the combination of two drugs that, in part, elicit their efficacy by creating a disruption in the redox regulatory pathways in *P. falciparum*. It has been shown that *P. falciparum* may be vulnerable to redox cycling drugs that are able to disrupt redox homeostasis maintained within the parasite. These drugs are then able to increase intracellular ROS levels and overwhelm the parasite homeostasis mechanisms.[125,126]

Redox cycling drug combinations rely on the oxidant and redox-active drug to work together to establish and maintain the intracellular ROS production. The parent redox molecule is reduced in the presence of reduced flavin cofactors, such as $FADH_2$ and $FMNH_2$. The oxidation of the reduced conjugate by intracellular oxygen restores the

parent redox molecule, whilst reducing the oxygen in a reaction that produces ROS. The regenerated parent molecule is available again for reduction by the reduced flavin cofactors, resulting in redox cycling and build-up of ROS. Additionally, the oxidant drug component interrupts the electron transfer by the abrupt oxidation of reduced flavin cofactors.[77]

An example of the action of the oxidant drug, as discussed previously in Section 1.2.3.2, is the reduction of artemisinin to the inert deoxyartemisinin, producing overwhelming build-up of ROS in the parasite (Figure 1-8) resulting in parasite death. However, redox homeostasis in *P. falciparum* are able to resume once artemisinin is depleted, curbing these effects.[77,124] As seen with MB, disulfide reductases such as GR and TrxR catalyse the reduction of MB by NADPH. As shown in Figure 1-14, the resulting LMB is then rapidly oxidized by oxygen, while producing H_2O_2.[78,126,127] With every reaction cycle, NADPH and oxygen are consumed in the respective oxidation/reduction reactions and concurrently increasing the production of ROS.[127] Blank *et* al. proposed that the mechanism for the biological effects of MB are likely due to its redox cycling abilities together with modification of the lipophilicity of MB upon reduction to LMB through electron exchange.[128] Through this action, the redox component of combination therapy ensures that the generation of ROS is not diminished after artemisinin exhaustion (Figure 1-15).

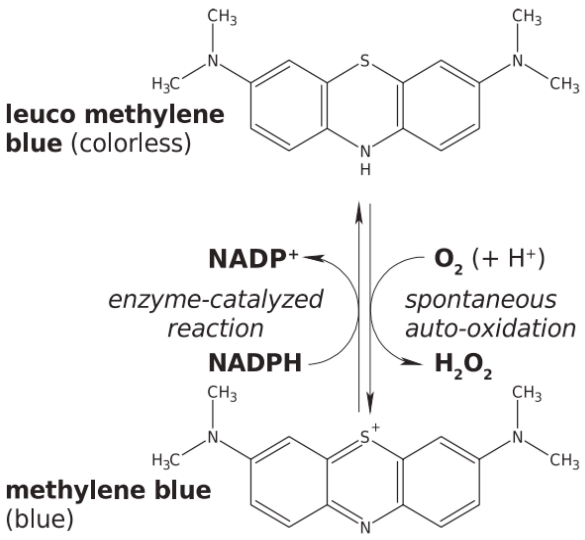

Figure 1-14: Redox cycling of MB. MB is reduced by disulfide reductases such as GR and TrxR in the presence of NADPH, to the colourless LMB, which in turn is auto-oxidized back to MB, resulting in the production of ROS.[127]

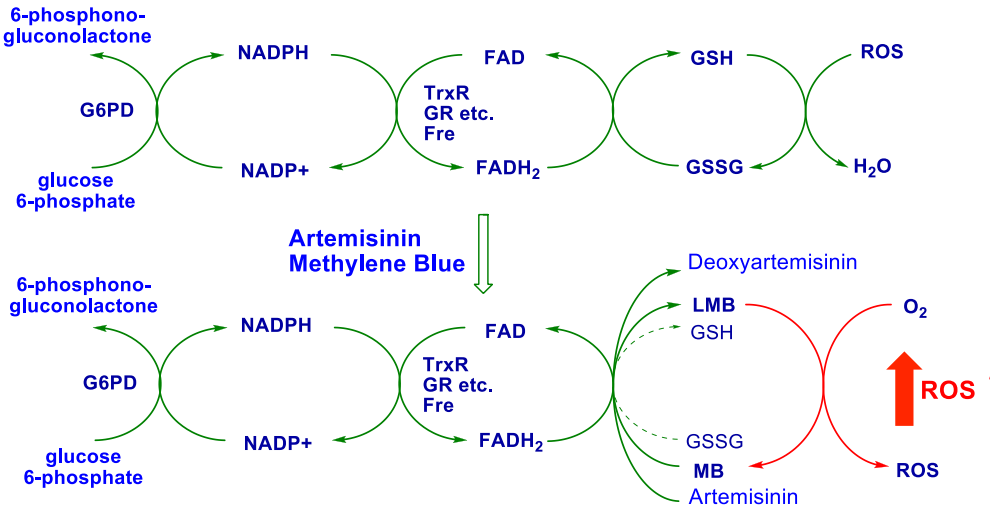

Figure 1-15: Proposed enhancement of intracellular ROS by the combination of redox compounds such as MB with peroxidic antimalarials such as artemisinin, resulting in the loss of redox homeostasis in the parasite .[78]

While redox-active compounds like MB[129] or 1,4-naphthoquinones[66] have shown to increase oxidative stress within the erythrocyte, Belorgey *et al*. suggested that higher levels of oxidative stress may serve as protection against malaria infection by increasing ring-stage phagocytosis rather than by direct inhibition of parasite growth.[125] Furthermore, the safety and efficacy of MB was assessed in a clinical study in Burkina-Faso in G6PD-deficient patients with uncomplicated *falciparum* malaria.[130,131] Combinations of MB with artesunate or amodiaquine administered to children with uncomplicated malaria demonstrated enhanced overall efficacy by the addition of the redox partner.[132] Therefore, MB-like compounds are excellent candidates for drug combinations and their potential as new antimalarial treatments.

1.4 Drug development for malaria

The drug discovery pipeline can be divided in two main areas of research: pre-clinical (non-human models) and clinical research (human studies). Pre-clinical research can further be subdivided into various areas of speciality, in which each area filters the best potential candidates that could qualify for clinical studies.[133] Figure 1-16 depicts the flow of compounds from early identification, to lead evaluation, rational design, and finally candidate selection. Drug development of novel antimalarial compounds can be achieved by many different approaches. Efforts have been made to improve drugs that are currently used in antimalarial therapy, for example, by optimising the parent scaffold for which parasites have acquired resistance. However, the discovery of novel classes of antimalarials more often relies on high-throughput screening (HTS) of compound libraries.[134]

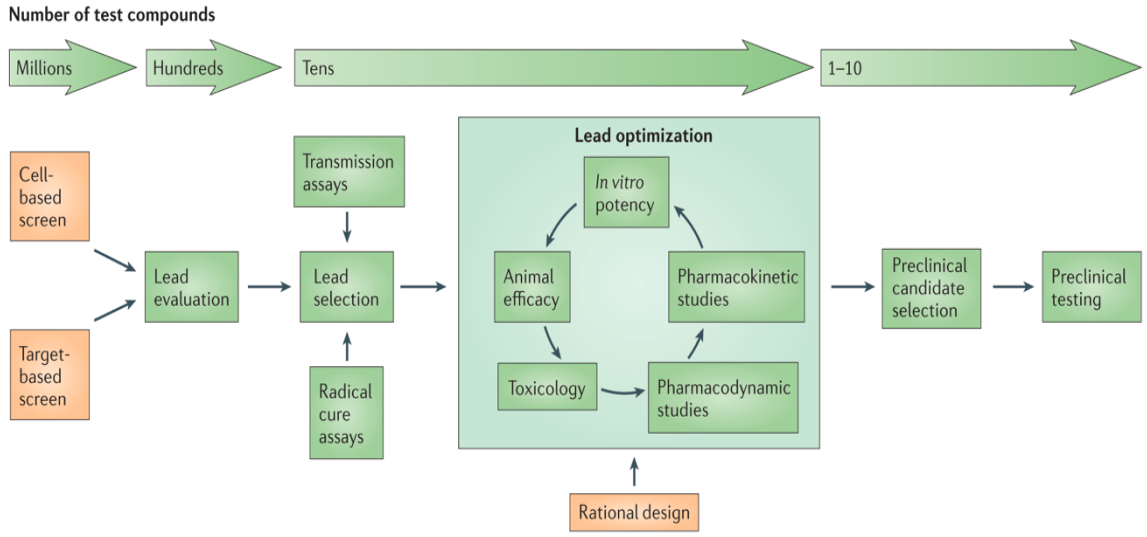

Figure 1-16: Drug development strategy for novel antimalarial drugs.[134]

Drug discovery starts from the simplest (biochemical assays) and continues to increasingly complex models. The pipeline produces data from a chain of experiments and ultimately completes the PK/PD picture of the compound.[135] The pre-clinical drug discovery phase involves the initial prediction of the behaviour of compounds in cells or

the human body. *In silico* studies use computational models that mimic biological processes and environment genomic-, proteomic-, and metabolomic-derived information identifies potential targets to be used by computer-based methods.[136] These methods are, however, limited as living systems consist of complex components and *in silico* studies are only able to give a preliminary overview of potential drug behaviour.[137,138]

In vitro studies represent the biology of the disease model more closely as they use cells which are isolated either freshly from an organ or from cultures of cells and tissues. These models use homogenous, characterized cells that provide an economic solution for investigating efficacy, toxicity, and physicochemical characteristics of new compounds. However, the predictive power of *in vitro* models are limited by their isolation from the true physiological setting of a living organism, as many hormonal and nutritional factors, heterogeneity, and cellular interactions are absent.[139] While it should be acknowledged that cellular models lack the complexity of animal models, *in vitro* studies are preferred for identifying lead compounds by by-passing the ethical issues and concerns associated with animal testing.[136,137] It is advised that data from *in silico* and *in vitro* studies be combined during the identification of lead compound, as they provide preliminary PK data.[140]

1.4.1 Antimalarial drug-sensitivity screening

Drug discovery and development typically involves screening a library of compounds with several modifications or variations to a scaffold, to identify new compounds that possess useful activity. For this approach to be feasible and efficient, HTS methodologies should be in place in order to ensure fast turn-around time of data between medicinal chemists and biologists. The Medicines for Malaria Venture (MMV) have created an open source drug discovery concept that allows the research community access to hundreds of unique compounds for screening of antiplasmodial activity. This “Malaria Box” of potential chemical starting points can be obtained from the MMV and can be used to investigate potential antimalarials and identify how these compounds function.[134,141]

Many different techniques and technologies have evolved to evaluate potential antimalarial compounds. *In vitro* screening of potential antimalarial compounds is the fundamental method of identifying compounds with antiplasmodial activity and is made possible through the ability to culture *P. falciparum* parasites *in vitro* in human

erythrocytes. This involves the proliferation of parasites in culture medium (CM) containing human erythrocytes, serum, and controlled atmospheric conditions, typically at 37°C under reduced oxygen concentration.[142] A variety of well-characterised drug-sensitive and drug-resistant clinical parasite isolate strains have been culture-adapted and are available from the Malaria Research and Reference Reagent Resource Centre (MR4).

New compounds are typically screened against a drug-sensitive parasite strain, such as 3D7 or D10, but should also be screened against a drug-resistant parasite strain, such as W2 or Dd2. Using both types of strains, one can determine if the compound is susceptible to cross resistance, in which resistance to one drug is extended to other drugs with similar modes of action.[143] Continuous culturing of parasite strains supports the development of antimalarial drug-sensitivity assay systems. These antiplasmodial activity screens are used to identify promising novel or improved drug candidates, their potential interactions in drug-combinations, and to assess the emergence of drug-resistant parasite strains.[144]

For decades, the gold standard assay for testing efficacy *in vitro* has been the tritiated (^{3}H) hypoxanthine uptake assay, developed in 1979 by Desjardins.[145] This assay is based on the principle that multiplying parasites require exogenous purines to incorporate into their DNA. Radiolabelled hypoxanthine is a DNA precursor that is incorporated into parasite DNA and is therefore a direct measure of parasitaemia, making it a very accurate method of determination of parasite viability.[146] Parasites are incubated with the test compounds in CM. ^{3}H-hypoxanthine is added to the wells and incubated for an additional incubation period. The cells are harvested, and the radioactive counts are measured using a scintillation counter. The 50% maximal inhibitory concentration (IC_{50}) values are determined by linear regression analyses of the resulting dose–response curves.[147]

The hypoxanthine assay is still widely used; however, it is a radioactive product and requires costly consumables, expensive instrumentation and has several steps to follow which makes it more challenging to use in a HTS environment. Furthermore, many laboratories are moving away from the use of radioactivity for the detection for parasite growth inhibition, as it adds to the complexity and cost of the assay.[95,144,148] The parasite lactate dehydrogenase (pLDH) assay, a colorimetric screening technique, was developed by Makler *et al*. in 1993.[149] This assay indirectly measures the number of viable parasites by the measuring of absorbance of formazan, a product of the metabolic reaction of pLDH by viable parasites. Although this assay is widely used for pre-clinical drug screening, it is

considered unfavourable for HTS environments, since it involves expensive reagents and multistep procedures.[149]

A low-cost alternative for determining the antiplasmodial activity is to determine the parasitaemia of treated and control parasites by counting GIEMSA-stained parasites by light microscopy. However, this method is labour-intensive and is also subject to individual variability. Even when microscopists are highly trained, variability in counting and assessing developmental stages of parasites may occur.[148]

One assay that seems to solve the issue of time and cost is the SYBR Green (SG) fluorescence-based assay developed by Smilkstein and co-workers in 2004.[150] The assay is reported to be as sensitive as the hypoxanthine assay and more suited for HTS environments due to fast results and inexpensive preparation.[147] Following incubation of parasites with candidate antimalarial compounds, the samples are incubated with SG where intercalation of the SG dye with parasite DNA occurs. As the dye intercalates with DNA, it becomes highly fluorescent, and fluorescence readings are obtained with a plate reader.[151] Although the assay is preferred in laboratory settings for the HTS of compound libraries, drawbacks such as the indiscretion of the dye between parasite and other double stranded DNA present limitations to the sensitivity of field/clinical samples where host DNA is present in white blood cells.[151]

Downstream efficacy evaluation involves *in vivo* methods which have been developed in murine models able to sustain *Plasmodium* infections. The oldest assays are those known as the 4-day suppressive test, developed for rodent malaria strains such as the *P. berghei* strain.[152] Rodent models have been used successfully for the identification of several antimalarials, for example, mefloquine and artemisinin derivatives. The investigation of efficacy in animal models have proven to be a fundamental phase in the drug discovery and development pathway, as they provide useful information on efficacy, PK relationships and host-parasite interactions.[95] The drawback of non-primate animal models are that the *Plasmodium* species that infect humans, are unable to infect non-primate animal models. The exception to this is the humanized mouse model, in which immunocompromised mice were developed to sustain a *P. falciparum* infection by means of continuous engraftment with uninfected human erythrocytes.[153]

1.4.2 Absorption, distribution, metabolism, and elimination–properties and toxicity

The importance of investigating the ADME properties and toxicity and the role these properties play in the success of new drug candidates, were highlighted in a review by Li published in 2001. These properties play an essential role in the bioavailability, metabolism and efficacy of successful drug candidates.[154] Furthermore, Kola and Landis have indicated that the major reasons for attrition of drugs in the discovery and development pipeline arises because of lack of clinical efficacy and safety.[155] Therefore, early introduction of ADME and toxicity screening during the drug discovery process is advised.[154]

Time constrained methodologies for rapid data turnaround of a large number of compounds, however, are a major challenge with regards to early screening.[156] The fact that *in vitro* assays are designed to be simple and offer HTS, comes as both an advantage and disadvantage. A disadvantage is that they do not control for, or consider, complex factors that would otherwise be observed *in vivo*. The absence of the effect and control of physiological factors such as blood flow, protein binding, and pH implies that there is no absolute correlation between the *in vitro* and *in vivo* systems. Interpretation of different assays often have interrelated relationships such as solubility, efficacy, and PK.[157] For this reason, Eddershaw *et al.* advises that *in vitro* screens should be used as a tool to rank compounds for further study, rather than for absolute rejection of potential candidates based on a single parameter.[158] The goal of ADME characterization is, therefore, to preliminarily predict *in vivo* behaviour of compounds through a variety of experimental assays. These include assays to determine physicochemical properties and biological assays using subcellular fractions, cell culture tissues, and whole organs.[156]

1.4.2.1 Absorption

The oral delivery of drugs is the favoured route of administration due to ease of administration. This creates a criterion for screening of new compounds, as absorption should be effective in order to achieve *in vivo* efficacy.[159] Passive diffusion across the intestinal epithelium driven by a concentration gradient is considered the major mechanism of absorption. Physicochemical factors of drugs that have an impact on the extent of absorption include permeability and lipophilicity, enzymatic stability,

dissolution rate, acid dissociation constant (pKa), molecular size, and affinity for transporters.[160] The gastrointestinal tract (GIT) is a complex environment and therefore many biological factors can influence absorption such as the stomach emptying rate, intestinal transit time, pre-systemic metabolism by enzymes of the GIT, and the first-pass effect of the liver.[161] The permeability of a drug cannot be accurately estimated from physicochemical factors, such as pKa, lipophilicity and solubility, alone. One of the main reasons for this is because multiple drug-transport pathways exists. An *in vitro* model is required for a more accurate representation of the intestinal mucosa. The Caco-2 cell based-assay is currently the most widely accepted model for intestinal permeability.[154] Caco-2 cells are cultured in 24-well plates and incubated with test compound to measure the uptake from the apical side to the basolateral side, which represents the intestinal lumen and blood, respectively.[162]

1.4.2.2 Distribution

For a drug to exert its clinical effect, it needs to be distributed to the relevant tissues upon absorption into the blood stream. The distribution to tissues depends on blood flow to those sites, drug solubility, and uptake into tissues. For an average adult human (70 kg),[163] the total body water is between 50–70% of body weight, which is distributed between four compartments namely: intracellular fluid (40%), plasma (5%), interstitial fluid (15%) and transcellular fluid (1%). Drugs move across epithelial barriers out of the plasma towards other fluid compartments or back into the plasma to establish equilibrium. Drug molecules exist in different compartments either bound to tissues or as unbound, free molecules, as well as in equilibrium between ionized and unionized forms. Therefore, the distribution of a drug between compartments are influenced by its physicochemical- and biochemical properties, such as the pH partition, the lipid-water partition, cell membrane permeability and the extent of protein binding within the compartments.[164]

In terms of PK parameters, the volume of distribution (Vd) is the theoretical volume reflecting the relative distribution of drugs between the plasma and tissue compartments. As the extent of distribution depends largely on the protein binding and lipophilicity of the drug, those that are mostly confined to the plasma will have a small Vd, while those that bind significantly to tissues will exhibit a large Vd.[164,165]

Exploring the plasma protein binding of a compound not only enhances our understanding of its PK profile, but also how tissue distribution, cell entry, receptor interactions, and availability for elimination influence its pharmacological effects.[166] The determination of the protein binding of a drug candidate is not a parameter by which a decision regarding a candidate's longevity is determined, but rather provides insight on its performance during *in vitro* and *in vivo* assays. Therefore, the determination of protein binding is encouraged early in drug discovery in order to aid in the understanding of distribution or mechanism of action.[166]

1.4.2.3 Metabolism

After a drug has been taken orally, it is absorbed into the bloodstream and transported to the liver via the hepatic portal vein, where it is metabolised by liver enzymes. Highly lipophilic molecules are transformed and metabolised for eventual excretion. The liver is also responsible for the inactivation of other biologically active molecules and detoxification of potentially toxic chemicals.[154,167] Typically, the parent drug is subject to transformation to more polar molecules which results in more water-soluble metabolites that can be easily excreted form the body through the kidneys or bile.

Drug metabolism can be divided into two categories. Phase I metabolism consists of enzymes from the cytochrome (CYP) P450 family. The CYP3A4 human isoform is responsible for almost 50% of xenobiotic metabolism. Phase II enzymes are responsible for conjugation of the drug or metabolite and include uridine diphosphate-glucuronosyltransferase, phenol sulfotransferase, and GSH-S-transferase. Multiple isoforms of Phase II enzymes also exists in a similar fashion to the CYP family.[154]

Metabolic stability screening is performed using liver microsomes, isolated enzymes, or isolated hepatocytes.[168] Microsomes express the major drug-metabolizing CYP enzymes and glucuronosyltransferase that are responsible for drug metabolism. For this reason, they are typically used for the determination of metabolic stability.[169]

1.4.2.4 Elimination

Drug elimination is the permanent removal of a drug from the body. The drug is either excreted chemically unchanged, or as chemically modified active or inactive metabolites. The body uses several pathways of elimination, which mainly involve the kidneys.[170] Renal excretion relies on the elimination of polarized, water soluble molecules, either unchanged or as their metabolites. If drugs are too lipophilic, they will not be excreted by the kidney and instead require modification by the liver to increase their hydrophilicity, via Phase I or II biotransformation. Following metabolism by the liver, the drug will pass through the large intestine to be excreted in the faeces. In some cases, the drug may be re-absorbed in the small intestine and distributed in the body, depending on its chemical properties. This is known as enterohepatic recirculation.[171] Other pathways of excretion include the lungs, milk, sweat, tears, skin, hair or saliva and are considered secondary processes of excretion.[172]

1.4.2.5 Toxicity

Unexpected drug toxicity is an important factor for the withdrawal of a drug from the late-stage development phases or even from market. Cytotoxicity may arise from drug-drug interactions, metabolism, or because of species or organ-specific interactions.[173] Therefore, investigation of drug toxicity is vital to the process of drug discovery.

Screening methodologies are routinely used for evaluation of toxic mechanisms in early pre-clinical studies for the guidance of chemical-structure modification by medicinal chemists. These assays mostly use tumour cell lines which contain little drug-metabolizing capacity and, therefore, reflect the compound's intrinsic toxicity. Metabolic stability screening using liver microsomes such as human hepatocytes, is preferable, however, because it enables metabolite formation and may predict *in vivo* human hepatotoxicity more accurately.[154]

1.4.3 *In vivo* animal model

Various animal models are used throughout the stages of the drug discovery pipeline. Despite the ethical concerns mentioned in section 1.4, *in vivo* evaluation in an appropriate animal model can be instrumental in combination with *in vitro* screening assays, to help

clarify *in vivo* outcomes. Animal models are very useful in describing the relationships between tissue concentrations and those in plasma or whole blood.[174] During pre-clinical characterization of efficacy and toxicity, *in vivo* models can detail the time-course relationship between plasma and drug concentrations (PK profile). These measurements can then be correlated with the time course of efficacy (pharmacodynamics).[174] Various animal species are used during these investigations and may include mice, rats, dogs or monkeys.[175] Animal models are utilized in PK investigations which can determine the concentration-time profiles, tolerable dose, drug interaction and toxicity of novel compounds during the candidate screening process.[176,177] PK studies involve taking multiple blood samples over a period of time after a dose of the drug was administered to healthy animals.[178] Compounds can be dosed singly or as part of a cassette dosing strategy, which involves the dosing of multiple compounds to a single animal. The latter method has the advantage of HTS of candidate compounds, however this method also increases the likelihood of potential drug interactions.[179] The biological samples are quantitatively analysed and the resulting PK parameters allow interpretation of the ADME properties of the drug.[178] While ADME screening is a relatively accessible *in vitro* system for studying the ADME properties of drug candidates, *in vivo* studies are still considered to deliver the most conclusive data on overall drug behaviour.[180] Furthermore, data from preclinical models are useful in describing or predicting clinical expectations. The use of mathematical tools, such as physiology based PK modelling, allows estimation of PK parameters to be attained in clinical studies.[181] The modelling of preclinical PK data together with pharmacodynamic data further enables the projection of a potential clinical dose range. These models and simulations not only aim to provide more thorough understanding of the efficacy and toxicity, but also to decrease the uncertainty of clinical outcomes and attrition of drug in downstream development.[182]

1.5 Study aim and objectives

1.5.1 Aim

The aim of this project is to identify compounds that are active and selective against sensitive and resistant strains of *P. falciparum.* Favourable compounds will have their PK evaluated in order to identify compounds with desirable properties. Lastly, further exploration in an *in vitro* combination model aims to identify favourable drug combinations with an artemisinin derivative as a partner drug.

1.5.2 Objectives

- Identify and select compounds that are active against drug-sensitive and resistant *P. falciparum* strains and which could potentiate generation of ROS and redox cycling.
- Develop and partially validate quantitative LC-MS/MS methods for the selected compounds.
- Determine the ADME drug-like properties of the compounds using the following *in vitro* assays: kinetic solubility, lipophilicity, membrane permeability, plasma stability, plasma protein binding (PPB), microsomal protein binding, and metabolic stability.
- Evaluate the intravenous and oral PK profiles of the compounds over 24 hours in a mouse model.
- Select the compound(s) with the most favourable properties for progression into *in vitro* combination analysis with an artemisinin derivative.
- Test the compounds *in vitro* for potential synergistic interaction against the NF54 drug-sensitive parasite strain.

2 Identification of potential antimalarial drug candidates

2.1 Introduction

In recent years, the effort to develop new and effective antimalarial drugs, particularly for treatment of malaria caused by *P. falciparum,* the most severe of the five *Plasmodium* parasite species that infect humans, has greatly increased. Although mortality due to infection by *P. falciparum* has steadily declined over the last decade,[79] the *P. falciparum* parasite has shown signs of developing resistance to first-line therapies.[54,79] As discussed in Chapter 1, treatment with the current first line antimalarial drugs, collectively referred to as ACTs, has experienced increased parasite clearance times which suggests emerging resistance against the artemisinin component in the combination therapy. More recently, it has been demonstrated that resistance to the partner drug in the ACT is also emerging [79,183,184]. In response to the threat of emerging resistance, the efforts to find effective, well-tolerated and high-quality drugs for use in combination therapies malaria have increased.[185,186]

To ensure that artemisinins remain effective, the new partner drugs chosen for the proposed combinations should clearly have high efficacy, fast action, and work to limit the development of resistance, by having a different mechanism of action and longer half-life.[187] Achieving the goal of malaria eradication also requires a shift in the consideration of the type of molecules considered as drug candidates. Several biological target sites have been identified within the various stages of the parasite life cycle and drugs can be designed to target those specific sites. Asexual blood stages are the logical target site, as these proliferating parasites are responsible for the clinical manifestations of the disease.[188] Furthermore, the importance of activity against sexual blood stage gametocytes that are responsible for transmission of the malaria parasites from the human to mosquito is now especially emphasized. Any drug which can block transmission of resistant parasite phenotypes for example will greatly assist in the aim of quenching the spread of resistant malaria, and eventually assist in the final task of eradicating malaria.

The drug discovery pipeline is constantly fed with new compounds. The MMV has proposed a set of target candidate profiles (TCP) which may be applied to the compound moving through the early screening phases. Although not a prerequisite, these assist in prioritization of the many leads identified during screening of compound libraries (Table 2-1).[189] Novel compounds presenting IC_{50} values in the nanomolar range (<1 μM) during

HTS against drug-sensitive and drug-resistant malaria strains, are deemed sufficiently active and are progressed to the next phase.[26,185]

Table 2-1: Overview of MMV target-candidate profiles for lead identification and prioritization during drug screens.[189]

Profile	Intended use
TCP-1	Molecules that clear asexual blood-stage parasitemia
TCP-2	Profile retired
TCP-3	Molecules with activity against hypnozoites (mainly *P. vivax*)
TCP-4	Molecules with activity against hepatic schizonts
TCP-5	Molecules that block transmission (targeting parasite gametocytes)
TCP-6	Molecules that block transmission by targeting the insect vector (endectocides)

Whilst antiplasmodial potency of any new compound is critical, its cytotoxicity against mammalian cells must be assessed in order to decide on the suitability of the compounds. As the mechanism of action of many new compounds highly active against the malaria parasite may not be known, it is important that toxicity towards mammalian cells is established, in order to ensure that these have acceptable therapeutic indices.

The strategy applied in the collaborative research project is to protect the artemisinin component by including new partner pro-oxidant compounds which, via redox cycling, maintains the level of oxidative stress induced in an incipient sense by the artemisinins.[68] The inclusion of a third partner for development of a potential TACT was also investigated, which involved derivatives of decoquinate (DQ), as their antiplasmodial activity is well established.[190] Through the addition of a long acting third partner in the combination, like DQ, any parasites remaining in circulation should be eliminated and result in reducing the risk of recrudescence.

The compounds investigated in this project were selected from five different series of derivatives prepared in the Centre of Excellence for Pharmaceutical Sciences at North-West University, South Africa and the School of Biomedical Sciences at Charles Sturt

University, Australia. Compounds were selected based on their favourable *in vitro* activity against CQ-sensitive (CQS) and CQ-resistant (CQR) strains of *P. falciparum*, and cytotoxicity against mammalian cells. The compounds are representative of several different parent compounds from which they are derived, namely phenothiazines (AD01) based on MB, phenoxazines (PhX6), artemisinins (WHN012), thiosemicarbazones (DpNEt) and quinolones (RMB005) and quinolines (RMB059 and RMB060) derived from DQ. The antiplasmodial activities against *P. falciparum* and the cytotoxicity of these compounds are presented in this chapter.

2.2 Materials

All materials used in this chapter are listed in Appendix A. Only materials of analytical grade or higher were used. Compound preparation was completed by the following institutions:

WHN012: Dr Ho Ning Wong, Centre of Excellence for Pharmaceutical Sciences, Faculty of Health Sciences, North-West University, Potchefstroom, South Africa.[191]

AD01: Prof. Jacques Petzer, Centre of Excellence for Pharmaceutical Sciences, Faculty of Health Sciences, North-West University, Potchefstroom, South Africa

PhX6 & DpNEt: Prof Chris Parkinson, School of Biomedical Sciences, Charles Sturt University, Orange, NSW, Australia.

RMB005, -059 and -060: Dr. Richard Beteck, Centre of Excellence for Pharmaceutical Sciences, Faculty of Health Sciences, North-West University, Potchefstroom, South Africa.[192]

2.2.1 Sample preparation

The preparation of all samples used in this chapter is described in Appendix A.

2.2.2 Methods

Parasite culturing methods and parasite survival assay methods are described in Appendix A.

All activity and cytotoxicity screening were completed by the Division of Clinical Pharmacology at the University of Cape Town, except for RMB005, RMB059 and RMB060 which were previously completed by Beteck *et al.*,[192,193] as referenced in Table 2-3. The author of this thesis determined the *in vitro* antiplasmodial activity of PhX6 and AD01 against the NF54 CQS *P. falciparum* parasites.

2.2.2.1 Culturing of parasites

In brief, parasite stocks obtained from MR4 were maintained at 5% haematocrit in CM and washed O+ human RBCs, according to the modified method of Trager and Jensen.[142] Cultures were kept under an atmosphere of 3% O_2, 4% CO_2, 93% N_2, and incubated at 37°C. Medium was replaced every 48 hours under sterile conditions.

2.2.2.2 pLDH metabolic assay

The pLDH assay is a metabolic method described by Makler *et al.* to indirectly determine parasite survival from a sigmoidal dose response curve.[149] Compounds were diluted in CM at the highest concentration of the dosing curve and subsequently serially diluted. A thin blood smear slide of synchronous, ring-stage CQS (NF54 *P. falciparum*) or CQR (Dd2 *P. falciparum*) parasite strains was prepared on a glass slide and fixed with methanol. The slide was rinsed and stained with Giemsa staining solution. A light microscope with an oil emersion lens (100 x objective) was used to view the slides. Parasitaemia was calculated as a percentage of the infected RBCs counted, over the total number of cells counted (500 – 700 cells). A stock culture of synchronous ring stage *P. falciparum* parasites was diluted to a 2% parasitaemia with a 2% haematocrit, using washed type O positive human RBCs in CM. The ring-culture parasites were added to the plate containing the compounds in CM which resulted in an 1% in-well parasitaemia. Plates were incubated for 72 hours at 37°C in airtight chambers and gassed with 3% O_2, 4% CO_2, 93% N_2. The parasites were exposed to the test compounds and controls for 72 hours, as this is the time window in which the parasites were expected to be in a trophozoite-dominant growth phase. Trophozoite stage parasites are required during the endpoint analysis, as this growth phase is much more metabolically active than ring stage parasites. Plates were frozen at -80°C and thawed to kill all surviving parasites. Each well of the plate was supplemented with Malstat reagent; containing acetylpyridine adenine dinucleotide (APAD) and lactate; and nitroblue tetrazolium (NBT) reagents. The pLDH from infected cells oxidize lactate to pyruvate in the presence of APAD+, which is subsequently reduced to APADH. The yellow NBT is reduced to a purple formazan salt by APADH which was measured spectrophotometrically at 620 nm. The data was used to generate a sigmoidal dose-response curve from which the IC_{50} was calculated. Experiments were repeated at least three times on three separate occasions. The viability of the assay was determined at each end point through the comparison of calculated IC_{50} values of the two positive controls

(CQ, 7-21 nM; AS, 5-10 nM, based on in-house data for NF54). Secondly, it was expected that the wells containing only parasitized RBCs would have increased in parasitaemia and thus result in a significant reduction of the NBT. The assay was considered to have 'failed' when the IC_{50} of either of the control compounds fell outside the suggested range or if weak formation of the purple formazan salt was observed in the parasitized RBC control wells. This could be due to many experimental factors, including underestimation of starting parasitaemia, incorrect or insufficient gassing of the chambers or in the case where a gassing chamber leaked.

2.2.2.3 Maintenance of mammalian cell lines

Cellular growth is monitored consistently to obtain high quality cultures. Confluency is reached when 80% of the culture flask surface is covered with cells. At this point the culture is ready for subculturing in fresh medium or for seeding into plates for assays.[194] Confluency of the Chinese Hamster Ovarian (CHO) cells was observed under a light microscope (40 x objective). Upon confirmation, cells were detached using trypsin and washed with CM. The pellet was transferred to a new sterile flask containing CM and incubated at 37°C with 5% CO_2. The medium was replaced after 48 hours.

2.2.2.4 Cytotoxicity screening assay

The quantitative colorimetric assay described by Mosmann, was used to determine the survival of mammalian cells.[195] Briefly, mammalian cells were prepared at a concentration of 105 cells/mL in CM and added to a sterile 96-well plate. Plates were incubated for 24 hours at 37°C with 5% CO_2 to allow the cells to attach. Compounds were serially diluted in CM and added to the cells. Cells were exposed to the compounds for 48 hours at 37°C. A solution of 3-(4,5-dimethylthiazol-2-yl)-2,5-diphenyl tetrazolium bromide (MTT) was added to each well. Plates were left to develop in the dark, as the MTT is light sensitive. After MTT is reduced to its formazan salt by active mitochondria in viable cells. Dimethyl sulfoxide (DMSO) was added to dissolve the formazan crystals and absorbance was measured at 570 nm. The data was used to generate a sigmoidal dose-response curve from which the IC_{50} was calculated. Cytotoxicity was ranked in three levels of toxicity: high toxicity, IC50 values <10 μM; moderate toxicity, IC50 values 10 – 100 μM or low toxicity, >100 μM.

2.2.3 Calculations

The ability of the given compound to selectively kill *P. falciparum*, was determined by calculation of the selectivity index (SI).[196] The SI is the ratio of the cytotoxicity to the antiplasmodial activity; this indicates whether a compound is selectively toxic to the parasites, and does not induce non-specific killing of healthy tissues (Equation 2-1). A compound with a SI value >10 is considered acceptable for progression to animal experiments.[197]

Equation 2-1: Determination of selectivity index

$$\boldsymbol{SI = \frac{Cytotoxicity\ IC_{50}}{Efficacy\ IC_{50}}}$$

The resistance index (RI) is the ratio of the activity against CQR parasites to that of CQS parasites (Equation 2-2).[198] This ratio indicates the susceptibility of a compound to develop cross-resistance with other drug resistant strains.[199] The RI can vary greatly between parasite strains and a lower RI does not necessarily indicate lower resistance, as the therapeutic response in vivo is much more complex. A RI value <10 indicates intermediate resistance, while a value above that is typical of drug resistance.[200]

Equation 2-2: Determination of resistance index

$$\boldsymbol{RI = \frac{Drug\ resistant\ strain\ IC_{50}}{Drug\ susceptible\ strain\ IC_{50}}}$$

2.3 Results and discussion

2.3.1 Determination of antiplasmodial activity against *Plasmodium falciparum* parasites

Five structurally diverse compound series were previously screened for antiplasmodial activity. The IC_{50} values of the compounds mentioned above were assessed against asexual blood stages of the CQS NF54 and CQR Dd2 or K1 strains of *P. falciparum*. From a total of 138 compounds, seven were determined as suitable candidates for further investigation based on their high antiplasmodial activity (Table 2-2). These compounds include the amino-artemisinin WHN012, the phenothiazine AD01, the phenoxazine PhX6, the thiosemicarbazone DpNEt, and derivatives derived from decoquinate, namely the

decoquinate amide RMB005 and the quinoline ethyl ester carbamates RMB059 and RMB060.

Antiplasmodial potency below 100 nM was observed in both the CQS NF54 strain (1.2 nM to 41.8 nM) and CQR Dd2 and K1 strains (1.4 nM to 64.8 nM) (Table 2-3). The highest activity was seen for WHN012, RMB059, and RMB060 against the CQS NF54 strain (1.2 nM, 6.9 nM and 1.5 nM, respectively) and for AD01, WHN012, and RMB060 against the CQR Dd2 or K1 strain (11.9 nM, 9.2 nM and 1.4 nM, respectively). Antiplasmodial activity of each compound is discussed in more detail below.

Table 2-2: Compounds selected for this study.

Compound	**Classification**	**Molecular weight (g/mol)**	**Formula**	**Structure**
WHN012	Amino artemisinin	489.6	$C_{26}H_{36}FN_3O_5$	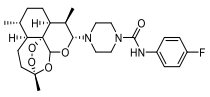
AD01	Phenothiazine	340.5	$C_{20}H_{26}N_3S$	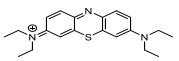
PhX6	Phenoxazine	394.5	$C_{25}H_{22}N_4O$	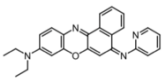
DpNEt	Thiosemicarba-zone	285.4	$C_{14}H_{15}N_5S$	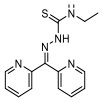
RMB005	DQ amide	476.6	$C_{26}H_{40}N_2O_6$	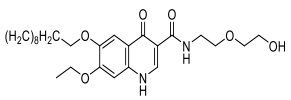
RMB059	Quinoline ethyl ester carbamate	530.6	$C_{29}H_{42}N_2O_7$	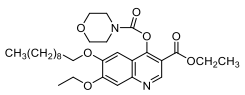
RMB060	Quinoline ethyl ester carbamate	607.7	$C_{29}H_{41}N_3O_9S$	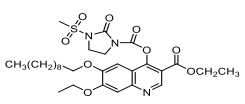

Table 2-3: Antiplasmodial and cytotoxicity values of the selected compounds, parent compounds, and controls.

Compounds	*P. falciparum* IC_{50} (nM)[a]			Mammalian cell toxicity[b] (μM)	Resistance Index[c]	Selectivity Index[d]	
	NF54	Dd2	Other			CHO/sensitive *Pf* strain	CHO/resistant *Pf* strain
WHN012	1.2 ± 0.04	9.2 ± 1.9		>204 ± ND	7.6	>1000	>1000
AD01	23.1 ± 2.5	11.9 ± 2.8		74 ± 9.4	0.5	>1000	>1000
PhX6	41.8 ± 0.04	16.2 ± 2.4		192 ± 4.6	0.4	>1000	>1000
DpNEt	40.7 ± 1.4	28.6 ± 4.0		11 ± 4.2	0.7	270	384
RMB005	40.4 ± 1.3[h]		64.8 ± 7.2 (K1)[h]	> 21 ± ND	1.9	528	326
RMB060	1.5 ± 0.5[i]		1.4 ± 0.6 (K1)[i]	> 88 ± ND	0.9	>1000	>1000
RMB059	6.9 ± 3.9[i]		14.4 ± 6.3 (K1)[i]	> 188 ± ND	2.1	>1000	>1000
CQ[e]	9.9 ± 0.4	142 ± 16.8		nd	14.3	nd	nd
AS[e]	6.9 ± 1.4	18.1 ± 7.1		>354 ± ND[f]	2.6	>1000	>1000
DHA[f]	0.8 ± 0.1	5.7 ± 2.0		25.2 ± 3.7[f]	7.1	>1000	>1000
MB[g]			3.6 ± 2.2 (D6) 3.9 ± 2.3 (W2)	52.6 ± 4.5[f]	1.1	>1000	>1000
DQ	26.6 ± 1.4[h]		64.9 ± 8.8 (K1)[h]	>100 ± ND[j]	2.4	>1000	>1000
Emetine[k]	nd	nd		0.1 ± 0.002	nd	nd	nd

[a] Values are mean ± standard deviation (n = 3), [b] CHO cells, mean ± standard deviation (n = 3), [c] Resistance index = IC_{50} (resistant strain)/ IC_{50} (sensitive strain), [d] Selectivity Index = Cytotoxicity IC_{50}/Activity IC_{50}, [e] Positive control for antiplasmodial assays, [f] Value from reference (Coertzen *et al.*, 2018), [g] Value from reference (Vennerstrom *et al.*, 1995), against drug-sensitive D6 and drug resistant W2 parasites, [h] Value from reference (Beteck *et al.*, 2016), tested against drug-sensitive NF54 and resistant K1 parasites, [i] Value from reference (Beteck et al., 2018), tested aganst drug-sensitive NF54 and resistant K1 parasites [j] Cytotoxicity against WI-38 cell line of normal human fetal lung fibroblast (HFLF), [k] Positive control for cytotoxicity assays, nd = not determined; AS, artesunate; CQ, chloroquine; DHA, dihydroartemisinin; DQ, decoquinate; MB, methylene blue. Results shown are the mean IC_{50} values and SD from at least three independent experiments.

2.3.1.1 WHN012

Artemisinins as oxidant drugs were previously discussed in Chapter 1. New derivatives have exhibited potent *in vitro* activity and improvement of safety profiles.[201] Moreover, they are known to have useful biological activities in other therapeutic areas such as anti-HIV therapy,[202] immunosuppression,[203] anticancer[204] and antitubercular activity.[205] In effort to develop more stable and economic preparations from artemisinins, as discussed in the literature review, a series of DHA-piperazines were prepared by Haynes *et al*. with demonstrated efficacy and economic preparation.[206] Further conversion of this series further aimed to optimise DHA-piperazines which provided the aryl urea derivatives, discussed here.

WHN012 (Figure 2-1), presented pronounced activity against the CQS NF54 parasites (1.2 nM) and CQR Dd2 parasites (9.2 nM). An approximate eight-fold loss of activity in the CQR strain was observed and a RI value of 7.6 was calculated. Application of the two-tailed unpaired t test revealed a statistical significance between activity in CQS and CQR parasite strains (P=.0019, N = 3, t = 7.2912). Despite this, WHN012 was still a candidate of further development, as its activity is arguably in the low nanomolar range, which is similar to the parent compound DHA. A parallel RI value of 7.1 was calculated for DHA.[207] As the RI of WHN012 suggests potential cross resistance to CQR strains, the extent thereof should be investigated in other multidrug-resistant strains, specifically those resistant to artemisinins. WHN012 presented an IC_{50} of >204 μM and therefore had selective inhibition of CQS and CQR parasites (SI >1000). WHN012 was not expected to show toxicity and was therefore suitable to progress to *in vivo* animal experiments.

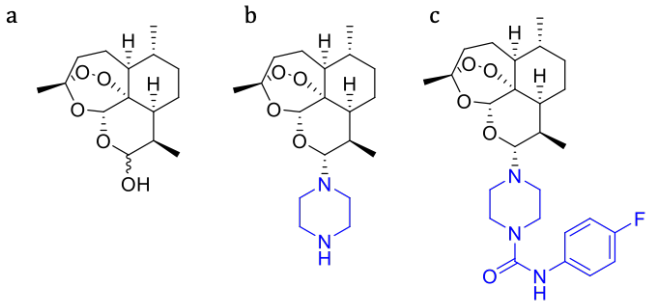

DHA	DHA-piperazine	WHN012
NF54 IC_{50}: 0.8 nM	NF54 IC_{50}: 3.2 nM	NF54 IC_{50}: 1.2 nM
Dd2 IC_{50}: 5.7 nM	Dd2 IC_{50}: 1.7 nM	Dd2 IC_{50}: 9.2 nM

Figure 2-1: Structures of DHA, the DHA-piperazine derivatives derived from DHA, and the arylurea derivative WHN-12 derived from DHA-piperazine.[207]

DHA is the metabolite common to all artemisinin analogues registered for clinical use. However, high doses have been found to cause neurotoxicity which limit their use.[208,209] Derivatization of DHA by replacing the hydroxyl group at C-10 by other groups incapable of providing DHA on metabolism is encouraged in an effort to improve the overall stability of the artemisinins.

The thermal instability of DHA itself poses problems during formulation and storage, as investigated and discussed by Ng *et al.*, 2007.[210] Further investigation of various derivatives derived from the C-10 amino derivative DHA-piperazine (Figure 2-1)[207] revealed remarkable early and late stage gametocytocidal activity. WHN012 presented nanomolar activities against early stage (IC_{50} 36.0 ± 10.2), as well as late stage (IC_{50} 17.0 ± 7.0) NF54 gametocytes satisfying both TCP-1 and TCP-5 criteria (Table 2-1).[191] WHN012 was therefore selected based on the high potency towards asexual blood stage parasites and sexual gametocytes.

2.3.1.2 AD01

MB is an example of a phenothiazinium salt and is the oldest known synthetic antimalarial compound with its first use reported in 1891.[211] AD01 is a derivative of MB in which the methyl groups of MB are replaced with ethyl groups (Figure 2-2). Thus, the compound is expected to be more lipophilic than MB. Many theories regarding the mechanism by which MB exhibits its antiplasmodial activity have been postulated.[125,127,128,211] One such mechanism is the ability of MB to undergo redox cycling,[212] as described in Chapter 1. Thus, AD01 is very likely to undergo redox cycling.

AD01 was considered a viable candidate for further investigation, based on its antiplasmodial activity in the low-nanomolar range against both CQS NF54 (23.1 nM) and CQR Dd2 (11.9 nM) parasite strains (Table 2-3). The activity of AD01 lies within the range similar to that recorded for phenothiazine derivatives by Vennerstrom *et al.* The activity of MB was recorded as 3.6 nM against the CQS D6 strain and 3.9 nM against CQR W2 strain of *P. falciparum*.[199] Calculation of the RI for MB indicated that there was no observable shift in activity towards CQR parasites (RI 1.1) and the SI indicated selective inhibition towards parasite development (SI >1000). While the RI value was <1 for AD01, antiplasmodial activity was comparable between the CQS NF54 (32.1 nM) and CQR Dd2 strain (11.9 nM). AD01 did not have significant cellular toxicity (74 µM) and demonstrated selective inhibition of CQS and CQR parasites (SI >1000). AD01 was considered a suitable candidate for *in vivo* studies as the SI values surpassed the threshold considerably.

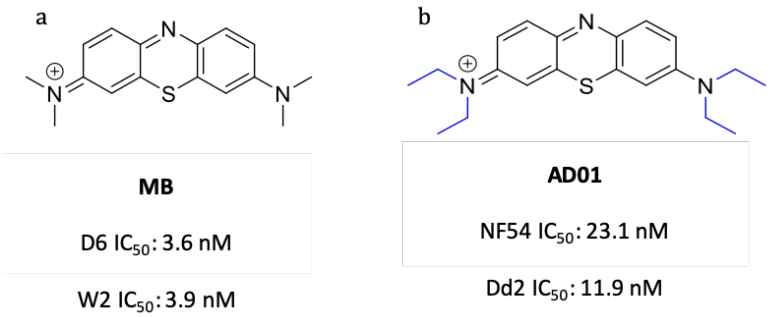

Figure 2-2: The structures of (a) parent compound MB and (b) the derivative AD01. The difference between MB and AD01 are highlighted in blue.

2.3.1.3 PhX6

The phenoxazine class of compounds are heterocyclic compounds with an oxazine fused to two benzene rings and found to be naturally present in insect pigments, mold metabolites and actinomycins.[213] The first simple angular benzo[alpha]phenoxazine was first reported by Goldstein and Semelicht in 1919.[214] Phenoxazine derivatives have reportedly diverse biological activities including antimycobacterial activity,[215] antitumor activity,[216] and antiprotozoal activity.[217] Their mechanism remains poorly understood, but it is postulated that the nitrogen group is able to undergo reduction in redox reactions, resulting in ROS production.[218]

The structure of PhX6 bearing a benzene ring fused to the phenoxazine nucleus is referred to as a benzo[α]phenoxazine (Figure 2-3). PhX6 was more active against the CQR strain Dd2 (16.2 nM) than the CQS strain NF54 (41.8 nM), with an RI value of 0.4. Statistical significance was observed between antiplasmodial activity in CQS and CQR parasite strains (unpaired t test, $P<0.001$, N = 3, t = 18.4726). PhX6 had an IC50 of 192 µM against the CHO mammalian cells, denoting that it selectively targets the parasites with SI values of >1000 for both CQS and CQR parasite strains.

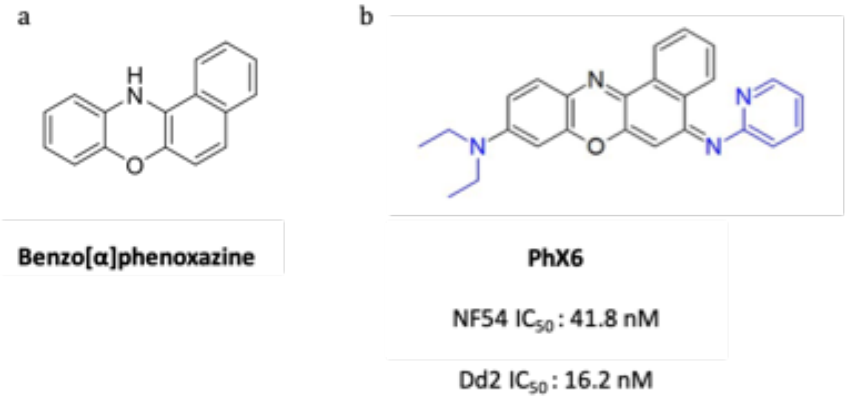

Figure 2-3: The structures of a) the benzo[α]phenoxazine scaffold and b) the derivative PhX6. The differences between PhX6 and the benzo[α]phenoxazine nucleus are highlighted in blue.

Various benzo[α]phenoxazines were demonstrated by Katsamaks *et al.*, to display activities *in vitro* in the low-nanomolar range against drug-sensitive and drug-resistant *P. falciparum* .[219] Follow-up work conducted by Ge *et al.*, identified one such derivative SSJ-

183 (Figure 2-4) with close structural resemblance to PhX6, which displayed nanomolar activity against the CQR *P. falciparum* K1 strain (IC_{50} 7.6 nM) and high selectivity when tested against L6 myoblastoma cell lines (IC_{50} 55.7 μM, SI >1000).[220] Administration of this benzo[α]phenoxazine derivative in a *P. berghei* mouse model cured infected mice after three daily oral doses of the compound. The researchers concluded that these benzo[α]phenoxazines are promising compounds for further investigation as new drug candidates.[220]

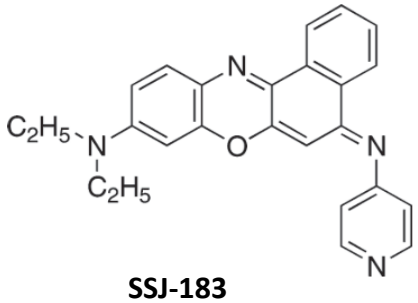

SSJ-183

NF54 IC_{50}: 11.0 nM
K1 IC_{50}: 7.6 nM

Figure 2-4: The structures of the benzo[α]phenoxazine derivative SSJ-183.[221]

2.3.1.4 DpNEt

Thiosemicarbazone derivatives such as DpNEt (Figure 2-5), have been examined as anticancer molecules.[222,223] This class of compounds are modified from the oxygen-containing semicarbazide.[224,225] As these compounds are able to chelate intracellular metal ions, Richardson *et al.* hypothesized the potential mechanism of their biological activity as being able to generate free radicals by forming redox-active iron complexes from intracellular iron.[222] This mechanism will prove useful as an antimalarial therapy and new combination therapies, since the disruption of parasitic redox homeostasis is a key aspect of this research approach. DpNEt presented nanomolar potency against the CQS NF54 and CQR Dd2 parasites (40.7 nM and 28.6 nM, respectively). DpNEt had a lower IC_{50} of 11 μM against the CHO cells. The IC_{50} was not problematic as the calculated SI values remained appreciably above the threshold of suitability for animal studies (270 and 384 for CQS and CQR parasite strains, respectively). Furthermore, the cytotoxicity was nearly 100-fold lower than that of control compound emetine (0.1 μM). However, this

should be closely monitored in future compound optimisation studies of this series, as toxicity could present in other toxicity models, for example, the hERG model.

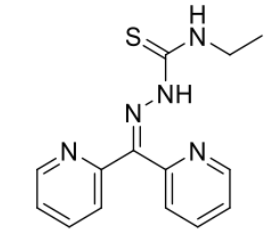

DpNEt

NF54 IC_{50}: 40.7 nM

Dd2 IC_{50}: 28.6 nM

Figure 2-5: The structure of DpNEt

2.3.1.5 RMB005, RMB059, and RMB060

DQ, a carboxyquinolone, was first described in 1968[226] and is a widely-used coccidiostat in various animal species with an acceptable food safety profile.[227] Its mechanism of action against malaria parasites is through the selective inhibition of the plasmodial mitochondrial *bc* (1) complex.[228] DQ was converted by Beteck *et al*. into the derivatives RMB005, RMB059, and RMB060 (Figure 2-6).[192] DQ showed low nanomolar *in vitro* activities against CQS NF54 asexual parasites (26.6 nM),[193] as well as strong potency against liver and sexual gametocyte stages of the *P. falciparum*. While DQ showed limited cross-resistance to atovaquone resistant parasites and prophylactic efficacy as a single oral dose,[229,230] its instability, low aqueous solubility, and high lipophilicity renders DQ a less favourable drug to apply to the drug development cascade.[193,231] In the review by Beteck *et al.*, the authors acknowledge that DQ is very affordable and satisfies several MMV TCP criteria (TCP-1, 4, and 5) for malaria eradication. However, optimization is needed with regards to its physiochemical properties.[231] The aims of recent studies were to generate new derivatives of DQ which have enhanced metabolic stabilities and solubilities.[192,193]

The ethyl ester group in DQ was replaced by a secondary amide group to yield the amide derivative RMB005 (Figure 2-6b). RMB005 presented similar antiplasmodial activity against CQS NF54 (40.4 nM) and CQR K1 (64.8 nM) *P. falciparum* parasites compared to the parent compound DQ (26.6 nM in CQS NF54 and 64.9 nM in CQR K1).[192] An RI of 1.9 was calculated for RMB005 against K1 parasites. Similarly, an RI of 2.4 was calculated for the parent compound DQ, against the resistant K1 strain. While the three RMB compounds were analysed using the SYBR green-I assay, a comparative study by Zhang *et al.* has shown that antiplasmodial data from this assay and the pLDH assay are not statistically different.[232] RMB005's antiplasmodial values are comparable to artesunate (RI 2.6) and indicate lack of susceptibility to cross resistance. However, further investigation is required against other multiple drug resistant strains to determine the susceptibility of the quinolones to cross resistance. RMB005 was included in this study to investigate potential improvement of *in vivo* physiochemical properties of the parent compound DQ.

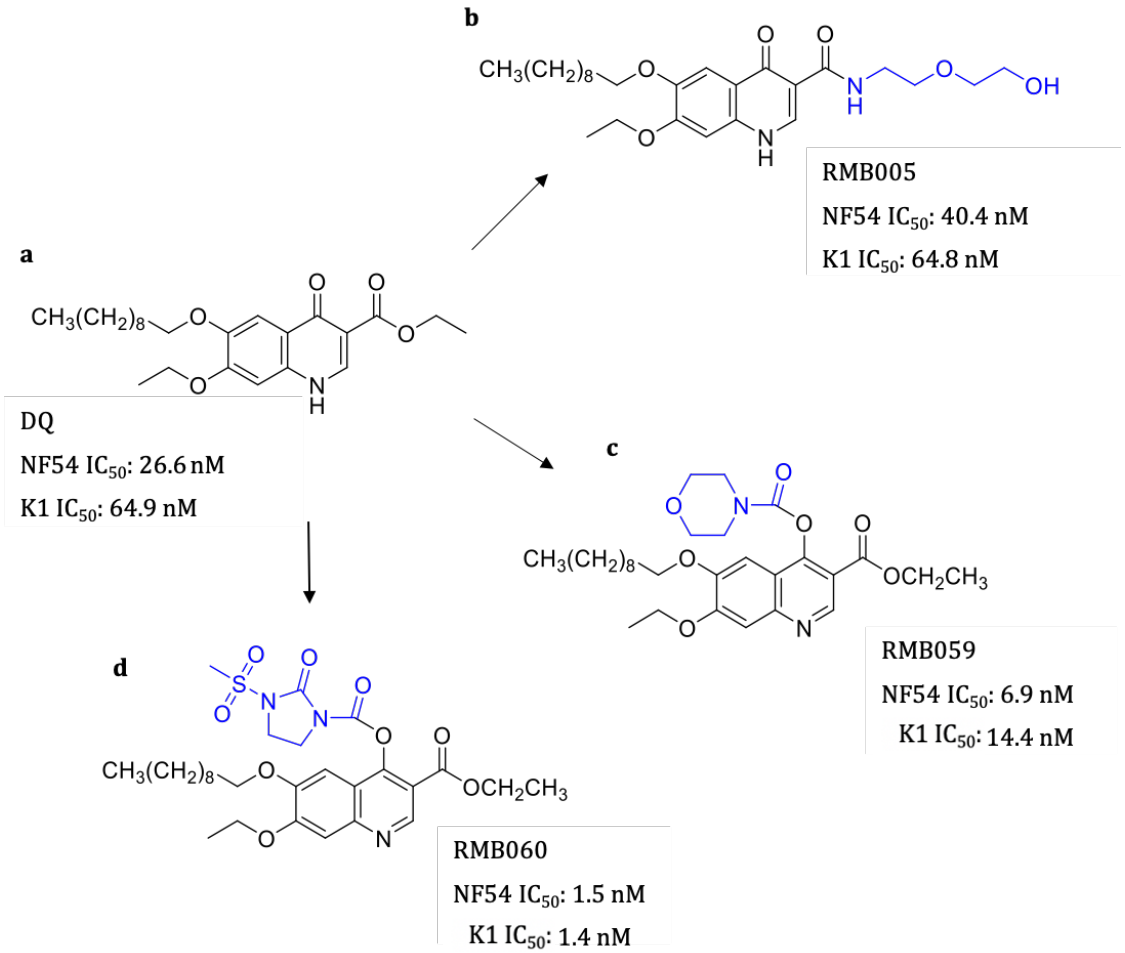

Figure 2-6: The structures of parent compound DQ and derivatives with IC_{50} data against CQS NF54 and CQR K1 *P. falciparum*. Modifications to the original molecule are

illustrated in blue to yield the DQ amide derivative RMB005 and the quinoline ethyl ester carbamate derivatives RMB059 and RMB60.

RMB059 and RMB060 are quinoline ethyl ester carbamate derivatives of DQ (Figure 2-6c and d). Beteck *et al.* modified the parent compound by addition of side chains to the quinolone nucleus, in an effort to potentially increase the extent of exposure *in vivo* through improved absorption.[232] RMB059 and RMB060 presented low nanomolar activities of 6.9 nM and 1.5 nM respectively against CQS *P. falciparum* strain NF54. These compounds have superior activity profiles to DQ, and similar potency to CQ and artesunate in the CQS NF54 strain. The activity of RMB059 and RMB060 to CQR K1 strain was 14.4 nM and 1.4 nM, respectively. The RI of RMB060 of < 1 indicates no cross-resistance against CQR strains. RMB059 had an RI of 2.1, which may be an indication of potential cross resistance to CQR strains. However, the value is still within acceptable range in comparison to artesunate (RI = 2.6). Further studies by Beteck *et al.* showed that RMB059 and RMB060 presented 20–40% inhibition of early and late stage NF54 gametocytes during single concentration experiments and therefore both satisfy MMV TCP-5 (Table 2-1).[192] This property is especially beneficial if more than one partner drug in triple-combination therapy presents activity against sexual stages and could potentially augment transmission blocking. The mammalian cytotoxicity IC_{50} values of RMB005 (>21 μM), RMB059 (>88 μM) and RMB060 (>188 μM) were used to calculate the SI values. Overall, the compounds showed selective inhibition of the CQS NF54 *P. falciparum* strain (SI >528) as well as the CQR K1 *P. falciparum* strain (SI >384), indicating that they are suitable candidates to progress to animal studies.

2.3.2 Cytotoxicity and selectivity of highly active compounds

All the potent compounds were subject to cytotoxicity screening assays against the CHO cell line. The high micromolar IC_{50} ranges for all seven compounds indicated no significant cellular toxicity (Table 2-3) and all compounds had substantially higher IC_{50} values than the control, emetine (IC_{50} = 0.1 μM). Furthermore, selectivity indices showed all seven of the compounds selectively inhibited the malaria parasite, as demonstrated by the high SI values (Table 2-3). This ratio is vitally important for enabling the progression of compounds to further *in vivo* studies. *In vivo* PK studies will be conducted for all seven compounds, as the SIs are above the minimum required value of 10 for the parasite strains tested (NF54 and Dd2/KI).[199]

2.4 Summary and conclusions

A small diversity-oriented library was screened for antiplasmodial activity. Seven structurally diverse, highly active compounds (IC_{50} <1 μM) which lack nonspecific inhibition of mammalian cells were selected from this screening. The ultimate aim was to discover new partner compounds for use in ACTs. The compounds PhX6, AD01, DpNEt, WHN012, RMB005, RMB059, and RMB060 were selected based on their nanomolar antiplasmodial activity in CQS and CQR strains of *P. falciparum* and their lack of non-specific cellular toxicity in mammalian CHO cells. The RIs of all compounds were found to be below that of CQ (0.4 – 7.6), which indicate low susceptibility of cross resistance. The RI values of PhX6, AD01, DpNEt, RMB005, RMB060, and RMB059 were below that of artesunate (<2.6).

Future work will include extensive screening to investigate multiple drug-resistant and artemisinin-resistant strains to further determine the potential of cross-resistance and viability as potential drug candidates.

The ambition of the MMV is to discover novel compounds that will maintain the continuous development process of effective malaria therapies which will support the ultimate eradication of malaria. They have compiled TCP criteria to aid researchers in identification of lead compounds. All compounds selected comply with TCP-1, at minimum, which requires all compounds to be active against asexual blood stage parasites (Table 2-1). Additional results obtained for WHN012 and RMB060 indicate that the compounds show both early- and late-stage gametocytocidal activity.[191,192] WHN012 and RMB060 thus also comply with TCP-5, which specifies transmission-blocking activity by targeting parasite gametocytes (Table 2-1).

The compounds belonging to the RMB class are novel derivatives of an existing antimicrobial drug DQ, whose physiochemical properties are expected to have been improved by chemical modification. Similarly, AD01 is a more lipophilic analogue of MB and is expected to show poorer solubility and absorption. Although great emphasis is placed on the potency of antiplasmodial compounds, the need for suitable physiochemical properties should also be stressed, as aqueous solubility and lipophilicity may aid in the interpretation of activity data and determination of drug-like properties. Further

investigation will determine their *in vitro* physiochemical and *in vivo* PK properties. The evaluation of these properties is discussed in the following chapters.

3 Physicochemical and biochemical characterization of biologically-active compounds

3.1 Introduction

The antiplasmodial activity and toxicity of seven compounds, namely the amino-artemisinin WHN012, the ethyl analogue AD01 of MB, the phenoxazine PhX6, the thiosemicarbazone DpNEt, and the decoquinate derivatives RMB005, RMB059, and RMB060 which were selected for this project have been discussed in the previous chapter. For convenience, the structures of the compounds to be examined here are given in Figure 3-1. As all compounds have promising biological activities *in vitro* (Table 2-3), it is essential to establish suitability for taking these compounds forward by assessing their physicochemical properties with respect to drug development.

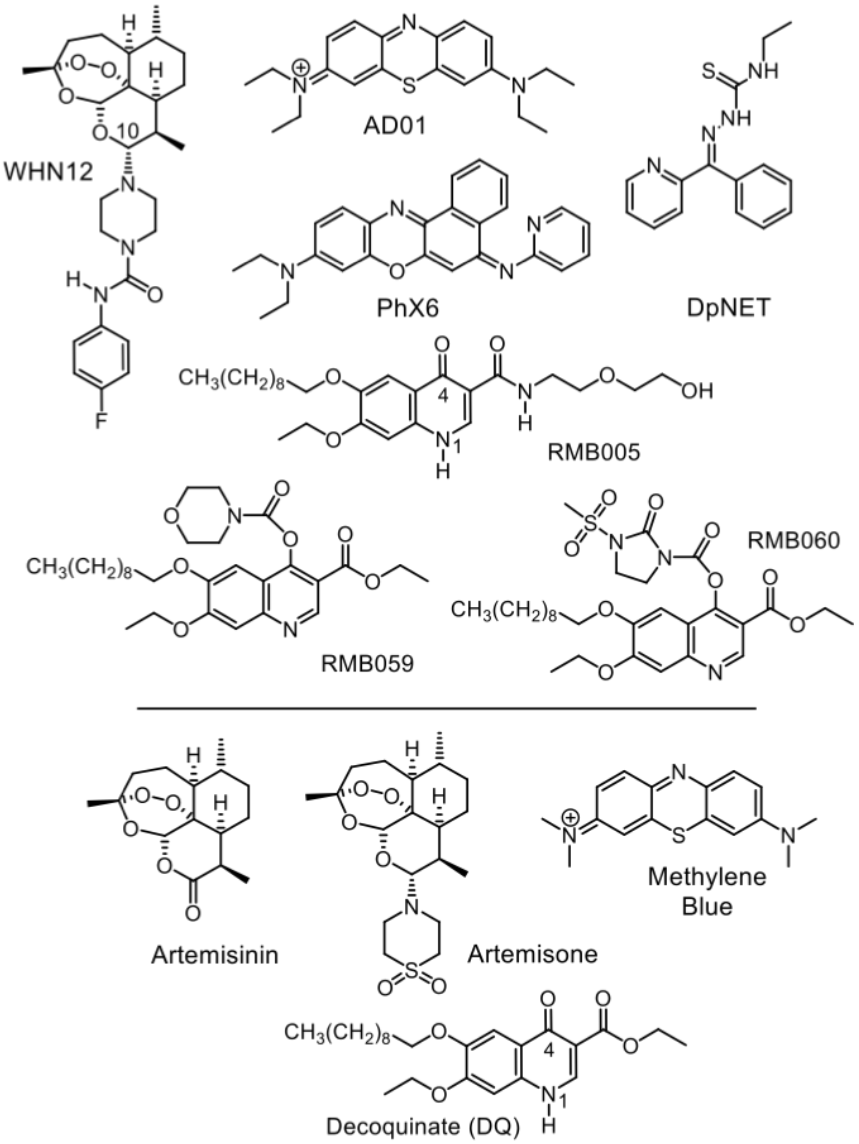

Figure 3-1: Structures of compounds selected for evaluation of physicochemical and biochemical properties required to establish their suitability as drugs, and their comparator compounds, where applicable.

In drug discovery, screening of the biological activity of compounds is followed by assessment of their ADME properties. Then, depending upon these properties, certain compounds may be selected for conducting PK studies in animals.[233]

Most drugs are administered orally and must overcome physiological barriers to reach pharmacological targets so as to exert their therapeutic effects. The early investigation of ADME properties enables acquisition of incipient knowledge that will help to indicate how the *in vitro* potency of the compounds will translate to *in vivo* efficacy. This information is not only important for the structural design and modification of new compounds, but it also enables an assessment of the viability of new compounds in a drug development programme and whether these should be taken forward for further investigation.[155]

Within the context of this project, ADME properties of the biologically active compounds were investigated with various assays that simulate the physiological environments to which the drugs might be exposed *in vivo*, as discussed in Chapter 1. *In vitro* assays included assessment of solubility; permeability; lipophilicity; plasma and metabolic stability; and protein binding. The ADME assays were conducted in parallel to the *in vivo* PK assays in order to gain an appreciation of the PK profiles in a living model.

3.1.1 Solubility

Solubility may be broadly defined as the amount of a substance that dissolves in a volume of solvent.[234] A kinetic-solubility assay was used to determine the aqueous solubilities of the compounds in buffer solutions with pH's ranging between 2–7.4, which closely relates to assay conditions in pre-clinical investigations. Investigation of solubilities may also provide insight into how well the drug may be absorbed at the various pH values of the gastrointestinal tract (GIT).[140,235]

The aqueous solubility, among other physicochemical properties of a compound, determines if a molecule will be delivered to, and interact with, the pharmacological target.[140,236] Consequently, compounds should be soluble within the physiological pH range. Solubility is a key parameter that enhances bioavailability (BA) of orally administered drugs. A compound that displays high activity *in vitro*, but has a low solubility may elicit problems in the later stages of drug development.[140,236]

3.1.2 Lipophilicity

The affinity of a compound for a lipid or aqueous environment is determined by the lipophilicity assay, which is expressed as a distribution coefficient (LogD) of a compound between 1-octanol and an aqueous buffer.[140] LogD is an important parameter as it significantly impacts ADME properties and gives valuable insights into structure-activity and structure-property relationships.

In conjunction with solubility, the extent of lipophilicity will affect permeation across cellular membranes. Absorption, distribution, and BA of a drug is greatly influenced by its distribution between polar and non-polar environments.[237] Thus, crossing of epithelial cells of the intestinal lumen and the lipid bilayer of RBCs requires optimal lipophilicity.[7,238]

LogD values between 1–3 are considered ideal for gastrointestinal absorption via passive permeation and have the potential to increase oral BA. Values below 1 indicate the compounds may be too hydrophilic and this could limit absorption from the GIT, while values >3 indicate the compounds are highly lipophilic. For such compounds, tissue binding becomes a problem.[237,239]

3.1.3 Permeability

Apparent permeability (P_{app}) is determined by the parallel artificial membrane permeability assay (PAMPA), which was first introduced by Kansy *et al.*[240] The assay provides an *in vitro* model for passive diffusion and assists in the interpretation of drug absorption. The assay essentially measures the movement of the drug from a donor to an acceptor chamber, through an artificial hexadecane membrane.[240] In order for a drug to be absorbed and reach a pharmaceutical target, it should be able to cross the membranes of physiological barriers such as those found in the gastrointestinal wall during absorption from the GIT and diffusion across lipid membranes of RBCs.[238]

Movement across cells can occur either by paracellular or transcellular transport. The former involves movement of small molecules between tight junctions of adjacent cells and does not require energy or specific transporters.[241] The latter occurs either by passive transport, which utilizes a concentration gradient, or an active transport mechanism

which requires energy.[240] The relationship between permeability, solubility and lipophilicity greatly influences intestinal absorption and ultimately BA.[140,242]

3.1.4 Plasma stability

Plasma stability of the compounds is determined by incubating a single concentration of compound and measuring the signal intensity over time. The test samples are compared to freshly prepared reference samples, to determine the percentage remaining after the incubation period. The plasma stability was expressed as a half-life which was calculated from the percentage remaining. Drug metabolism can occur in the liver, GIT, or by enzymes present in the plasma.[243] The stability of a compound in whole blood or plasma is an important parameter to consider during drug development, as it can contribute to rapid clearance and short half-lives, resulting in poor *in vivo* performance. Ultimately, poor plasma stability will lead to low concentrations and decreased *in vivo* efficacy.[140,243]

3.1.5 Plasma protein binding

Protein binding influences the distribution, metabolism, and elimination of a compound and considered to be one of the sources of complexity that is integral to the *in vivo* system.[244] Increased importance is placed on PPB in describing PK/PD relationships. The free-drug theory states that only free, unbound drug (f_u) in plasma is available to interact with, and elicit an effect on, the pharmacological target; and should reflect the pharmacologically relevant concentration of unbound drug in tissue.[245]

Drug exposure at the target site is impacted by highly protein bound drugs and this will also impact the interpretation of *in vivo* pharmacodynamic data required to establish PK/PD relationships.[244] Furthermore, undesired non-specific PPB may result in drug displacement when more than one drug interacts with plasma proteins.[246] The extent to which compounds bind to proteins is determined by their structure and physicochemical properties.[244] The most abundant of these proteins are human serum albumin (HSA) and globulin protein, alfa-1 acid glycoprotein (AAG).[247] Acidic drugs, like atovaquone, and neutral drugs bind to albumin while basic drugs like quinine, AM, and primaquine bind to AAG.[247,248] PPB is, thus, an important parameter in relation to toxicity and drug-drug interactions.

3.1.6 Microsomal protein binding

The extent of binding to microsomal proteins is important for prediction of *in vivo* clearance. The intrinsic clearance is the rate at which the liver is able to irreversibly remove a drug from the circulation–excluding the effects of protein binding or flow limitations. Within an *in vivo* system, the free drug equilibrates between the plasma and hepatocyte cytosol and this allows the drug to enter the liver and exposes it to the drug metabolising enzymes. Most drugs are lipophilic, organic compounds and are subject to non-specific binding to the lipid-protein milieu of the microsomal membrane.[249] Therefore, investigation of the extent of microsomal binding results in more accurate predictions of *in vivo* clearance.[250]

3.1.7 Metabolic stability

The metabolic stability of compounds is determined using mouse and human liver microsomes. Homogenised liver tissue is centrifuged to produce a supernatant (S9 fraction) and pellet containing mitochondria and lysosomes. Further centrifugation of the S9 fraction forms a pellet which contains remnants of the cellular endoplasmic reticulum. During this process, spheres of membranes called microsomes are formed in the presence of calcium. As such, microsomes are considered artefacts of hepatic subcellular fraction preparation, but are fundamental for understanding hepatic clearance *in vitro* as they contain all membrane bound proteins.[251] Although metabolic studies involving microsomes are considered incomplete–as they do not account for non-oxidative processes and metabolism by cytosolic enzymes, they remain crucial for the identification of metabolically-unstable compounds.[252]

The liver transforms xenobiotics into more polar compounds to be readily eliminated from the system via the kidneys or bile.[235] Clearance from the liver is a vital parameter as it directly impacts the BA of orally administered drugs.[253] This occurs during Phase I and Phase II metabolism. Phase I metabolism primarily involves oxidation, reduction and hydrolytic reactions that expose an existing functional group in a compound (e.g. demethylation) or create a new functional group (e.g. hydroxylation). Phase I metabolism is mainly driven by cytochrome P450 isoforms–found in high abundance in

microsomes.[254] Phase II metabolism involves conjugation reactions of pre-existing functional groups, or such groups generated by Phase I metabolism on a drug substrate– to create very polar, water-soluble metabolites that are easily excreted.[235] However, acetylation of compounds containing a primary amino group results in a more hydrophobic conjugate in a reaction that converts the ionised primary ammonium group to an uncharged amide.[255] By investigating compounds in both mouse and human microsomes, it is possible to scale the intrinsic clearance to expected *in vivo* clearance.[250,256,257]

3.2 Materials

All materials used in this chapter are listed in Appendix B. Only materials of analytical grade or higher were used.

3.3 Methods

3.3.1 Sample preparation

3.3.1.1 Sample preparation for method development

The solid compounds were dissolved to prepare solutions of 1 mg/mL stock solutions in DMSO. Compound stock solutions were prepared and diluted to required concentrations as needed for direct infusion, chromatographic method development, and validation experiments.

3.3.1.2 Sample preparation for ADME assays

The preparation of reagents and samples used during ADME assays are described on pg. 193-195 of Appendix B.

3.3.2 Bioanalytical method development

Analytical methods were developed on a LC-MS/MS system which consisted of a Schimadzu high-performance liquid chromatography (HPLC) system (Kyoto, Japan), coupled to an AB Sciex 3200 Q TRAP mass spectrometer (AB Sciex, Massachusetts, USA).

Compounds were prepared for infusion at concentrations between 100–500 ng/mL in various mixtures of mobile phases from stock solutions. A 1 mL Hamilton glass syringe was used for direct infusion into the mass spectrometer at 10 μL/min. Different analytical columns and ratios of aqueous and organic mobile phases were explored during method development to find the optimal chromatographic conditions for the compounds. Initial product scan mass spectra, MRM transitions and final mass spectrometer conditions and representative chromatograms of all compounds are listed in Appendix C.

3.3.3 Bioanalytical validation experiments

In order to ensure the methods were robust and provided accurate and reproducible data, several tests were applied to determine if the methods were fit for the intended analyses associated with the *in vitro* ADME and *in vivo* PK sections. This included assessment of stock solution stability; matrix stability; autosampler stability; recovery and matrix effects; accuracy and precision; and carryover.

The nature of this project did not justify a full validation, as prescribed by the U.S. Food and Drug Administration (FDA) and European Medicines Agency (EMA) international guidelines.[258,259] Instead, the FDA guidelines that give recommendations for chromatographic assays more relevant to pre-clinical research under the 'fit-for-purpose' (FFP) concept were followed.[258] The conditions allow for less stringent validation criteria as the data will not be used for clinical or regulatory purposes. It was determined that, at this level of validation, a percentage difference between the average peak ratio for the reference standard and test solution, should not exceed 20% (%Nom), and a percentage coefficient of variability (CV) not exceeding 15%. Validation of analytical methods require some key questions to be addressed, which were implemented under the FFP approach[258] and includes the following:

- Is the method able to measure the intended analyte without any interference and with acceptable selectivity and specificity?

- Does the method deliver accurate and precise results, within the acceptable variability range?
- What is the range in measurements that provide reliable data?
- Is the reliability of the data from the bioanalytical method affected by sample collection, handling and storage?

In summary, the validation determined if the optimised methods are suited to the analysis of the study samples. Validation experiments are described in Appendix D.

3.3.4 ADME assays

Standard operating procedures for ADME assays were developed and validated in the Division of Clinical Pharmacology, Department of Medicine at the University of Cape Town by the H3D Drug Discovery and Development Centre. Chemicalize was used for prediction of pKa values, ChemAxon (https://www.chemaxon.com).

3.3.4.1 Kinetic solubility

Aqueous solubility of the compounds was determined at various pH levels, using a miniaturised shake-flask method.[235,236] A three-point calibration curve of each control and test compound was prepared from stock solutions in DMSO. Test samples were prepared in phosphate buffer saline (PBS) solutions at pH 2, 6.5 and 7.4 in flat-bottomed 96-well plates. Plates were agitated on an orbital shaker at room temperature for 2 hours at 200 rpm and subsequently analysed with HPLC-DAD (Agilent 1200 Rapid Resolution HPLC with diode array detector). Control (reserpine and hydrocortisone) and test compound concentrations were calculated from the peak area in the UV chromatogram by extrapolation from the calibration curve, using the relationship in Equation 3-1.

Equation 3-1. Linear regression relationship of concentration versus instrument response.

$$y = ax + b$$

Where a is the slope and b is the intercept.

3.3.4.2 Lipophilicity

The preference of a compound to distribute into a lipid or aqueous environment was determined by a shake-flask lipophilicity (LogD) assay, modified from Alelyunas *et al.*[237] Stock solutions of control (hydrocortisones, verapamil and ouabain) and test compounds were diluted to 100 μM in a deep well 96-well deep-well plate containing 1-octanol and a phosphate buffer (pH 7.4). Plates were shaken vigorously on an orbital shaker at 750 rpm for 2 hours. The organic and buffer layers of each well were transferred separately to a new analysis plate. The samples were analysed with HPLC-DAD and $LogD_{7.4}$ was calculated from the integrated peak areas using Equation 3-2.

Equation 3-2

$$Log\ D_{7.4} = Log_{10} \times \left(\frac{octanol\ phase\ peak\ area/injection\ volume}{buffer\ phase\ peak\ area/injection\ volume}\right)$$

3.3.4.3 Permeability assay

Passive permeability was determined by measuring the diffusion of compounds across an artificial membrane *in vitro*, using the PAMPA assay.[240] Reference (warfarin) and test compound samples were diluted to 1 mM in a donor buffer (pH 6.5) from DMSO stock solutions. Total donor solution was prepared by diluting 10 μL of 1 mM test compound with 10 μL Lucifer Yellow solution and 980 μL donor buffer. In triplicate, 150 μL of this solution was added to the apical (donor) side of a multiscreen plate containing the artificial hexadecane membrane (Figure 3-2). The acceptor-buffer solution was prepared by adding 10 μL DMSO to 990 μL acceptor buffer (pH 7.4) and 250 μL were added to the basolateral (acceptor) wells. The donor plate was carefully inserted into the acceptor plate and incubated at room temperature for 4 hours. Theoretical equilibrium samples were prepared by adding 150 μL of donor solutions to 250 μL acceptor solutions and left at room temperature. After the incubation period, 50 μL of samples from the acceptor plate were transferred to a round bottom 96-well plate, together with 30 μL of donor buffer for matrix matching. For the prepared theoretical equilibrium samples, 80 μL were added to the analysis plate. Lastly, 160 μL ISTD was added to all acceptor and equilibrium samples, and samples were submitted for LC-MS/MS analysis. $LogP_{app}$ (apparent permeability) was calculated using equations 3-3 and 3-4.

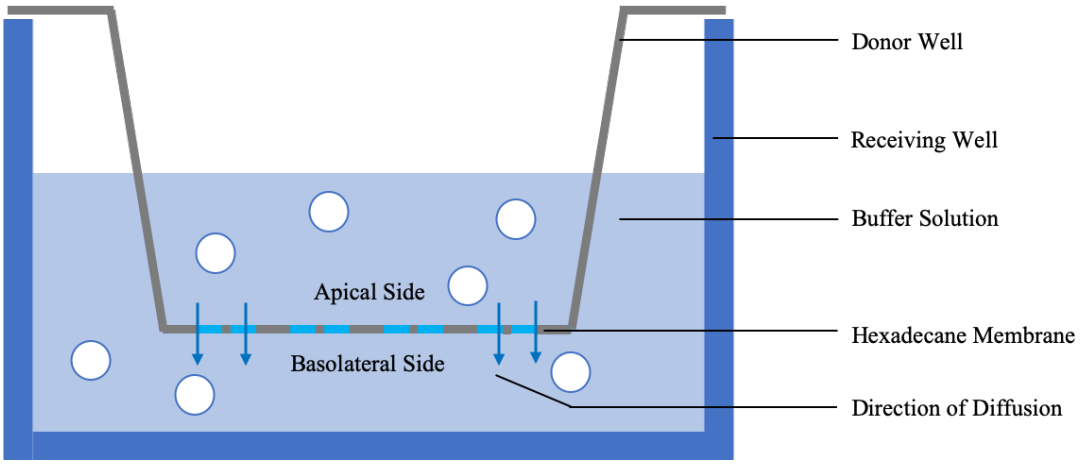

Figure 3-2: The experimental setup of the Multiscreen filter plate containing the artificial membrane. The donor plate is slotted on top of the acceptor plate with the membrane submerged in the acceptor buffer solution.

Equation 3-3

$$C = \frac{V_D \times V_A}{(V_D + V_A) \times A \times t}$$

where VA = volume of donor compartment (0.15 cm^3), VD = volume of acceptor compartment (0.25 cm^3), A = accessible filter area (0.24 cm^2) and t = incubation time (14 400 seconds).

Equation 3-4

$$P_{app} = C \times -\ln\left(1 - \frac{[drug_{acceptor}]}{[drug_{equilibrium}]}\right)$$

Where $[drug_{acceptor}]$ is the analyte to internal standard peak area ratio of the test compound in the acceptor compartment and $[drug_{equilibrium}]$ is the analyte to internal standard peak area ratio of the combined total donor and acceptor compartments.

3.3.4.4 Plasma stability

The stability of compounds in human plasma was determined using a 5-point stability assay.[235,243] Control (procaine and vinpocetine) and test compound stock solutions were diluted in thawed human plasma in deep well 96-well plates. An aliquot was placed in six different deep well plates labelled with different time-points (t_0, t_5, t_{15}, t_{30}, t_{60}, and t_{180} minutes). The t_0 samples were immediately precipitated with ice cold acetonitrile containing the internal standard (ISTD) (0.1 μM carbamazepine) and stored at -20°C until analysis. The remaining plates were placed in a water bath at 37°C and precipitated at the indicated time. After samples of the final timepoint were precipitated, the supernatant was transferred to a round bottom 96-well plate for analysis with LC-MS/MS. Peak areas of the chromatograms were integrated and normalised with the ISTD peak area. The normalised peak areas were used to calculate the percentage compound remaining after 3 hours incubation, using Equation 3–5. A time versus percentage remaining scatter plot was constructed for each compound and the regression line was used to calculate the *in vitro* half-life of a compound in human plasma, using Equation 3-6.

Equation 3-5

$$\%\ Stability\ (parent\ remaining) = \frac{normalised\ peak\ area\ at\ t_x}{normalised\ peak\ area\ at\ t_0} \times 100$$

where t_x is the time of incubation.

Equation 3-6

$$Half - life\ (minutes) = \frac{-0.693}{\lambda}$$

where λ is the slope of Ln percentage remaining versus time.

3.3.4.5 Plasma protein binding

The extent of protein binding was determined by using human plasma.[166] Stock solutions (10 mM) of control (caffeine, warfarin and MMV390048) and test compounds were diluted to 10 μM in plasma, in deep well 96-well plates. An aliquot of each compound was removed in duplicate and immediately precipitated with ice cold acetonitrile containing

the ISTD (0.1 μM carbamazepine). These served as "total concentration samples" (TCS). The rest of the samples were incubated in a water bath at 37°C for one hour and then transferred to ultracentrifuge tubes. Samples were centrifuged for 4 hours at 37°C and 30 000 g. Following centrifugation, the supernatant was transferred to the plate containing TCS and precipitated with ice cold acetonitrile containing ISTD. Plates were centrifuged at 3500 rpm and the supernatant transferred to round bottom 96-well analysis plates and analysed by LC-MS/MS. The percentage of bound drug was calculated from normalised peak areas of integrated chromatograms, using Equations 3-7 and compound degradation was calculated using Equation 3-8.

Equation 3-7

$$\%\ Bound = 100\ \times \frac{normalised\ \text{peak}\ area\ \text{of}\ TCS - normalised\ \text{peak}\ area\ sample}{normalised\ \text{peak}\ area\ TCS}$$

where TCS is total concentration samples

Equation 3-8

$$\%\ Degradation = 100\ \times \frac{normalised\ \text{peak}\ area\ control\ sample}{normalised\ \text{peak}\ area\ of\ TCS}$$

3.3.4.6 Microsomal binding

Stock solutions of control (warfarin and propranolol) and test compounds were diluted to 1 μM in buffered solution containing 0.4 mg/mL microsomal protein. TCS and centrifuged samples were prepared in the same fashion as described in Section 3.3.4.5. Following centrifugation, the supernatant was transferred to the plate containing TCS and precipitated with ice cold acetonitrile containing ISTD (0.1 μM carbamazepine). The supernatant was transferred to round bottom 96-well analysis plates and analysed by LC-MS/MS. The percentage bound drug was calculated from normalised peak areas of integrated chromatograms, using Equations 3-7 and 3-8.

3.3.4.7 Metabolic stability

Determination of the *in vitro* rate of metabolism of the compounds was achieved by using a 5-point metabolic stability assay in human and mouse liver microsomes.[257,260] Stock solutions of control (midazolam, MMV390048 and propranolol) and test compounds were diluted in buffered solution containing 0.4 mg/mL microsomes, in deep well 96-well plates. Deep well plates were labelled with time points t_0, t_5, t_{15}, $t_{30,}$ and t_{60} minutes. Aliquots were transferred to each of the plates in duplicate. The t_0 samples were immediately precipitated with ice cold acetonitrile containing the ISTD (0.1 μM carbamazepine) and stored at -20°C until analysis. NADPH was added to the remaining plates to initiate the metabolic reaction and plates were placed in a water bath at 37°C and precipitation of the solutions in the plates was carried out at the indicated times. Following precipitation, the supernatant was transferred to a round bottom 96-well plate for LC-MS/MS analysis. Peak areas of the chromatograms were integrated and normalised with the ISTD peak area. The normalised peak areas were used to calculate the percentage parent remaining at each incubation, using Equation 3-5.[257] Calculation of *in vitro* half-lives was carried out as described in Section 3.4.3.4 using Equation 3-6. Intrinsic clearance values were calculated using Equation 3-9. The constant Z refers to the liver mass per body weight in kilograms for mouse and human species, as 87.5 mg/kg and 25.7 mg/kg, respectively.[252]

Equation 3-9

$$Cl_{int} = \frac{0.693}{in\ vitro\ t_{1/2}} \times \frac{volume\ of\ incubation}{mg\ microsomes} \times \frac{45\ mg\ microsomes}{g\ liver} \times \mathrm{Z}$$

Obach has argued that the most accurate *in vivo* hepatic clearance (CL_H) predictions are achieved when including both plasma and microsomal non-specific binding for acidic, basic, and neutral drugs.[257] The predicted hepatic clearance presented in Table 3-10 was calculated by Equation 3-10 and included protein binding data from Section 3.4.3.5. and 3.4.3.6.

Equation 3-10

$$CL_H = \frac{Q \times f_{u(plasma)} \times \frac{CL_{int}}{f_{u(mic)}}}{Q + f_{u(plasma)} \times \frac{CL_{int}}{f_{u(mic)}}}$$

where Q is the hepatic blood flow of mouse (90 mL/min/kg) or human (20.7 mL/min/kg).

Equation 3-11 was used in the case of AD01, RMB059 and RMB060, where protein-binding data were not available.

Equation 3-11

$$CL_H = \frac{Q \times CL_{int}}{Q + CL_{int}}$$

3.3.5 Data analysis

Data from validation and ADME experiments were analysed in Excel (Microsoft Office Excel, 2013) to obtain mean ± standard error of the mean and %CV, where applicable. Graphs were constructed using Excel and GraphPad Prism version 5 for Windows (GraphPad Software Inc., La Jolla, California).

3.4 Results and discussion

3.4.1 Solubility

Kinetic solubility at pH 2, 6.5, and 7.4 was evaluated for 2 hours at 25°C. Solubility was categorised as very low, low, moderate, or high according to Kerns and Di (Table 3-1).[239] Solubility data of the biologically active compounds is presented in Table 3-2.

Table 3-1: Solubility classification.

Solubility Class	**Concentration (μM)**
Very low	<5
Low	5 – 49
Moderate	50 – 150
High	≥150

Table 3-2: Aqueous solubility of the seven biologically active compounds.

Compound	**Kinetic solubility (μM)**		
	pH 2	pH 6.5	pH 7.4
WHN012	10	24	27
AD01	>150	>150	>150
PhX6	>150	<5	<5
DpNEt	>150	>150	>150
RMB005	<5	<5	<5
RMB059	<5	<5	<5
RMB060	nd	nd	nd
Reserpine	135	5	<5
Hydrocortisone	>150	>150	>150

nd, not determined

WHN012 (pKa 5.65/13.7), AD01 (pKa 3.96) and DpNEt (pKa 2.38/11.3) had similar solubilities at the different pH levels tested, indicating their solubility profiles are unaffected by the change in pH. WHN012, an aminoartemisinin derivative (Figure 3-1), had low solubility across all pH levels (10–27 μM); this contrasts with the solubility of artemisone (AMS) (220 μM, pH 7.2) and artemisinin (225 μM, pH 7.2).[261] The MB analogue AD01 and the thionosemicarbazone DpNEt were highly soluble (>150 μM) at all pH levels tested. The phenoxazine PhX6 (pKa 3.90) had very low solubility at pH 6.5 and 7.4 (<5 μM), and high solubility at pH 2 (>150 μM). This was evidently due to the compound existing in the protonated conjugate acid form at lower pH. The decoquinate derivatives RMB005 (pKa -1.02/11.8) and RMB059 (pKa 4.73) were poorly soluble across all pH levels, and were comparable to the parent compound DQ (pKa -1.55/9.95, 0.14 μM).[262] The ester carbamate RMB060 (pKa 4.71) was unstable in solution and reliable evaluation was not possible.

3.4.2 Lipophilicity

The distribution coefficient of the compounds in 1-octanol and buffer at pH 7.4 ($LogD_{7.4}$) was used as a measure of lipophilicity. As described in Section 3.1.2., lipophilicity is considered ideal in the range of LogD 1-3. The LogD data is presented in Table 3-3.

Table 3-3: The distribution coefficient $LogD_{7.4}$ as measure of lipophilicity.

Compound	**Lipophilicity ($LogD_{7.4}$)**
WHN012	1.9
AD01	0.2
PhX6	1.0
DpNEt	2.3
RMB005	3.2
RMB059	2.9
RMB060	2.9
Artemisone	2.5[a]
Artemisinin	2.9[b]
MB	0.1[c]
DQ	7.8[a]
Hydrocortisone	1.6
Verapamil	2.5
Ouabain	-1.8

[a]value from Burger *et al.*, 2018; [b]value from Shah *et al.*, 2012; [c]value from Usacheva *et al.*, 2001.

WHN012 (pKa 5.65/13.7) has moderate lipophilicity within the ideal range ($LogD_{7.4}$ 1.9), and is slightly less lipophilic than artemisinin (LogP 2.9)[263] and its semi-synthetic analogue AMS (LogP 2.5).[264] It should be noted that artemisinin does not possess any ionisable groups and thus the LogP value obtained by Shah *et al.*, would be equal to the Log D at any pH. Using the equation for calculating LogD at a specified pH by Xing and Glen, the calculated LogD of artemisinin and AMS was very similar to their LogP values.[265]

AD01 (pKa 3.96) had a low lipophilicity ($LogD_{7.4}$ 0.2), which compares with the reported lipophilicity of MB (pKa 3.14).[266,267] The lipophilicity of PhX6 (pKa 3.90) was on the lower end of the ideal range ($LogD_{7.4}$ 1.0), while the LogD of DpNEt (pKa 2.38/11.3) was classified as ideal ($LogD_{7.4}$ 2.3). RMB005 (pKa -1.02/11.8) had lipophilicity above the ideal range ($LogD_{7.4}$ 3.2). LogD values of RMB059(pKa 4.73) and RMB060 (pKa 4.71) were classified within the ideal range of lipophilicity ($LogD_{7.4}$ 2.9) which was much lower than the parent compound DQ, (pKa -1.55/9.95) which has a LogD of 7.8.[264]

3.4.3 Permeability (PAMPA)

Permeability was determined via LC-MS/MS quantification following a 4-hour incubation at room temperature and at pH 6.5. This pH resembles more closely the section of the GIT where most of the passive intestinal absorption takes place.[268,269] Permeability was classified according to ranges provided in the instructions of the manufacturer Biofocus (based on Kansy *et al.*)[240] as shown in Table 3-4. The results are presented in Table 3-5 as the logarithm of apparent permeability ($LogP_{app}$).

Table 3-4: PAMPA classification.

Permeability class	**$LogP_{app}$**
Low	<-6.5
Moderate	-5.5 to -6.5
High	>-5.5

Table 3-4: Permeability through an artificial hexadecane membrane at pH 6.5.

Compound	**Permeability ($LogP_{app}$)**
WHN012	-3.2
AD01	-6.4
PhX6	-4.4
DpNEt	-3.7
RMB005	-6.3
RMB059	-5.8
RMB060	-6.3
Warfarin	-3.8

Overall, the compounds exhibited moderate to high permeability. High apparent permeability was observed for WHN012 ($LogP_{app}$ -3.2), PhX6 ($LogP_{app}$ -4.4) and DpNEt ($LogP_{app}$ -3.7), suggesting that passive diffusion contributes significantly to the absorption of these compounds and the extent of absorption was predicted to be high.[270] It should be noted that PhX6 was poorly soluble at pH 6.5 which may have resulted in the apparently lower rate of passive diffusion. According to Richardson *et al.*, the high permeability of DpNEt may be partly supportive of the correlation with the high biological activity, which allows it to access intracellular iron (Fe) pools.[222] AD01 ($LogP_{app}$ -6.4), RMB005 ($LogP_{app}$ -6.3), RMB059 ($LogP_{app}$ -5.8), and RMB060 ($LogP_{app}$ -5.8) expressed moderate apparent permeability, indicating the quantity of compound that was able to cross from the apical to the basolateral side of the membrane was limited. In similar fashion, the poor apparent permeability observed was potentially due to the poor solubility at pH 6.5 and might suggest that the RMB compounds were not completely in solution on the apical side of the membrane and thereby unable to cross sufficiently to the basolateral side.

3.4.4 Plasma stability

The stability of compounds in plasma was assessed using the human plasma stability assay. Compounds were incubated in fresh plasma at 37°C and quantified via LC-MS/MS analysis. Half-lives in plasma were calculated from percentage remaining plots and are presented in Table 3-5.

Table 3-5: Stability of the seven compounds in human plasma.

Compound	% Remaining	Projected half-life(min)
WHN012	91	>150
AD01	21	85
PhX6	88	>150
DpNEt	87	>150
RMB005	91	>150
RMB059	68	66
RMB060	<7	<8
Procaine	<7	<8
Vinpocetine	100	>150

WHN012 was not subject to significant degradation in plasma. AD01 had low stability in plasma with only 21% remaining after 3 hours. PhX6, DpNEt, and RMB005 had good stability and >150 minutes half-life in plasma, comparable to the reference control vinpocetine. RMB059 and RMB060 were unstable in plasma and half-lives were calculated as 66 min and <8 min, respectively. Some functional groups are 'soft spots' susceptible to hydrolysis, such as the ester and carbamate groups on RMB059 and RMB060. It was suspected that DQ could potentially be a degradation product of RMB059 and RMB060. Transition ions were, thus, included in the LC-MS/MS method for detection during analysis of the plasma stability assay. Peak area ratios versus time of RMB and DQ were plotted on the same graph to illustrate the change in concentrations of the compounds (Figure 3-3). The degradation of RMB059 exhibited in Figure 3-3a suggested that the compound was metabolised in a linear fashion over the 180 min assay period, while RMB060 (Figure 3-3b) was rapidly converted to DQ within the first 20 minutes of

the assay. It is interesting to note the extent of conversion that differs between the two compounds and it is recommended that further metabolic identification studies be done to determine the formation of other metabolites. The implication of hydrolysis on *in vivo* experiments could have a profound effect because it could mean that as soon as RMB is introduced into systemic circulation, it would be rapidly converted to DQ. This was however thought to be advantageous as DQ is poorly absorbed and if RMB presented improved absorption, it could act as "prodrug" for DQ delivery. This effect may also improve the efficacy profile of these quinolones as there will be both parent and converted active metabolite in circulation to increase the extent and duration of efficacy.

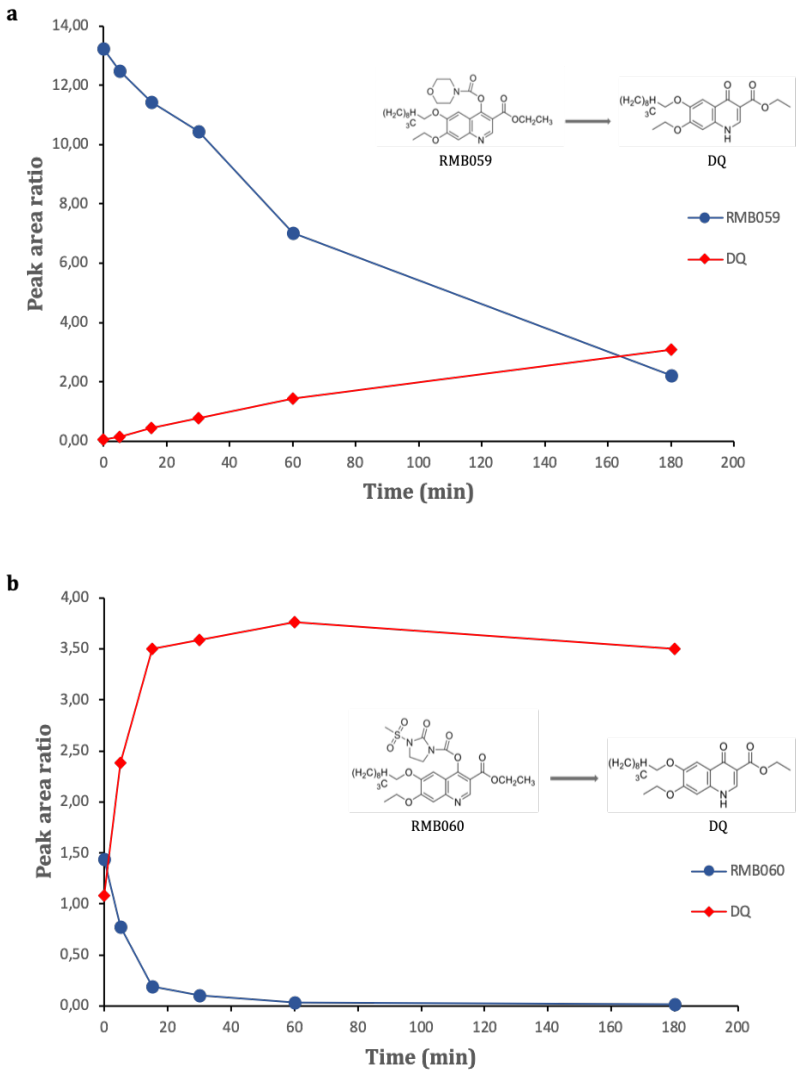

Figure 3-3: The change in concentration of parent compounds a) RMB059 and b) RMB060 to the metabolite DQ during the 3 hour incubation period in human plasma.

3.4.5 Plasma protein binding

The non-specific binding of compounds to plasma proteins was investigated using an ultracentrifuge method. As discussed in the previous section, AD01, RMB059, and RMB060 were excluded from protein-binding analysis due to their susceptibility to degradation in plasma. The acceptable value for percentage compound remaining during incubation was set at 85%. Plasma protein binding was classified as high, moderate, or low, as shown in Table 3-6.[250] MMV390048 was used as an in-house control of moderate binding, as it has been well characterised by Paquet *et al.*[26] Results are summarised below in Table 3-7.

Table 3-6: Protein binding classification.

Protein binding class	**Fraction unbound (fu)**
Low	>0.5
Moderate	0.5 to 0.05
High	<0.05

Table 3-7: Non-specific binding to human plasma proteins.

Compound	**% Plasma protein binding (fu)**
WHN012	98 (0.02)
AD01	nd
PhX6	90 (0.10)
DpNEt	94 (0.06)
RMB005	92 (0.08)
RMB059	nd
RMB060	nd
Caffeine	30 (0.70)
Warfarin	99 (0.01)
MMV390048	87 (0.13)

f_u, fraction unbound; HLM, human liver microsomes; nd, not determined

WHN012 was highly bound to plasma proteins (98%) similar to that of mefloquine (98%)[244] while PhX6, DpNEt and RMB005 were only moderately bound (Table 3-7). Navaratnam *et al.* determined that artemisinin and its derivatives are moderately bound to human plasma proteins. Artemisinin, AS and artemether were 64%, 59% and 76% bound to plasma proteins, respectively,[271] while Li *et al.* found that DHA (43%) has a low protein binding.[272]

3.4.6 Microsomal binding

Microsomal protein binding was determined by incubation in mouse and human liver microsomes, using the same ultracentrifugation method described in Section 3.3.4.5. Microsomal protein binding was classified using Table 3-6.[273] Binding data for AD01, RMB059 and RMB060 was not possible, as compound integrity was lost over the 4-hour assay period (i.e. <85% remaining).

Table 3-8: Microsomal protein binding for mouse and human.

Compound	**% Microsomal protein binding (f_u)**	
	Mouse	Human
WHN012	54 (0.46)	61 (0.39)
AD01	nd	nd
PhX6	99 (0.01)	99 (0.01)
DpNEt	16 (0.84)	25 (0.75)
RMB005	99 (0.01)	99 (0.01)
RMB059	nd	nd
RMB060	nd	nd
Warfarin	1 (0.99)	2 (0.98)
Propranolol	33 (0.67)	38 (0.62)

f_u, fraction unbound; MLM, mouse liver microsomes; nd, not determined

The mouse and human microsomal binding for WHN012 are moderate. Binding of PhX6 to microsomal proteins are high in both species. Weakly basic compounds like PhX6 are,

however, more likely to bind extensively to microsomal protein.[249] DpNEt had low binding and RMB005 was highly bound to microsomal proteins. No significant interspecies variability was expected as studies by Barr *et al.* and Riccardi *et al.* determined that binding across multiple species exhibit similar trends.[274,275]

3.4.7 Metabolic stability in mouse and human liver microsomes

Metabolic stability was measured using a 5-time point assay, as outlined in Section 3.3.4.7. Predicted *in vivo* clearances were calculated by accounting for microsomal and protein binding.[257] Metabolic stability was classified based on predicted hepatic clearance, as shown in Table 3-9 and as defined by Li *et al.*[276] The results are presented in Table 3-10.

Table 3-9: Classification of predicted hepatic clearance values.

Species	**Hepatic clearance rate (mL/min/kg)**		
	High CL_H (>70% Q)	Intermediate CL_H	Low CL_H (<30% Q)
Mouse	>63	30 - 60	<27
Human	>14.4	7 - 14	<6.21

CL_H, hepatic clearance; Q, hepatic blood flow

The predicted human hepatic clearance of WHN012 (11.8 mL/min/kg) was comparable to artesunate and artemisinin (12.3 and 9.8 mL/min/kg, respectively)[276] and suggests that WHN012 would be cleared at an intermediate rate in humans. Intermediate hepatic clearance was predicted for WHN012 in mice. PhX6 and DpNEt presented similar intrinsic clearance values that were longer in the mouse but shorter in the human species, and comparable to propranolol. Predicted CL_H for PhX6 was high for both mouse (88.2 mL/min/kg) and human (20.2 mL/min/kg) species.[277] DpNEt presented low predicted human hepatic clearance rates (4.00 mL/min/kg). AD01, RMB059, and RMB060 had high predicted clearance in both species (>75.2 mL/min/kg and 16.2 mL/min/kg for mouse and human, respectively). This may be as result of rapid metabolism due to their chemical structure, but this may also highlight the compounds' general lability. RMB005 was

metabolically more unstable in mouse liver microsomes (CL_H 81.2 mL/min/kg, high) than in human microsomes (CL_H 12.6 mL/min/kg, intermediate).

Table 3-10: Prediction of hepatic clearance from *in vitro* metabolic stability assays.

Compound	**Species**	**% remaining (after 60 min)**	**Intrinsic clearance (mL/min/kg)**	**Predicted hepatic clearance (mL/min/kg)**	**Predicted hepatic extraction ratio (EH)**
WHN012	Mouse	2	2485	49.1	0.55
	Human	3	531	11.8	0.57
AD01	Mouse	2	772	80,6*	0.47*
	Human	27	74	16.2*	0.44*
PhX6	Mouse	9	446	88.2	0.98
	Human	23	82	20.2	0.98
DpNEt	Mouse	14	416	22.3	0.25
	Human	34	62	4.00	0.19
RMB005	Mouse	55	104	81.2	0.90
	Human	85	4	12.6	0.61
RMB059	Mouse	22	457	75.2*	0.46*
	Human	10	410	19.7*	0.49*
RMB060	Mouse	17	541	77.2*	0.46*
	Human	12	183	18.6*	0.47*
Midazolam	Mouse	6	1895	49.0a	0.54
	Human	9	794	14.2a	0.69
MMV390048	Mouse	92	11	nd	0.11
	Human	95	3	nd	0.14
Propranolol	Mouse	3	632	62.0b	0.69
	Human	56	32	6.8b	0.33

*protein binding data not included; [a]protein binding value from Obach, 1999[257]; [b]protein binding value from Obach, 1997.[250]

3.4.8 Overall interpretation

The most important drug-like properties of the compounds relating to the different phases of ADME once it enters a living system, were determined from the assays performed in this study.

The absorption of a drug is dependent on its solubility, lipophilicity, and permeability. Different pH levels were included in the solubility assay, as fluctuation of the pH gradient throughout the GIT and various conditions throughout the *in vivo* environment can alter dissolution of drugs.[234]

Solubility was measured in aqueous buffer at pH 2, which represents the pH of the stomach (1.4–2) and pH 6.5 and 7.4 which represents the pH of the intestine, where absorption takes place (6.8–8).[278] WHN012, RMB005 and RMB060 exhibited low solubility across the physiological pH levels tested and could, therefore, have limited absorption and greater variability of uptake *in vivo*.[279] Within the context of malaria, drugs need to be soluble in blood and able to cross membranes of capillaries and RBCs to reach the target, as the clinical presentation of the disease is located outside the plasma.

Moreover, conditions within intracellular compartments become important for drugs that elicit their mechanism of action by accumulation in such compartments. Although the cytosolic pH of infected erythrocytes is not significantly different to normal cells (pH 7.4), other compartments with a lower pH, such as the acidic food vacuole of the parasite (pH 4.9–5.0) is important when considering solubility-performance of a drug.[280] This is demonstrated by CQ, a basic drug, that accumulates in the digestive vacuoles of *P. falciparum*.[281]

As PhX6 is a weak base, it was expected that solubility would be optimal in low pH environments. This was demonstrated by high solubility at pH 2 (>150 μM, Table 3-1). PhX6 showed poor solubility at pH 6.5 and 7.4. However, the observation that PhX6 has biological activity in the nanomolar range suggests that the compound is at least marginally soluble in CM (pH 7.4). This behaviour is similar to that of the antimicrobial bedaquiline. Bedaquiline is practically insoluble across a wide pH range in aqueous buffer, but shows excellent anti-tuberculosis activity.[282] In this case, its pKa of 8.9 allows it to be mostly protonated at pH 7.4 and therefore its solubility would exceed that of PhX6. PhX6 was expected to display high permeability in similar fashion to that of BDQ. Contrastingly,

the high solubility of MB analogue AD01 and the thionosemicarbazone DpNEt, suggest that these compounds will have good absorption *in vivo*.

It is suggested as a rule of thumb that hydrophobicity is inversely correlated to hydrophilicity.[283] This was demonstrated by some of the compounds investigated in this study, particularly through the high solubility and below-ideal lipophilicity observed for AD01. Correlation of lipophilicity within the ideal range was expected to present good intestinal absorption, higher protein binding, and lower Vd *in vivo*.[283] The relationship of LogD with free-drug PK and metabolism has been well described,[257,283] and is discussed later.

Permeation is largely controlled by the physicochemical properties of a drug, namely lipophilicity, charge, and size of the compound. Furthermore, the extent of absorption may be substantially impacted by various transporter proteins such as P-glycoprotein.[284] Although WHN012 was poorly soluble at pH 6.5, small amounts going into solution could be able to permeate the phospholipid layer very well.

In a study carried out by Senarathna *et al.*, it was demonstrated that artemisinin-derivative artesunate had moderate permeability; it was proposed that it would suffer incomplete absorption in the GIT as passive diffusion was not the main mechanism of absorption.[270] In contrast, AMS has a similar high passive diffusion ($LogP_{app}$ -4.2) to WHN012 and was found not to be subject to P-glycoprotein- (P-gp) mediated efflux transport.[270] The PAMPA assay is unable to distinguish whether compounds like AD01, with high solubility and moderate permeability, are dependent on active transcellular transport; or to what extent it could be subject to P-gp mediated efflux. It is evident through this example, that solubility and lipophilicity are opposing, inversely related parameters that should be balanced in order to obtain optimal drug permeability and exposure.

Although AD01 was very soluble at physiological pH that is typical of the GIT, lower extent of permeation could result in low oral BA due to incomplete absorption in the intestine. Biological models of permeability such as Caco-2 cell-based assays could determine if AD01 disposition is predominantly dependent on active transport. Senarathna *et al.* also investigated the permeability of MB and found that poor permeability ($LogP_{app}$ -5.7) could be attributed to its hydrophilicity; this appears to be the case of AD01. MB was found to be subject to P-gp efflux and this will result in decreased drug accumulation and

absorption *in vivo*.[140,270] Because of close similarity in structure, this could potentially be observed with AD01.

The information obtained from the kinetic solubility and permeability studies of these compounds can be arranged in a relationship described as the biological classifications system (BCS). The BCS was first proposed by Amidon and colleagues[285] as a guideline to classify compounds and assist decision making for downstream development. This framework classifies compounds based on aqueous solubility and apparent permeability (Figure 3-4). This classification system can be applied to the *in vitro* data to correlate *in vivo* profiles of the compounds.

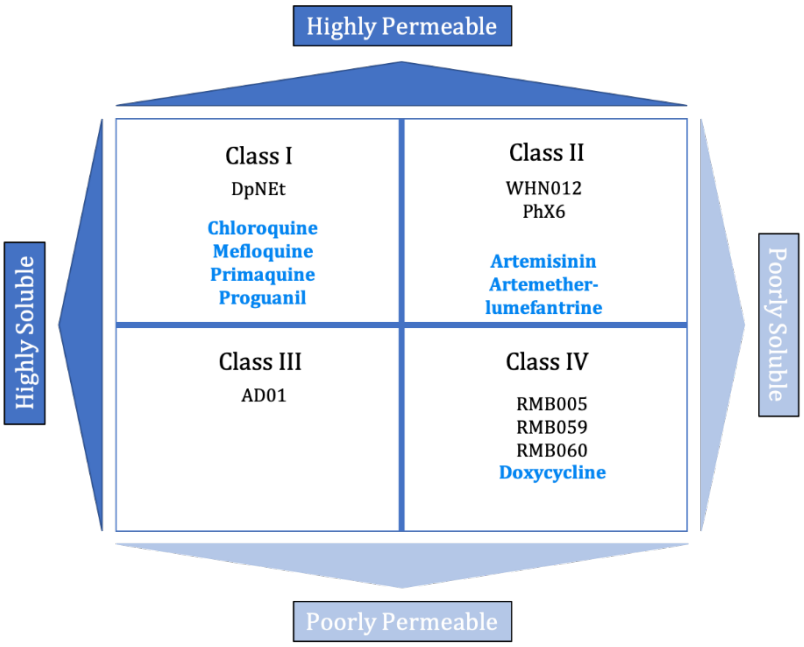

Figure 3-4: The relationship of permeability to solubility within the four categories of the BCS described by Amidon *et al.*[285] Classification of clinically used antimalarials are shown in blue, as listed by Kasim *et al.*[286]

Highly soluble compounds fall within Class I and III, while highly-permeable compounds fall within Class I and II of the BCS (Figure 3-4). *In vitro-in vivo* correlation of a Class I compound exhibiting high solubility and high permeability, such as DpNEt, is expected to show good extent of absorption, but low exposure due to the first pass effect in the liver. CQ, mefloquine, primaquine, and proguanil, among others, are clinically used antimalarial drugs which are classified as Class I drugs. Compounds WHN012 and PhX6 were classified as Class II compounds, which had low solubility and high permeability. Included in this

class is the clinically applied artemisinin and artemether-lumefantrine combination. Drug dissolution is expected to be the rate-limiting factor and high systemic variability is expected due to slow and variable absorption for WHN012 and PhX6. AD01 was the only Class III compound that presented high solubility and moderate to low permeability. It is expected that AD01 would present variable absorption rate and extent of exposure due to the variability in gastro-intestinal transport and membrane permeability-solubility interplay. RMB059 and RMB060 were classified as Class IV having low solubility and low permeability, which potentiates difficulty with oral drug delivery.[285,287]

Other biochemical interactions such as the effects from protein binding and metabolism, occur in the human body once a drug has been administered and absorbed. The binding of drugs to protein and tissues are common for many drugs and will impact the distribution and elimination. For antimalarial drugs, the impact of protein binding is of prime interest because it is the free, unbound drug at the site of action/infection that exerts the therapeutic effect.[244] The binding to human plasma proteins of the compounds investigate in this study were classified as moderately to highly bound. Downstream *in vivo* investigations of potential candidates should be vigilant of differences in protein concentration resulting from disease, since the effect of alteration of drug concentration of new compounds is unknown.[288] It is known that malaria infection decreases the concentration of albumin and increases AAG by approximately 25% and 50%, respectively.[289] Therefore, the free concentration of compounds such as WHN012–that are highly bound to protein, could alter its therapeutic effectiveness *in vivo*. Another important consideration is that efficacious antimalarial therapy is principally reliant on combination therapy. Highly protein-bound drugs could become susceptible to drug interactions by displacement from bound proteins, especially if partner drugs competitively bind to plasma proteins.[245,290]

It was found by Obach that microsomal binding has significant impact in the scaling of *in vitro* intrinsic clearance to the *in vivo* hepatic clearance. Thus, for accurate prediction and correlation of *in vitro-in vivo* data, the microsomal binding needs to be determined and incorporated into microsomal stability equations.[257] When binding of the drug occurs on the membrane of microsomes, where most of the metabolising enzymes reside, it is unavailable for interaction with the microsome, which decreases the extent of hepatic metabolism. This can cause an over estimation of the stability of a compound, especially in the case of lipophilic compounds such as WHN012, PhX6, DpNEt and RMB005 as they

are more likely to associate with membranes. Free, unbound drugs in systemic circulation are metabolised by enzymes found in the plasma and liver. If the molecule is bound to protein, the interaction with enzymes is hindered. This could likely result that the compounds will present lower clearance rates in an *in vivo* model.[257]

The artemisinins are known to have metabolic labilities by reductive metabolism of the peroxide bridge,[291,292,] and, thus, WHN012 could undergo extensive metabolism. The physicochemical properties of DpNEt suggested that it could be well absorbed, and thus, may present high BA, as further suggested by the clearance data. Compounds with low free fraction in plasma ($f_u \leq 0.1$) are expected to be less available for first pass metabolism *in vivo*. DpNEt displayed non-specific binding to microsomes of between 16–25%, and $f_u < 0.1$ in human plasma. Because metabolic stability involving liver microsomes are predominantly attributed to Phase I and Phase II reactions, the low predicted clearance of DpNEt may suggest that metabolism could be substantially mediated by other, nonoxidative processes and cytosolic enzymes.[251,252]

As mentioned previously, data of low-solubility drugs should be interpreted with caution. The poor solubility of RMB005 could cause the compound to precipitate during the assay, leaving it unavailable for the microsomes to metabolise and then resuspended upon precipitation with organic solvent. This could result in false presentation of stability, i.e. overprediction of the percentage remaining following incubation over 60 minutes. Metabolic stability of compounds RMB059 and RMB060 could be misleading, as they have shown to be relatively unstable compounds in human plasma (Figure 3-3). The apparent high rate of metabolism is not an accurate prediction, but rather, reflective of the compounds' expected lability under the assay conditions.

3.4.9 Correlation with *in vitro* biological assays

The observed *in vitro* biological activities of the compounds, as described in Chapter 2, showed correlation to some of the physicochemical and biochemical characteristics investigated in this chapter. Good solubility presented by AD01 (Section 3.4.1) was represented by biological activities (Section 2.3.1.2).

The parent compound MB was reported to have a LogP of 0.1 by Usacheva and colleagues, indicating it is hydrophilic.[266] The structural analogue AD01 showed slightly improved lipophilicity ($LogD_{7.4}$ 0.2), while reflective of its good *in vitro* activity.

Compounds that presented low solubility, which included WHN012, RMB005, and PhX6, only require a small portion of compound in solution and to present high potency. The most surprizing discovery was that RMB059 and RMB060 were converted to the parent DQ when exposed to hydrolytic enzymes in biological matrix. Although the degradation of RMB059 and RMB060 was significant over time, this was not reflected in the biological assays, as one would expect decreased biological activity as result of poor stability. The biological activity from the RMB compounds could be explained by a prodrug-effect whereby compounds were added to the incubation plate and are converted into the more stable parent DQ during antiplasmodial screening assays. High biological activity of the ester carbamates could also indicate a fast mechanism of action, as hydrolysis was expected to occur quickly, and surviving parasites to be killed as the concentration of DQ increased over time.

3.5 Summary and conclusions

The characterization of physicochemical properties included solubility, lipophilicity, and permeability. While biochemical properties included stability and protein binding. As expected, profiles were significantly different for each of the compounds.

Solubility ranged from poor to high. The results of the analyses of sparingly soluble compounds were interpreted with caution, as these may give erroneous data of *in vitro* assays carried out in similar conditions and solutions with specific pH's. In contrast, *in vitro* biological evaluation suggested that a sufficient fraction of the compound remained in solution in order to produce the pharmacological effect. This observation was an example of the potency and permeability being dependent on minimum required solubility and should be taken into consideration as it may ultimately influence oral dosing concentrations.[140,293]

Lipophilicity and permeability correlated well, and it was expected that those with high permeability be well absorbed and present good exposure *in vivo*. Protein binding predicted that all qualifying compounds would have low free fractions *in vivo* and it would

be important consider this in future investigation in disease models, as malaria infection significantly alters different plasma protein levels.[289] High protein binding of lipophilic compounds could result in the underprediction of clearance. Subsequently, the available binding data was factored into *in vitro* intrinsic clearance data to obtain more accurate hepatic clearance predictions for *in vivo* investigations.[257]

Clearance is a crucial parameter in the prediction of doses to be administered, as higher oral clearance requires higher oral dosages. Unfortunately, determination of plasma and microsomal protein binding for AD01, RMB059, and RMB060 were not possible as stability was very low. Rapid formation of metabolites from these compounds is likely to be observed during *in vivo* studies. The data from the ADME studies are used together with *in vivo* data described in the next chapter in order to assist interpretation of the PK profiles of the compounds.

4 Pharmacokinetic evaluation in a mouse model

4.1 Introduction

In the previous chapter the determination of the ADME properties of the amino-artemisinin WHN012, the ethyl analogue AD01 of MB, the phenoxazine PhX6, the thiosemicarbazone DpNEt, and the decoquinate derivatives RMB005, RMB059, and RMB060 (Fig. 3-1, Chapter 3) *in vitro* is described.

While *in vitro* ADME assays offer high-throughput lead candidate identification, it lacks the physiological integration and complexity of a dynamic living model in which the ADME systems are interrelating.[294] *In vivo* models area also able to provide much more information on a drug's oral BA, duration of exposure, systemic clearance (CL) and distribution, as discussed later. The murine model for pharmacokinetic investigations offer a comprehensive and inexpensive evaluation of novel compounds in a living system. However, variability resulting from species differences should be kept in mind. For example, protein binding can differ across species and therefore it is crucial to evaluate protein binding in all species of animals used during pre-clinical investigation.[295] Furthermore, concentration measurements at some sample collection sites can differ between mice and humans. For example, drugs can penetrate epithelial lung fluid to a different extent between species and therefore result in less accurate PK interpretation.[296] In the case of rapidly metabolising drugs, murine metabolism can be altered to more closely mimic clearance or metabolism in humans.[297] C57BL/6 mice, an inbred strain, were used rather than outbred strains (Swiss, CD-1, NMRI) because of their genetic homogeneity resulting in minimized intrastrain differences and variability.[298]

By using animal models, one can evaluate the onset, duration, and intensity of a drug's effect following administration. This is established by determination of PK parameters, that is, determining what the body does to the drug. The relevant parameters include the CL, elimination half-life ($t_{1/2}$) , Vd, and BA, maximum concentration (C_{max}) and the time (T_{max}) to reach C_{max}, and the area under the concentration-time curve (AUC) of the drug.[299]

CL, $t_{1/2}$, Vd, and BA are essential properties associated with the PK of a drug.[299] Plasma (total or systemic) CL is determined by all the individual metabolizing/eliminating organ clearances.[300] Various organs are responsible for elimination of drugs including the kidneys and lungs, among others, although the liver is considered to have the highest capacity for drug metabolism.

The systemic CL, thus, results from the additive effects of various organ eliminations, as demonstrated by Equation 4-1 (Figure 4-1).[299] CL is estimated from the plasma or whole blood concentrations of a single intravenous dose. The total dose considered should be the amount which ultimately gains access to the systemic circulation. This is calculated by dividing the administered dose by the area under the concentration-time curve and is expressed as volume per unit time (Equation 4-2, Figure 4-1).[300] CL is usually further defined as blood, plasma, or free drug CL and their use is dependent on the concentration of drug used.

The $t_{1/2}$ of a drug is dependent on both the plasma CL and extent of distribution. Therefore, different drugs may present similar CL rates but distinctly different half-lives, as their degree of distribution will influence the rate at which they are eliminated from the body. Terminal plasma $t_{1/2}$ is defined as the time required to reduce the plasma concentration by 50% after reaching pseudo-equilibrium. Then, terminal $t_{1/2}$ is computed when the decrease in drug plasma concentration is due only to drug elimination, and the term 'elimination $t_{1/2}$' is applicable. Half-life for a drug following first-order elimination kinetics is computed by division of the natural logarithm of 2 by the elimination rate constant and is expressed as a unit of time (Equation 4-3, Figure 4-1).[301]

Along with CL, the Vd can have significant implications on the duration of action of a drug through their relationship to $t_{1/2}$.[302] Vd is defined as the theoretical volume that would be necessary to contain the total amount of an administered drug at the same concentration that it is observed in the blood plasma.[303]As expressed in Equation 4-4 (Figure 4-1), the Vd is calculated by division of the administered dose by the plasma concentration at time zero, and is expressed in litres.

BA is defined as the amount of drug that is absorbed and reaches the target site unchanged following different routes of administration and is a good indicator of the extent of absorption from the site of administration to the systemic circulation.[303] The BA of a drug which is administered via intravenous route, is assumed to be 100%, as the bolus dose is introduced directly into the systemic circulation. Other routes of administration often result in incomplete BA levels which may be due to solubility, dosage form effects, site of administration effects or membrane effects. For example, the BA following an oral dose would be lower than that of an intravenous dose; due to the fact that the drug is subject to hepatic first pass metabolism during absorption.[299] BA may further be influenced by first pass extraction of the drug via the gut wall during absorption or through efflux

transporters located in the intestinal epithelium or hepatocytes.[251] Absolute BA is calculated from the dose-corrected area under the curve for an extravascular (oral) dose and an intravenous dose and expressed as a percentage (Equation 4-5, Figure 4-1).

In general, PK data is either analysed by model fitting using non-linear regression analysis, or non-compartmental analysis techniques. The latter is generally the preferred method of choice for the determination of the PK parameters listed earlier, as it requires fewer assumptions than model-based approaches.[304]

An ideal PK profile depends largely on the pharmacological target site. In the case of the disease target for malaria infection, the major pharmacological target is confined within the systemic circulation – the RBCs. Some PK parameters are fundamental regardless of site of action, such as adequate intestinal absorption following oral administration. Compounds are able to enter the systemic circulation through many known mechanisms, but the major mechanism is through passive diffusion, as discussed in Section 3.1.3.[238,305] Upon absorption into the bloodstream from the GIT, blood is circulated through the liver via the hepatic portal vein. The liver may metabolize the drug, resulting in its elimination. This process is known as first pass extraction and has an immense impact on the BA of a drug. Compounds that are readily absorbed, but survive major metabolism by liver enzymes, are likely to have a prolonged $t_{1/2}$ resulting in substantial exposure.[154]

Importantly, understanding the PK in relationship with pharmacodynamics of the compound *in vivo*, could enhance understanding of the action of a drug. The observed pharmacodynamic effect in a given preclinical model system is associated with a specific PK driver such as parameters AUC, C_{max}, or the lowest concentration of a drug in the blood, compared to the *in vitro* potency measure.[36,306] Within the context of malaria, compounds that exhibit high levels of activity *in vitro* and display slow elimination, high exposure, and BA *in vivo* will be favoured over those deficient in these PK properties.

As mentioned in Chapter 3, characterisation of ADME properties were done in parallel to PK evaluation. Interestingly, analysis of the carbamate derivatives (RMB059 and RMB060) posed challenges which influenced the interpretation of their data, for example erratic, highly variable recovery values during extraction method optimisation. Prior to PK sample processing and analysis, it was discovered that the compounds were generally unstable, especially in the whole blood matrix. The PK analysis of these compounds was approached by quantifying DQ as a product of the compounds administered, by

integrating the peak areas of DQ during LC-MS/MS analysis and calculating the concentrations of PK samples from a DQ calibration curve. As such, DQ was included in all validation experiments, where applicable. The PK properties of compounds necessary for progression to combination studies are identified in this chapter.

Equation 4-1: Total clearance

$$\boldsymbol{CL_{total} = CL_{liver} + CL_{renal} + CL_{other}}$$

Equation 4-2: Calculation of plasma clearance

$$\boldsymbol{CL = \frac{dose}{AUC_{0-\infty}}}$$

Equation 4-3: Calculation of half-life

$$\boldsymbol{t_{1/2} = \frac{0.693}{k_{el}}}$$

Equation 4-4: Calculating volume of distribution

$$\boldsymbol{V_d = \frac{total\ amount\ of\ drug\ in\ the\ body}{drug\ plasma\ concentration}}$$

Equation 4-5: Calculation of absolute bioavailability

$$\boldsymbol{BA = \frac{[AUC]_{oral}}{[AUC]_{intravenous}} \times \frac{Dose_{intravenous}}{Dose_{oral}} \times 100}$$

Figure 4-1: Summary of equations used to calculate essential properties

4.2 Materials

Materials used during preparation and analysis of PK experiment samples are listed in Appendix C. Only materials of analytical grade or higher were used.

4.3 Methods

4.3.1 Ethical statement

Despite the ethical concerns mentioned in Section 1.4, all animal studies and procedures were conducted with prior approval of the Ethics Committee of University of Cape Town (approval number 013/028) in accordance with the South African National Standards (SANS 10386:2008) for the Care and Use of Animals for Scientific Purposes,[307] and guidelines from the Department of Health.[308] The benefits of *in vivo* assessment are vast, as per Section 1.4.3.

4.3.2 Environmental conditions for animals

Healthy C57BL/6 mice weighing approximately 25 g were kept at the University of Cape Town animal facility. Mice were housed in 27x21x28 cm cages (n=3) under controlled environmental conditions at 22 ± 2°C, humidity of 55% ± 15% and a 12 hour light/dark cycle. The cage floor was covered in dried wood shavings. Paper strips and cardboard tubes were provided for building material and shelter. Mice were acclimatised to the experimental environment for 4–5 days prior to beginning the experiments. Food and water were available *ad libitum*.

4.3.3 Formulations

Dosing was with aqueous or organic solutions for oral and intravenous administration; the aqueous solution consisted of either 100% Millipore water, or an aqueous solution of hydroxypropyl methylcellulose (HPMC) containing 0.2% Tween 80. The weighed compound was dissolved in water and vortexed for 2 minutes or suspended in the HPMC solution and vortexed for 2 minutes. The aqueous solutions were used for oral dosing. For intravenous dosing, the weighed compound was added to either 100% Millipore water,

or an organic vehicle consisting of 10% dimethylacetamide (DMA), 30% polyethylene glycol 400 (PEG), 50% polypropylene glycol (PPG) and 10% ethanol. Dosing solutions were tested the day before the scheduled experiment to ensure that the compound is soluble in the solution; solubility was confirmed by visual inspection of the dosage solution before administration. Suspensions were vigorously vortexed and sonicated to obtain a clear and even suspension. Fresh dosing solutions were again prepared similarly the following day for use in the experiment.

4.3.4 Preparation of test compound and administration

Solutions or suspensions for oral and intravenous administration were prepared freshly on the day of the experiment. A predetermined mass of the test compound was weighed for oral and intravenous dosing groups. The mass of the compound used was based on the average weight of the mice, determined the morning of the experiment. Mr Trevor Finch (animal technician) from the Division of Clinical Pharmacology at the University of Cape Town performed all animal handling, compound administration, and blood collection. The volume of dosing solution administered to oral and intravenous groups of mice was calculated based on the average weight of the mice allocated to the respective group. Oral dosing solutions of AD01 and PhX6 consisted of 100% Millipore water. WHN012, DpNEt, RMB005, RMB059, and RMB060 were prepared in an aqueous suspension of 0.5% HPMC (w/v) with 0.2% Tween 80 (v/v). For oral administration, between 160 and 200 µL of the dosing solution was administered by oral gavage. Mice in the intravenous dosing group were anesthetised and compounds were administered via the penile dorsal vein. Intravenous dosing solution for AD01 and PhX6 consisted of 100% Millipore water. WHN012, DpNEt, RMB005, RMB059, and RMB060 were prepared in a solution of DMA, PEG 400, PPG and ethanol (1:3:5:1, v/v). Between 60–120 µL dosing solution was slowly administered over 1 minute. Administration was carried out within 30 minutes of preparation of the solutions of suspensions containing the compound

4.3.5 Sample collection

Animal study samples were collected via tail tip bleeding in heparinised collection tubes and gently vortexed to prevent coagulation. Mice were placed in a restraining device to

assist the process of blood sampling. Whole blood samples for analysis were collected for all compounds except for WHN012. Plasma samples were prepared from whole blood samples for this compound because a reliable extraction method in whole blood could not be developed, as determined during extraction method development (Section 4.3.7). Whole blood samples for WHN012 were collected at pre-determined time points (0.08, 0.25, 0.5, 1.5, 2.5, and 4 hours) for both the oral and intravenous groups and centrifuged for 5 minutes at 5590 g to obtain the plasma layer. Plasma was transferred to clean collection tubes and frozen at -80°C. For the oral dose of AD01, PhX6, DpNEt, RMB005, RMB059, and RMB060, blood samples were collected at 0.5, 1, 3, 5, 8, 10 and 24 hours, gently vortexed and kept on ice. Additionally, the intravenous study group had an extra time point at 0.16 hours. Approximately 20 µL of blood was sampled at each time point and no more than approximately 160 µL of blood was collected throughout the 24-hour sampling period, which is well within the guidelines. Blood samples were frozen at -80°C.

4.3.6 Calibration standards and quality control sample preparation

Blank whole blood collected in lithium heparin tubes from C57BL/6 mice, was used for the preparation of calibration standards (STDs) and quality control (QC) samples. Various solutions for spiking blank matrix were tested to optimize the spiking method and improve reproducibility. Weighed amounts of the compounds were dissolved in DMSO to generate solutions at concentrations of 1 mg/mL, on the day of calibration STDs and QC preparation. Stock solutions of WHN012, AD01, and PhX6 were spiked at the highest nominal concentration directly into the matrix from the freshly prepared DMSO stock solutions, and serially diluted with blank matrix across the calibration range (Table 4-1). Each calibration standard was vortexed vigorously for one minute between each dilution.

In the case where serial dilutions did not produce acceptable accuracy and precision, a parallel spiking method from working solutions were used. Working solutions were prepared in a spiking solution (1:1 mix of mobile phases, v/v) from freshly prepared stock solutions and spiked in parallel at equal volumes across the concentration range to achieve the nominal concentrations of STDs and QCs in blood. DpNEt and RMB005 were prepared as working solutions in spiking solutions.

STDs for WHN012 were prepared in mouse plasma at the highest nominal concentration from the freshly prepared 1 mg/mL DMSO stock solution, and serially diluted across the

calibration range. The same approach was carried out for preparation of QC samples. Preparation of STDs and QC samples in mouse whole blood or plasma were completed in Eppendorf tubes immersed in an ice bath (at 0°C) and all samples were frozen at -80°C. Details of mobile phases used for STD and QC preparation are described in Appendix B.

Table 4-1: Calibration standard concentration range

Compound	**Standard curve range (ng/mL)**	
	Low	High
WHN012	3.90	4000
AD01	7.80	4000
PhX6	3.90	4000
DpNEt	15.6	4000
RMB005	2.00	3000
DQ	2.00	4000

4.3.7 Extraction methods

PK analysis requires reliable and selective extraction methods to be developed and optimized for biological matrices prior to analysis. Various extraction methods from blood or plasma were investigated to determine the maximal recovery and reproducibility from the matrix. This included protein precipitation extraction (PPE) with acidified and basified organic solvents such as acetonitrile (ACN) and methanol (MeOH), mixtures of ACN and MeOH or liquid-liquid extraction (LLE) over a broad pH range (pH 3–11).

Briefly, WHN012 required liquid-liquid extraction with aqueous buffer at pH 8 and ethyl acetate. The plasma samples (15 μL) were vortexed with 35 μL buffer containing an appropriate concentration of the ISTD and 350 μL ethyl acetate for 2 minutes. The samples were centrifuged at 5590 g for 5 minutes. The organic phase (300 μL) was transferred to clean polypropylene test tubes and was evaporated to dryness under a

steady stream of nitrogen. The dried samples were reconstituted with a mixture of aqueous and organic mobile phases (1:1, v/v), transferred to a 96-well analysis plate and analysed with LC-MS/MS.

For the analysis of PhX6, AD01, DpNEt, RMB005, and DQ, 20 μL of whole blood sample was precipitated with 100 μL ice cold organic solvent (Table 4-2) containing an appropriate concentration of the ISTD and vortexed for 1 minute. Following centrifugation at 5590 g for 5 minutes, 50 μL of the supernatant was transferred to a 96-well analysis plate. Fifty microliters of aqueous mobile phase were added to the samples before submission for LC-MS/MS analysis. Adequately high and reproducible recovery was obtained with the above described methods, as shown by the percentage recovery and precision in Table 4-2.

Table 4-2: Summary of optimized extraction methods from biological matrices and recovery

Compound	Matrix	Extraction method	Mean % recovery (% CV)
WHN012	Plasma	LLE (pH 8)	112 (3.9)
PhX6	Whole blood	PPE[a]	95 (2.3)
AD01	Whole blood	PPE[a]	106 (8.6)
DpNEt	Whole blood	PPE[a]	88 (11.3)
RMB005	Whole blood	PPE[b]	62 (0.1)
DQ	Whole blood	PPE[b]	60 (11.1)

ACN, acetonitrile; FA, formic acid; LLE, liquid-liquid extraction; PPE, protein precipitation extraction; [a]0.1% FA in ACN; [b]100% ACN

4.3.8 LC-MS/MS quantifications

The transitions used for quantification of the compounds are listed in Appendix C. These transitions were followed on an AB Sciex 3200 QTRAP mass spectrometer. Quantification accuracy and precision were measured for the calibration range of the standard curve and the quality controls samples. The quantification statistics of each compound are shown in

Appendix D. Overall the analytical methods performed well during PK sample analysis with standard and QC samples achieving an accuracy (%Nom) between 81.3–114.8% for all samples, with precision (%CV) below 14.8%, indicating good reproducibility.

Correlation coefficients for all curves were greater than 0.998. Carryover was assessed during each experiment using an extracted blank matrix sample injected right after the highest calibration standard. No significant carryover was observed.

4.3.9 Validation experiments

The validation guidelines from the FDA[258] and EMEA[259], as referred to in Chapter 3, suggest that bioanalytical methods used during preclinical development should be validated as FFP. The validation of sample handling, processing, and analysis during PK experiments were done to ensure reliability of the results. The following validation experiments were conducted: stability of compounds in stock solutions and working solutions, autosampler stability, carry-over, matrix effects, stability in matrix, specificity, and extraction recovery. The validation data of all compounds are presented in Appendix D.

4.3.10 Data analysis

Whole blood and plasma concentrations of the compounds were determined using the same optimised quantitative LC-MS/MS analytical methods described in Appendix C. Quantification of the analytes (metabolites) was done using quadratic regression of peak area ratio versus concentration with 1/concentration (1/x) weighting. Experimental sample concentrations were calculated from the calibration curve. All calibration curves showed regression above 0.988. Calibration curves of all compounds are listed in Appendix D.

4.3.11 Non-compartmental analysis

Study samples were analysed in terms of concentration versus time. The concentrations obtained from the calibration curves were used during non-compartmental analysis

(NCA), using Microsoft Excel Add-In PKSolver[309] to determine the following PK parameters:

- C_{max} in μM
- T_{max} in hours
- $t_{1/2}$ in hours
- Area under the concentration-time curve from zero to infinity ($AUC_{0-\infty}$) in min·μmol/L
- CL in mL/min/kg
- Vd in L/kg
- BA in percentage

4.4 Results and discussion

The seven compounds were administered orally and intravenously to healthy mice. Although the experimental endpoint of sample collection was at 24 hours, not all compounds remained above the limit of quantitation. The exception to this was WHN012, for which sample collection only continued until 4 hours. The limit of quantitation for the compounds were as follows: 2.00 ng/mL (RMB005 and DQ); 3.9 ng/mL (WHN012 and PhX6); 7.80 ng/mL (AD01) and 15.6 ng/mL (DpNEt).

In order to determine if the methods applied to analyse the PK samples were reliable and robust, several validation tests were evaluated. Overall, the methods used to administer, extract, and process the samples, proved to be robust in providing accurate and reproducible results. Results from validation tests are summarised in Appendix D.

4.4.1 WHN012

Table 4-3: Summary of *in vitro* ADME characteristics of WHN012

	***In vitro* ADME assays**								
Compound	Solubility (uM, pH 2/6.5/7.4)	LogD (pH 7.4)	$LogP_{app}$ (pH 6.5)	Plasma $t_{1/2}$ (min)	PPB (%)	Microsomal protein binding (%)		Predicted hepatic CL (mL/min/kg)	
						Mouse	Human	Mouse	Human
WHN012	10/24/27	1.9	-3.2	>150	98	54	61	49.1	11.8

WHN012 was administered as described in Section 4.3.4. The concentration administered to animals were increased from in-house standard dosing concentrations from 20 mg/kg to 50 mg/kg for the oral (PO) group and 5 mg/kg to 10 mg/kg for the intravenous (IV) groups (n=3 per group). The latter decision was made since the current clinical artemisinins are highly susceptible to metabolism and characterized by short half-lives and rapid elimination.[271,310] Initially, the absorption and metabolism of WHN012 was of main interest through a more intensive 4 hour sampling schedule. If WHN012 had shown more promising data, this would have warranted a follow-up 24-hour PK study. The plasma profiles of WHN012 obtained from intravenous and oral dosing groups are graphically represented in Figure 4-2. Calculated PK parameters are shown in Table 4-4.

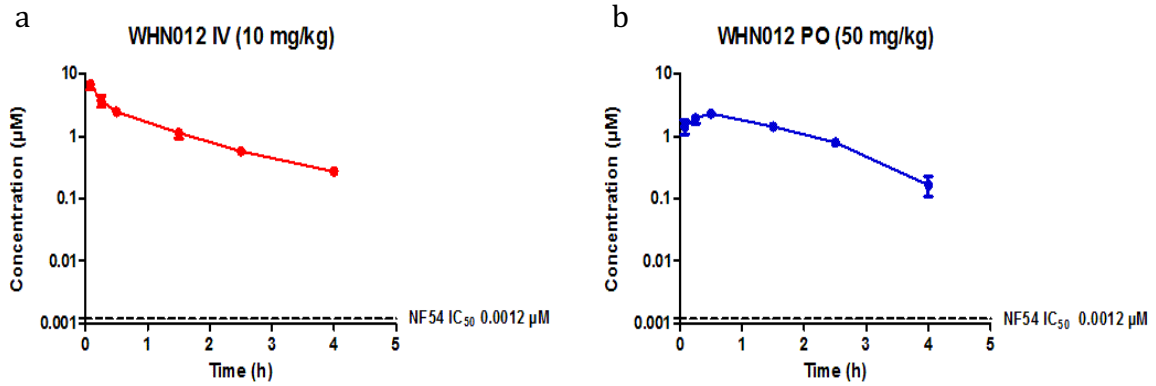

Figure 4-2: The concentration-time profiles of WHN012 after a) intravenous and b) oral administration of the compound. The IC_{50} of the NF54 parasite strain is indicated by the dashed line. Values are mean ± SEM.

Table 4-4: Summary of PK parameters of WHN012 following oral and intravenous administration in mice.

	Value of the parameter by administration route (mean ± SEM)	
Parameter	PO (50 mg/mL)	IV (10 mg/mL)
C_{max} (µM)	2.32 ± 0.34	
T_{max} (h)	0.50 ± 0.00	
Elimination $t_{1/2}$ (h)		1.34 ± 0.28
CL (mL/min/kg)		58.90 ± 2.01
Vd (L/kg)		6.92 ± 1.71
$AUC_{0-\infty}$ (min·µmol/L)	289 ± 31	347 ± 11
BA (%)	17 ± 2	

Following single oral administration of 50 mg/kg, the plasma concentration rapidly increased to a C_{max} of 2.32 µM after 30 minutes (T_{max}). The plasma concentration of WHN012 remained above the *in vitro* IC_{50} for at least 4 hours as indicated in Figure 4-2a and b. The mean area under the curve ($AUC_{0-\infty}$) was 289 ± 31 min·µmol/L.

Following intravenous administration of a single 10 mg/kg dose, there was a slightly faster elimination phase that lasted for the first 30 min, after which the rate of elimination was apparently constant. The elimination $t_{1/2}$ was 1.34 ± 0.28 hours. This was reflected by a moderate CL rate of 58.90 ± 2.01 mL/min/kg. The Vd was 6.92 L/kg and the mean $AUC_{0-\infty}$ values of WHN012 after intravenous dosing was 347 ± 11 min·µmol/L. The absolute oral BA was calculated by comparison of the intravenous an oral dose to their respective AUC's. A low BA of 17% was observed for WHN012.

The predicted *in vitro* ADME characteristics of WHN012 correlated well with the *in vivo* PK profile. Although the predicted solubility at physiological pH could have limited intestinal absorption of WHN012, the compound was rapidly absorbed, as indicated by the T_{max}, owing to ideal lipophilicity and permeability properties. The AUC's from intravenous and oral dosing were low, considering the high dosing concentration. The $AUC_{0-\infty}$ from intravenous dosing was expected to be higher, as 100% of the drug is

administered into circulation, which may be consequential of the fast rate of CL.[257,276] C_{max}, the point at which absorption of WHN012 was greater than the distribution and elimination, is an important parameter to consider, as it could indicate if plasma concentration levels could cause toxicity, especially from higher doses. Fortunately, WHN012 had high selectivity (SI>1000) towards parasites, as the compound expressed very low general toxicity (IC_{50} >200 μM).

The calculated elimination $t_{1/2}$ was short ($t_{1/2}$ 1.34 h) following intravenous administration and, though not as rapid as artemisinin ($t_{1/2}$ 0.8 h),[311] still comparable to other artemisinins.[310,312,313] Fast eliminating drugs used for malaria therapy, such as the artemisinin class of compounds which have very short half-lives, are advised to be used in combination with longer $t_{1/2}$ drugs to prevent the development of resistance by parasites.

The systemic CL of 58.90 ± 2.01 mL/min/kg was considered moderate to high.[276] The idea behind incorporation of the electronegative fluorine atom into the aromatic group in the WHN series was to render the compounds more resistant to metabolic oxidation during Phase I metabolism; as has previously been demonstrated in other fluorinated artemisinin derivatives as well as quinine derivatives.[314–318] Unfortunately, the use of the *p*-fluorophenyl group in WHN012 did not have a marked effect–the compound still presented moderate to high CL. The hepatic CL predicted from the *in vitro* intrinsic CL (49.1 mL/min/kg) was slightly lower than the observed CL. In addition, the *in vivo* intrinsic CL of the unbound fraction ($CL_{int,u}$) was calculated–as this offers the most accurate interpretation of CL.[251] The actual $CL_{int,u}$ value of 2950 mL/min/kg, so derived, suggested that CL was in fact much faster, as was predicted from the metabolic stability assays described in Chapter 3. Although plasma protein binding was determined in human plasma, it offered valuable insights in the interpretation of PK data, as demonstrated by the *in vivo* $CL_{int,u}$.

The elimination trend of the intravenous profile in Figure 4-2a suggested that WHN012 expressed first order elimination kinetics, by which a constant fraction of drug is eliminated per unit time. The AUC0-∞ indicates the total exposure of the compound in the system. By comparing the intravenous and oral profiles, the oral $AUC_{0-\infty}$ is lower than that of the intravenous. This suggests that poor solubility, as characterized during *in vitro* ADME evaluations (Section 3.4.1), could significantly hamper absorption of WHN012. In addition, WHN012 could suffer first pass metabolism after absorption when passing

through the liver upon oral dosing, as the first pass effect is avoided during intravenous administration. It is also important to consider that extraction by the gut-wall could potentially contribute to the low AUC values.[251]

The intravenous profile of WHN012 incorporates a high Vd, indicating that the compound distributes to the tissues and other compartments. In relationship to the lipophilicity ($LogD_{7.4}$ 1.94) and high protein binding (f_u 0.02) determined from the *in vitro* investigations, it is possible that WHN012 could bind non-specifically to other tissues. Substantial distribution into tissue could result in low AUC of the compound. The BA of WHN012 was low (17%) and below that observed for artemisinin, DHA and artemether which ranges from 19-35% in rats.[271,310] Although these values are considered very low, the high intrinsic activities can partially counter the effect of low oral BA. In the context of this project, further optimization to the WHN series in terms of solubility and stability are imperative for the development of newer, more efficient artemisinin derivatives.

4.4.2 AD01

Table 4-5: Summary of in vitro ADME characteristics of AD01

	***In vitro* ADME assays**								
Compound	Solubility (uM, pH 2, 6.5 and 7.4)	LogD (pH 7.4)	$LogP_{app}$ (pH 6.5)	Plasma $t_{1/2}$ (min)	PPB (%)	Microsomal protein binding (%)		Predicted hepatic CL (mL/min/kg)	
						Mouse	Human	Mouse	Human
AD01	>150/>150 />150	0.2	-6.4	85	nd	nd	nd	80.6	16.2

The analogue of MB was administered orally (n=5) and intravenously (n=5) to mice as described in Section 4.3.4. AD01 is a salt with a chloride counter ion; this results in the net molecular mass of 340.5 g/mol. As a result, the net concentration of AD01 'active compound' upon dosing was calculated as 18.1 mg/kg and 4.6 mg/kg for oral and intravenous dosing, respectively. Whole blood concentration-time profiles of AD01 obtained from intravenous and oral dosing groups are graphically represented in Figure

4-3a and 4-3b, respectively. The PK parameters were determined by NCA and shown in Table 4-6 below.

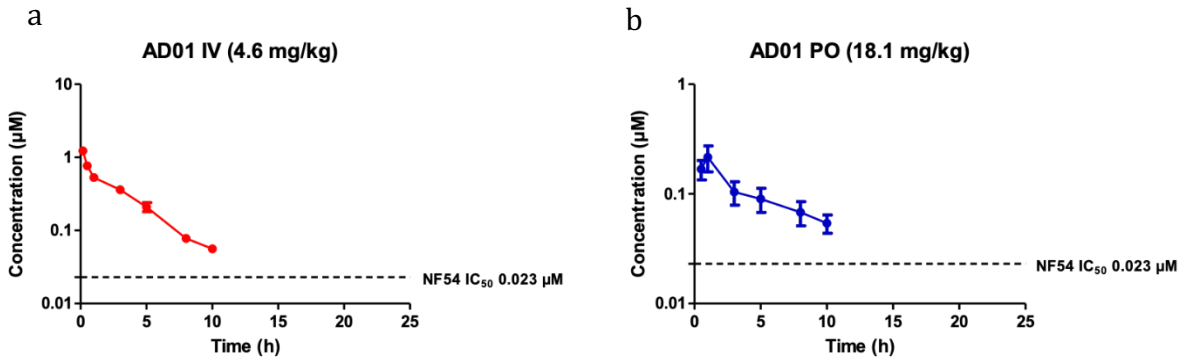

Figure 4-3: The concentration-time profiles of AD01 after a) intravenous (n=5) and b) oral (n=5) administration of the compound. The IC_{50} of the NF54 parasite strain is indicated by the dashed line. Values are mean ± SEM.

Table 4-6: Summary of PK parameters of AD01 following oral and intravenous administration in mice.

	Value of the parameter by administration route (mean ± SEM)	
Parameter	PO (18.1 mg/mL)	IV (4.6 mg/mL)
C_{max} (µM)	0.25 ± 0.05	
T_{max} (h)	0.88 ± 0.13	
Elimination $t_{1/2}$ (h)		2.51 ± 0.07
CL (mL/min/kg)		74.41 ± 6.68
Vd (L/kg)		16.24 ± 1.73
$AUC_{0-\infty}$ (min·µmol/L)	101 ± 19	186 ± 15
BA (%)	15 ± 4	

Following a single oral administration of 18.1 mg/kg, AD01 reached a C_{max} of 0.25 µM in whole blood at 0.88 hours. The C_{max} achieved after oral administration reached a concentration higher than the *in vitro* IC_{50} (0.023 µM), and the exposure levels remained

above the IC_{50} for at least 10 hours. AD01 had very high selectivity towards the parasites (SI = >1000). The $AUC_{0-\infty}$ was 101 ± 19 min·µmol/L.

AD01 blood concentrations were detectable for 10 hours after IV administration, after which the signal fell below the limit of quantitation (7.80 ng/mL). An apparent elimination $t_{1/2}$ of 2.51 hours was calculated, which was reflective of the rapid rate of CL (74.41 mL/min/kg). The apparent Vd was 16.24 L/kg and $AUC_{0-\infty}$ was 186 ± 15 min·µmol/L. Consequently, a low BA of 15% was observed for AD01.

The overall *in vivo* PK profile of AD01 correlated well with the *in vitro* ADME characteristics. It was predicted that AD01 would present high solubility at a low and physiological pH levels, low partitioning to lipid environments (LogD < 1) and low passive transcellular permeability. Lipophilicity and permeability influence the extent of absorption from the oral dose. The low C_{max} value observed from oral dosing (Table 4-6) suggested that passive diffusion over the intestinal membrane was limited by the low lipophilicity and ionization of the compound in solution.[319]

In vitro microsomal stability assays allowed scaling of the CL_{int} to predicted *in vivo* hepatic CL. The compound was expected to be rapidly cleared with a predicted hepatic CL_H value of 80.6 mL/min/kg. The calculated *in vivo* CL (74.41 ± 6.68 mL/min/kg) was very similar to the predicted CL, both indicating that AD01 was rapidly cleared from the system. Unfortunately, intrinsic *in vivo* CL values could not be reported, as determination of protein binding was not possible for AD01.

AD01 was unstable during investigation of stability in human plasma (Section 3.4.4), which suggested non-CYP biotransformation potentially contributed to the metabolism of AD01.[320] The relatively short $t_{1/2}$ and rapid CL of AD01 resulted in an incomplete profile with shorter observation time for the whole blood concentrations, above the limit of quantitation, following intravenous dosing. The elimination trend of the intravenous graph suggests that AD01 is subject to first order elimination kinetics. A fast CL rate also impacted the extent of exposure, which was reflected by the AUC's.

The low AUC observed in oral PK profile indicate the oral BA of AD01 is very low: this was calculated to be 15%. This could be due to many reasons, such as first pass metabolism in the gut wall or liver, poor absorption due to low partitioning to lipid environments, low passive transcellular permeability and potential efflux transport. The latter was investigated by Sanarathna *et al.* in a study which strongly suggest that MB is a substrate

for P-gp and multidrug resistance protein which mediated its transport out of cells.[270] Because AD01 and MB are structurally so similar, these findings suggest that AD01 could also be highly susceptible to efflux transport. Additionally, the stability of AD01 in plasma was low and suggested chemical interactions, such as hydrolysis in plasma, also limited the BA of AD01.[321] If the circulating whole blood concentrations following oral dosing is unable to remain above the IC_{50}, more frequent dosing would be required to maintain potentially therapeutic levels.

With the above in mind, the effective combination of AD01 with a fast-acting artemisinin and potentially a third partner quinolone, could remain beneficial in the redox drug combination rationale. AD01 presented a high apparent Vd (16.24 ± 1.73 L/kg, Table 4-6), similar to MB. In a study carried out by Peter *et al.*, the PK profile of MB and its distribution into organs in rats was established. It was found that MB was subjected to extensive 'first-pass distribution' to the brain, intestinal wall, liver, and bile, following intravenous and intraduodenal administration.[322] The researchers concluded that this was a likely reason for large difference in the observed AUC values.

The target of antimalarial therapy resides predominantly in the blood. Intravenous administration, which resulted in higher circulating concentrations, would be preferred. However, this route of administration poses its own challenges with regards to patient compliance, storage, and access to treatment. Considering the well-known synergy of MB with artemisinins,[207,323] it is worth investigating the potential interaction of AD01 with an artemisinin, as this can further guide and encourage optimisation of MB analogues in future studies.

4.4.3 PhX6

Table 4-7: Summary of in vitro ADME characteristics of PhX6.

	***In vitro* ADME assays**								
Compound	Solubility (uM, pH 2, 6.5 and 7.4)	LogD (pH 7.4)	$LogP_{app}$ (pH 6.5)	Plasma $t_{1/2}$ (min)	PPB (%)	Microsomal protein binding (%)		Predicted hepatic CL (mL/min/kg)	
						Mouse	Human	Mouse	Human
PhX6	>150/<5/ <5	1.0	-4.4	>150	90	99	99	88.2	20.2

The phenoxazine derivative PhX6 was administered orally (n=5) and intravenously (n=5) to mice as described in Section 4.3.4. PhX6 was provided as the conjugate acid with a nitrate (NO_3^-) counterion and the dosing concentrations were adjusted according to salt formation. The whole blood concentration profiles of PhX6 obtained from intravenous and oral dosing groups are graphically represented in Figure 4-4a and 4-4b, respectively. Following PK samples analysis, NCA was used to determine the PK parameters shown in Table 4-8, below.

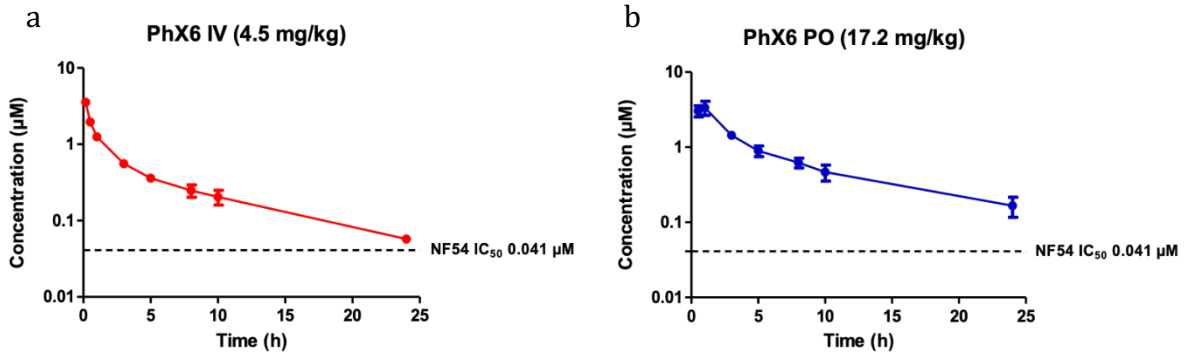

Figure 4-4: The concentration-time profiles of PhX6 after a) intravenous and b) oral administration of the compound. The IC_{50} of the NF54 parasite strain is indicated by the dashed line. Values are mean ± SEM.

Table 4-8: Summary of PK parameters of PhX6 following oral and intravenous administration in mice.

	Value of the parameter by administration route (mean ± SEM)	
Parameter	PO (17.2 mg/mL)	IV (4.5 mg/mL)
C_{max} (μM)	3.45 ± 0.68	
T_{max} (h)	0.80 ± 0.12	
Elimination $t_{1/2}$ (h)		7.96 ± 0.73
CL (mL/min/kg)		21.47 ± 1.76
Vd (L/kg)		14.92 ± 2.09
$AUC_{0-\infty}$ (min·μmol/L)	1150 ± 216	540 ± 44
BA (%)	60 ± 12	

Following oral administration at a single dose of 17.2 mg/kg (Figure 4-4b), PhX6 reached a C_{max} concentration of 43.45 ± 0.68 μM. Thereafter, the concentration declined as a multiphasic elimination curve. The exposure concentrations of PhX6 remained above the *in vitro* IC_{50} of activity for the duration of the study. PhX6 proved to be highly selective towards parasites with a SI > 1000 (Table 2.3, Section 2.3). The observed C_{max} was reached at approximately 0.80 hours. The mean $AUC_{0-\infty}$ was 1150 ± 216 min·μmol/L and indicated encouraging overall exposure of the compound following oral administration.

PhX6 was slowly cleared from the systemic circulation at 21.47 ± 1.76 mL/min/kg which resulted in a long $t_{1/2}$ of 7.96 hours. The Vd was 14.90 L/kg and the mean $AUC_{0-\infty}$ after IV dosing was 540 ± 44 min·μmol/L. Of all the compounds investigated in this chapter, PhX6 presented the highest oral BA of 60%.

The *in vitro* ADME characteristics correlated well with the *in vivo* observed PK profile of PhX6. The lipophilicity and passive transcellular permeability of PhX6 allowed for good absorption from the oral dose, as indicated by the C_{max} and AUC values. The *in vitro* kinetic solubility assay predicted that PhX6 would have limited solubility at pH 7.4 and 6.5, and high solubility at pH 2. The physiological pH range of the intestinal environment is between 6.8–8, where drugs are predominantly absorbed.[278] Comparing the apparent permeability (-4.4) and solubility (greater than 150 μM at pH 2 and less 5 μM at pH 6.5

and pH 7.4, respectively), it is possible that as ionised PhX6 molecules leave the stomach (pH 1.4–2.1) it gradually transformed to the unionized species as it passes though the intestine (pH 4.4–6.6) in balance between soluble (ionised) and permeable (unionised) species.[324] PhX6 is probably absorbed from early sections of the duodenum where the stomach contents from gastric emptying first enters the intestine.[269] A test preparation of PhX6 in the dosing formulation (deionised water) was prepared before the experiment to test the solubility. The apparent satisfactory solubility which was observed during *in vivo* evaluation, may be attributed to the difference in compound preparation during *in vitro* solubility testing, as the dosing formulation preparation was directly in aqueous solution.

The microsomal assays predicted extensive liver metabolism (CL_H 88.2 mL/min/kg). However, this was not observed in the mouse PK study (21.47 ± 1.76 mL/min/kg). Additionally, the derived $CL_{int,u}$ suggested a much faster CL (214.7 mL/min/kg). The elimination phase of PhX6, as indicated in Figure 4-4a, shows multiphasic elimination. Following intravenous administration, PhX6 presented a long $t_{1/2}$ of approximately 8 hours. Compounds with longer half-lives are favoured for use in combination with faster acting, short $t_{1/2}$ drugs. The AUC obtained from oral administration shows that the compound is significantly absorbed in the bloodstream. This suggested that PhX6 can be maintained in the system and offers better potential to elicit its pharmacological effect. Therefore, greater exposure of a drug in the system could translate to greater concentrations of the compound available at the therapeutic site of action.[36] Subsequently, combinations of PhX6 with artemisinins would further encourage its development as a redox drug candidate.

Benzo(α)phenoxazines that were previously investigated[325] showed similar PK profiling to PhX6. Benzo(α)phenoxazine derivatives possessing the aminopyridine ring not only presented comparable activity to MB, but also have superior PK profiles to derivatives containing, for example, alkyl halides. The *in vitro* selectivity and PK properties of PhX6 are encouraging for further development.

4.4.4 DpNEt

Table 4-9: Summary of in vitro ADME characteristics of DpNEt.

	***In vitro* ADME assays**								
Compound	Solubility (uM, pH 2, 6.5 and 7.4)	LogD (pH 7.4)	$LogP_{app}$ (pH 6.5)	Plasma $t_{1/2}$ (min)	PPB (%)	Microsomal protein binding (%)		Predicted hepatic CL (mL/min/kg)	
						Mouse	Human	Mouse	Human
DpNEt	>150/>150 />150	2.3	-3.7	>150	94	16	25	22.3	4.00

The thiosemicarbazone derivative DpNEt was administered orally (n=5) and intravenously (n=5) as described in Section 4.3.4. The experimental samples were analysed with LC-MS/MS and the whole blood concentration profiles obtained from intravenous and oral dosing groups are graphically represented in Figure 4-5. The data was analysed with NCA analysis in order to determine the PK parameters listed in Table 4-10 below.

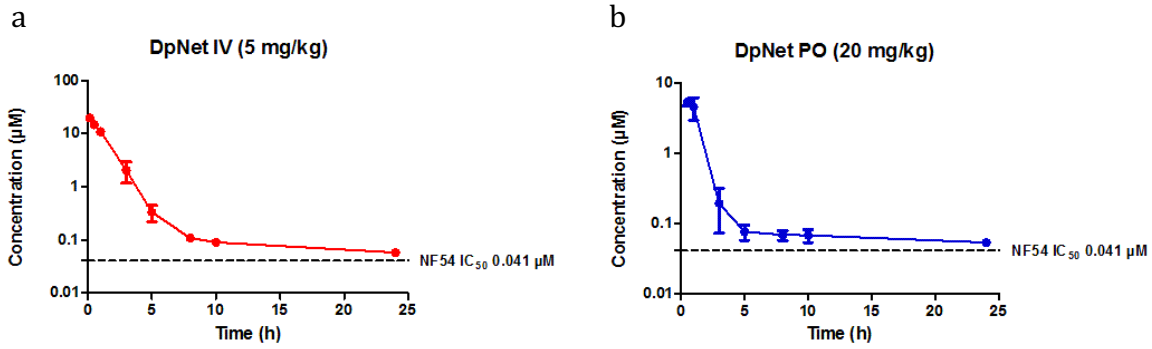

Figure 4-5: The concentration-time profiles of DpNEt after a) intravenous and a) oral administration of the compound. The IC_{50} of the NF54 parasite strain is indicated by the dashed line. Values are mean ± SEM.

Table 4-10: Summary of PK parameters of DpNEt following oral and intravenous administration in mice.

	Value of the parameter by administration route (mean ± SEM)	
Parameter	PO (20 mg/mL)	IV (5 mg/mL)
C_{max} (µM)	6.32 ± 1.15	
T_{max} (h)	0.70 ± 0.12	
Elimination $t_{1/2}$ (h)		1.12 ± 0.13
CL (mL/min/kg)		10.20 ± 0.93
Vd (L/kg)		1.00 ± 0.16
$AUC_{0-\infty}$ (min·µmol/L)	550 ± 148	1795 ± 198
BA (%)	8 ± 2	

Following a single oral dose of 20 mg/kg, DpNEt exhibited a mean C_{max} concentration of 6.32 ± 1.15 µM after 0.70 hours. The exposure concentrations of DpNEt remained above the IC_{50} for the duration of the experimental time period. The mean $AUC_{0-\infty}$ was 550 ± 148 min·µmol/L. The elimination $t_{1/2}$ was short (1.12 ± 0.13 h). DpNEt was slowly cleared from the system (10.20 ± 0.93 mL/min/kg). The mean IV group $AUC_{0-\infty}$ was quantified as 1795 ± 198 min·µmol/L and the Vd was 1 L/kg. The BA was calculated as 8%.

The properties of DpNEt predicted from the *in vitro* ADME assays suggested that DpNEt would be well absorbed across the intestinal membrane (Table 4-9). High solubility was observed across all pH levels tested (>150 µM), as well as high apparent passive transcellular permeability ($LogP_{app}$ -3.7). DpNEt also expressed ideal lipophilicity in the range which facilitates the absorption across membranes. Although a high C_{max} was achieved, suggesting good absorption, high BA was not achieved.

BA relies on two main parameters, namely absorption and CL.[251] It is worth considering the possibilities why DpNEt had a low BA, despite the extent of absorption. Firstly, the predicted hepatic CL obtained from *in vitro* metabolic stability assays (CL_H 22.3 mL/min/kg, Table 4-9) correlated well with the *in vivo* blood CL (10.2 mL/min/kg). However, when including the effect of protein binding to determine $CL_{int,u}$, a value of 170

mL/min/kg was calculated. Thus, the systemic CL did not correlate with the low BA. One may speculate that the liver is not the main route of CL for DpNEt.

Three physiological processes are involved during CL of xenobiotics from the system namely metabolic transformation, renal excretion, and hepatobiliary excretion. The physiochemical properties of a compound may give indications of which rate-determining mechanism would be favoured. In the case of a lipophilic compound, metabolic transformation by the liver is favoured, whereas hydrophilic or polar compounds are more likely to be cleared by active or passive excretion.[251]

The hydrophilicity and polar nature of DpNEt in conjunction with the *in vivo* parameters suggest that the route of elimination of DpNEt is more likely to be via hepatobiliary or renal excretion. During hepatobiliary excretion, drugs are actively transported by organic-anion-transporting polypeptides, breast cancer resistance protein (BCRP), P-gp and multidrug resistance protein uptake/efflux transporters expressed on the hepatocyte membrane. Transporter proteins recognize substrates in the blood and secrete them into the bile via canalicular transporters (Figure 4-6).[251,326] CL by the kidneys are mediated by glomerular filtration. Compounds that are not highly bound to plasma proteins, such as DpNEt, are able to pass through the glomeruli into the proximal convoluted tubule, or be deposited into the renal blood flow by active transporters expressed at the proximal convoluted tubule.[251]

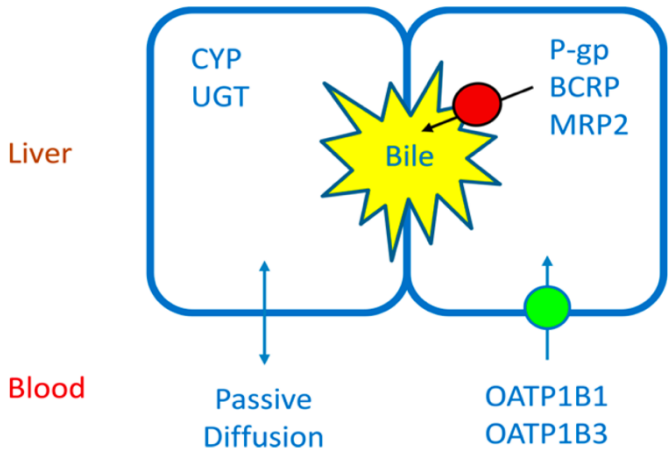

Figure 4-6: Schematic of the hepatobiliary system. Reprinted with permission from Smith D.A, Beaumont K., Maurer T.S, Di L., Clearance in drug design. J Med Chem. 2019;62(5):2245–55. Copyright (2019) American Chemical Society.[251]

Transport proteins responsible for active uptake such as P-gp, MRP-2, MRP-4 and BCRP, are also widely present on the apical side of enterocyte membranes.[327] Many clinically used drugs for various diseases encounter the obstacle of multidrug resistance induced by molecular 'pumps' which actively remove xenobiotics from cells. These may comprise a family of protein transporters collectively known as the adenosine triphosphate ATP-binding cassette superfamily, of which P-gp is the most prevalent.[328,329] According to Aller *et al.*, P-gp transport proteins are partial to hydrophobic and aromatic interactions[330] and thus aromatic rings such as those found in DpNEt could make the compound more likely to be a substrate for P-gp. However, this needs to be confirmed with cell-based assays in order to obtain more conclusive results.

The thiosemicarbazone chelators have proven their antimalarial potency and potential as antimalarial drug candidates.[331–333] Parkinson *et al.* evaluated the efficacies of a series of thiosemicarbazones in both *in vitro* and *in vivo* and identified the thiosemicarbazone TSC3 with a structure similar to DpNEt as highly effective (ED_{50} 1.2 mg/kg/day) in suppressing *Plasmodium berghei* ANKA-strain parasites in the Peters 4-day test after once daily oral dosing of 16 mg/kg over a 4 day period.[334] Further evaluation in a modified Thompson test revealed that TSC3 had a cure rate of 58% at 16 mg/kg administered orally for 3 days. These promising data encourages the optimization of this series of compounds through conduct of careful PK and pharmacodynamic studies. However, the surprisingly low oral BA of DpNEt precludes further investigation in combination studies.

4.4.5 RMB005

Table 4-11: Summary of in vitro ADME characteristics of RMB005.

	***In vitro* ADME assays**								
Compound	Solubility (uM, pH 2, 6.5 and 7.4)	LogD (pH 7.4)	$LogP_{app}$ (pH 6.5)	Plasma $t_{1/2}$ (min)	PPB (%)	Microsomal protein binding (%)		Predicted hepatic CL (mL/min/kg)	
						Mouse	Human	Mouse	Human
RMB005	<5/<5/<5	3.2	-6.3	>150	92	99	99	81.2	12.6

The DQ amide RMB005 was used as aqueous suspension and organic dosing formulations, as described in Section 4.3.4. The whole blood concentration profiles of RMB005 obtained from intravenous (n=5) and oral (n=5) dosing groups are graphically represented in Figure 4-7. The data was analysed by NCA to determine the parameters listed below in Table 4-12.

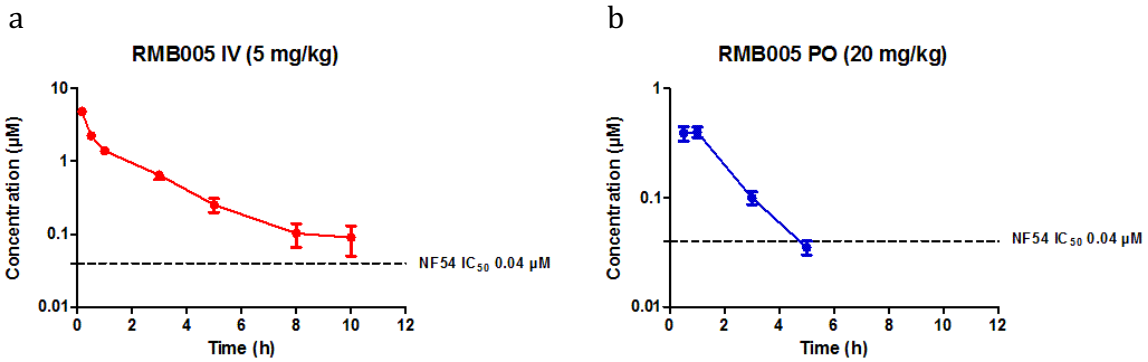

Figure 4-7: The concentration-time profiles of RMB005 after a) intravenous and b) oral administration of the compound. The IC_{50} of the NF54 parasite strain is indicated by the dashed line. Values are mean ± SEM.

Table 4-12: Summary of PK parameters of RMB005 following oral and intravenous administration in mice.

	Value of the parameter by administration route (mean ± SEM)	
Parameter	PO (20 mg/mL)	IV (5 mg/mL)
C_{max} (µM)	0.49 ± 0.02	
T_{max} (h)	0.70 ± 0.12	
Elimination $t_{1/2}$ (h)		2.62 ± 0.61
CL (mL/min/kg)		28.50 ± 2.17
Vd (L/kg)		6.59 ± 1.83
$AUC_{0-\infty}$ (min·µmol/L)	59 ± 2	377 ± 32
BA (%)	4 ± 0.3	

Following a single oral dose of 20 mg/kg, the mean whole blood C_{max} reached a maximum of 0.49 ± 0.02 µM at approximately 0.70 hours (Table 4-12). Even though the total systemic exposure of RMB005 was considered poor, the C_{max} was above the *in vitro* IC_{50} (0.04 µM, Fig 4-7). The whole blood concentrations were, however, below the reliable limit of quantification after five hours and fell below that of the IC_{50}. The mean $AUC_{0-\infty}$ was 59 ± 2 min·µmol/L. After a single intravenous dose of 5 mg/kg, the CL was classified as relatively low (28.50 ± 2.17 mL/min/kg), and the $t_{1/2}$ was relatively short (2.62 ± 0.61). The mean $AUC_{0-\infty}$ was 377 ± 32 min·µmol/L and the BA was low (4%).

The *in vivo* profile of RMB005 correlates well with the predicted *in vitro* ADME parameters in terms of solubility and exposure. Although RMB005 was quickly absorbed, the extent of exposure was limited–presumably by the poor solubility (<5 µM). The dynamic state of equilibrium at which solubility functions in a living system, as described in Chapter 3, likely did not favour membrane permeability of the small amount of compound that was available in solution, as the passive permeability was also very low ($LogP_{app}$ -6.3). Consequently, the low AUC observed following oral dosing is an intricate product of the lack of solubility as well as the restricted membrane permeability and resulted in very low BA. The BA was relative to DQ, which showed a 6% relative BA after an 80 mg/kg oral microsuspension dose in mice.[229]

In terms of efficacy at the pharmacological target, RMB005 would potentially not be able to passively cross membranes, even if only a small amount is able to remain in solution. The calculation of CL_{int} which corrected for the free fraction (f_u 0.08), produced a CL value much higher than the original parameter (356 mL/min/kg). As RMB005 is moderately to highly bound to plasma proteins, the inclusion of the unbound fraction allows for more appropriate interpretation of the compound being metabolised in the system[251] and is reflected by the short $t_{1/2}$ (2.62 h). Poor PK properties of this compound precludes further investigation.

4.4.6 RMB059 and RMB060

Table 4-13: Summary of in vitro ADME characteristics of RMB059 and RMB060.

	***In vitro* ADME assays**								
Compound	Solubility (uM, pH 2, 6.5 and 7.4)	LogD (pH 7.4)	$LogP_{app}$ (pH 6.5)	Plasma $t_{1/2}$ (min)	PPB (%)	Microsomal protein binding (%)		Predicted hepatic CL (mL/min/kg)	
						Mouse	Human	Mouse	Human
RMB059	<5/<5/<5	2.9	-5.8	66	nd	nd	nd	75.2	19.7
RMB060	nd	2.9	-6.3	<8	nd	nd	nd	77.2	18.6

As discussed in Chapter 2, RMB059 and RMB060 were synthesised from DQ as newer decoquinate derivatives. These compounds were introduced and investigated subsequently to RMB005. The aim in this investigation was to establish if RMB059 and RMB060 had improved PK profiles in terms of solubility, stability and exposure relative to RMB005. RMB059 and RMB060 were administered orally (n=3) and intravenously (n=3) as described in Section 4.3.4.

During LC-MS/MS assay development, it was discovered that the compounds RMB059 and RMB060 were very unstable. Further investigation and method validation tests for potential explanations revealed that the compounds were converted to DQ, the 'parent' compound from which they were synthesized.

The major challenge of working with the carbamate quinolone derivatives RMB059 and RMB060 was their stability in whole blood. The compounds were generally unstable in whole blood which suggests that they would be labile as soon as being inserted or absorbed into the systemic circulation, and potentially be hydrolysed in the stomach.

The validation of bioanalytical methods of DQ are summarised in Appendix D. NCA analysis of DQ (as metabolite of RMB059 and RMB060) was carried out (Table 4-14 and 4-15, respectively). The whole blood concentration profiles of DQ obtained from intravenous and oral dosing of RMB059 and RMB060 are graphically represented in Figures 4-8 and 4-9, respectively.

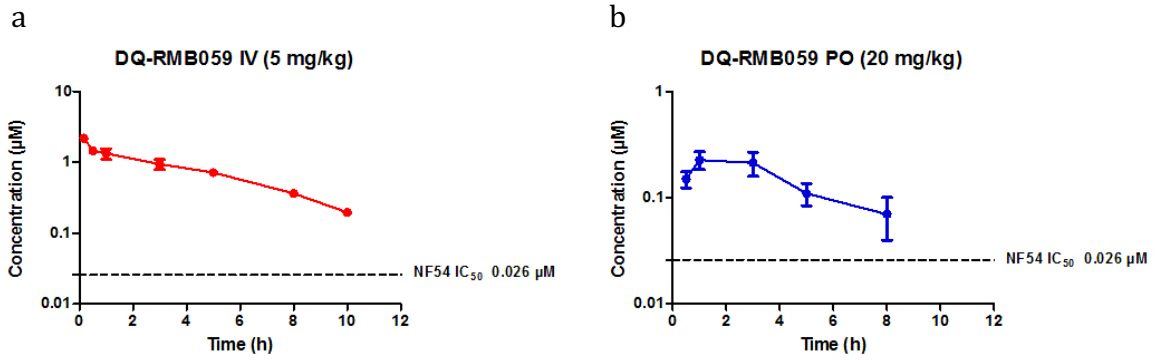

Figure 4-8: The concentration-time profiles of DQ after a) intravenous and b) oral administration of RMB059. The IC_{50} of the NF54 parasite strain is indicated by the dashed line. Values are mean ± SEM.

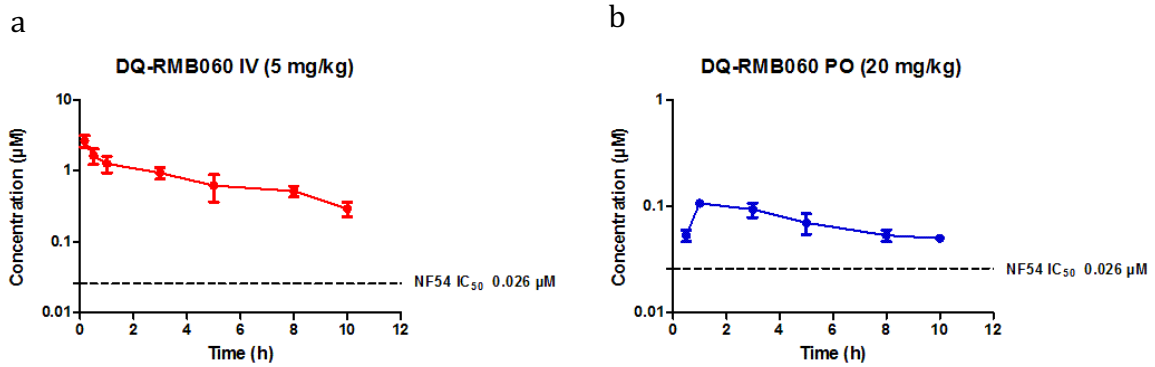

Figure 4-9: The concentration-time profiles of DQ after a) intravenous and a) oral administration of RMB060. The IC_{50} of the NF54 parasite strain is indicated by the dashed line. Values are mean ± SEM.

Table 4-14: Summary of PK parameters of DQ following oral and intravenous administration of RMB059 in mice.

	Value of the parameter by administration route (mean ± SEM)	
Parameter	PO (20 mg/mL)	IV (5 mg/mL)
C_{max} (µM)	0.23 ± 0.05	
T_{max} (h)	1.67 ± 0.67	
Elimination $t_{1/2}$ (h)		4.79 ± 1.66
CL (mL/min/kg)		19.40 ± 3.14
Vd (L/kg)		8.00 ± 2.96
$AUC_{0-\infty}$ (min·µmol/L)	101 ± 44	573 ± 98
BA (%)	nd	

Table 4-15: Summary of PK parameters of DQ following oral and intravenous administration of RMB060 in mice.

	Value of the parameter by administration route (mean ± SEM)	
Parameter	PO (20 mg/mL)	IV (5 mg/mL)
C_{max} (µM)	0.11 ± 0.01	
T_{max} (h)	1.67 ± 0.67	
Elimination $t_{1/2}$ (h)		4.66 ± 1.16
CL (mL/min/kg)		21.50 ± 3.38
Vd (L/kg)		8.88 ± 2.87
$AUC_{0-\infty}$ (min·µmol/L)	63 ± 9	592 ± 108
BA (%)	nd	

The mean C_{max} of DQ after oral dosing of RMB059 was 0.23 ± 0.05 µM. The low C_{max} was probably a combination of hydrolysis in the stomach and blood hydrolysis of RMB059. The C_{max} of DQ was observed at approximately 1.67 hours post-dose as depicted in Figure 4-7B, where after it slowly declined. The whole blood concentrations of DQ remained above the IC_{50} (0.026 µM) for at least 8 hours, after which the concentrations fell below the lower limit of quantitation (LLOQ). The mean $AUC_{0-\infty}$ was 101 ± 44 min·µmol/L. The elimination $t_{1/2}$ was 4.79 hours and CL of DQ was relatively slow (19.40 ± 3.14 mL/min/kg). The Vd was 8 L/kg and the mean $AUC_{0-\infty}$ of DQ following intravenous administration of RMB059 was 573 ± 98 min·µmol/L.

DQ presented a C_{max} concentration of 0.11 µM at 1.67 hours from a single oral dose of RMB060 and the exposure was low (63 ± 9 min·µmol/L). Following the single intravenous administration of RMB060, the elimination $t_{1/2}$ of DQ was 4.66 ± 1.16 hours, which was very similar to RMB059. DQ also demonstrated a slow hepatic CL of 21.50 ± 3.38 mL/min/kg. The Vd was 8.88 L/kg and the mean $AUC_{0-\infty}$ was 592 ± 108 min·µmol/L. The whole blood concentrations of DQ remained above the IC_{50} until 10 hours, after which the concentrations fell below the LLOQ.

With reference to the rationale for investigating the derivatives RMB059 and RMB060, it is concluded that these compounds did not offer improved solubility, systemic exposure, or metabolic stability when compared to RMB005, even though enhancing BA was expected from the incorporation of carbamates.[62] Many physical properties play a critical role in the *in vivo* performance of compounds during PK studies, such as solubility and stability. RMB059 and RMB060 were converted to DQ at a significant rate. Additionally, the exceptionally poor solubility of DQ in water[229] further limited the extent of DQ absorption. From this, it can be concluded that the ethyl ester carbamate quinolone DQ derivative series need optimization in terms of both in terms of solubility, and in enhancing the stability of certain metabolic 'soft-spots' such as the esters, amides, and carbamates which are more susceptible to hydrolysis.[243]

4.5 Summary and conclusion

As described in Chapter 3, bioanalytical assays used during preclinical investigation should be robust, accurate, and precise, and validated according to "fit for purpose" FDA guideline criteria. Validation of the assays included matrix stability, recovery, matrix effects, carry over, and formulation stability. The assays proved to be robust and performed well during PK sample analysis. However, two compounds, RMB059 and RMB060 were exceptions to this outcome, as they were found to be very unstable in whole blood. An assay was developed for DQ (the 'metabolite' of RMB059 and RMB060) to indirectly evaluate PK properties of these compounds.

A summary of PK parameters of all compounds evaluated is shown in Table 4-16. *In vitro-in vivo* correlations were observed between ADME characterisation and PK profiles, and *in vitro* data aided in interpretation of PK parameters.

As described in Chapter 2, the rationale for development of the amino-artemisinin WHN012 and related derivatives originated with the demonstration that the amino-artemisinin AMS has improved PK properties with respect to the current clinically-used artemisinins.[261,335] However, it is found that AMS itself possesses superior solubility (220 μM at pH 7.2) and lipophilicity (LogD 2.49 at pH 7.4) when compared to WHN012.[261]

Haynes *et al.* concluded that AMS offered improved BA and stability in comparison to artemisinin.[261,336] For the purpose of this research project, AMS should be considered as the oxidant partner in the *in vitro* investigations to follow, for the fact that WHN012 did not present improved PK properties. Based on this outcome, AMS was selected as the preferred oxidant partner drug for combination experiments. As mentioned previously, systemic exposure of the compounds fundamentally impacts their efficacy.

The phenoxazine PhX6 and phenothiazine AD01, both potential redox compounds, had oral BA values of 60% and 15%, respectively. Of all the different compounds evaluated in this study, PhX6 had the best PK properties and was identified as the most successful compound to investigate further in *in vitro* combination experiments together with AMS. Additionally, due to previously established synergistic interaction between MB and artemisinins, AD01 was considered for investigation as well.

The PK evaluation of the RMB compounds, derivatives of decoquinate, indicate that these do not have improved PK properties in comparison to DQ, which are potentially due to poor solubility and lack of stability.

The aim of the work described in this chapter was to identify compounds with favourable PK properties for further development. In the next chapter, the *in vitro* combination experiments are discussed for PhX6, AD01, and AMS in fixed-ratio combination analysis.

Table 4-16: Summary of *in vivo* PK parameters after oral and intravenous administration in mice.

Parameter	**Compound**						
	WHN012	AD01	PhX6	DpNEt	RMB005	RMB059-DQ	RMB060-DQ
Intravenous							
Elimination $t_{1/2}$ (h)	1.34 ± 0.28	2.51 ± 0.07	7.96 ± 0.73	1.12 ± 0.13	2.62 ± 0.61	4.79 ± 1.66	4.66 ± 1.16
CL (mL/min/kg)	58.90 ± 2.01	74.41 ± 6.86	21.47 ± 1.76	10.20 ± 0.93	28.50 ± 2.17	19.40 ± 3.14	21.50 ± 3.38
Vd (L/kg)	6.92 ± 1.71	16.24 ± 1.73	14.92 ± 2.09	1.00 ± 0.16	6.59 ± 1.83	8.00 ± 2.96	8.88 ± 2.87
$AUC_{0-\infty}$ (min·µmol/L)	347 ± 11	186 ± 15	540 ± 44	1795 ± 198	377 ± 32	573 ± 98	592 ± 108
Oral							
C_{max} (µM)	2.32 ± 0.34	0.25 ± 0.05	3.45 ± 0.68	6.32 ± 1.15	0.49 ± 0.02	0.23 ± 0.05	0.11 ± 0.01
T_{max} (h)	0.50 ± 0.00	0.88 ± 0.13	0.80 ± 0.12	0.70 ± 0.12	0.70 ± 0.12	1.67 ± 0.67	1.67 ± 0.67
$AUC_{0-\infty}$ (min·µmol/L)	289 ± 31	101 ± 19	1150 ± 216	550 ± 148	59 ± 2	101 ± 44	63 ± 9
BA (%)	17 ± 2	15 ± 4	60 ± 12	8 ± 2	4 ± 0.3	nd	nd

AUC, area under the concentration-time curve; CL, clearance; C_{max}, maximum plasma concentration; T_{max}, time to reach C_{max}; Vd, volume of distribution. Intravenous and oral administered doses of all compounds were 5 mg/kg and 20 mg/kg, respectively, except for WHN012 which was 10 mg/kg and 50 mg/kg, respectively.

5 *In vitro* isobole analysis of drug interactions

5.1 Introduction

Successful treatment of many diseases, including cancer, tuberculosis, HIV, and malaria, relies on combination therapy. This strategy is preferred over monotherapy as it often achieves greater therapeutic efficacy and potentially shortens duration of treatment. In the case of infectious disease, it may also delay the development of drug resistance.[337] Currently, the continued use of first-line ACTs is threatened by the delay in parasite clearance times.[183] The WHO has strongly recommended against the administration of artemisinins, or any derivatives, in monotherapy for uncomplicated malaria, due to parasites developing resistance.[79] As a result, current drug development research focuses on finding new partner compounds to use in combination which will hopefully delay the onset of resistance to existing therapies.[338]

As described in Chapter 1, the overarching goal of the Flagship Project, of which this research forms part, is to develop new compounds that can be used together with the existing artemisinins, or new artemisinin derivatives that can protect the artemisinin component from emergence of resistance.

The partner compound should ideally be longer acting, have a different mechanism of action to the artemisinin and have a synergistic interaction. Extensive research on artemisinin derivatives have provided many active compounds, for example, hydroxyartemisinin derivatives,[339] triazolyl artemisinins[340] and endoperoxides which includes arterolane (OZ277) and artefenomel (OZ439).[341] AMS (Figure 5-1) is derived from DHA and has demonstrated *in vitro* antiplasmodial activities superior to those of the current artemisinins applied clinically. AMS was selected as the artemisinin component in the combination investigations described in this chapter, for its well-described activity profile, as well as lack of metabolism to DHA.[261,342] Additionally, a lack of neurotoxicity has been established for AMS.[261,343] AMS exhibited superior efficacy and PK over clinically used artemisinins and improved antiplasmodial potency against an array of parasite life stages.[207,261]

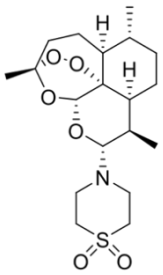

Figure 5-1: Structure of artemisone.

As described in Chapter 1, oxidant drugs should be considered for combination with redox compounds and investigated as potential antimalarial drug candidates, for the overall benefit that the oxidant abruptly induces oxidative stress, which is then maintained or enhanced by redox cycling of the redox drug partner. From the initial group of compounds identified in Chapter 2, two compounds were selected for investigation *in vitro* based on their high antiplasmodial activity towards *P. falciparum*, PK profiles and expected favourable interaction with artemisinins. These compounds are predicted to have redox cycling potential, based on the classes of compounds they belong to. It is predicted that they will potentiate antimalarial efficacy by amplification of oxidative stress.[127]

The first compound selected for isobole analysis was PhX6. The compound presented nanomolar activity against CQS and CQR *P. falciparum* parasite strains *in vitro* and demonstrated high selectivity toward the parasites. *In vitro* ADME analysis and *in vivo* PK studies displayed favourable physiological properties. PhX6 was absorbed well from oral administration in a healthy murine model and achieved a BA of 60% (Section 4.4.3). The elimination $t_{1/2}$ from the mouse model was 8 hours, which would be ideal for delivering a longer duration of treatment after the faster eliminating AMS.

AD01 was selected for its chemical similarity to MB, being the slightly more lipophilic ethyl analogue of the redox parent. *In vivo* PK analysis revealed a lower exposure and shorter $t_{1/2}$ of the compound in comparison to PhX6. However, if the compound shows synergistic interaction with AMS, exposure levels *in vivo* could potentially be enough to elicit a sufficient pharmacological effect. These compounds (Figure 5-2) were evaluated for their potential synergistic interactions *in vitro* as this result could greatly enhance their efficacy *in vivo*.[344] It is important to note here that the expression of therapeutic

efficacy is not only dependent on biological activity of the compounds, but also on PK and metabolic components which are likely to influence the observation *in vivo*.[338,345]

Compounds AD01 and PhX6 were analysed in combination with AMS by a modified fix-ratio isobologram analysis originally described by Fivelman *et al.*[337] The method was adapted and simplified from the traditional checkerboard assay.[346] Fivelman argues the fixed ratio method is simpler, with easier calculations and is more accurate compared to the checkerboard assay, which is affected by day to day variations in single initial IC_{50} concentrations. The main aim of the work described in this chapter was to determine if an oxidant drug (AMS) together with a redox compound (AD01 or PhX6) would produce synergistic interactions, where synergy is defined as compounds delivering greater efficacy together than when used alone.[347]

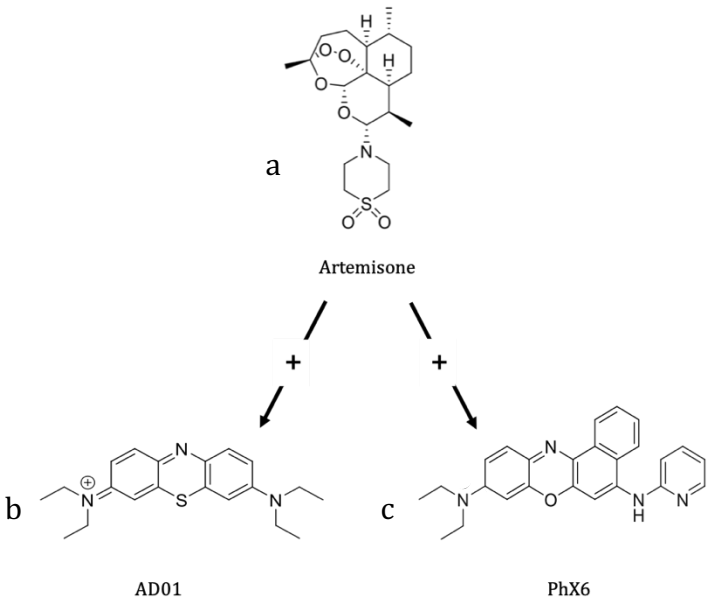

Figure 5-2: Molecular structures of compounds tested in *in vitro* combinations. Artemisone (a) was tested in combination against either AD01 (b) or PhX6 (c).

5.2 Materials

All materials used in this chapter are listed in Appendix A. Only materials of analytical grade or higher were used.

5.3 Methods

5.3.1 Sample preparation

The preparation of all samples used in this chapter is described in Appendix A.

Compound stock solution were prepared in 100% DMSO (2 mM) except for CQ which was dissolved in distilled water (20 mg/mL).

5.3.2 Parasite survival assay

Parasite culturing methods and parasite survival assay methods are described in Appendix A. The 72-hour pLDH parasite survival assay against the CQS NF54 parasite strain was used to achieve isobole analysis.

5.3.3 Fixed-ratio combination experiments

AMS, a 10-alkylaminoartemisinin derivative of DHA, was selected as the oxidant partner drug for investigation in combination studies. AMS was investigated in combination with PhX6 or AD01 using the modified fixed-ratio method against CQS NF54 *P. falciparum* parasites in the standard 72-hour pLDH assay.[149]

The two compounds were tested alone and in combination at ratios of 3:1, 1:1, 1:3 and 1:9, and were prepared as six solutions (Table 5-1). The first (C1) and last (C6) combination solution contained either drug A (AMS) or drug B (AD01 or PhX6) alone. Compounds were diluted from 2 mM DMSO stock solutions and combination solutions were prepared in CM from working solutions to obtain the final in-well concentration fraction of each compound in combination. Concentration ranges for combinations were prepared from the predetermined single IC_{50} values; such that the IC_{50} of the individual compounds would fall in the middle of the plate.

The solutions were added to the sterile assay plate and serial dilutions were made in subsequent wells across the plate with a multichannel pipette (Figure 5-3). The final concentration of DMSO, once diluted in the plate, was less than 0.05% and did not have any effect on the cultures. The plates were incubated for 72 hours, as described on pg. 184-186, Appendix A.

Table 5-1: Combination solutions labelled C1 to C6 for the fixed ratios in each combination and final in-well concentrations of each fraction of drug in combinations, after addition of pRBC's.

Combinations	**Fraction of A**	**Fraction of B**	**Concentration (nM)**		
			Compound A	Compound B	
			AMS	AD01 or	PhX6
C1	1	0	100	0	0
C2	3	1	75	25	200
C3	1	1	50	50	400
C4	1	3	25	75	600
C5	1	9	10	90	720
C6	0	1	0	100	800

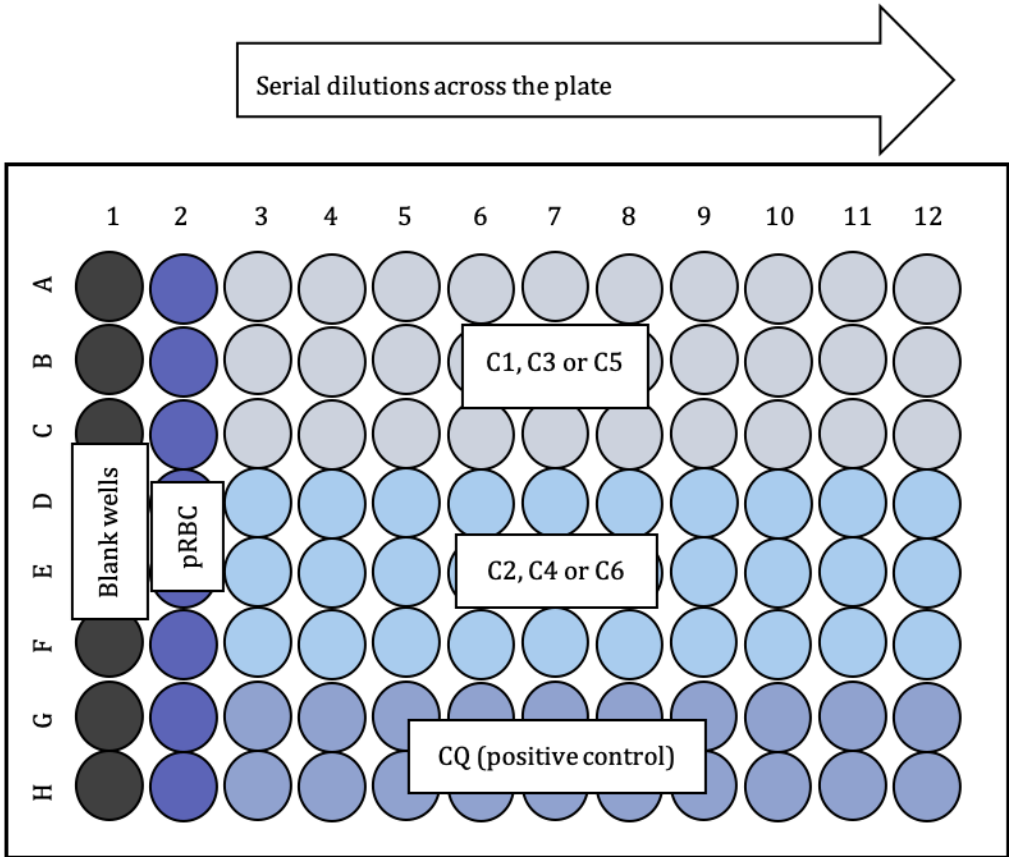

Figure 5-3: Representation of the assay plate layout. The highest concentration of combination samples was added in triplicate to column 3. Three 96-well plates were prepared similarly, with row A–C and Row D–F of the first plate containing C1 and C2, the second plate containing C3 and C4 and the third plate containing C5 and C6. Column 1 contained only CM which served to account for absorbance from uninfected RBC's in medium. Column 2 contained parasitized RBC's in medium and served as negative control (100% parasite growth). The positive control CQ was added in duplicate to row G–H on all three plates.

5.3.4 Data analysis

The absorbance of the plates was read at 620 nm. Data sets of each combination were used to generate sigmoidal dose-response curves using GraphPad Prism version 5 for Windows (GraphPad Software Inc., La Jolla, California). Each data point obtained from the combination samples was represented in two data sets. Each combination (C2, C3, C4, and C5) was thus represented by two curves–one curve for each of the drugs in the combination with respect to its concentration range. A single curve was generated for each of the single compounds tested. Therefore, 10 sigmoidal dose-response curves were

constructed during one experiment. Compounds were tested in technical triplicates and on three separate occasions.

5.3.5 Calculation of FIC_{50} values

The IC_{50} values were used to calculate the 50% fractional inhibitory concentrations (FIC_{50}) of drug A within the respective combination (Equation 5-1), i.e. the extent of growth inhibition by the combination (drug A + drug B) divided by the inhibition by application of the drug alone (drug A) (Equation 5-1). The same was done for FIC_{50} calculation of drug B (Equation 5-2). The sum of FICs was calculated by addition of FIC_{50} (A) and FIC_{50} (B) (Equation 5-3) in order to determine the interaction of the compounds. The same equations were used to determine the FIC_{90} values from the IC_{90}'s. A value derived from Equation 5-3 of < 0.80 indicated synergy; > 1.4 indicated antagonism and =1 indicated addition.[347,348]

Equation 5-1: FIC_{50} of compound A

$$\boldsymbol{FIC_{50}(A) = \frac{IC_{50}\ (A+B)}{IC_{50}\ A}}$$

Equation 5-2: FIC_{50} of compound B

$$\boldsymbol{FIC_{50}(B) = \frac{IC_{50}\ (B+A)}{IC_{50}\ B}}$$

Equation 5-3: Sum of FIC_{50}

$$\boldsymbol{\sum FIC_{50} = FIC_{50\,(A)} + FIC_{50\,(B)}}$$

Finally, FIC_{50} values of compounds in respective combinations were plotted on a graph as an isobologram (Figure 5-4). Addition interaction (blue field) would be observed for data points plotted around the midline (1,1). Synergistic interactions (green field) would have data points below the midline and data points of antagonistic interactions (red field)

would lie above the midline. In addition, the shape of the isobologram gave an indication of the interaction in the combination. A concave shape indicates synergy and convex shape indicates antagonism. Data points around a straight line indicate addition.

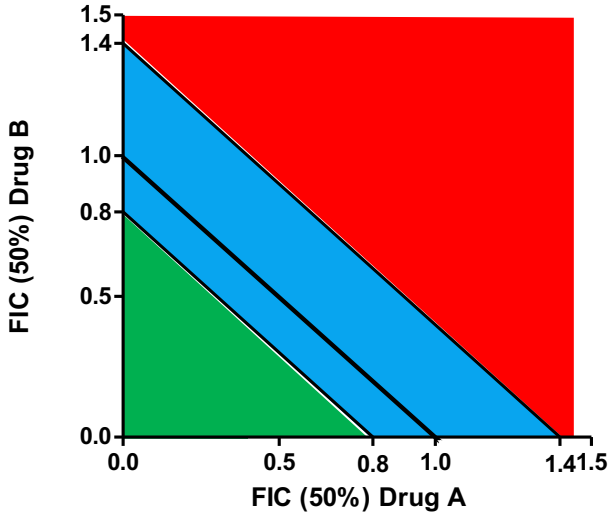

Figure 5-4: Representative graph of classification areas for ∑FIC values. ∑FIC values are classified as 'synergistic' (<0.8) if plotted in the green field, 'additive' (0.8–1.4) when plotted in the blue field and 'antagonistic' (>1.4) when plotted in the red field. (FIC, fractional inhibitory concentration).

5.3.6 Statistical testing

Statistical testing for the significance of shift in the $\sum FIC_{50}$'s was achieved by a one-way analysis of variance (ANOVA) test (with statistical significance accepted for $p < 0.05$) with Tukey's Multiple Comparison test using GraphPad Prism version 5 for Windows (GraphPad Software Inc., La Jolla, California).

5.4 Results and discussion

Isobole analysis requires the determination of individual IC_{50} values for the compounds, before fixed ratio concentration ranges can be set. The single compound IC_{50}'s of AD01 (CQS NF54 23.1 nM) and PhX6 (CQS NF54 41.8 nM) were determined previously, as discussed in Chapter 2. The pLDH parasite survival assay, as described in Appendix A, was used to determine the IC_{50} of AMS. An IC_{50} of 4.50 ± 2.42 nM against the CQS NF54 parasite

strain was obtained for AMS and was consistent with values in the literature.[207] The IC_{50}s from the combination assays were used to determine mean FIC_{50}'s and Sum of FIC_{50}'s ($\sum FIC_{50}$'s) in each combination of AMS + AD01 and AMS + PhX6, as described earlier[337,347] and is shown in Table 5-2.

The combination of AMS and AD01 at different ratios presented IC_{50} values between 3.40 nM to 1.35 nM for AMS and 10.35 nM to 0.92 nM for AD01 (Table 5-2a). Combination experiments with AD01 showed the IC_{50} values were lowered across all the combination ratios, i.e. the combination IC_{50}'s were lower than those of either AMS (6.16 nM) or AD01 (23.31 nM) alone. This indicated that these worked better together than as single compounds. IC_{50}'s from the combination of AMS and PhX6 revealed similar trends with values ranging from 1.84 nM to 0.61 nM for AMS and 21.21 nM to 3.20 nM for PhX6, compared to the IC_{50} of AMS (2.86 nM) and PhX6 (45.61 nM) alone (Table 5-2a).

The FIC_{50} of AMS in combination with AD01 or PhX6 in respective combination experiments were used to calculate the $\sum FIC_{50}$'s of each combination. Isobolograms were constructed from resulting $\sum FIC_{50}$'s and curve shapes were observed to determine synergy, antagonism or addition. Both AMS + AD01 and AMS + PhX6 combinations produced a concave curve shape (Figure 5-5a and 5c) which indicated synergistic interactions. To clearly define interaction of two compounds, the $\sum FIC_{50}$ values were classified as the following: values below 0.8 indicate synergism, above 1.4 indicate antagonism and between 0.8 and 1.4 indicate addition.[349] $\sum FIC_{50}$ ranged between 0.61 and 0.71 for AMS + AD01 and between 0.73 and 0.87 for AMS + Phx6. Therefore, all combinations were classified as having synergistic interactions, except the 1:9 ratio of AMS + PhX6, which was weakly additive ($\sum FIC_{50}$ 0.87). The IC_{90} values were also calculated (Table 5-2b) and used to construct an isobologram from the FIC_{90}'s (Figure 5-5b and 5d), in order to confirm the trends seen at IC_{50} level. A similar trend of interaction is seen for both sets of combination experiments between the IC_{50} and IC_{90} levels.

Table 5-2a: FIC_{50} and $\sum FIC_{50}$ of artemisone (drug A) in fixed-ratio combination with AD01 or PhX6 (Drug B).

Combination	**Combination Ratio (A:B)**	**[a]MeanIC_{50} ± SD (nM)**		**[a]Mean FIC_{50}**		**$\sum FIC_{50}$**	**Interaction**
		Drug A	Drug B	Drug A	Drug B		
AMS + AD01	1:0	6.16 ± 2.92	nd	1.00 ± 0.0	nd	1.00	
	3:1	3.40 ± 1.44	0.92 ± 0.40	0.56 ± 0.08	0.04 ± 0.02	0.60	Synergy
	1:1	1.97 ± 0.83	2.04 ± 0.78	0.34 ± 0.07	0.09 ± 0.04	0.43	Synergy
	1:3	1.14 ± 0.38	3.63 ± 1.53	0.20 ± 0.05	0.16 ± 0.08	0.36	Synergy
	1:9	1.35 ± 0.54	10.35 ± 2.40	0.25 ± 0.13	0.46 ± 0.15	0.71	Synergy
	0:1	nd	23.31 ± 2.49	nd	1.00 ± 0.0	1.00	
AMS + PhX6	1:0	2.86 ± 1.01	nd	1.00 ± 0.0	nd	1.00	
	3:1	1.84 ± 0.59	3.20 ± 1.34	0.65 ± 0.02	0.09 ± 0.05	0.73	Synergy
	1:1	1.46 ± 0.46	7.88 ± 3.67	0.51 ± 0.06	0.20 ± 0.09	0.72	Synergy
	1:3	0.91 ± 0.31	14.17 ± 6.13	0.32 ± 0.01	0.38 ± 0.20	0.70	Synergy
	1:9	0.61 ± 0.35	21.21 ± 2.22	0.21 ± 0.05	0.67 ± 0.17	0.87	Addition
	0:1	nd	45.61 ± 5.69	nd	1.00 ± 0.0	1.00	

[a] Results shown are the mean IC_{50} values and SD from at least three independent experiments

Table 5-2b: FIC_{90} and $\sum FIC_{90}$ of artemisone (drug A) in fixed-ratio combination with AD01 or PhX6 (Drug B).

Combination	**Combination Ratio (A:B)**	**[a]Mean IC_{90} ± SD (nM)**		**[a]Mean FIC_{90}**		**$\sum FIC_{90}$**	**Interaction**
		Drug A	Drug B	Drug A	Drug B		
AMS + AD01	1:0	9.56 ± 6.78	nd	1.00 ± 0.00	nd	1.00	
	3:1	5.25 ± 3.82	1.53 ± 0.88	0.58 ± 0.16	0.04 ± 0.02	0.62	Synergy
	1:1	3.63 ± 1.74	3.62 ± 1.76	0.47 ± 0.24	0.09 ± 0.05	0.55	Synergy
	1:3	2.20 ± 1.05	7.09 ± 4.62	0.27 ± 0.08	0.17 ± 0.11	0.43	Synergy
	1:9	2.18 ± 1.19	15.76 ± 5.01	0.27 ± 0.12	0.37 ± 0.15	0.64	Synergy
	0:1	nd	44.71 ± 11.37	nd	1.00 ± 0.00	1.00	
AMS + PhX6	1:0	5.20 ± 1.48	nd	1.00 ± 0.00	nd	1.00	
	3:1	2.75 ± 0.77	4.94 ± 2.24	0.53 ± 0.01	0.08 ± 0.06	0.61	Synergy
	1:1	2.70 ± 1.28	13.63 ± 5.09	0.50 ± 0.10	0.20 ± 0.11	0.71	Synergy
	1:3	1.44 ± 0.76	120.52 ± 5.92	0.27 ± 0.07	0.33 ± 0.23	0.59	Synergy
	1:9	1.09 ± 0.85	47.38 ± 8.81	0.19 ± 0.10	0.65 ± 0.18	0.85	Addition
	0:1	nd	78.94 ± 34.25	nd	1.00 ± 0.00	1.00	

[a] Results shown are the mean IC_{90} values and standard deviation (SD) from at least three independent experiments.

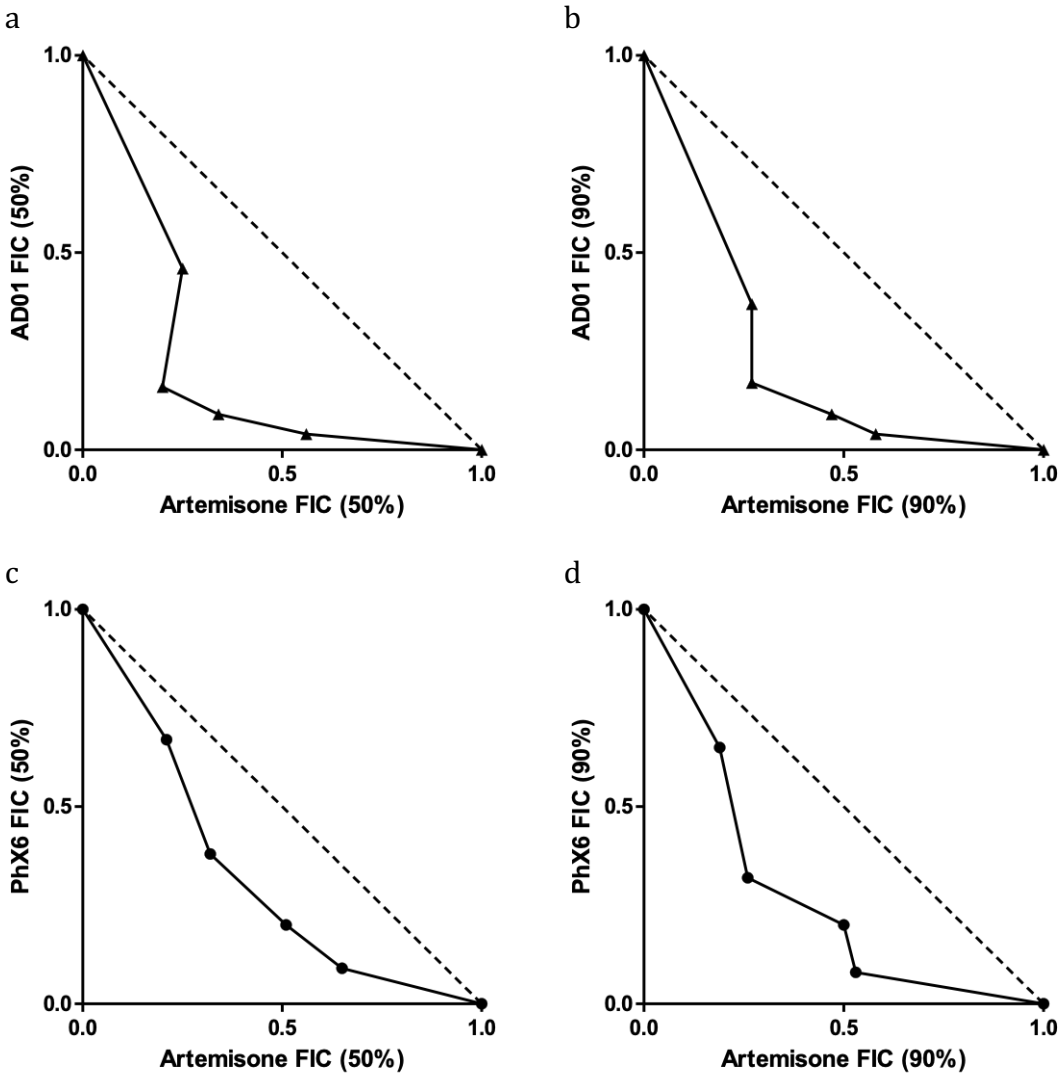

Figure 5-5: FIC_{50} (left) and FIC_{90} values (right) of AMS and AD01 (top) or PhX6 (bottom) determined at various ratios (3:1, 1:1, 1:3 and 1:9) for a CQS (NF54) strain of *P. falciparum*. The resulting synergistic effects of the compounds in combination is indicated by the concave isobolograms. Independent dose-response curves of the fixed drug combinations were determined using the pLDH assay against intraerythrocytic asexual parasites for 72 hours. The dashed line corresponds to an indifferent interaction. The solid line indicates the respective isobole curve of the drug combination. Data are the means of 3 independent experiments. (FIC, fractional inhibitory concentration).

The combination of AMS with AD01 or PhX6 in a fixed combination ratio against CQS NF54 parasites presented a marked shift in the mean IC_{50}'s of AMS. In order to determine the significance of the shift, combination $\sum FIC_{50}$'s of AMS were compared to the $\sum FIC_{50}$ of AMS alone, using the one-way ANOVA test ($p < 0.05$) (Figure 5-6). For AMS in combination with AD01, the combination ratios with the most significant shift was observed for 1:1 and 1:3 (One-way ANOVA, $p \leq 0.001$, $F = 14.08$, $df = 4$). Combination ratio 3:1 was also calculated

to be significantly different ($p \leq 0.05$), but less so than the formerly mentioned combinations. For AMS + PhX6, combination ratio 1:3 was the only combination to show a significant shift (One-way ANOVA, $p \leq 0.05$, $F = 6.091$, $df = 4$).

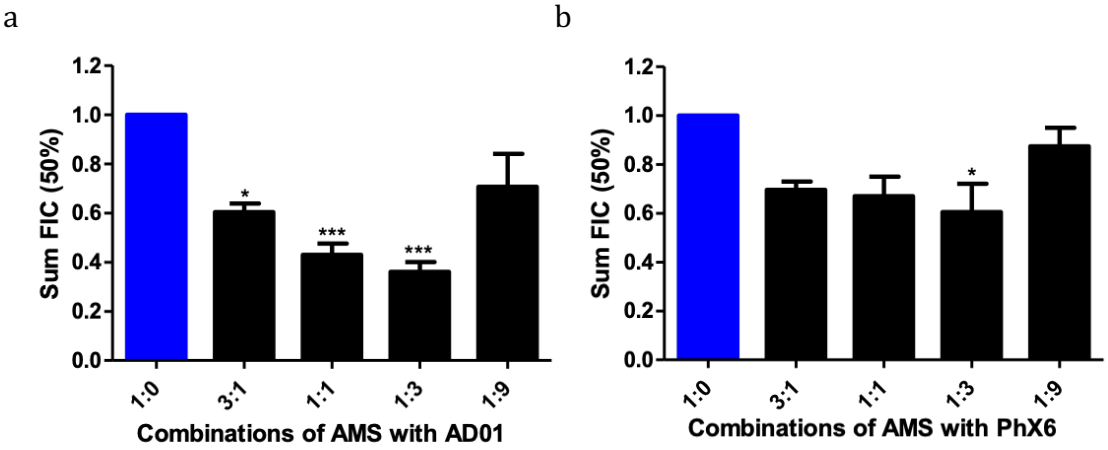

* $p \leq 0.05$; ** $p \leq 0.01$; *** $p \leq 0.001$

Figure 5-6: $\sum FIC_{50}$ values of a) AMS + AD01 and b) AMS + PhX6 combinations at difference combination ratios and tested against the single concentrations (blue bar). Significant differences were measured between fixed drug combinations using a one-way ANOVA test ($p < 0.05$).

Pro-oxidant redox compounds, such as MB, have been investigated previously with artemisinins and are associated with notably favourable interactions.[207,323,350] AMS was shown to be very synergistic with MB *in vitro*, and had a mean $\sum FIC_{50}$ value of 0.75 and 0.61, respectively against early and late stage gametocytes.[207] The authors concluded that the *in vitro* gametocytocidal effects of artemisinin derivatives may be augmented with strategic combination of MB and that the findings encourage further investigation in order to supplement the evidence of redox combinations. The high efficacy of MB-based combinations[207,344,351207] strongly encourages further investigation into synergistic interaction between artemisinins and redox compounds like MB.

It was anticipated that synergism between AMS in combination with AD01 and PhX6 would be observed, because of their structural similarities to compounds previously

tested in the same class, as well as the principle of their proposed redox mechanism.[207,352] Overall, AD01 and PhX6 presented favourable *in vitro* interactions with AMS and showed a noticeable shift in the IC_{50}'s of AMS. These findings strongly suggest that the synergistic effects of AD01 and PhX6 with AMS are a consequence of their biochemical mechanism by the redox cycling principle.

These results are beneficial because the positive interaction with artemisinins support the hypothesis of including redox compounds in artemisinin-based therapy, as artemisinins are currently the most active antimalarial drugs both in terms of the dosage amounts required, and rapidity in inducing parasite clearance. Furthermore, using artemisinin derivatives such as AMS as the oxidant drug in the combination is beneficial as it has a PK profile superior to artemisinin, artesunate, and DHA. It is also simple and inexpensive to produce AMS and the drug has shown to have improved safety compared to the other artemisinins.[261,353]

In vivo efficacy does not only rely on biological activity but is also highly dependent on PK. As discussed in Chapter 2, successful and efficient combinations with the artemisinins are dependent on a second partner compound with a longer $t_{1/2}$, to prevent the formation of resistant parasites. AD01 and PhX6 were both selected for evaluation in the fixed-ratio combination assays. As AD01 is structurally similar to MB, it was expected to show some degree of synergistic interaction with AMS.[207] PhX6, on the other hand, was the leading compound to be evaluated for combinations, as its PK profile was far superior to all the other compounds evaluated in Chapter 4. The combination ratio 1:3 revealed a significant synergistic interaction of AMS with PhX6. Therefore, it is suggested that PhX6 is a better partner for AMS than AD01. Although synergistic activity with AD01 was greater than PhX6 in combination ratio 1:1 and 1:3, it probably will not be chosen for further studies. Because of its superior PK profile, coupled with its synergism with AMS, PhX6 will be taken forward.[342] Clearly, whilst AD01 has excellent efficacies (Section 2.3) and is strongly synergistic with AMS, newer more lipophilic and metabolically more stable analogues of AD01 are required.

5.5 Summary and Conclusion

Two redox compounds, AD01 and PhX6, were assessed *in vitro* in combination with AMS using the modified fixed-ratio method to identify potential synergistic interactions.[337] Both compounds improved the IC_{50} of AMS in combination compared to that of AMS alone. The $\sum FIC_{50}$'s were all classified as predominantly synergistic and an ANOVA test was applied to distinguish significant interactions according to the $\sum FIC_{50}$'s of each concentration ratio. Significant synergistic interactions were identified for AD01 in the combination ratios of 3:1, 1:1 and 1:3 as well as PhX6 in combination ratio of 1:3.

Although the significance of interaction of AD01 with AMS was greater than that of PhX6, it is important to consider that highly efficacious drugs need good PK properties to be successful as clinically used therapies. With regards to malaria, high level of efficacy together with drugs that have multiple mechanisms and different elimination half-lives are essential in overcoming disease burden and preventing the emergence of resistance.[338] With this in mind, PhX6 was identified as having the most favourable PK profile of all compounds evaluated, as well as having significant synergistic interaction with AMS. This will increase the potential of therapeutic efficacy of PhX6 *in vivo* in combination with AMS. These findings strongly encourage further investigation of efficacy *in vivo* in order to ascertain if the synergistic interactions are translatable to a living model.

6 Conclusions and future work

The effective treatment and control of malaria is increasingly threatened by the development of drug-resistant parasites. Drugs that were once used in highly effective therapies in malaria endemic areas have been replaced by ACTs. Even though artemisinins are the most rapidly acting and effective drugs, their efficacy for the global control and cure of malaria is threatened by increased emergence of resistance. Guidelines such as the WHO Global Technical Strategy for Malaria for 2016–2030,[1] which aims to drastically reduce incidence and eventually eliminate malaria, highlights the need for ongoing development of new drugs.

As outlined in Chapter 1, the concept underpinning this research is of potentiating oxidative stress within the parasite's proliferating environment by combining an oxidant drug with a redox drug capable of maintaining high levels of ROS through its redox cycling ability. The concept was tested, establishing whether compounds presented selective activity against CQS and CQR *P. falciparum* parasites, whether they possess suitable PK properties to be rationally selected for further evaluation in drug combinations and if they demonstrated anticipated drug interactions with an artemisinin derivative in preliminary *in vitro* combination investigations.

In this thesis seven compounds are identified from a compound library constructed from a multidisciplinary collaboration. These were initially selected based on their antiplasmodial activity. The compounds were artemisinin derivatives, phenoxazines, phenothiazines, thiosemicarbazones, and quinolone derivatives. The compounds were evaluated for their antiplasmodial activity against the CQS NF54 strain and the CQR Dd2, K1, and W2 parasites. Additionally, general toxicity evaluation with the mammalian CHO cell line showed that the inhibitory activity of compounds WHN012, AD01, PhX6, DpNEt, RMB005, RMB059 and RMB060 were very selective for the parasites, as indicated by the selectivity index (SI>270; Table 2-3).

WHN012, an aryl urea derived from DHA-piperazine, was selected as the oxidant compound. The compound showed remarkably good activity against both CQR and CQS parasite strains. Although the artemisinins are regarded the most active antimalarial drugs, they are known to be very unstable. It was expected that the electronegative *p*-fluorophenyl functional group would make the compound less susceptible to liver metabolism and thereby improve total exposure. However, WHN012 had high *in vitro* and *in vivo* CL, and ultimately did not show improved BA over other artemisinin derivatives. After considering the data, it was decided that AMS should be considered as the oxidant

drug for combination experiments to follow. The exceptional activity and selectivity of the WHN compound class certainly do justify their worth for further investigation and generating yet newer compounds optimised in terms of stability and solubility.

AD01 is an ethyl derivative of MB, a known redox drug. Although AD01 showed excellent solubility, the lack of lipophilicity and poor passive permeability limited its absorption and contributed to low BA (14%). Poor stability of AD01 was observed in the plasma stability assay and this was also reflected in the animal experiments. The susceptibility of the compound to metabolism may indicate that active metabolites are being formed. Future studies will focus on this possibility.

Phenoxazines like PhX6 have been shown to be active redox cycling compounds and express good antiplasmodial activity. Despite poor solubility at higher pH's, PhX6 showed a remarkably good BA of 60% in the mouse model and together with being highly active against both CQS and CQS strains of the parasite, was clearly a good candidate to progress to combination experiments. PhX6 was tested in combination with AMS and showed a distinct shift in the activity of AMS, indicating a significant synergistic interaction. AD01 was also considered for *in vitro* combination work as its close similarity to MB suggests that synergy with AMS was likely. Both PhX6 and AD01 showed significant synergy with AMS *in vitro*. The results indicate that redox cycling between an oxidant and redox-active drug is potentially driving the synergistic interaction between the compounds. Overall, these findings suggested that PhX6 is the ideal candidate for further investigation with AMS for future *in vivo* combination studies.

DpNEt, that is structurally different to the phenoxazines and phenothiazines, was another redox compound selected based on its high activity and selectivity and. The compound displayed promising physicochemical properties. However, evaluation of the PK profile showed that DpNEt had surprisingly low BA (8%). The predicted hepatic CL, *in vivo* systemic CL and low Vd raised the question of whether DpNEt was subject to other routes of elimination. It was hypothesised that DpNEt, although being absorbed well, was potentially a substrate for P-gp transporters that could ultimately influence concentrations seen in whole blood.

Lastly, the RMB compounds derived from decoquinate (DQ) were investigated as potential longer acting third partner compounds to the redox cycling combination. The amide derivative of DQ, RMB005 was expected to show improved physicochemical

properties to DQ, but it turned out to have poor solubility and permeability, resulting in very low BA (4%). The carbamate derivatives RMB059 and RMB060 were expected to show improved physicochemical properties over RMB005. However, these compounds turned out to be very unstable under physiological conditions and were rapidly converted to DQ under the assay conditions. Stability, together with solubility and permeability, plays a key role in candidate selection and should therefore be optimised before further investigation of this series of compounds.

The work discussed in this thesis centres on a novel set of compounds having efficient and selective inhibition of CQS and CQR *P. falciparum* parasites, as well as promising *in vitro* and *in vivo* properties. The evaluation of the PK properties and *in vitro* combinations resulted in the identification of the potentially efficacious PhX6+AMS combination. Considering these results, it is highly recommended that this combination be further investigated.

Research limitations can result in the incomplete or incorrect interpretation of results from a study and thus influence downstream research based on those data. Firstly, AD01 and DpNEt are suspected to be subject to active transport mechanisms, based on their PK profiles obtained from the mouse model. For the determination of membrane permeability using the PAMPA assay, the permeability mechanism is limited to the passive diffusion as the assay does not possess the capacity to facilitate active transport. Therefore, a cell-based model, such as the Caco-2 permeability assay is required in order to determine if these compounds, that may be subject to active transport *in vivo*, are being absorbed and eliminated through other mechanisms.[278] Although the PAMPA assay is considered to be relatively basic, it remains the preferred model in HTS environments and is a more economic model to use.

The general stability of the RMB compounds should be addressed. As mentioned previously, RMB059 and RMB060 were too unstable and whole blood concentrations from murine experiments could not be quantified. Whole blood concentrations of the parent DQ was calculated instead. In this case it was not possible to determine the BA of DQ that was available for absorption into the bloodstream and indirectly determine the extent to which RMB059 and RMB060 were converted to DQ. Another question was raised regarding how the RMB compounds were able to retain their activity during initial *in vitro* activity screening, whilst showing stability issues under assay conditions. Future

investigations in this class of compounds should aim to determine if they potentially act as prodrugs to DQ, and indeed if these have superior kill kinetics to DQ itself.

Although the work described in this thesis answered several research questions, some new research questions arose that were beyond the scope of this study and should be addressed in future studies.

In order to fully understand the synergistic interaction of PhX6+AMS, this combination should be evaluated in an *in vivo* efficacy model in order to establish the relationship between PK and efficacy of the compounds. This can be achieved with the SCID humanised mouse model. Furthermore, from these investigations, one will not only be able to determine the pharmacodynamics of these compounds, but also gain insight on how their PK profiles are affected in a diseased model. The SCID model should ultimately be used to determine if the combination of PhX6+AMS is able to retain its high activity and remain synergistic in a dynamic, living system. Additionally, gametocyte and transmission-blocking activity are a central focus for drug discovery for antimalarials. In the efforts to eradicate malaria this should be investigated in potential antimalarial compounds such as PhX6. While AMS has shown significant gametocytocidal activity and synergistic interaction with MB, it would be valuable to determine if PhX6 could synergize the redox imbalance in transmissible gametocyte stages.

Lastly, combinations were completed *in vitro* against the NF54 CQS parasite strain only. While this shows promising and confirmatory data on the expected interaction between an oxidant and redox-active drug, it should be noted that activity in resistant strains, specifically artemisinin resistant strains, also play a key role in the progression of a compound in preclinical research. This is a research objective that should be addressed in future studies, as it would provide valuable additional information regarding the potential to overcome or delay resistance formation.

7 References

1. World Health Organization. World Malaria Report 2019. Geneva, Switzerland; 2019.

2. Chew CH, Lim YAL, Lee PC, Mahmud R, Chua KH. Hexaplex PCR detection system for identification of five human Plasmodium species with an internal control. J Clin Microbiol. 2012;50(12):4012–9.

3. Sitali L, Miller JM, Mwenda MC, Bridges DJ, Hawela MB, Hamainza B, et al. Distribution of Plasmodium species and assessment of performance of diagnostic tools used during a malaria survey in Southern and Western Provinces of Zambia. Malar J. 2019;18(1):130.

4. Ridley RG. Medical need, scientific opportunity and the drive for antimalarial drugs. Nature. 2002;415(6872):686–93.

5. Winzeler EA. Malaria research in the post-genomic era. Nature. 2008;455(7214):751–6.

6. Bozdech Z, Llinás M, Pulliam BL, Wong ED, Zhu J, DeRisi JL. The transcriptome of the intraerythrocytic developmental cycle of Plasmodium falciparum. PLoS Biol. 2003;1(1).

7. Miller LH, Ackerman HC, Su XZ, Wellems TE. Malaria biology and disease pathogenesis: Insights for new treatments. Nat Med. 2013;19(2):156–67.

8. Delves M, Plouffe D, Scheurer C, Meister S, Wittlin S, Winzeler EA, et al. The activities of current antimalarial drugs on the life cycle stages of plasmodium: A comparative study with human and rodent parasites. PLoS Med. 2012;9(2):e1001169.

9. Maier AG, Matuschewski K, Zhang M, Rug M. Plasmodium falciparum. 2018;

10. Bartoloni A, Zammarchi L. Clinical aspects of uncomplicated and severe malaria. Mediterr J Hematol Infect Dis. 2012;4(1).

11. Warhurst D, Williams J. Laboratory diagnosis of malaria. J Clin Pathol.

1996;49(7):533–8.

12. Aguilar R, Magallon-Tejada A, Achtman AH, Moraleda C, Joice R, Cisteró P, et al. Molecular evidence for the localization of Plasmodium falciparum immature gametocytes in bone marrow. Blood. 2014;123(7):959–66.

13. Gebru T, Lalremruata A, Kremsner PG, Mordmüller B, Held J. Life-span of in vitro differentiated Plasmodium falciparum gametocytes. Malar J. 2017;16(1):330.

14. Eichner M, Diebner HH, Molineaux L, Collins WE, Jeffery GM, Dietz K. Genesis, sequestration and survival of Plasmodium falciparum gametocytes: Parameter estimates from fitting a model to malariatherapy data. Trans R Soc Trop Med Hyg. 2001;95(5):497–501.

15. Josling GA, Llinás M. Sexual development in Plasmodium parasites: Knowing when it's time to commit. Nat Rev Microbiol. 2015;13(9):573–87.

16. Miura K, Crompton PD. What goes around comes around: Modeling malaria transmission from humans back to mosquitos. J Clin Invest. 2018;128(4):1264–6.

17. Crutcher J, Hoffman S. Malaria. In: Medical Microbiology. 4th ed. Texas; 1996.

18. Arnot DE, Gull K. The Plasmodium cell-cycle: Facts and questions. Ann Trop Med Parasitol. 1998;92(4):361–5.

19. Bhatt S, Weiss DJ, Cameron E, Bisanzio D, Mappin B, Dalrymple U, et al. The effect of malaria control on Plasmodium falciparum in Africa between 2000 and 2015. Nature. 2015;526(7572):207–11.

20. White MT, Verity R, Griffin JT, Asante KP, Owusu-Agyei S, Greenwood B, et al. Immunogenicity of the RTS,S/AS01 malaria vaccine and implications for duration of vaccine efficacy: Secondary analysis of data from a phase 3 randomised controlled trial. Lancet Infect Dis. 2015;15(12):1450–8.

21. Acharya P, Garg M, Kumar P, Munjal A, Raja KD. Host-parasite interactions in human malaria: Clinical implications of basic research. Front Microbiol. 2017;8:1–16.

22. Hooft Van Huijsduijnen R, Wells TN. The antimalarial pipeline. Curr Opin Pharmacol. 2018;42:1–6.

23. Huskey SEW, Zhu CQ, Fredenhagen A, Kühnöl J, Luneau A, Jian Z, et al. KAE609 (Cipargamin), a new spiroindolone agent for the treatment of malaria: Evaluation of the absorption, distribution, metabolism, and excretion of a single oral 300-mg dose of [14C]KAE609 in healthy male subjects. Drug Metab Dispos. 2016;44(5):672–82.

24. Rosling JEO, Ridgway MC, Summers RL, Kirk K, Lehane AM. Biochemical characterization and chemical inhibition of PfATP4-associated Na-ATPase activity in Plasmodium falciparum membranes. J Biol Chem. 2018;293(34):13327–37.

25. Djimde A, Grobusch MP, Zoleko Manego R, Mombo-Ngoma G, Picot S, Sagara I, et al. OC 8721 WANECAM II – a clinical trial programme to assess safety, efficacy and transmission-blocking properties of a new antimalarial KAF156 (ganaplacide) in uncomplicated malaria in west and central africa. BMJ Glob Heal. 2019;4(Suppl 3):A17.3-A18.

26. Paquet T, Le Manach C, Cabrera DG, Younis Y, Henrich PP, Abraham TS, et al. Antimalarial efficacy of MMV390048, an inhibitor of Plasmodium phosphatidylinositol 4-kinase. Sci Transl Med. 2017;9(387).

27. Deshpande S, Kuppast B. 4-Aminoquinolines: An overview of antimalarial chemotherapy. Med Chem (Los Angeles). 2016;6(1):1–11.

28. Mishra M, Mishra VK, Kashaw V, Iyer AK, Kashaw SK. Comprehensive review on various strategies for antimalarial drug discovery. Eur J Med Chem. 2017;125:1300–20.

29. Tan KR, Magill AJ, Parise ME, Arguin PM. Doxycycline for malaria chemoprophylaxis and treatment: Report from the CDC expert meeting on malaria chemoprophylaxis. Am J Trop Med Hyg. 2011;84(4):517–31.

30. World Health Organization. Guidelines for the treatment of malaria. 3rd ed. Geneva, Switzerland; 2015.

31. Alecrim MG, Lacerda M V., Mourãdieo MP, Alecrim WD, Padilha A, Cardoso BS, et al. Successful treatment of Plasmodium falciparum malaria with a six-dose regimen of artemether-lumefantrine versus quinine-doxycycline in the western Amazon region of Brazil. Am J Trop Med Hyg. 2006;74(1):20–5.

32. Winstanley PA, Ward SA, Snow RW. Clinical status and implications of antimalarial drug resistance. Microbes Infect. 2002;4(2):157–64.

33. Ocan M, Akena D, Nsobya S, Kamya MR, Senono R, Kinengyere AA, et al. Persistence of chloroquine resistance alleles in malaria endemic countries: A systematic review of burden and risk factors. Malar J. 2019;18(1):76.

34. Aikawa M. High-resolution autoradiography of malarial parasites treated with 3 H-chloroquine. Am J Pathol. 1972;67(2):277–84.

35. Olafson KN, Ketchum MA, Rimer JD, Vekilov PG. Mechanisms of hematin crystallization and inhibition by the antimalarial drug chloroquine. Proc Natl Acad Sci U S A. 2015;112(16):4946–51.

36. White NJ. Pharmacokinetic and pharmacodynamic considerations in antimalarial dose optimization. Antimicrob Agents Chemother. 2013;57(12):5792–807.

37. Taylor WRJ, Thriemer K, von Seidlein L, Yuentrakul P, Assawariyathipat T, Assefa A, et al. Short-course primaquine for the radical cure of Plasmodium vivax malaria: a multicentre, randomised, placebo-controlled non-inferiority trial. Lancet. 2019 Sep 14;394(10202):929–38.

38. Meltzer E, Schwartz E. Utility of 8-aminoquinolines in malaria prophylaxis in travelers. Vol. 21, Current Infectious Disease Reports. 2019.

39. Bousema T, Okell L, Shekalaghe S, Griffin JT, Omar S, Sawa P, et al. Revisiting the circulation time of Plasmodium falciparum gametocytes: molecular detection methods to estimate the duration of gametocyte carriage and the effect of gametocytocidal drugs. Malar J. 2010;9(1):136.

40. Staines HM, Krishna S. Treatment and prevention of malaria. Staines H, Krishna S, editors. Basel: Springer; 2012.

41. Melariri P, Kalombo lonji, Nkuna P, Dube admire. Oral lipid-based nanoformulation of tafenoquine enhanced bioavailability and blood stage antimalarial efficacy and led to a reduction in human red blood cell loss in mice. Int J Nanomedicine. 2015;10:1493–503.

42. Chu CS, Phyo AP, Turner C, Win HH, Poe NP, Yotyingaphiram W, et al. Chloroquine

versus dihydroartemisinin-piperaquine with standard high-dose primaquine given either for 7 days or 14 days in plasmodium vivax malaria. Clin Infect Dis. 2019 Apr 8;68(8):1311–9.

43. Chu CS, Bancone G, Moore KA, Win HH, Thitipanawan N, Po C, et al. Haemolysis in G6PD heterozygous females treated with primaquine for Plasmodium vivax malaria: A nested cohort in a trial of radical curative regimens. Garner P, editor. PLoS Med. 2017 Feb 7;14(2):e1002224.

44. Bancone G, Chowwiwat N, Somsakchaicharoen R, Poodpanya L, Moo PK, Gornsawun G, et al. Single low dose primaquine (0.25mg/kg) does not cause clinically significant haemolysis in G6PD deficient subjects. Gutman J, editor. PLoS One. 2016 Mar 24;11(3):e0151898.

45. Phommasone K, van Leth F, Peto TJ, Landier J, Nguyen TN, Tripura R, et al. Mass drug administrations with dihydroartemisinin-piperaquine and single low dose primaquine to eliminate Plasmodium falciparum have only a transient impact on Plasmodium vivax: Findings from randomised controlled trials. Diemert DJ, editor. PLoS One. 2020;15(2):e0228190.

46. Camarda G, Jirawatcharadech P, Priestley RS, Saif A, March S, Wong MHL, et al. Antimalarial activity of primaquine operates via a two-step biochemical relay. Nat Commun. 2019;10(1):1–9.

47. Tekwani BL, Walker LA. 8-Aminoquinolines: Future role as antiprotozoal drugs. Curr Opin Infect Dis. 2006;19(6):623–31.

48. Nzila A. The past, present and future of antifolates in the treatment of Plasmodium falciparum infection. J Antimicrob Chemother. 2006;57(6):1043–54.

49. Ndyomugyenyi R, Magnussen P, Clarke S. The efficacy of chloroquine, sulfadoxine-pyrimethamine and a combination of both for the treatment of uncomplicated Plasmodium falciparum malaria in an area of low transmission in western Uganda. Trop Med Int Heal. 2004;9(1):47–52.

50. Staedke SG, Kamya MR, Dorsey G, Gasasira A, Ndeezi G, Charlebois ED, et al. Amodiaquine, sulfadoxine/pyrimethamine, and combination therapy for treatment of uncomplicated falciparum malaria in Kampala, Uganda: A randomised trial.

Lancet. 2001;358(9279):368–74.

51. Zhao L, Pi L, Qin Y, Lu Y, Zeng W, Xiang Z, et al. Widespread resistance mutations to sulfadoxine-pyrimethamine in malaria parasites imported to China from Central and Western Africa. Int J Parasitol Drugs Drug Resist. 2020 Apr 1;12:1–6.

52. White NJ. Assessment of the pharmacodynamic properties of antimalarial drugs in vivo. Antimicrob Agents Chemother. 1997;41(7):1413–22.

53. Schwarz NG, Oyakhirome S, Pötschke M, Gläser B, Klouwenberg PK, Altun H, et al. 5-Day nonobserved artesunate monotherapy for treating uncomplicated Falciparum malaria in young Gabonese children. Am J Trop Med Hyg. 2005;73(4):705–9.

54. Tu Y. Artemisinin—A gift from traditional Chinese medicine to the world. Angew Chemie - Int Ed. 2016;55(35):10210–26.

55. Meshnick SR. Artemisinin: Mechanisms of action, resistance and toxicity. Int J Parasitol. 2002;32(13):1655–60.

56. Faurant C. From bark to weed: The history of artemisinin. Parasite. 2011;18(3):215–8.

57. Butler AR, Khan S, Ferguson E. A brief history of malaria chemotherapy. J R Coll Physicians Edinb. 2010;40(2):172–7.

58. Klonis N, Crespo-Ortiz MP, Bottova I, Abu-Bakar N, Kenny S, Rosenthal PJ, et al. Artemisinin activity against Plasmodium falciparum requires hemoglobin uptake and digestion. Proc Natl Acad Sci U S A. 2011;108(28):11405–10.

59. Krishna S, Uhlemann AC, Haynes RK. Artemisinins: Mechanisms of action and potential for resistance. Drug Resist Updat. 2004;7(4–5):233–44.

60. Edikpo N, Ghasi S, Elias A, Oguanobi N. Artemisinin and biomolecules: The continuing search for mechanism of action. Mol Cell Pharmacol. 2013;5(2):75–89.

61. Avery MA, Gao F, Chong WKM, Mehrotra S, Milhous WK. Structure—activity relationships of the antimalarial agent artemisinin. 1. Synthesis and comparative molecular field analysis of C-9 analogs of artemisinin and 10-deoxoartemisinin. J

Med Chem. 1993;36(26):4264–75.

62. Igarashi Y, Yanagisawa E, Ohshima T, Takeda S, Aburada M, Miyamoto KI. Synthesis and evaluation of carbamate prodrugs of a phenolic compound. Chem Pharm Bull. 2007;55(2):328–33.

63. Ye B, Wu YL, Li GF, Jiao XQ. Antimalarial activity of deoxoqinghaosu. Yao Xue Xue Bao. 1991;26(3):228–30.

64. Ginsburg H, Atamna H. The redox status of malaria-infected erythrocytes: An overview with an emphasis on unresolved problems. Parasite. 1994;1(1):5–13.

65. Jortzik E, Becker K. Thioredoxin and glutathione systems in Plasmodium falciparum. Int J Med Microbiol. 2012;302(4–5):187–94.

66. Müller T, Johann L, Jannack B, Brückner M, Lanfranchi DA, Bauer H, et al. Glutathione reductase-catalyzed cascade of redox reactions to bioactivate potent antimalarial 1,4-naphthoquinones - A new strategy to combat malarial parasites. J Am Chem Soc. 2011;133(30):11557–71.

67. Mohring F, Pretzel J, Jortzik E, Becker K. The redox systems of Plasmodium falciparum and Plasmodium vivax: comparison, in silico analyses and inhibitor studies. Curr Med Chem. 2014;21(15):1728–56.

68. Rathore S, Datta G, Kaur I, Malhotra P, Mohmmed A. Disruption of cellular homeostasis induces organelle stress and triggers apoptosis like cell-death pathways in malaria parasite. Cell Death Dis. 2015;6(7):1803–1803.

69. Goyal M, Alam A, Bandyopadhyay U. Redox regulation in malaria: current concepts and pharmacotherapeutic implications. Curr Med Chem. 2012;19(10):1475–503.

70. Müller S. Redox and antioxidant systems of the malaria parasite Plasmodium falciparum. Mol Microbiol. 2004;53(5):1291–305.

71. Atamna H, Krugliak M, Shalmiev G, Deharo E, Pescarmona G, Ginsburg H. Mode of antimalarial effect of methylene blue and some of its analogues on Plasmodium falciparum in culture and their inhibition of P. vinckei petteri and P. yoelii nigeriensis in vivo. Biochem Pharmacol. 1996;51(5):693–700.

72. Becker K, Rahlfs S, Nickel C, Schirmer RH. Glutathione - Functions and metabolism in the malarial parasite Plasmodium falciparum. Biol Chem. 2003;384(4):551–66.

73. Krauth-Siegel RL, Bauer H, Schirmer RH. Dithiol proteins as guardians of the intracellular redox milieu in parasites: Old and new drug targets in trypanosomes and malaria-causing plasmodia. Angew Chemie - Int Ed. 2005;44(5):690–715.

74. Kinoshita A, Nakayama Y, Kitayama T, Tomita M. Simulation study of methemoglobin reduction in erythrocytes: Differential contributions of two pathways to tolerance to oxidative stress. FEBS J. 2007;274(6):1449–58.

75. Schirmer RH, Müller JG, Krauth-Siegel RL. Disulfide-Reductase inhibitors as chemotherapeutic agents: The design of drugs for trypanosomiasis and malaria. Angew Chemie Int Ed English. 1995;34(2):141–54.

76. Hunt NH, Stocker R. Oxidative stress and the redox status of malaria-infected erythrocytes. Blood Cells. 1990;16(2–3):499–526.

77. Haynes RK, Cheu KW, Chan HW, Wong HN, Li KY, Tang MMK, et al. Interactions between artemisinins and other antimalarial drugs in relation to the cofactor model-a unifying proposal for drug action. ChemMedChem. 2012;7(12):2204–26.

78. Haynes RK, Chan WC, Wong HN, Li KY, Wu WK, Fan KM, et al. Facile oxidation of leucomethylene blue and dihydroflavins by artemisinins: Relationship with flavoenzyme function and antimalarial mechanism of action. ChemMedChem. 2010 Aug 2;5(8):1282–99.

79. World Health Organization. World Malaria Report 2018. Geneva, Switzerland; 2018.

80. Nosten F, Luxemburger C, Ter Kuile FO, Woodrow C, Pa Eh J, Chongsuphajaisiddhi T, et al. Treatment of multidrug-resistant plasmodium falciparum malaria with 3-day artesunate-mefloquine combination. J Infect Dis. 1994;170(4):971–7.

81. World Health Organization. Antimalarial drug combination therapy: Report of a WHO Technical Consultation. World Health Organization, Geneva WHO. Geneva, Switzerland; 2001.

82. Mishra N, Kaitholia K, Srivastava B, Shah NK, Narayan JP, Dev V, et al. Declining

efficacy of artesunate plus sulphadoxine-pyrimethamine in northeastern India. Malar J. 2014;13(1):1–12.

83. Nosten F, Van Vugt M, Price R, Luxemburger C, Thway KL, Brockman A, et al. Effects of artesunate-mefloquine combination on incidence of Plasmodium falciparum malaria and mefloquine resistance in western Thailand: A prospective study. Lancet. 2000;356(9226):297–302.

84. van der Pluijm RW, Tripura R, Hoglund RM, Pyae Phyo A, Lek D, ul Islam A, et al. Triple artemisinin-based combination therapies versus artemisinin-based combination therapies for uncomplicated Plasmodium falciparum malaria: a multicentre, open-label, randomised clinical trial. Lancet. 2020;395(10233):1345–60.

85. Rosenthal PJ. Are three drugs for malaria better than two? Lancet. 2020;395(10233):1316–7.

86. Woodrow CJ, White NJ. The clinical impact of artemisinin resistance in Southeast Asia and the potential for future spread. FEMS Microbiol Rev. 2017;41(1):34–48.

87. Dondorp AM, Nosten F, Yi P, Das D, Phyo AP, Tarning J, et al. Artemisinin resistance in Plasmodium falciparum malaria. N Engl J Med. 2009;361(5):455–67.

88. Dhingra SK, Small-Saunders JL, Ménard D, Fidock DA. Plasmodium falciparum resistance to piperaquine driven by PfCRT. Lancet Infect Dis. 2019;19(11):1168–9.

89. Tilley L, Straimer J, Gnädig NF, Ralph SA, Fidock DA. Artemisinin action and resistance in Plasmodium falciparum. Trends Parasitol. 2016;32(9):682–96.

90. World Health Organization. Status report on artemisinin and ACT resistance. Geneva, Switzerland; 2015.

91. Phyo AP, Nkhoma S, Stepniewska K, Ashley EA, Nair S, McGready R, et al. Emergence of artemisinin-resistant malaria on the western border of Thailand: A longitudinal study. Lancet. 2012 May;379(9830):1960–6.

92. Ashley EA, Dhorda M, Fairhurst RM, Amaratunga C, Lim P, Suon S, et al. Spread of artemisinin resistance in Plasmodium falciparum malaria. N Engl J Med. 2014;371(5):411–23.

93. Ariey F, Witkowski B, Amaratunga C, Beghain J, Langlois AC, Khim N, et al. A molecular marker of artemisinin-resistant Plasmodium falciparum malaria. Nature. 2014;505(7481):50–5.

94. Phyo AP, Jittamala P, Nosten FH, Pukrittayakamee S, Imwong M, White NJ, et al. Antimalarial activity of artefenomel (OZ439), a novel synthetic antimalarial endoperoxide, in patients with Plasmodium falciparum and Plasmodium vivax malaria: an open-label phase 2 trial. Lancet Infect Dis. 2016 Jan 1;16(1):61–9.

95. Fidock DA, Rosenthal PJ, Croft SL, Brun R, Nwaka S. Antimalarial drug discovery: efficacy models for compound screening. Nat Rev Drug Discov. 2004;3(6):509–20.

96. Okombo J, Chibale K. Recent updates in the discovery and development of novel antimalarial drug candidates. Medchemcomm. 2018;9(3):437–53.

97. Guerin PJ, Olliaro P, Nosten F, Druilhe P, Laxminarayan R, Binka F, et al. Malaria: Current status of control, diagnosis, treatment, and a proposed agenda for research and development. Lancet Infect Dis. 2002;2(9):564–73.

98. Dorsey G, Vlahos J, Kamya MR, Staedke SG, Rosenthal PJ. Prevention of increasing rates of treatment failure by combining sulfadoxine-pyrimethamine with artesunate or amodiaquine for the sequential treatment of malaria. J Infect Dis. 2003;188(8):1231–8.

99. World Health Organization. The sixth meeting of the Greater Mekong Subregion (GMS) Therapeutic Efficacy Studies (TES) Network. Manila, Philippines; 2019.

100. Nsanzabana C. Resistance to artemisinin combination therapies (ACTs): Do not forget the partner Drug! Trop Med Infect Dis. 2019 Feb 1;4(1):26.

101. Martinelli A, Moreira R, Cravo P. Malaria combination therapies: advantages And shortcomings. Mini-Reviews Med Chem. 2008;8(3):201–12.

102. Pabón A, Carmona J, Burgos LC, Blair S. Oxidative stress in patients with non-complicated malaria. Clin Biochem. 2003;36(1):71–8.

103. Sorci G, Faivre B. Inflammation and oxidative stress in vertebrate host-parasite systems. Philos Trans R Soc B Biol Sci. 2009;364(1513):71–83.

104. Castro L, Freeman BA. Reactive oxygen species in human health and disease. Nutrition. 2001;17(2):161–5.

105. Karihtala P, Soini Y. Reactive oxygen species and antioxidant mechanisms in human tissues and their relation to malignancies. Apmis. 2007;115(2):81–103.

106. Ignarro L. Physiology and pathophysiology of nitric oxide. Kidney Int Suppl. 1996;55.

107. Jayshree RS, Ganguli NK, Dubey ML, Mohan K, Mahajan RC. Generation of reactive oxygen species by blood monocytes during acute Plasmodium knowlesi infection in rhesus monkeys. APMIS. 1993 Jul 1;101(7–12):762–6.

108. Francis SE, Sullivan DJ, Goldberg and DE. Hemoglobin metabolism in the malaria parasite Plasmodium falciparum. Annu Rev Microbiol. 1997;51(1):97–123.

109. Becker K, Tilley L, Vennerstrom JL, Roberts D, Rogerson S, Ginsburg H. Oxidative stress in malaria parasite-infected erythrocytes: Host-parasite interactions. Int J Parasitol. 2004;34(2):163–89.

110. Banerjee R, Liu J, Beatty W, Pelosof L, Klemba M, Goldberg DE. Four plasmepsins are active in the Plasmodium falciparum food vacuole, including a protease with an active-site histidine. Proc Natl Acad Sci U S A. 2002;99(2):990–5.

111. Tilley L, Loria P, Foley M. Chloroquine and other quinoline antimalarials. In: Antimalarial Chemotherapy Infectious Disease. Totowa, NJ: Humana Press; 2001.

112. Egan TJ, Combrinck JM, Egan J, Hearne GR, Marques HM, Ntenteni S, et al. Fate of haem iron in the malaria parasite Plasmodium falciparum. Biochem J. 2002;365(2):343–7.

113. Wunderlich J, Rohrbach P, Dalton J. The malaria digestive vacuole. Front Biosci. 2012;4:1424–48.

114. Kehrer JP. The Haber-Weiss reaction and mechanisms of toxicity. Toxicology. 2000 Aug 14;149(1):43–50.

115. Kavishe RA, Koenderink JB, Alifrangis M. Oxidative stress in malaria and artemisinin combination therapy: Pros and Cons. FEBS J. 2017;284(16):2579–91.

116. Simões APCF, van den Berg JJM, Roelofsen B, Op den Kamp JAF. Lipid peroxidation in Plasmodium falciparum-parasitized human erythrocytes. Arch Biochem Biophys. 1992;298(2):651–7.

117. Rahlfs S, Nickel C, Deponte M, Schirmer RH, Becker K. Plasmodium falciparum thioredoxins and glutaredoxins as central players in redox metabolism. Redox Rep. 2003;8(5):246–50.

118. Couto N, Wood J, Barber J. The role of glutathione reductase and related enzymes on cellular redox homoeostasis network. Free Radic Biol Med. 2016;95:27–42.

119. Kanzok SM, Schirmer RH, Türbachova I, Iozef R, Becker K. The thioredoxin system of the malaria parasite Plasmodium falciparum. J Biol Chem. 2000;275(51):40180–6.

120. Krnajski Z, Gilberger TW, Walter RD, Müller S. The malaria parasite Plasmodium falciparum possesses a functional thioredoxin system. Mol Biochem Parasitol. 2001;112(2):219–28.

121. Rahlfs S, Becker K. Interference with redox-active enzymes as a basis for the design of antimalarial drugs. Mini-Reviews Med Chem. 2006;6(2):163–76.

122. Kawazu SI, Tsuji N, Hatabu T, Kawai S, Matsumoto Y, Kano S. Molecular cloning and characterization of a peroxiredoxin from the human malaria parasite Plasmodium falciparum. Mol Biochem Parasitol. 2000;109(2):165–9.

123. Krnajski Z, Gilberger TW, Walter RD, Cowman AF, Müller S. Thioredoxin reductase is essential for the survival of Plasmodium falciparum erythrocytic stages. J Biol Chem. 2002 Jul 19;277(29):25970–5.

124. Mohring F, Jortzik E, Becker K. Comparison of methods probing the intracellular redox milieu in Plasmodium falciparum. Mol Biochem Parasitol. 2016;206:75–83.

125. Belorgey D, Antoine Lanfranchi D, Davioud-Charvet E. 1,4-Naphthoquinones and other NADPH-dependent glutathione reductase- catalyzed redox cyclers as antimalarial agents. Curr Pharm Des. 2013;19(14):2512–28.

126. Haynes RK, Cheu KW, Tang MMK, Chen MJ, Guo ZF, Guo ZH, et al. Reactions of antimalarial peroxides with each of leucomethylene blue and dihydroflavins: flavin

reductase and the cofactor model exemplified. ChemMedChem. 2011;6(2):279–91.

127. Buchholz K, Schirmer RH, Eubel JK, Akoachere MB, Dandekar T, Becker K, et al. Interactions of methylene blue with human disulfide reductases and their orthologues from Plasmodium falciparum. Antimicrob Agents Chemother. 2008;52(1):183–91.

128. Blank O, Davioud-Charvet E, Elhabiri M. Interactions of the antimalarial drug methylene blue with methemoglobin and heme targets in Plasmodium falciparum: A physico-biochemical study. Antioxidants Redox Signal. 2012;17(4):544–54.

129. Gallo V, Schwarzer E, Rahlfs S, Schirmer RH, van Zwieten R, Roos D, et al. Inherited glutathione reductase deficiency and Plasmodium falciparum malaria - a case study. PLoS One. 2009;4(10):e7303.

130. Mandi G, Witte S, Meissner P, Coulibaly B, Mansmann U, Rengelshausen J, et al. Safety of the combination of chloroquine and methylene blue in healthy adult men with G6PD deficiency from rural Burkina Faso. Trop Med Int Heal. 2005;10(1):32–8.

131. Meissner PE, Mandi G, Witte S, Coulibaly B, Mansmann U, Rengelshausen J, et al. Safety of the methylene blue plus chloroquine combination in the treatment of uncomplicated falciparum malaria in young children of Burkina Faso [ISRCTN27290841]. Malar J. 2005;4(1):1–9.

132. Zoungrana A, Coulibaly B, Sié A, Walter-Sack I, Mockenhaupt FP, Kouyaté B, et al. Safety and efficacy of methylene blue combined with artesunate or amodiaquine for uncomplicated falciparum malaria: A randomized controlled trial from Burkina Faso. PLoS One. 2008 Feb 20;3(2):23–6.

133. Rezaee R, Abdollahi M. The importance of translatability in drug discovery. Expert Opin Drug Discov. 2017;12(3):237–9.

134. Flannery EL, Chatterjee AK, Winzeler EA. Antimalarial drug discovery-approaches and progress towards new medicines. Nat Rev Microbiol. 2013;11(12):849–62.

135. Tudor M, Hermes J, Li J. Translatability: What does it mean in drug discovery? Drug Discov Today. 2016;21(6):865–7.

136. Saeidnia S, Manayi A, Abdollahi M. From in vitro experiments to in vivo and clinical studies; pros and cons. Curr Drug Discov Technol. 2016;12(4):218–24.

137. Saeidnia S, Manayi A, Abdollahi M. The pros and cons of the in-silico pharmaco-toxicology in drug discovery and development. Int J Pharmacol. 2013;9(3):176–81.

138. Ekins S, Mestres J, Testa B. In silico pharmacology for drug discovery: Applications to targets and beyond. Br J Pharmacol. 2007;152(1):21–37.

139. Shetab-Boushehri SV, Abdollahi M. Current concerns on the validity of in vitro models that use transformed neoplastic cells in pharmacology and toxicology. Int J Pharmacol. 2012;8(6):594–5.

140. Di L, Kerns EH. Profiling drug-like properties in discovery research. Curr Opin Chem Biol. 2003;7(3):402–8.

141. Van Voorhis WC, Adams JH, Adelfio R, Ahyong V, Akabas MH, Alano P, et al. Open source drug discovery with the Malaria Box compound collection for neglected diseases and beyond. PLoS Pathog. 2016;12(7):e1005763.

142. Trager W, Jensen J. Human malaria parasites in continuous culture. Science (80-). 1976;193(4254):637–75.

143. World Health Organization. Artemisinin resistance and artemisinin-based combination therapy efficacy. Geneva, Switzerland; 2018.

144. Leidenberger M, Voigtländer C, Simon N, Kappes B. SYBR® green I-based fluorescence assay to assess cell viability of malaria parasites for routine use in compound screening. In: Gilbert DF, Friedrich O, editors. Cell Viability Assays, Methods and Protocols. New York: Humana Press Inc.; 2017. p. 97–110.

145. Desjardins RE, Canfield CJ, Haynes JD, Chulay JD. Quantitative assessment of antimalarial activity in vitro by a semiautomated microdilution technique. Antimicrob Agents Chemother. 1979;16(6):710–8.

146. Maji AK. Drug susceptibility testing methods of antimalarial agents. Trop Parasitol. 2018;8(2):70–6.

147. Abiodun OO, Gbotosho GO, Ajaiyeoba EO, Happi CT, Hofer S, Wittlin S, et al.

Comparison of SYBR Green I-, PicoGreen-, and [3H]-hypoxanthine- based assays for in vitro antimalarial screening of plants from Nigerian ethnomedicine. Parasitol Res. 2010;106(4):933–9.

148. Noedl H, Wongsrichanalai C, Wernsdorfer WH. Malaria drug-sensitivity testing: New assays, new perspectives. Trends Parasitol. 2003;19(4):175–81.

149. Makler MT, Ries JM, Williams JA, Bancroft JE, Piper RC, Gibbins BL, et al. Parasite lactate dehydrognase as an assay for Plasmodium falciparum drug sensitivity. Am J Trop Med Hyg. 1993;48(6):739–41.

150. Smilkstein M, Sriwilaijaroen N, Kelly JX, Wilairat P, Riscoe M. Simple and Inexpensive fluorescence-based technique for high-throughput antimalarial drug screening. Antimicrob Agents Chemother. 2004;48(5):1803–6.

151. Vossen MG, Pferschy S, Chiba P, Noedl H. The SYBR green I malaria drug sensitivity assay: Performance in low parasitemia samples. Am J Trop Med Hyg. 2010;82(3):398–401.

152. Peters W, O BR-E by: Z, M S, 1999 U. Handbook of Animal Models of Infection. Aust Vet J. 2000;78(7):482–482.

153. Jiménez-Díaz MB, Mulet T, Viera S, Gómez V, Garuti H, Ibáñez J, et al. Improved murine model of malaria using Plasmodium falciparum competent strains and non-myelodepleted NOD-scid IL2Rγnullmice engrafted with human erythrocytes. Antimicrob Agents Chemother. 2009;53(10):4533–6.

154. Li AP. Screening for human ADME/Tox drug properties in drug discovery. Drug Discov Today. 2001;6(7):357–66.

155. Kola I, Landis J. Can the pharmaceutical industry reduce attrition rates? Nat Rev Drug Discov. 2004;3(8):711–5.

156. Yu H, Adedoyin A. ADME-Tox in drug discovery: Integration of experimental and computational technologies. Drug Discov Today. 2003;8(18):852–61.

157. Lin JH. Applications and limitations of interspecies scaling and in vitro extrapolation in pharmacokinetics. Drug Metab Dispos. 1998;26(12):1202–12.

158. Eddershaw PJ, Beresford AP, Bayliss MK. ADME/PK as part of a rational approach to drug discovery. Drug Discov Today. 2000;5(9):409–14.

159. Moroz E, Matoori S, Leroux JC. Oral delivery of macromolecular drugs: Where we are after almost 100 years of attempts. Adv Drug Deliv Rev. 2016;101:108–21.

160. Lin L, Wong H. Predicting oral drug absorption: mini review on physiologically-based pharmacokinetic models. Pharmaceutics. 2017;9(4):41.

161. Ashford M. Gastrointestinal tract–physiology and drug absorption. In: Aulton M, Taylor K, editors. Alton's pharmaceutics e-book: the design and manufacture of medicines. 5th ed. China: Elsevier Ltd; 2017. p. 296–313.

162. Hidalgo IJ, Raub TJ, Borchardt RT. Characterization of the human colon carcinoma cell line (Caco-2) as a model system for intestinal epithelial permeability. Gastroenterology. 1989;96(2):736–49.

163. Pai MP. Drug dosing based on weight and body surface area: Mathematical assumptions and limitations in obese adults. Pharmacotherapy. 2012 Sep;32(9):856–68.

164. Chillistone S, Hardman JG. Factors affecting drug absorption and distribution. Anaesth Intensive Care Med. 2017;18(7):335–9.

165. Davis PJ, Bosenberg A, Davidson A, Jimenez N, Kharasch E, Lynn AM, et al. Pharmacology of pediatric anesthesia. In: Smith's Anesthesia for Infants and Children. 8th ed. Philadelphia, PA: Elsevier Inc.; 2011. p. 179–261.

166. Cohen LH. Plasma protein-binding methods in drug discovery. In: Yan Z, Caldwell G, editors. Optimization in Drug Discovery. Totowa, NJ: Humana Press Inc.; 2004. p. 111–22.

167. Kang YJ. Drug metabolism and transport. Lash L, editor. Totowa, NJ: Humana Press Inc.; 2005.

168. Li AP, Lu C, Brent JA, Pham C, Fackett A, Ruegg CE, et al. Cryopreserved human hepatocytes: Characterization of drug-metabolizing activities and applications in higher throughput screening assays for hepatotoxicity, metabolic stability, and drug-drug interaction potential. Chem Biol Interact. 1999;121(1):17–35.

169. Knights KM, Stresser DM, Miners JO, Crespi CL. In vitro drug metabolism using liver microsomes. Curr Protoc Pharmacol. 2016;74(1):7–8.

170. Aldred E. Drug excretion. In: Pharmacology. Philadelphia, PA: Elsevier; 2009. p. 133–6.

171. Lu J Da, Xue J. Poisoning: Kinetics to therapeutics. In: Critical Care Nephrology. 3rd ed. Elsevier Inc.; 2019. p. 600–29.

172. Kapusta D. Drug excretion. In: Enna S, Bylund D, editors. xPharm: The Comprehensive Pharmacology Reference. Elsevier Inc.; 2007. p. 1–2.

173. Li AP. Primary hepatocyte cultures as an in vitro experimental model for the evaluation of pharmacokinetic drug-drug Interactions. In: Advances in Pharmacology. Academic Press; 1997. p. 103–30.

174. Andes D, Craig WA. Animal model pharmacokinetics and pharmacodynamics: A critical review. Int J Antimicrob Agents. 2002;19(4):261–8.

175. Yeleswaram K, McLaughlin LG, Knipe J, Schabdach D. Pharmacokinetics and oral bioavailability of exogenous melatonin in preclinical animal models and clincal implications. J Pineal Res. 1997;22:45–51.

176. Tolman JA, Nelson NA, Bosselmann S, Peters JI, Coalson JJ, Wiederhold NP, et al. Dose tolerability of chronically inhaled voriconazole solution in rodents. Int J Pharm. 2009;379(1–2):25–31.

177. Gibbons JA, de Vries M, Krauwinkel W, Ohtsu Y, Noukens J, van der Walt JS, et al. Pharmacokinetic drug interaction studies with enzalutamide. Clin Pharmacokinet. 2015;54(10):1057–69.

178. Steinstraesser A, Wesch R, Frick A. Clinical pharmacokinetic studies. In: Drug Discovery and Evaluation: Safety and Pharmacokinetic Assays, Second Edition. Springer Berlin Heidelberg; 2013. p. 1139–210.

179. Smith NF, Raynaud FI, Workman P. The application of cassette dosing for pharmacokinetic screening in small-molecule cancer drug discovery. Mol Cancer Ther. 2007;6(2):428–40.

180. Tang C, Prueksaritanont T. Use of in vivo animal models to assess pharmacokinetic drug-drug interactions. Pharm Res. 2010;27(9):1772–87.

181. Valic MS, Prof GZ. Research tools for extrapolating the disposition and pharmacokinetics of nanomaterials from preclinical animals to humans. Theranostics. 2019;9(11):3365–87.

182. Chien JY, Friedrich S, Heathman MA, de Alwis DP, Sinha V. Pharmacokinetics/pharmacodynamics and the stages of drug development: Role of modeling and simulation. AAPS J. 2005;7(3).

183. Ouji M, Augereau JM, Paloque L, Benoit-Vical F. Plasmodium falciparum resistance to artemisinin-based combination therapies: A sword of Damocles in the path toward malaria elimination. Parasite. 2018;25(24):1–12.

184. Amato R, Lim P, Miotto O, Amaratunga C, Dek D, Pearson RD, et al. Genetic markers associated with dihydroartemisinin–piperaquine failure in Plasmodium falciparum malaria in Cambodia: a genotype–phenotype association study. Lancet Infect Dis. 2017;17(2):164–73.

185. Burrows JN, Burlot E, Campo B, Cherbuin S, Jeanneret S, Leroy D, et al. Antimalarial drug discovery - The path towards eradication. Parasitology. 2014;141(1):128–39.

186. Duparc S, Lanza C, Ubben D, Borghini-Fuhrer I, Kellam L. Optimal dose finding for novel antimalarial combination therapy. Trop Med Int Heal. 2012;17(4):409–13.

187. Greenwood BM, Fidock DA, Kyle DE, Kappe SHI, Alonso PL, Collins FH, et al. Malaria : progress , perils , and prospects for eradication. J Clin Invest. 2008;188(4):1266–1276.

188. Tolia NH, Enemark EJ, Sim BKL, Joshua-Tor L. Structural basis for the EBA-175 erythrocyte invasion pathway of the malaria parasite Plasmodium falciparum. Cell. 2005;122(2):183–93.

189. Burrows JN, Duparc S, Gutteridge WE, Hooft Van Huijsduijnen R, Kaszubska W, Macintyre F, et al. New developments in anti-malarial target candidate and product profiles. Malar J. 2017;16(1):26.

190. Ryley JF, Peters W. The antimalarial activity of some quinolone esters. Ann Trop

Med Parasit. 1970;64(2):209–22.

191. Wong HN, Padín-Irizarry V, van der Watt ME, Reader J, Liebenberg W, Wiesner L, et al. Optimal 10-aminoartemisinins with potent transmission-blocking capabilities for new artemisinin combination therapies–activities against blood stage p. falciparum including PfKI3 C580Y mutants and liver stage P. berghei parasites. Front Chem. 2020;7:901.

192. Beteck RM, Seldon R, Coertzen D, van der Watt ME, Reader J, Mackenzie JS, et al. Accessible and distinct decoquinate derivatives active against Mycobacterium tuberculosis and apicomplexan parasites. Commun Chem. 2018;1(1):62.

193. Beteck RM, Coertzen D, Smit FJ, Birkholtz LM, Haynes RK, N'Da DD. Straightforward conversion of decoquinate into inexpensive tractable new derivatives with significant antimalarial activities. Bioorganic Med Chem Lett. 2016;26(13):3006–9.

194. Straube T, Muller C. How to do a proper cell culture quick check [Internet]. Leica Microsystems. 2016 [cited 2020 Sep 14]. Available from: https://www.leica-microsystems.com/science-lab/how-to-do-a-proper-cell-culture-quick-check/

195. Mosmann T. Rapid colorimetric assay for cellular growth and survival: Application to proliferation and cytotoxicity assays. J Immunol Methods. 1983;65:55–63.

196. Macuamule CJ, Tjhin ET, Jana CE, Barnard L, Koekemoer L, De Villiers M, et al. A pantetheinase-resistant pantothenamide with potent, on-target, and selective antiplasmodial activity. Antimicrob Agents Ch. 2015;59(6):3666–8.

197. Batista R, García PA, Castro MA, Del Corral JMM, Speziali NL, De P. Varotti F, et al. Synthesis, cytotoxicity and antiplasmodial activity of novel ent-kaurane derivatives. Eur J Med Chem. 2013;62:168–76.

198. Bagavan A, Rahuman AA, Kaushik NK, Sahal D. In vitro antimalarial activity of medicinal plant extracts against Plasmodium falciparum. Parasitol Res. 2011;108(1):15–22.

199. Vennerstrom JL, Makler MT, Angerhofer CK, Williams JA. Antimalarial dyes revisited: Xanthenes, azines, oxazines and thiazines. Antimicrob Agents Ch. 1995;39(12):2671–7.

200. Nzila A, Mwai L. In vitro selection of Plasmodium falciparum drug-resistant parasite lines. J Antimicrob Chemother. 2009;65(3):390–8.

201. Soomro S, Langenberg T, Mahringer A, Konkimalla VB, Horwedel C, Holenya P, et al. Design of novel artemisinin-like derivatives with cytotoxic and anti-angiogenic properties. J Cell Mol Med. 2011;15(5):1122–35.

202. Jana S, Iram S, Thomas J, Hayat MQ, Pannecouque C, Dehaen W. Application of the triazolization reaction to afford dihydroartemisinin derivatives with anti-HIV activity. Molecules. 2017;22(2):303.

203. Fan M, Li Y, Yao C, Liu X, Liu J, Yu B. DC32, a dihydroartemisinin derivative, ameliorates collagen-induced arthritis through an Nrf2-p62-keap1 feedback loop. Front Immunol. 2018;9.

204. Gour R, Ahmad F, Prajapati SK, Giri SK, Lal Karna SK, Kartha KPR, et al. Synthesis of novel S-linked dihydroartemisinin derivatives and evaluation of their anticancer activity. Eur J Med Chem. 2019;178:552–70.

205. Kalani K, Alam S, Chaturvedi V, Singh S, Khan F, Srivastava SK. In vitro, in dilico and ex vivo studies of dihydroartemisinin derivatives as antitubercular agents. Curr Top Med Chem. 2019;19(8):633–44.

206. Wu Y, Parapini S, Williams ID, Misiano P, Wong HN, Taramelli D, et al. Facile preparation of N-glycosylated 10-piperazinyl artemisinin derivatives and evaluation of their antimalarial and cytotoxic activities. Molecules. 2018;23(7):1713.

207. Coertzen D, Reader J, Van Der Watt M, Nondaba SH, Gibhard L, Wiesner L, et al. Artemisone and artemiside are potent panreactive antimalarial agents that also synergize redox imbalance in plasmodium falciparum transmissible gametocyte stages. Antimicrob Agents Ch. 2018;62(8):e02214-17.

208. Wesche DL, DeCoster MA, Tortella FC, Brewer TG. Neurotoxicity of artemisinin analogs in vitro. Antimicrob Agents Ch. 1994;38(8):1813–9.

209. Brewer TG, Grate SJ, Peggins J, Peter J, Petras JM, Levine BS, et al. Fatal neurotoxocity of arteether and artemether. Am J Trop Med Hyg. 1994;51(3):251–9.

210. Ng N-C, Williams ID, Shek LY, Gomes MF, Wong H-N, Lung C-M, et al. Artesunate and dihydroartemisinin (DHA): unusual decomposition products formed under mild conditions and comments on the fitness of DHA as an antimalarial drug. ChemMedChem. 2007;2(10):1448–63.

211. Wainwright M, Amaral L. The phenothiazinium chromophore and the evolution of antimalarial drugs. Trop Med Int Heal. 2005;10(6):501–11.

212. Schirmer RH, Adler H, Pickhardt M, Mandelkow E. "Lest we forget you - methylene blue..." Neurobiol Aging. 2011;32(12):2325-e7.

213. Katz E, Weissbach H. Biosynthesis of the actinomycin chromophore; enzymatic conversion of 4-methyl-3-hydroxyanthranilic acid to actinocin. J Biol Chem. 1962;237(3):882–6.

214. Goldstein H, Ludwig-Semilitch Z. Sur les 1,2-naphtophénazoxines. Helv Chim Acta. 1919;2(1):655–62.

215. Shimizu S, Suzuki M, Tomoda A, Arai S, Taguchi H, Hanawa T, et al. Phenoxazine compounds produced by the reactions with bovine hemoglobin show antimicrobial activity against non-tuberculosis mycobacteria. Tohoku J Exp Med. 2004;203(1):47–52.

216. Shimamoto T, Yaguchi M, Tomoda A, Ohyashiki K. Antitumor effects of a novel phenoxazine derivative on human leukemia cell lines through activation of caspase-3 and telomerase. Blood. 2000;96(11 PART II).

217. Shi XL, Ge JF, Liu BQ, Kaiser M, Wittlin S, Brun R, et al. Synthesis and in vitro antiprotozoal activities of 5-phenyliminobenzo[a] phenoxazine derivatives. Bioorganic Med Chem Lett. 2011;21(19):5804–7.

218. Alberti A, Bolognese A, Guerra M, Lavecchia A, Macciantelli D, Marcaccio M, et al. Antitumor agents 4. Characterization of free radicals produced during reduction of the antitumor drug 5H-pyridophenoxazin-5-one: An EPR study. Biochemistry. 2003 Oct 21;42(41):11924–31.

219. Katsamakas S, L. Zografos A, Sarli V. Advances of phenoxazines: synthesis, reactivity and their medicinal applications. Curr Med Chem. 2016;23(26):2972–99.

220. Ge JF, Arai C, Yang M, Bakar Md. A, Lu J, Ismail NSM, et al. Discovery of novel benzo[a]phenoxazine SSJ-183 as a drug candidate for malaria. ACS Med Chem Lett. 2010;1(7):360–4.

221. Mizukawa Y, Ge JF, Bakar Md A, Itoh I, Scheurer C, Wittlin S, et al. Novel synthetic route for antimalarial benzo[a]phenoxazine derivative SSJ-183 and two active metabolites. Bioorganic Med Chem. 2014;22(14):3749–52.

222. Richardson DR, Sharpe PC, Lovejoy DB, Senaratne D, Kalinowski DS, Islam M, et al. Dipyridyl thiosemicarbazone chelators with potent and selective antitumor activity form iron complexes with redox activity. J Med Chem. 2006;49(22):6510–21.

223. Bernhardt P V., Kalinowski DS, Lovejoy DB, Richardson V, Islam M, Sharpe PC, et al. 2-Acetylpyridine thiosemicarbazones are potent iron chelators and antiproliferative agents: redox activity, iron complexation and characterization of their antitumor activity. J Med Chem. 2009;52(5):1459–70.

224. Tang J, Yin HY, Zhang JL. Luminescent zinc complexes as bioprobes for imaging molecular events in live cells. In: Inorganic and Organometallic Transition Metal Complexes with Biological Molecules and Living Cells. Academic Press; 2017. p. 1–53.

225. Li M, Lu Y, Yang M, Li Y, Zhang L, Xie S. One dodecahedral bismuth(iii) complex derived from 2-acetylpyridine N(4)-pyridylthiosemicarbazone: Synthesis, crystal structure and biological evaluation. Dalt T. 2012;41(41):12882–7.

226. Anadón A, Martínez-Larrañaga MR. Veterinary drugs residues: Coccidiostats. In: Encyclopedia of Food Safety. Elsevier; 2014. p. 63–75.

227. Taylor MA, Bartram DJ. The history of decoquinate in the control of coccidial infections in ruminants. J Vet Pharmacol Ther. 2012;35(5):417–27.

228. Da Cruz FP, Martin C, Buchholz K, Lafuente-Monasterio MJ, Rodrigues T, Sönnichsen B, et al. Drug screen targeted at plasmodium liver stages identifies a potent multistage antimalarial drug. J Infect Dis. 2012;205(8):1278–86.

229. Wang H, Li Q, Reyes S, Zhang J, Zeng Q, Zhang P, et al. Nanoparticle formulations of decoquinate increase antimalarial efficacy against liver stage Plasmodium

infections in mice. Nanomedicine Nanotechnology, Biol Med. 2014;10:57–65.

230. Nam TG, McNamara CW, Bopp S, Dharia N V, Meister S, Bonamy GMC, et al. A chemical genomic analysis of decoquinate, a Plasmodium falciparum cytochrome b inhibitor. ACS Chem Biol. 2011;6(11):1214–22.

231. Beteck RM, Smit FJ, Haynes RK, N'Da DD. Recent progress in the development of anti-malarial quinolones. Malar J. 2014;13(1):339.

232. Zhang M, Lu F, Cao J, Gao Q. [Comparative study of assay methods for in vitro antimalarial drug efficacy testing in Plasmodium falciparum]. Zhongguo xue xi chong bing fang zhi za zhi = Chinese J schistosomiasis Control. 2015 Apr;27(2):146–51.

233. Wang J, Urban L. The impact of early ADME profiling on drug discovery and development strategy. Drug Discov World. 2004;5(4):73–86.

234. Alsenz J, Kansy M. High throughput solubility measurement in drug discovery and development. Adv Drug Deliv Rev. 2007;59(7):546–67.

235. Kerns E, Di L, Carter G. In vitro solubility assays in drug discovery. Curr Drug Metab. 2008;9(9):879–85.

236. Hill AP, Young RJ. Getting physical in drug discovery: A contemporary perspective on solubility and hydrophobicity. Drug Discov Today. 2010;15(15–16):648–55.

237. Alelyunas YW, Pelosi-Kilby L, Turcotte P, Kary MB, Spreen RC. A high throughput dried DMSO Log D lipophilicity measurement based on 96-well shake-flask and atmospheric pressure photoionization mass spectrometry detection. J Chromatogr A. 2010;1217(12):1950–5.

238. Porat D, Dahan A. Active intestinal drug absorption and the solubility-permeability interplay. Int J Pharm. 2018;537(1–2):84–93.

239. Kerns E, Di L. Drug-like properties: Concepts, structure design and methods from ADME to toxicity optimization. 1st ed. Burlington, MA: Academic Press; 2008.

240. Kansy M, Senner F, Gubernator K. Parallel artificial membrane permeation assay in the description of passive absorption processes. J Med Chem. 1998;41(7):1007–10.

241. Seki T, Kanbayashi H, Nagao T, Chono S, Tabata Y, Morimoto K. Effect of cationized gelatins on the paracellular transport of drugs through caco-2 cell monolayers. J Pharm Sci. 2006;95(6):1393–401.

242. Wexler DS, Gao L, Anderson F, Ow A, Nadasdi L, McAlorum A, et al. Linking solubility and permeability assays for maximum throughput and reproducibility. J Biomol Screen. 2005;10(4):383–90.

243. Di L, Kerns EH, Hong Y, Chen H. Development and application of high throughput plasma stability assay for drug discovery. Int J Pharm. 2005;297(1–2):110–9.

244. Gonzalez D, Schmidt S, Derendorf H. Importance of relating efficacy measures to unbound drug concentrations for anti-infective agents. Clin Microbiol Rev. 2013;26(2):274–88.

245. Bohnert T, Gan LS. Plasma protein binding: From discovery to development. J Pharm Sci. 2013;102(9):2953–94.

246. Rimac H, Debeljak Ž, Bojić M, Miller L. Displacement of drugs from human serum albumin: From molecular interactions to clinical significance. Curr Med Chem. 2017;24(18):1930–47.

247. Zsila F, Visy J, Mády G, Fitos I. Selective plasma protein binding of antimalarial drugs to α1-acid glycoprotein. Bioorganic Med Chem. 2008;16(7):3759–72.

248. Zsila F, Fitos I. Combination of chiroptical, absorption and fluorescence spectroscopic methods reveals multiple, hydrophobicity-driven human serum albumin binding of the antimalarial atovaquone and related hydroxynaphthoquinone compounds. Org Biomol Chem. 2010;8(21):4905–14.

249. McLure JA, Miners JO, Birkett DJ. Nonspecific binding of drugs to human liver microsomes. Br J Clin Pharmacol. 2000;49(5):453–61.

250. Obach RS. Nonspecific binding to microsomes: Impact on scale-up of the in vitro intrinsic clearance to hepatic clearance as assessed through examination of warfarin, imipramine, and propranolol. Drug Metab Dispos. 1997;25(12):1359–69.

251. Smith DA, Beaumont K, Maurer TS, Di L. Clearance in drug design. J Med Chem. 2019;62(5):2245–55.

252. Richmond W, Wogan M, Isbell J, Gordon WP. Interstrain differences of in vitro metabolic stability and impact on early drug discovery. J Pharm Sci. 2010;99(11):4463–8.

253. Shah P, Kerns E, Nguyen DT, Obach RS, Wang AQ, Zakharov A, et al. An automated high-throughput metabolic stability assay using an integrated high-resolution accurate mass method and automated data analysis software. Drug Metab Dispos. 2016;44(10):1653–61.

254. Waring RH, Ramsden DB, Jarratt PDB, Harris RM. Biomarkers of endocrine disruption: Cluster analysis of effects of plasticisers on Phase 1 and Phase 2 metabolism of steroids. Int J Androl. 2012;35(3):415–23.

255. Silverman RB, Holladay MW, Silverman RB, Holladay MW. Drug metabolism. In: The Organic Chemistry of Drug Design and Drug Action. 3rd ed. Academic Press; 2014. p. 357–422.

256. Rane A, Wilkinson GR, Shand DG. Prediction of hepatic extraction ratio from in vitro measurement of intrinsic clearance. J Pharmacol Exp Ther. 1977;200(2):420–4.

257. Obach RS. Prediction of human clearance of twenty-nine drugs from hepatic microsomal intrinsic clearance data: An examination of in vitro half-life approach and nonspecific binding to microsomes. Drug Metab Dispos. 1999;27(11):1350–9.

258. US Food and Drug Administration. Guidance for industry: bioanalytical method validation guidance for industry bioanalytical method validation. Silver Spring, MD; 2018.

259. European Medicines Agency. Guideline on bioanalytical method validation. London, UK; 2011.

260. Di L, Kerns EH, Li SQ, Petusky SL. High throughput microsomal stability assay for insoluble compounds. Int J Pharm. 2006;317(1):54–60.

261. Haynes RK, Fugmann B, Stetter J, Rieckmann K, Heilmann HD, Chan HW, et al. Artemisone - A highly active antimalarial drug of the artemisinin class. Angew Chemie - Int Ed. 2006;45(13):2082–8.

262. Bampidis V, Azimonti G, Bastos M de L, Christensen H, Dusemund B, Kouba M, et al.

Safety and efficacy of Deccox® (decoquinate) for chickens for fattening. EFSA J. 2019;17(1):1–29.

263. Shah SNH, Shahzad Y, Ansari MT, Haneef M, Malik M, Badshah A, et al. Permeation kinetics studies of physical mixtures of artemisinin in polyvinylpyrrolidone. Dissolution Technol. 2012;19(4):6–13.

264. Burger C, Aucamp M, du Preez J, Haynes RK, Ngwane A, du Plessis J, et al. Formulation of natural oil nano-emulsions for the topical delivery of clofazimine, artemisone and decoquinate. Pharm Res. 2018;35(10).

265. Xing L, Glen RC. Novel methods for the prediction of logP, Pka, and logD. J Chem Inf Comput Sci. 2002;42(4):796–805.

266. Usacheva MN, Teichert MC, Biel MA. Comparison of the methylene blue and toluidine blue photobactericidal efficacy against gram-positive and gram-negative microorganisms. Lasers Surg Med. 2001;29(2):165–73.

267. Wagner SJ, Skripchenko A, Robinette D, Foley JW, Cincotta L. Factors affecting virus photoinactivation by a series of phenothiazine dyes. Photochem Photobiol. 1998;67(3):343–9.

268. Berggren S, Hoogstraate J, Fagerholm U, Lennernäs H. Characterization of jejunal absorption and apical efflux of ropivacaine, lidocaine and bupivacaine in the rat using in situ and in vitro absorption models. Eur J Pharm Sci. 2004;21(4):553–60.

269. Zheng N, Ruan J, Zhang Y. Pharmacokinetic study on absorption of stachyose. Zhongguo Zhong xi yi jie he za zhi Zhongguo Zhongxiyi jiehe zazhi = Chinese J Integr Tradit West Med. 2000;20(6):444–6.

270. Senarathna SG, Page-Sharp M, Crowe A. The interactions of P-glycoprotein with antimalarial drugs, including substrate affinity, inhibition and regulation. PLoS One. 2016;11(4):e0152677.

271. Navaratnam V, Mansor SM, Sit NW, Grace J, Li Q, Olliaro P. Pharmacokinetics of artemisinin-type compounds. Clin Pharmacokinet. 2000;39(4):255–70.

272. Li QG, Peggins JO, Lin AJ, Masonic KJ, Trotman KM, Brewer TG. Pharmacology and toxicology of artelinic acid: Preclinical investigations on pharmacokinetics,

metabolism, protein and red blood cell binding, and acute and anorectic toxicities. Trans R Soc Trop Med Hyg. 1998;92(3):332–40.

273. Centre for Drug Candidate Optimisation (CDCO) Standard Operating Procedure, Report. Monash Institute of Pharmaceutical Sciences Parkerville, VIC 3052 Australia; 2011.

274. Barr JT, Lade JM, Tran TB, Dahal UP. Fraction unbound for liver microsome and hepatocyte incubations for all major species can be approximated using a single-species surrogate. Drug Metab Dispos. 2019;47(4):419–23.

275. Riccardi K, Ryu S, Lin J, Yates P, Tess D, Li R, et al. Comparison of species and cell-type differences in fraction unbound of liver tissues, hepatocytes, and cell lines. Drug Metab Dispos. 2018;46(4):415–21.

276. Li XQ, Björkman A, Andersson TB, Gustafsson LL, Masimirembwa CM. Identification of human cytochrome P450s that metabolise anti-parasitic drugs and predictions of in vivo drug hepatic clearance from in vitro data. Eur J Clin Pharmacol. 2003;59(5–6):429–42.

277. Lavé T, Dupin S, Schmitt C, Valles B, Ubeaud G, Chou R, et al. The use of human hepatocytes to select compounds based on their expected hepatic extraction ratios in humans. Pharm Res. 1997;14(2):152–5.

278. Kratz JM, Teixeira MR, Koester LS, Simões CMO. An HPLC-UV method for the measurement of permeability of marker drugs in the Caco-2 cell assay. Brazilian J Med Biol Res. 2011;44(6):531–7.

279. Di L, Kerns EH. Biological assay challenges from compound solubility: strategies for bioassay optimization. Drug Discov Today. 2006;11(9–10):446–51.

280. Yayon A, Cabantchik ZI, Ginsburg H. Identification of the acidic compartment of Plasmodium falciparum-infected human erythrocytes as the target of the antimalarial drug chloroquine. EMBO J. 1984 Nov;3(11):2695–700.

281. Saliba KJ, Folb PI, Smith PJ. Role for the plasmodium falciparum digestive vacuole in chloroquine resistance. Biochem Pharmacol. 1998;56(3):313–20.

282. Committee for Medicinal Producs for Human Use. CHMP assessment report for

SIRTURO (International non-proprietary name: bedaquiline). London, UK; 2013.

283. Van De Waterbeemd H, Smith DA, Jones BC. Lipophilicity in PK design: Methyl, ethyl, futile. J Comput Aided Mol Des. 2001;15(3):273–86.

284. Wacher VJ, Salphati L, Benet LZ. Active secretion and enterocytic drug metabolism barriers to drug absorption. Adv Drug Deliv Rev. 1996;20(1):99–112.

285. Amidon GL, Lennernäs H, Shah VP, Crison JR. A theoretical basis for a biopharmaceutic drug classification: the correlation of in vitro drug product dissolution and in vivo bioavailability. Pharm Res An Off J Am Assoc Pharm Sci. 1995;12(3):413–20.

286. Kasim NA, Whitehouse M, Ramachandran C, Bermejo M, Lennernäs H, Hussain AS, et al. Molecular properties of WHO essential drugs and provisional biopharmaceutical classification. Mol Pharm. 2004;1(1):85–96.

287. L.X. Y, Amidon GL, Polli JE, Zhao H, Mehta MU, Conner DP, et al. Biopharmaceutics classification system: the scientific basis for biowaiver extensions. Pharm Res. 2002;19(7):921–5.

288. Kaneko J. Serum proteins and the dysproteinemias. In: Clinical biochemistry of domestic animals. Elsevier Inc.; 1977. p. 117–38.

289. Silamut K, White NJ, Looareesuwan S, Warrell DA. Binding of quinine to plasma proteins in falciparum malaria. Am J Trop Med Hyg. 1985;34(4):681–6.

290. Smith DA, Di L, Kerns EH. The effect of plasma protein binding on in vivo efficacy: Misconceptions in drug discovery. Nat Rev Drug Discov. 2010;9(12):929–39.

291. Lee I-S, Elsohle HN, Croom EM, Hufford CD. Microbial metabolism studies of the antimalarial sesquiterpene artemisninin. J Nat Prod. 1989;52(2):337–41.

292. Titulaer HAC, Zuidema J, Kager PA, Wetsteyn JCFM, Lugt CB, Merkus FWHM. The pharmacokinetics of artemisinin after oral, intramuscular and rectal administration to volunteers. J Pharm Pharmacol. 1990;42(11):810–3.

293. Lipinski CA. Drug-like properties and the causes of poor solubility and poor permeability. J Pharmacol Toxicol Methods. 2000;44(1):235–49.

294. Zhang D, Luo G, Ding X, Lu C. Preclinical experimental models of drug metabolism and disposition in drug discovery and development. Acta Pharm Sin B. 2012;2(6):549–61.

295. Roberts JA, Pea F, Lipman J. The clinical relevance of plasma protein binding changes. Clin Pharmacokinet. 2013;52(1):1–8.

296. Ambrose PG, Bhavnani SM, Ellis-Grosse EJ, Drusano GL. Pharmacokinetic-pharmacodynamic considerations in the design of Hospital-acquired or ventilator-associated bacterial pneumonia studies: Look before you leap! Clin Infect Dis. 2010 Aug;51(SUPPL. 1):S103–10.

297. Craig WA, Redington J, Ebert SC. Pharmacodynamics of amikacin in vitro and in mouse thigh and lung infections. J Antimicrob Chemother. 1991;27(SUPPL. C):29–40.

298. Löscher W, Ferland RJ, Ferraro TN. The relevance of inter- and intrastrain differences in mice and rats and their implications for models of seizures and epilepsy. Epilepsy Behav. 2017;73:214–35.

299. Benet LZ, Zia-Amirhosseini P. Basic principles of pharmacokinetics. Toxicol Pathol. 1995;23(2):115–23.

300. Toutain PL, Bousquet-Mélou A. Plasma clearance. J Vet Pharmacol Ther. 2004;27(6):415–25.

301. Toutain PL, Bousquet-Mélou A. Plasma terminal half-life. J Vet Pharmacol Ther. 2004;27(6):427–39.

302. Smith DA, Beaumont K, Maurer TS, Di L. Volume of distribution in drug design. J Med Chem. 2015;58(15):5691–8.

303. Mattison DR. Clinical pharmacology during pregnancy. In: Clinical Pharmacology During Pregnancy. 1st ed. Academic Press; 2013. p. 217–56.

304. Gabrielsson J, Weiner D. Non-compartmental analysis. In: Computational Toxicology. Humana Press; 2012. p. 377–89.

305. Borchardt RT, Hidalgo IJ, Hillgren KM, Hu M. Pharmaceutical applications of cell

culture: an overview. In: Pharmaceutical applications of cell and tissue culture to drug transport. Boston, MA: Springer; 1991. p. 1–14.

306. Tuntland T, Ethell B, Kosaka T, Blasco F, Zang R, Jain M, et al. Implementation of pharmacokinetic and pharmacodynamic strategies in early research phases of drug discovery and development at Novartis Institute of Biomedical Research. Front Pharmacol. 2014;5(174):1–16.

307. South African national standard: the care and use of animals for scientific purposes. In: South African Bureau of Standards. Edition 1. SABS Standards Division, Pretoria, South Africa; 2008.

308. Department of Health. Ethics in health research: principles, processes and structures. In: 2nd ed. Pretoria, South Africa; 2015.

309. Zhang Y, Huo M, Zhou J, Xie S. PKSolver: An add-in program for pharmacokinetic and pharmacodynamic data analysis in Microsoft Excel. Comput Methods Programs Biomed. 2010;99(3):306–14.

310. Li QG, Peggins JO, Fleckenstein LL, Masonic K, Heiffer MH, Brewer TG. The pharmacokinetics and bioavailability of dihydroartemisinin, arteether, artemether, artesunic acid and artelinic acid in rats. J Pharm Pharmacol. 1998;50(2):173–82.

311. Weathers PJ, Elfawal MA, Towler MJ, Acquaah-Mensah GK, Rich SM. Pharmacokinetics of artemisinin delivered by oral consumption of Artemisia annua dried leaves in healthy vs. Plasmodium chabaudi-infected mice. J Ethnopharmacol. 2014;153(3):732–6.

312. Benakis A, Paris M, Loutan L, Plessas CT, Plessas ST. Pharmacokinetics of artemisinin and artesunate after oral administration in healthy volunteers. Am J Trop Med Hyg. 1997;56(1):17–23.

313. Ashton M, Hai TN, Sy ND, Huong DX, Van Huong N, Niêu NT, et al. Artemisinin pharmacokinetics is time-dependent during repeated oral administration in healthy male adults. Drug Metab Dispos. 1998;26(1):25–7.

314. Pu YM, Torok DS, Ziffer H, Pan X-Q, Meshnick SR. Synthesis and antimalarial activities of several fluorinated artemisinin derivatives. J Med Chem.

1995;38(20):4120–4.

315. O'Neill PM, Hawley SR, Storr RC, Ward SA, Park BK. The effect of fluorine substitution on the antimalarial activity of tebuquine. Bioorganic Med Chem Lett. 1996;6(4):391–2.

316. Park BK, Kitteringham NR, O'Neill PM. Metabolism of fluorine-contatining drugs. Annu Rev Pharmacol Toxicol. 2001;41:443–70.

317. Nga TTT, Ménage C, Bégué J-P, Bonnet-Delpon D, Gantier J-C. Synthesis and antimalarial activities of fluoroalkyl derivatives of dihydroartemisinin. Artic J Med Chem. 1998;41:4101–8.

318. Gillis EP, Eastman KJ, Hill MD, Donnelly DJ, Meanwell NA. Applications of fluorine in medicinal chemistry. J Med Chem. 2015;58(21):8315–59.

319. Atkinson AJ, Tirona RG, Kim RB, Miller R, Markey SP, Flockhart DA, et al. Effect of liver disease on pharmacokinetics. In: Principles of Clinical Pharmacology. Third ed. Elsevier Inc.; 2012. p. 73–87.

320. Saravanakumar A, Sadighi A, Ryu R, Akhlaghi F. Physicochemical properties, biotransformation, and transport pathways of established and newly approved medications: A systematic review of the Top 200 Most Prescribed Drugs vs. the FDA-approved drugs between 2005 and 2016. Clin Pharmacokinet. 2019;58:1281–94.

321. Abay ET, Van Der Westuizen JH, Swart KJ, Gibhard L, Lawrence N, Dambuza N, et al. Efficacy and pharmacokinetic evaluation of a novel anti-malarial compound (NP046) in a mouse model. Malar J. 2015;14(1):8.

322. Peter C, Hongwan D, Küpfer A, Lauterburg BH. Pharmacokinetics and organ distribution of intravenous and oral methylene blue. Eur J Clin Pharmacol. 2000;56(3):247–50.

323. Akoachere M, Buchholz K, Fischer E, Burhenne J, Haefeli WE, Schirmer RH, et al. In vitro assessment of methylene blue on chloroquine-sensitive and -resistant Plasmodium falciparum strains reveals synergistic action with artemisinins. Antimicrob Agents Chemother. 2005;49(11):4592–7.

324. Kansy M, Gerber PR, Kratochwil NA, Huber W, Mu F. Predicting plasma protein binding of drugs : a new approach. Biochem Pharmacol. 2002;64(9):1355–74.

325. Schleiferböck S, Scheurer C, Ihara M, Itoh I, Bathurst I, Burrows JN, et al. In vitro and in vivo characterization of the antimalarial lead compound SSJ-183 in Plasmodium models. Drug Des Devel Ther. 2013;7:1377–84.

326. Kusuhara H, Suzuki H, Sugiyama Y. The role of P-glycoprotein and canalicular multispecific organic anion transporter in the hepatobiliary excretion of drugs. J Pharm Sci. 1998;87(9):1025–40.

327. Chan LMS, Lowes S, Hirst BH. The ABCs of drug transport in intestine and liver: Efflux proteins limiting drug absorption and bioavailability. Eur J Pharm Sci. 2004;21(1):25–51.

328. Kim RB. Drugs as P-glycoprotein substrates, inhibitors, and inducers. Drug Metab Rev. 2002;34(1–2):47–54.

329. Sharom FJ. ABC multidrug transporters: Structure, function and role in chemoresistance. Pharmacogenomics. 2008;9(1):105–27.

330. Aller S, Yu J, Ward A, Weng Y, Chittaboina S, Zhuo R, et al. Structure of P-glycoprotein reveals a molecular basis for poly-specific drug binding. Science (80-). 2009;323(5922):1718–22.

331. Scovill JP, Klayman DL, Lambros CL, Childs GE, Notsch JD. 2-Acetylpyridine thiosemicarbazones. 9. Derivatives of 2-acetylpyridine 1-oxide as potential antimalarial agents. J Med Chem. 1984;27(1):87–91.

332. Klayman DL, Bartosevich JF, Griffin TS, Mason CJ, Scovill JP. 2-Acetylpyridine thiosemicarbazones. 1. A new class of potential antimalarial agents. J Med Chem. 1979;22(7):855–62.

333. Greenbaum DC, Mackey Z, Hansell E, Doyle P, Gut J, Caffrey CR, et al. Synthesis and structure-activity relationships of parasiticidal thiosemicarbazone cysteine protease inhibitors against Plasmodium falciparum, Trypanosoma brucei, and Trypanosoma cruzi. J Med Chem. 2004;47(12):3212–9.

334. Parkinson CJ, Birrell GW, Chavchich M, Mackenzie D, Haynes RK, de Kock C, et al.

Development of pyridyl thiosemicarbazones as highly potent agents for the treatment of malaria after oral administration. J Antimicrob Chemother. 2019;74:2965–73.

335. Jing-Ming L, Ni Mu-Yun F, Al J-F. Structure and reaction of arteannuin. Acta Chim Sin. 1979;37(2):129–43.

336. Ansari M, Saify Z, Sultana N, Ahmad I, Saeed-Ul-Hassan S, Tariq I, et al. Malaria and artemisinin derivatives: an updated review. Mini-Reviews Med Chem. 2013;13(13):1879–902.

337. Fivelman QL, Adagu IS, Warhurst DC. Modified fixed-ratio isobologram method for studying in vitro interactions between atovaquone and proguanil or dihydroartemisinin against drug-resistant strains of Plasmodium falciparum. Antimicrob Agents Chemother. 2004;48(11):4097–102.

338. White NJ. Preventing antimalarial drug resistance through combinations. Drug Resist Updat. 1998;1(1):3–9.

339. Gaur R, Darokar MP, Ajayakumar P V, Shukla RS, Bhakuni RS. In vitro antimalarial studies of novel artemisinin biotransformed products and its derivatives. Phytochemistry. 2014;107:135–40.

340. Park GM, Park H, Oh S, Lee S. Antimalarial activity of C-10 substituted triazolyl artemisinin. Korean J Parasitol. 2017 Dec 1;55(6):661–5.

341. Rudrapal M, Chetia D, Singh V. Novel series of 1,2,4-trioxane derivatives as antimalarial agents. J Enzyme Inhib Med Chem. 2017;32(1):1159–73.

342. Vivas L, Rattray L, Stewart LB, Robinson BL, Fugmann B, Haynes RK, et al. Antimalarial efficacy and drug interactions of the novel semi-synthetic endoperoxide artemisone in vitro and in vivo. J Antimicrob Chemother. 2007;59(4):658–65.

343. Schmuck G, Temerowski M, Haynes R, Fugmann B. Identification of non-neurotoxic artemisinin derivatives in vivo and in vitro. Res Adv Antimicrob Agents Chemother. 2003;3:35–47.

344. Coulibaly B, Zoungrana A, Mockenhaupt FP, Schirmer RH, Klose C, Mansmann U, et

al. Strong gametocytocidal effect of methylene blue-based combination therapy against falciparum malaria: a randomised controlled trial. PLoS One. 2009;4(5):1–6.

345. Moreno L, Echevarria F, Muñoz F, Alvarez L, Sanchez Bruni S, Lanusse C. Dose-dependent activity of albendazole against benzimidazole-resistant nematodes in sheep: Relationship between pharmacokinetics and efficacy. Exp Parasitol. 2004;106(3–4):150–7.

346. Orhan G, Bayram A, Zer Y, Balci I. Synergy tests by E test and checkerboard methods of antimicrobial combinations against Brucella melitensis. J Clin Microbiol. 2005;43(1):140–3.

347. Berenbaum MC. A method for testing for synergy with any number of agents. Source J Infect Dis. 1978;137(2):122–30.

348. Ohrt C, Willingmyre GD, Lee P, Knirsch C, Milhous W. Assessment of azithromycin in combination with other antimalarial drugs against Plasmodium falciparum in vitro. Antimicrob Agents Chemother. 2002;46(8):2518–24.

349. Snyder C, Chollet J, Santo-Tomas J, Scheurer C, Wittlin S. In vitro and in vivo interaction of synthetic peroxide RBx11160 (OZ277) with piperaquine in Plasmodium models. Exp Parasitol. 2007;115(3):296–300.

350. Dormoi J, Pascual A, Briolant S, Amalvict R, Charras S, Baret E, et al. Proveblue (methylene blue) as an antimalarial agent: In vitro synergy with dihydroartemisinin and atorvastatin. Antimicrob Agents Chemother. 2012;56(6):3467–9.

351. Ohrt C, Li Q, Obaldia N, Im-Erbsin R, Xie L, Berman J. Efficacy of intravenous methylene blue, intravenous artesunate, and their combination in preclinical models of malaria. Malar J. 2014;13(1):1–8.

352. Akoachere M, Buchholz K, Fischer E, Burhenne J, Haefeli WE, Schirmer RH, et al. In vitro assessment of methylene blue on chloroquine-sensitive and -resistant Plasmodium falciparum strains reveals synergistic action with artemisinins. Antimicrob Agents Chemother. 2005;49(11):4592–7.

353. Nagelschmitz J, Voith B, Wensing G, Roemer A, Fugmann B, Haynes RK, et al. First assessment in humans of the safety, tolerability, pharmacokinetics, and ex vivo pharmacodynamic antimalarial activity of the new artemisinin derivative artemisone. Antimicrob Agents Chemother. 2008;52(9):3085–91.

354. Lambros C, Vanderberg JP. Synchronization of Plasmodium falciparum erythrocytic stages in culture. J Parasitol. 1979;65(3):418.

355. Steyn JD, Wiesner L, Du Plessis LH, Grobler AF, Smith PJ, Chan WC, et al. Absorption of the novel artemisinin derivatives artemisone and artemiside: Potential application of Pheroid™ technology. Int J Pharm. 2011;414(1–2):260–6.

356. Resende LA, da Silva PHR, Fernandes C. Quantitative determination of the antimalarials artemether and lumefantrine in biological samples: A review. J Pharm Biomed Anal. 2019;165:304–14.

357. Walter-Sack I, Rengelshausen J, Oberwittler H, Burhenne J, Mueller O, Meissner P, et al. High absolute bioavailability of methylene blue given as an aqueous oral formulation. Eur J Clin Pharmacol. 2009;65(2):179–89.

358. Rengelshausen J, Burhenne J, Fröhlich M, Tayrouz Y, Singh SK, Riedel KD, et al. Pharmacokinetic interaction of chloroquine and methylene blue combination against malaria. Eur J Clin Pharmacol. 2004;60(10):709–15.

359. Matuszewski BK. Standard line slopes as a measure of a relative matrix effect in quantitative HPLC-MS bioanalysis. J Chromatogr B Anal Technol Biomed Life Sci. 2006;830(2):293–300.

360. Matuszewski BK, Constanzer ML, Chavez-Eng CM. Strategies for the assessment of matrix effect in quantitative bioanalytical methods based on HPLC-MS/MS. Anal Chem. 2003;75(13):3019–30.

8 Appendices

Appendix A

Appendix A presents the materials, instruments, sample preparation and methods used during culturing of *P. falciparum* parasites and mammalian cells, and *in vitro* screening assays.

List of materials

Table 8-1: List of materials used for the culturing of *P. falciparum* parasites.

Materials used for tissue culture of parasites	**Supplier**
RPMI 1640 with glutamine, without sodium bicarbonate (R6504)	Sigma Life Science
HEPES (N-2-[hydroxyethyl]piperizine-N'-2-[ethanesulfonic acid])	
D-(+)-Glucose	
Hypoxanthine	
Gentamicin solution	
Sodium bicarbonate	
Sodium L-lactate	
D- Sorbitol	
Phosphate buffered saline (PBS) tablet	
Sodium chloride	Merck
Glycerine (1,2,3 – propantriol)	
Sodium dihydrogen phosphate	Merck
Oil for immersion lenses	
Giemsa's azur eosin methylene blue solution	
Albumax II	Gibco
Potassium chloride	Sigma

Table 8-2: List of materials used for the pLDH assays.

Materials used for the pLDH assays	**Supplier**
3-Acetylpyridine adenine dinucleotide (APAD)	Sigma Life Sciences
Calcium L-lactate hydrate	
Trizma base (Tris)	
Chloroquine ($C_{18}H_{26}ClN_3.2H_3PO_4$, Mw = 515.87 g/mol)	
Artesunate ($C_{19}H_{28}O_8$, Mw = 384.42 g/mol)	
Nitro blue tetrazolium salt (NBT)	Merck
Phenazine ethosulphate	
Dimethyl sulfoxide (DMSO)	Merck
Triton X 100	

Table 8-3: List of materials used for the culturing of mammalian cells.

Materials used for culture of mammalian cell lines	**Supplier**
Dulbecco's modified Eagles Medium (DMEM)	Merck
Sodium bicarbonate ($NaHCO_3$)	
Gentamicin solution	
HAM'S F-12	Thermo-Scientific
Trypsin	Sigma
Phosphate buffered saline (PBS) tablet	
Fetal calf serum	

Table 8-4: List of materials used for the mammalian cell survival assay.

Materials used for the MTT assay	**Supplier**
3-(4,5-dimethylthiazol-2-yl)-2,5-diphenyl tetrazolium bromide (MTT)	Thermo Scientific
Crystal violet	Merck
Emetine hydrochloride ($C_{29}H_{40}N_2O_4 \cdot 2HCl$, Mw = 553.56 g/mol)	

Instrumentation

Water bath

A GRANT digital Y6 water bath or a YIH DER BL-710 water bath was used throughout all *in vitro P. falciparum* studies. The temperature of the water was maintained at 37°C.

Incubator

A Labcon 508IU incubator maintained at 37°C was used to store all cultures of *P. falciparum*. A Nuaire Autoflow CO_2 Air Jacketed Incubator was used to store all mammalian cell lines.

Light microscope

A Laborlux 12 Leitz Light microscope was used to view thin films of malaria parasites on glass microscope slides, in order to determine parasitaemia by counting and determine the integrity of cultures. A Sigma bright line hemacytometer (Z353, 962-9) was used to determine cell counts.

Vortex

A Scientific Industries Vortex Genie2 (G560E) was used to homogenize all suspensions and solutions, where required.

Weighing balance

A Satorius CPA2P Micro-Analytical Balance was used to weigh out all compounds and standards.

Centrifuge

An Eppendorf Centrifuge 5810R or 5804 was used to centrifuge cultures in Greiner Falcon tubes (15 and 50 mL). An Eppendorf deep well plate attachment (A-2-DWP) was used for suspensions in 96-well plates.

pH meter

A bench Jenway 3510 pH meter fitted with a 924 007 glass Jenway electrode to determine and adjust the pH of all solutions. The pH meter was calibrated before use with buffer solutions at pH 4.00 ± 0.01 and 7.00 ± 0.01 kept at a room temperature of ~23°C. Electrodes were stored immersed in a 3 M KCl solution obtained from Sigma Aldrich.

Plate reader

A Turner Biosystems Modulus Plate Reader was used to determine the absorbance of the MTT- and NBT-treated plates, at 540 nm and 620 nm, respectively.

Software

GraphPad Prism version 5 (GraphPad Software Inc.) for Windows was used to analyse all data and calculate statistical significance (GraphPad Software Inc., La Jolla, California). ChemDraw Professional V16.0.1.4 (PerkinElmer) was used to generate chemical structures and figures.

Sample preparation – Lactate dehydrogenase assay

Preparation of compounds and reference controls

All novel compounds were dissolved in 100% DMSO, while chloroquine and artesunate (as positive controls) were dissolved in distilled water. Stocks were stored at -20°C until used. Wells containing uninfected RBCs in CM served as 'blank' controls, while wells containing only infected RBCs in CM served as parasite growth controls.

Preparation of CM

The following was added to 1 L distilled water for incomplete CM: 10.4 g/L RPMI 1640 (containing glutamine, but without sodium bicarbonate), 4 g/L D-(+)-glucose, 6 g/L HEPES, 0.088 g/L Hypoxanthine, 5 g/L Albumax and 0.05 g/L gentamycin. The medium was pre-filtered (0.45 µm filter) and then filter sterilized (0.22 µm membrane) into autoclaved bottles. Medium was stored at 4°C until used.

CM was made by adding 8.4 mL 5% sodium bicarbonate to 200 mL incomplete medium and stored at 4°C until used.

Wash medium was prepared in the same manner as incomplete medium but omitting the Albumax. The medium was stored at 4°C until used.

Sodium bicarbonate

A 5% solution of $NaHCO_3$ was prepared by adding 50 g $NaHCO_3$ to 1 L distilled water. The solution was stored at 4°C until used.

Sodium chloride (12%)

A 12% solution of sodium chloride was prepared by dissolving 12 g of NaCl in 100 mL of distilled water. The solution was filter sterilized (0.22 µm membrane) into an autoclaved glass bottle and stored at 4°C until needed.

Sodium chloride (1.8%)

The solution was prepared by dissolving 1.8 g of NaCl in 100 mL of distilled water. The solution was filter sterilized (0.22 µm membrane) into an autoclaved glass bottle and stored at 4°C until needed.

Sodium chloride (0.9%) with glycerine (0.2%)

The solution was prepared by dissolving 0.9 g of NaCl and 0.2 mL glycerine in 100 mL of distilled water. The solution was filter sterilized (0.22 µm membrane) into an autoclaved glass bottle and stored at 4°C until needed.

PBS

A phosphate buffer solution was prepared by dissolving 1 tablet in 200 mL of distilled water. The final solution consisted of 0.01 M phosphate buffer, 0.0027 M KCl and 0.14 M NaCl with a pH of 7.4 at 25°C.

Giemsa staining solution

A 10% Giemsa stain solution was prepared by adding 1:10 volumes of Giemsa stain to PBS.

Sorbitol solution

A 5% D- Sorbitol solution was prepared by dissolving 50 g of D-sorbitol in 1 L of distilled water. The solution was sterile filtered through a membrane (0.22 µm) into autoclaved glass bottles and stored at 4°C until needed.

Human red blood cells

Washed type O positive human RBCs were obtained from the Groote Schuur Hospital blood bank. Blood was washed twice with wash medium, by adding equal parts of blood and medium to a 50 mL Falcon tube, under sterile conditions. The blood was centrifuged

at 1200 x *g* for 5 minutes and the supernatant was aspirated. The washed blood was stored at 4°C.

MALSTAT solution

The following was dissolved in 150 mL of distilled water: 400 µL TritonX100, 4 g L-lactate, 1.32 g Tris buffer, and 22 mg of APAD. The pH was adjusted to 9 with 32% HCl and the final volume made up to 200 mL. The solution was stored at 4°C.

NBT solution

Nitrolbue tetrazolium and phenazine ethosulphate was weighed out at a 20:1 ratio, i.e. 0.16 mg/mL and 3.2 mg/mL, respectively. The solution was made up in distilled water and covered with aluminium foil, as the reagents are light sensitive. The solution was kept at 4°C until needed.

Sample preparation – 3-(4,5-dimethylthiazol-2-yl)-2,5-diphenyl tetrazolium bromide (MTT) assay

Preparation of compounds and reference control

All novel compounds were dissolved in 100% DMSO, while emetine (as positive control) was dissolved in distilled water. Stocks were stored at -20°C until used. Wells containing only culturing medium served as the 'blank' controls, while wells containing cells with culturing medium served as the cell growth control.

Preparation of CM

Incomplete Dulbecos Modified Eagles Medium (DMEM) was prepared by adding 13.53 g of DMEM powder and 3.7 g $NaHCO_3$ to 1L of distilled water. The resultant solution was stirred for 30 minutes and the pH adjusted to 7.1. Lastly, 500 µl/L gentamycin was added. The solution was pre-filtered (0.45 µm filter) and then filter sterilized through a membrane (0.22 µm) into autoclaved glass bottles.

Incomplete HAMS F-12 medium was prepared by adding one bottle of HAMS F-12 to 1 L. The solution was stirred for 30 minutes and the pH adjusted to 7.1. Lastly, 500 µl/L gentamycin was added. The solution was pre-filtered (0.45 µm filter) and then filter sterilized through a membrane (0.22 µm) into autoclaved glass bottles.

CM for the CHO cell line was made up by adding the following to an autoclaved glass bottle: 10% heat inactivated fetal calf serum: 45% DMEM: 45% HAMS F-12. The medium was stored at 4°C, until needed.

Thawing medium for the CHO cell line was made up by adding the following to an autoclaved glass bottle: 30% heat inactivated fetal calf serum: 35% DMEM: 35% HAMS F-12

Fetal calf serum (FCS)

Fetal calf serum was prepared by heat inactivation at 56°C for 30 minutes. The serum was stored at 4°C in sterile Falcon tubes for short term use.

PBS

A phosphate buffer solution was prepared by dissolving 1 tablet in 200 mL of distilled water, which yielded a solution consisting of 0.01 M phosphate buffer, 0.0027 M KCl, and 0.14 M NaCl with a pH of 7.4 at 25°C.

Trypsin

A 0.25% Trypsin solution was prepared by adding 0.10 g of Trypsin to 100 mL of PBS. The solution was stored at 4°C.

Crystal violet dye

A 10% crystal violet solution was prepared in PBS and stored at room temperature.

MTT

A 5mg/mL solution of MTT was prepared in PBS and filter sterilized (0.45 μm filter) into an autoclaved glass bottle. The solution was covered with aluminium foil, as MTT is light sensitive.

Methodology – Lactate dehydrogenase assay

Thawing of P. falciparum cultures

The CQS NF54 (derived from a patient near Schiphol, Amsterdam presumed to be of West African origin) and CQR Dd2 (derived from W2-MEF, Indochina III/CDC) *P. falciparum* parasite strains obtained from MR4 were used throughout the study.

Parasites were thawed by slowly adding 1 volume of 12% sodium chloride to 5 volumes of thawed parasites with constant mixing. After 5 minutes, 10 mL of 1.8% NaCl was added and centrifuged for 5 minutes at 400 x *g*. The supernatant was removed and 10 mL of 0.9% NaCl with glucose was added and allowed to stand for 5 minutes. The solution was centrifuged for 5 minutes at 400 x *g*. After removing the supernatant, the pellet was placed into culture.

Continuous culture of P. falciparum

Cultures were maintained under sterile conditions throughout cultivation process in washed O+ human RBC at a 5% haematocrit in CM. CQS and CQR strains were cultured according to a modified method of Trager and Jensen.[142] Cultures were transferred to sterile centrifuge tubes from the culture flask and centrifuged at 750 x *g* for 5 minutes. The supernatant was aspirated, and a thin blood smear slide was prepared on a glass slide. The slide was fixed with methanol, rinsed with tap water and stained with the Giemsa staining solution for 10 minutes. A light microscope with an oil emersion lens (100 x objective) was used to view the slide in order to determine the predominant phase of the culture. Parasitaemia was calculated as a percentage of the infected RBCs counted, over the total number of cells counted. For a trophozoite culture, the pellet was diluted with washed human RBCs to 5% parasitaemia in 40 mL fresh CM and transferred back to a clean flat-bottomed culture flask. In the case of a predominantly ring culture, the cells were incubated on the bench with 10 mL sorbitol, according to Lambros and Vanderberg,[354] to lyse the cells containing trophozoites. After 15 minutes, the cultures were centrifuged, and the supernatant carefully removed. The pellet was resuspended in fresh CM and transferred to a clean flat-bottomed culture flask. The flasks were gassed with a mixture of 3% O_2, 4% CO_2, and 93% N_2 for 1 minute and incubated at 37°C.

Lactate dehydrogenase assay

The CQS and CQR *P. falciparum* strains were used in the lactate dehydrogenase assay to determine *in vitro* antiplasmodial activity, with a modified method described by Makler *et al*.[149] All compounds tested in the study were prepared from powdered form to a stock concentration in DMSO, except for CQ, which was prepared in distilled water. Compounds were diluted in CM and 200 µL of the highest concentration was added to a sterile 96-well plate. A two-fold dilution was achieved across the plate by transferring 100 µL form the highest concentration into the adjacent well, containing equal volume of CM. A stock culture of synchronous ring stage *P. falciparum* parasites was diluted to a 2%

parasitaemia with a 2% haematocrit, using washed human RBCs in CM. By adding 100 µL of pRBC to the drug-containing wells, the final parasitaemia and haematocrit of 1% was achieved. Plates were incubated for 72 hours at 37°C in airtight chambers and gassed in the same manner as with maintaining continuous cultures.

Plates were frozen at overnight -80°C after completion of the incubation period and analysed as per the method of Makler *et al*.[149] Aliquots of 15 µL from each well was removed and transferred to wells containing 100 µL of the MALSTAT solution. After a 30-minute incubation at room temperature, 25 µL of NBT was added to each well and the plates were left to develop in the dark for approximately 10 minutes. Plates were read at 620 nm.

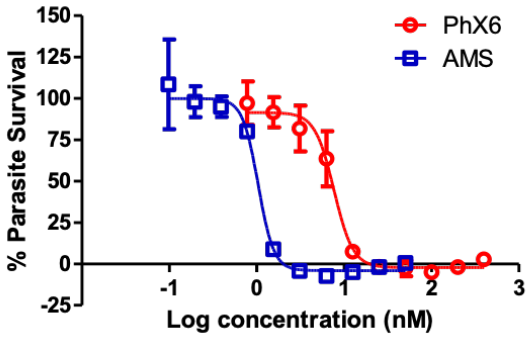

Figure 8-1: Representative dose-response curve for artemisone and PhX6

Methodology – MTT assay

Thawing of mammalian cell cultures

Vials containing aliquots of CHO cells were removed from liquid nitrogen and placed on ice. After slightly thawing on ice, the cells were transferred from cryotubes to sterile 15 mL Falcon tubes containing 9 mL of thawing medium. After the pellet thawed completely, the tubes were centrifuged at 750 x *g* for 5 minutes. The supernatant was aspirated, the pellet resuspended in 1 mL cold thawing medium and transferred to a cell suspension flask containing 9 mL thawing medium. The flask was incubated at 37°C (with 5% CO_2) and left for 48 hours to allow attachment.

Sub culturing of mammalian cell cultures

Viewing of flasks under a light microscope (100 x objective) allowed assessment of cell confluency. Elongated cells indicate attachment and appear round when detached from the flask surface. Medium was aspirated and the cells rinsed twice with sterile PBS. Trypsin was heated to 37 °C in a water bath and added to the flask to detach the cells. The flask was incubated for 5-10 minutes at room temperature and gently agitated to ensure detachment of all cells. After confirmation of detachment, 5 mL of heated CM was added to the flask to inhibit the Trypsin. The culture was transferred to sterile 15 mL Falcon tubes and centrifuged at 750 x *g* for 5 minutes. Medium was aspirated and the pellet resuspended in 5 mL CM, from which 1 mL of cell suspension was transferred to a new flask containing 9 mL CM. The flask was incubated at 37°C (with 5% CO_2).

MTT cytotoxicity assay

A cell culture stock was prepared at a concentration of 105 cells/mL. Cells were counted on a hemacytometer under a microscope (100 x objective) by adding 20 µL of cell suspension to 20 µL crystal violet dye and adding 20 µL of the mixture to a chamber on the hemacytometer.

The cell culture was added to a sterile 96-well plate and placed in the incubator at 37°C with 5% CO_2 for 24 hours to allow attachment. Tenfold dilutions of the compounds and standard were made in autoclaved Eppendorf tubes, in CM. The medium was carefully aspirated from the wells and 200 µL of the dilutions was added to the wells. Plates were covered with sterile lids and incubated for 48 hours.

As MTT is light sensitive, the staining and incubation process needed to be completed in the dark. Twenty-five microliters of sterile MTT was added to each well and left to incubate at room temperature for 4 h. Plates were covered with foil and centrifuged at 200 rpm for 10 minutes, the medium carefully aspirated and 100 µL of DMSO added to dissolve the crystals. After being briefly shaken, the absorbance was read at 540 nm on the plate reader.

Appendix B

Appendix B presents all materials and sample preparation used during *in vitro* ADME assays

List of materials

Table 8-5: Summary of materials used during ADME assays.

Materials used in all ADME assays	**Supplier**
KH_2PO_4 (MW = 136.09 g/mol)	Merck
K_2HPO_4 (MW = 174.19 g/mol)	Merck
Acetonitrile	Merck
DMSO	Sigma-Aldrich
Formic acid	Sigma
Purified water	Millipore
Carbamazepine (ISTD, $C_{15}H_{12}N_2O$, MW = 236.27 g/mol)	Sigma
Materials used in kinetic solubility assays	Supplier
Hydrocortisone (MW = 362.5 g/mol)	Sigma
NaCl (MW= 58.4 g/mol)	Sigma
KCl (MW = 74.6 g/mol)	Sigma
$Na_2HPO_4.7H_2O$ (MW = 286.1 g/mol)	Sigma
37% HCl	Sigma
Reserpine (MW = 608.7 g/mol)	AiBST Zimbabwe
Materials used in lipophilicity assays	Supplier
Octanol	Sigma
Ouabain ($C_{29}H_{44}O_{12}\cdot 8H_2O$, MW = 728.77 g/mol)	Sigma
Hydrocortisone ($C_{21}H_{30}O_5$, MW = 362.46 g/mol)	Sigma
Verapamil ($C_{27}H_{39}ClN_2O_4$, MW = 491.06 g/mol)	Sigma

Table 8-6: Summary of materials used during ADME assays (continued)

Materials used in plasma stability assay	**Supplier**
Procaine hydrochloride ($C_{13}H_{21}ClN_2O_2$, MW = 272.77 g/mol)	Sigma
Vinpocetin ($C_{22}H_{26}N_2O_2$, MW = 350.45 g/mol)	Sigma
Human plasma	Groote Schuur Hospital Blood bank
Materials used in metabolic stability assay	Supplier
NADPH	Sigma
Propranolol hydrochloride ($C_{16}H_{21}NO_2$·HCl, MW = 295.8 g/mol)	Sigma
Midazolam maleate salt ($C_{18}H_{13}ClFN_3 \cdot C_4H_4O_4$, MW = 441.8 g/mol)	AiBST Zimbabwe
MMV390048 (MW = 939.39 g/mol)	UCT, internal compound
Human and mouse liver microsomes	Xenotech
Materials used in plasma protein binding assay	Supplier
Caffeine ($C_8H_{10}N_4O_2$, MW = 194.19 g/mol)	Sigma
Warfarin ($C_{19}H_{16}O_4$, MW = 308.33 g/mol)	Sigma
Human plasma	Groote Schuur Hospital Blood bank
Materials used in microsomal protein binding assay	Supplier
Propranolol hydrochloride ($C_{16}H_{21}NO_2 \cdot HCl$, MW = 295.8 g/mol)	Sigma
Warfarin ($C_{19}H_{16}O_4$, MW = 308.33 g/mol)	Sigma
Human and mouse liver microsomes	Xenotech

Table 8-7: Summary of materials used during ADME assays (continued)

Materials used in PAMPA assay	**Supplier**
Sodium acetate anhydrous	BDH Chemicals
37% HCL	Sigma
NaCl (MW= 58.4 g/mol)	Sigma
NaOH (MW = 40 g/mol)	Sigma
KCl (MW = 74.6 g/mol)	Sigma
$Na_2HPO_4.7H_2O$ (MW = 286.1 g/mol)	Sigma
Lucifer Yellow CH dipotassium salt (MW = 521.57 g/mol)	Sigma
Warfarin ($C_{19}H_{16}O_4$, MW = 308.33 g/mol)	Sigma

Instrumentation

Water bath

A New Brunswick Scientific Innova 3100 Reciprocal water bath was used to incubate assay plates where required.

Vortex

A Scientific Industries Vortex Genie2 (G560E) was used to homogenize all suspensions and solutions, where required.

Weighing balance

A Satorius CPA2P Micro-Analytical Balance was used to weigh out all compounds and standards.

Ultracentrifuge

Optima L-80XP Beckman with a titanium fixed angle rotor (Type 42.2 Ti) was used to centrifuge microsamples at 42000 rpm.

pH meter

A bench Jenway 3510 pH meter fitted with a 924 007 glass Jenway electrode to determine and adjust the pH of all solutions. The pH meter was calibrated before use with buffer solutions at pH 4.00 ± 0.01 and 7.00 ± 0.01 kept at a room temperature of ~23°C. Electrodes were stored immersed in a 3 M KCl solution obtained from Sigma Aldrich.

Orbital plate shaker

Plates were agitated on an MS 3 Digital Shaker (IKA, Staufen, Germany).

HPLC-DAD

Samples were analysed by a HPLC-DAD (Agilent 1200 Rapid Resolution HPLC with a diode array detector) (Agilent, Little Falls, Wilmington, USA).

LC-MS/MS

Samples were analysed by LC-MS/MS which consisted of a Schimadzu high-performance liquid chromatography (HPLC) system (Kyoto, Japan), coupled to an AB Sciex 3200 Q TRAP mass spectrometer (AB Sciex, Massachusetts, USA).

Software

Analyst software version 1.6.2 (SCIEX, Massachusetts, USA) was used to analyse the data collected. Excel 2013 for Windows was used to do all calculations from raw data (Microsoft Office Excel 2010). GraphPad Prism version 5 for Windows was used construct all graphs, where applicable (GraphPad Software Inc., La Jolla, California).

Sample preparation

Preparation of reference controls and test compounds

All control and test compounds were dissolved in 100% DMSO and stored at -20°C until used.

Preparation of phosphate buffer at pH 7.4 and 6.5

Phosphate buffered saline (PBS) was prepared by adding 0.8 g NaCl, 0.2 mg KCl, 0.155 g $Na_2HPO_4.7H_2O$ and 0.2 g KH_2PO_4 to 100 mL purified water. The pH was measured and adjusted to pH 7.4 and 6.5 with 0.05 M HCL or 0.05 M NaOH.

Hydrochloric acid solution at pH 2

A hydrochloric acid solution was prepared by adding 83 μL of 37% HCl to 50 mL of purified water in a 100 mL volumetric flask. The flask was filled to the line with purified water and the pH was measured and adjusted to pH 2, if needed.

Potassium dihydrogen phosphate stock solution (1 M)

A stock solution of potassium dihydrogen phosphate was prepared by dissolving 13.6 g of KH_2PO_4 in 100 mL purified water. The solution was stored at 4°C until used.

Dipotassium phosphate stock solution (1 M)

A stock solution of dipotassium phosphate was prepared by dissolving 17.4 g of K_2HPO_4 in 100 mL purified water. The solution was stored at 4°C until used.

Potassium phosphate buffer (0.1 M)

A phosphate buffer was prepared by mixing 19.8 mL of potassium dihydrogen phosphate solution and 80.2 mL of dipotassium phosphate solution and diluting the mixture to 1 L in a glass bottle. The solution was stored at 4°C until used.

Lucifer yellow stock (10mM)

A 10 mM solution of lucifer yellow was prepared by dissolving 5.2 mg in 1 mL purified LC-MS/MS water. The solution was stored at -20°C until needed.

5% Hexadecane in Hexane

A 5% (v/v) stock solution of hexadecane in hexane artificial lipid solution was prepared and stored at room temperature for up to one month.

Preparation of the artificial membrane

Fifteen microliters of the 5% hexadecane solution were carefully added to each of the wells of the donor plate, as close as possible to the PAMPA membrane. The solution was evaporated in a fume hood for approximately 1 hour.

Measuring Lucifer Yellow for assessment of membrane integrity

To assess the integrity of the artificial membrane, 100 µL of acceptor samples, equilibrium samples, and blank acceptor buffer (pH 7.4) were added to a black 96-well plate. Fluorescence was measured using a plate reader (Blue filter; 490 nm excitation/510–570 nm emission wavelengths). If the fluorescence reading of acceptor samples are greater than 3 times the blank buffer readings, the membrane integrity of those samples were disrupted.

Carbamazepine internal standard solutions

A stock solution of carbamazepine was prepared by dissolving 5.9 mg in 250 mL purified water. A 0.1 µM working solution was prepared by diluting the stock solution 1:999 (v/v) in ACN. Both solutions were stored at -20°C until used.

Nicotinamide adenine dinucleotide phosphate solution (10 mM)

A solution of nicotinamide adenine dinucleotide phosphate was prepared by dissolving 8.3 mg of NADPH in 1 mL purified water. As the solution cannot be prepared in advance and stored, it was prepared right before addition to the assay plate.

Preparation of mobile phases for HPLC-DAD analysis

Aqueous mobile phases consisted of 0.1% formic acid solution in purified water with 5% organic mobile phase. The organic phase consisted of a 0.1% formic acid solution in acetonitrile (ACN).

Preparation of mobile phases for LC-MS/MS analysis

Aqueous and organic solutions were prepared for each compound identified during method development. Aqueous mobile phases consisted of either 0.1% formic acid solution in deionised water, 5 mM ammonium acetate in deionised water or 10 mM ammonium acetate with 0.1 % acetic acid in deionised water. The organic phase consisted of either 100% ACN, 0.1% acetic acid in ACN or 50:50 (v/v) solution of MeOH and ACN with 0.1% acetic acid.

Appendix C

Appendix C presents the details relating to the detection of the different analytes during LC-MS/MS analysis.

Table 8-8: Materials used during sample preparation and analysis of pharmacokinetic evaluation.

Material	**Supplier**
Methanol	Honeywell
Acetic acid	Merck
Formic acid	
Hydroxypropyl Methylcellulose (0.5%)	Sigma-Aldrich
Tween 80	
Dimethyl sulfoxide	
Dimethylacetamide	
Polyethylene glycol	
Propylene glycol	
Ethanol	

Table 8-9: Summary of aqueous and organic mobile phase preparation for LC-MS/MS analysis.

Compound	**Aqueous phase**	**Organic Phase**
WHN012	5 mM $NH_4CH_3CO_2$ + 0.1% AA	MeOH and ACN 1:1 (v:v) + 0.1% AA
PhX6	0.1% FA	100% ACN
AD01	0.1% FA	100% ACN
DpNEt	0.1% FA	100% ACN
RMB005	5 mM $NH_4CH_3CO_2$	100% ACN
RMB059	5 mM $NH_4CH_3CO_2$	100% ACN
RMB060	5 mM $NH_4CH_3CO_2$	100% ACN
DQ	5 mM $NH_4CH_3CO_2$ + 0.1% AA	0.1% AA in ACN

AA, acetic acid; ACN, acetonitrile; FA, formic acid; MeOH, methanol; $NH_4CH_3CO_2$, ammonium acetate.

Table 8-10: Details of the internal standards used for each of the compounds during analysis of the pharmacokinetic experiment samples

Compound analysed	**ISTD**	**Molecular Mass (g/mol)**	**Structure**
WHN012	WHN015	524.5	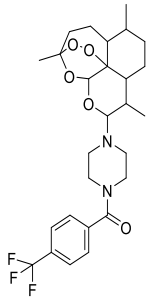
AD01 and PhX6	MMV902	392.4	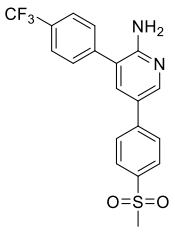
DpNEt	MMV390048	393.4	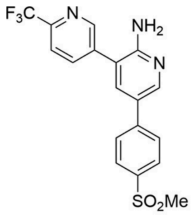
RMB005	DQ	417.5	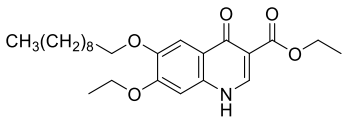
DQ	RMB073	520.3	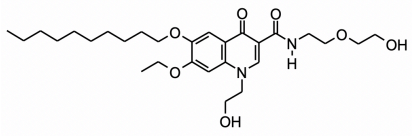

Compound infusions

Compounds WHN012, AD01, PhX6, DpNEt, RMB059, RMB060, and DQ were infused in positive electrospray ionization (ESI) mode at a rate of 10 µL/min. RMB005 was infused in negative ESI mode. The resulting initial product ions scans are shown in Figure 8-2 to 8-9.

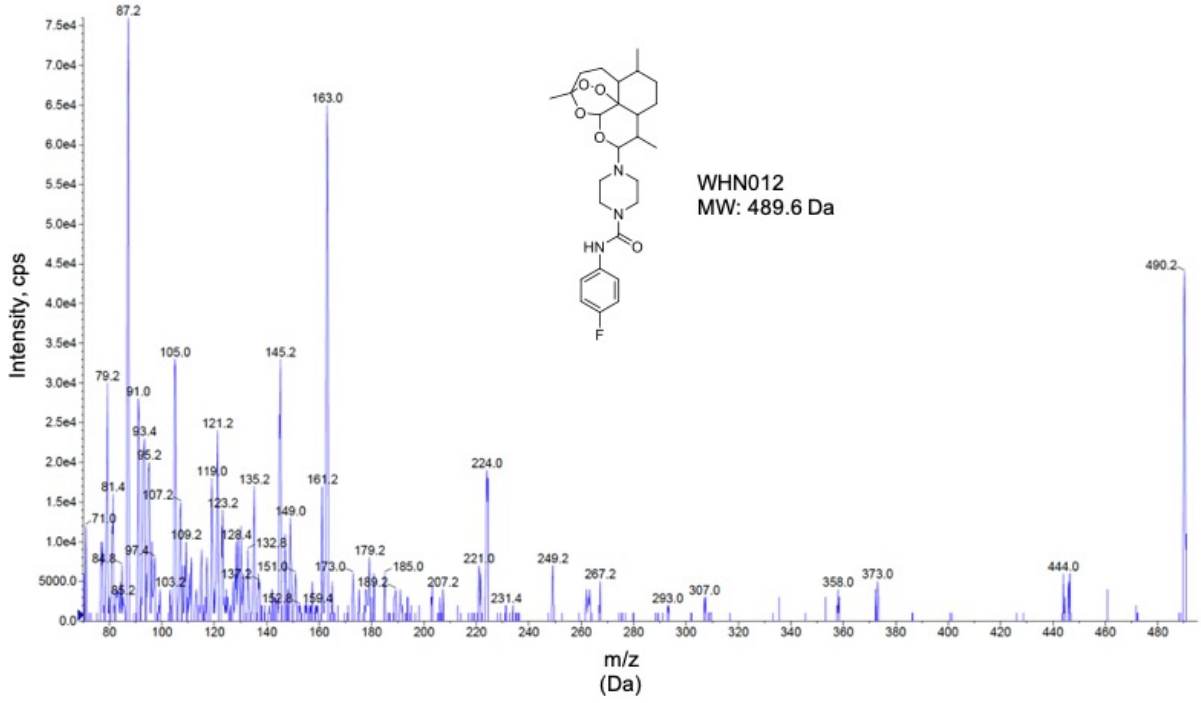

Figure 8-2: Product ion scan of WHN012.

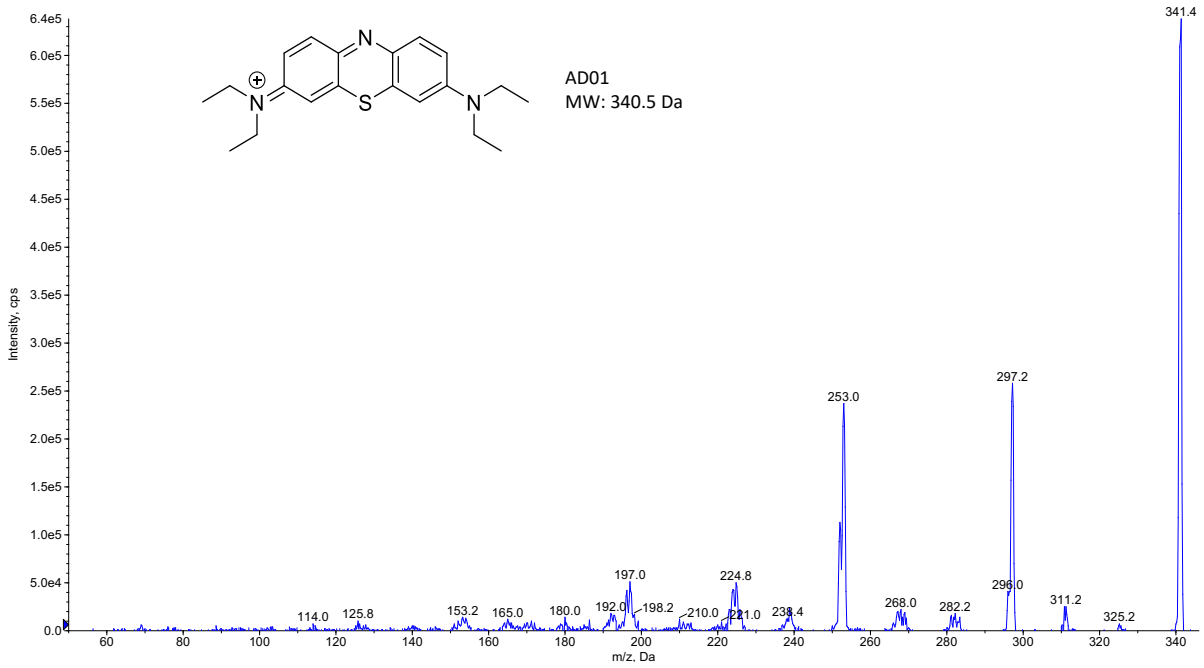

Figure 8-3: Product ion scan of AD01.

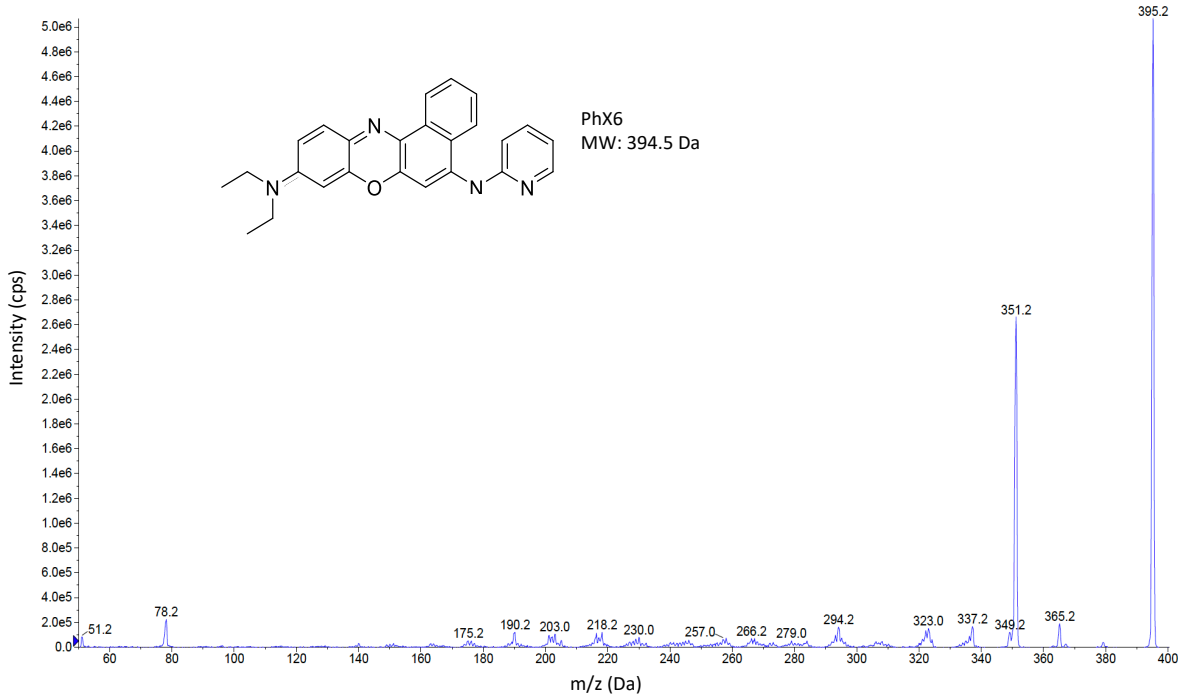

Figure 8-4: Product ion scan of PhX6.

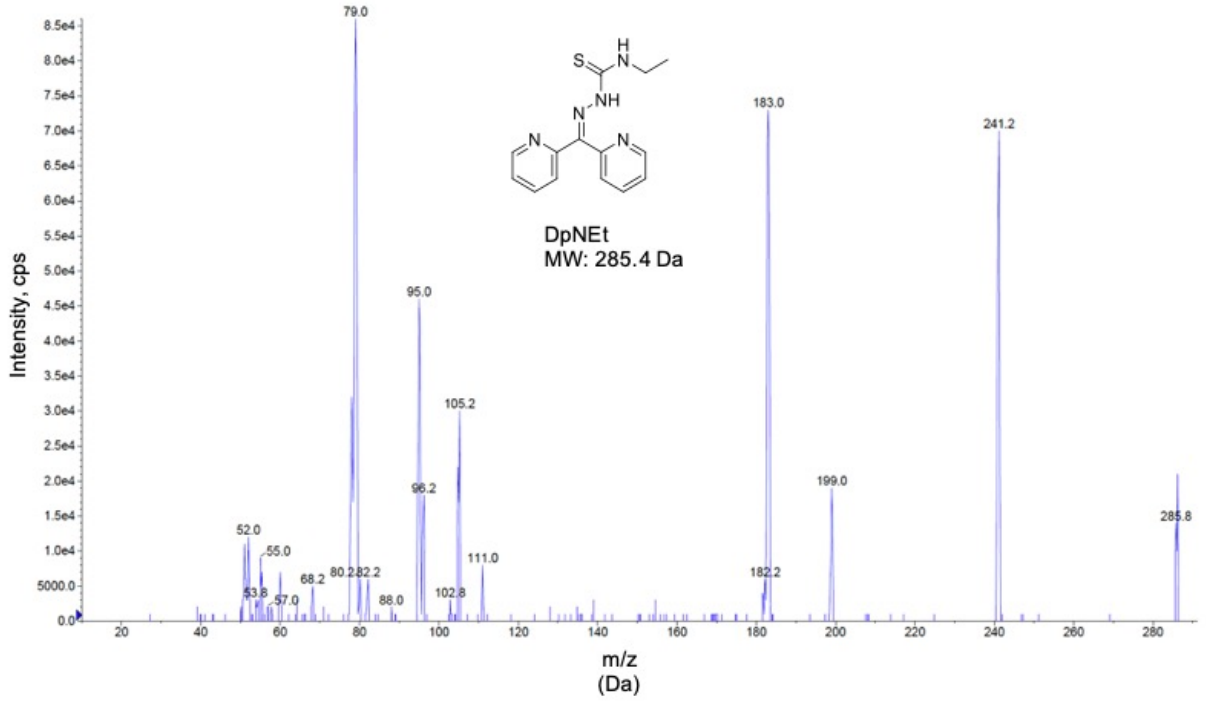

Figure 8-5: Product ion scan of DpNEt.

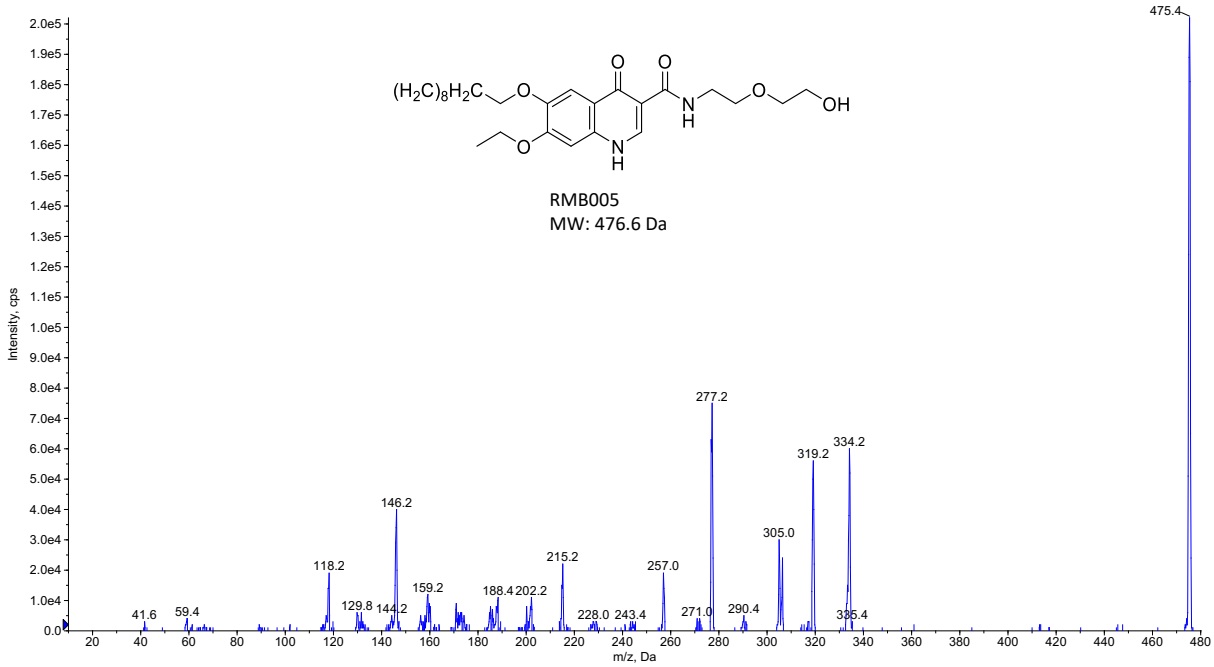

Figure 8-6: Product ion scan of RMB005.

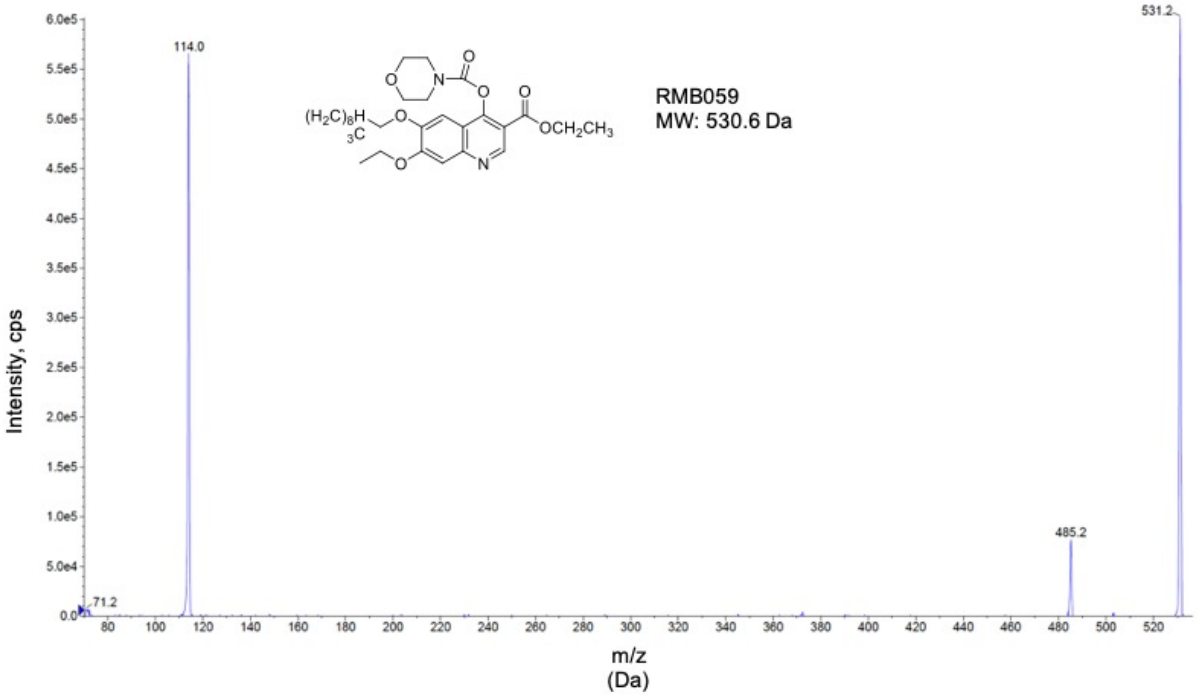

Figure 8-7: Product ion scan of RMB059.

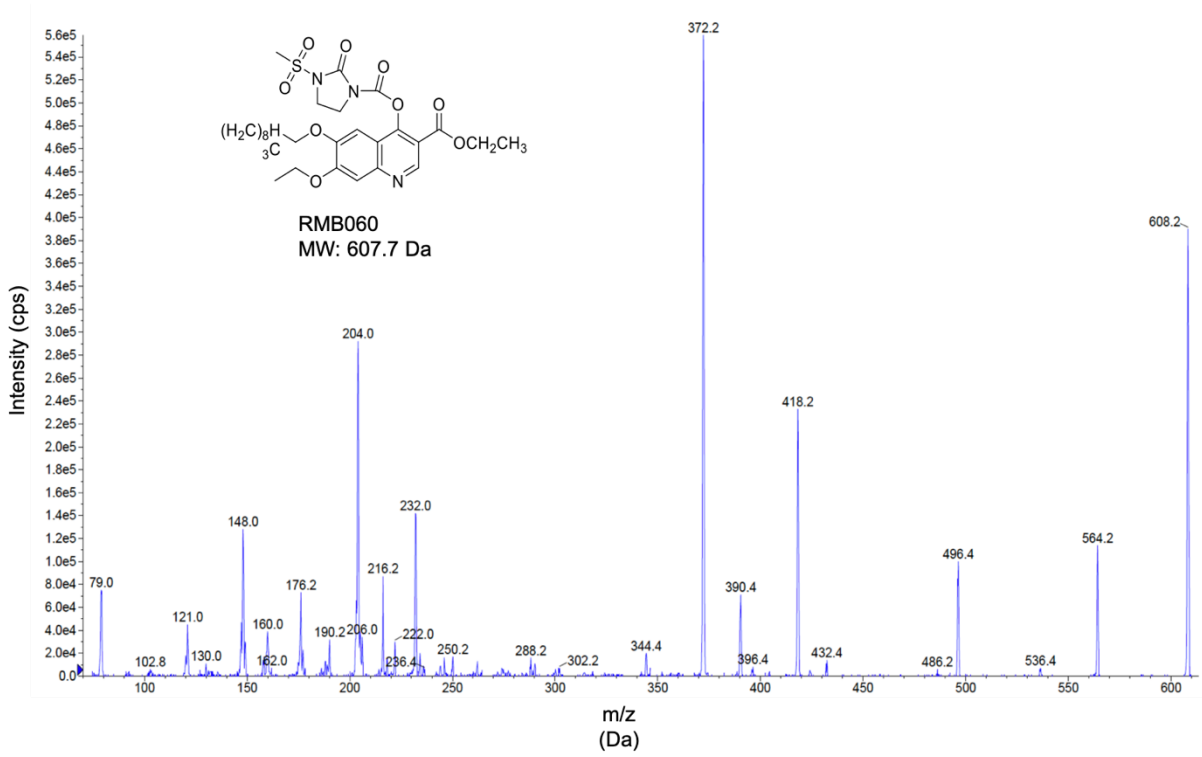

Figure 8-8: Product ion scan of RMB060.

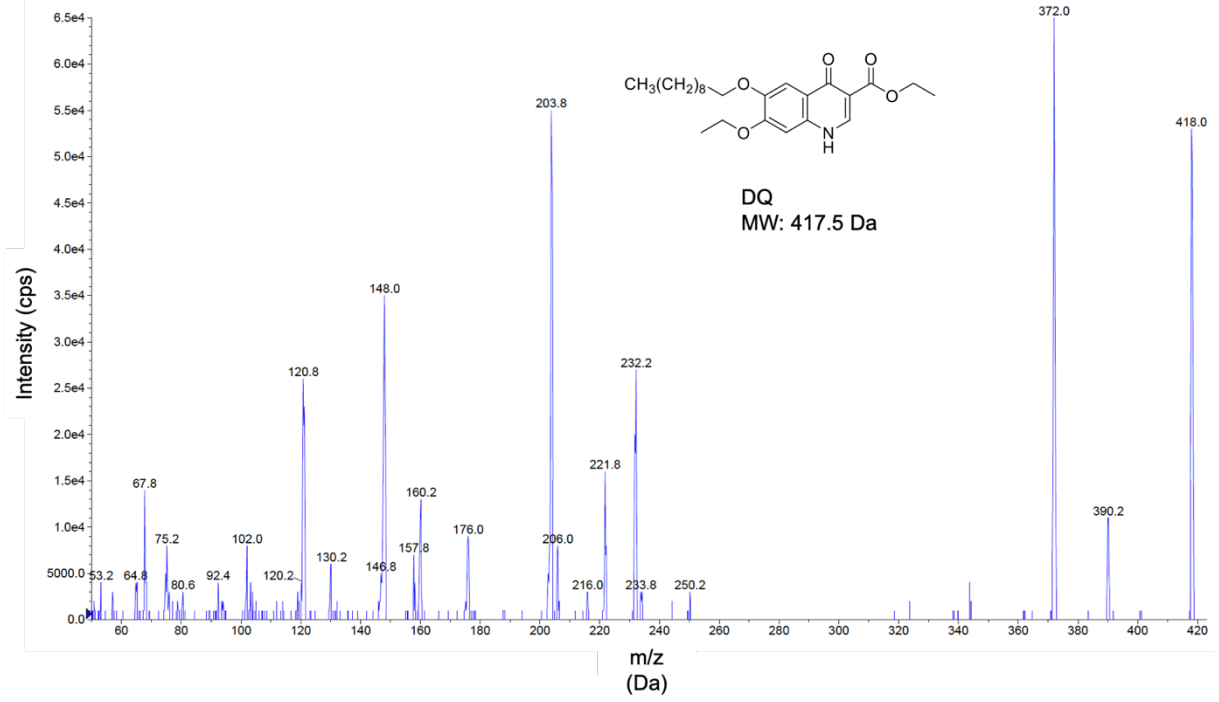

Figure 8-9: Product ion scan of DQ.

Chromatography

Liquid chromatography was developed by optimization of mobile phase conditions on different analytical columns in terms of finding optimal peak shapes and retention times (RT). Reversed phase gradient chromatography was superior to isocratic chromatography in analyte retention, peak shape, and reproducibility. A Phenomenex Gemini NX-C18 (5 µm, 2.1 mm x 50 mm) (California, USA) analytical column was selected for analysis of all compounds except RMB059. A Restek Raptor Biphenyl (5 µm, 2.1 mm x 50 mm) (Pennsylvania, USA) analytical column was selected for RMB059.

Optimal liquid chromatography of WHN012 was achieved with a gradient elution method consisting of 10 mM ammonium acetate (NH4CH3CO2) with 0.1% acetic acid (AA) for the aqueous mobile phase and a 1:1 mixture (v/v) of methanol (MeOH) and acetonitrile (ACN) for the organic phase, similar to previously described methods.[355,356] WHN012 had a retention time of approximately 3.3 min and the total run time was 7 min. During development of methods for basic compounds PhX6 and AD01, ideal ionisation was observed in 0.1% formic acid (FA) solution, in contrast to methods previously described

that worked better with ammonium acetate.[357,358] PhX6 eluted approximately at 3.2 min and AD01 at 2.5 min. DpNEt had a retention time of approximately 2.0 min on the Gemini-NX column. Greater ionization was obtained from an acidic aqueous mobile phase (0.1% FA) from direct infusion. The Gemini-NX column proved to be ideal for the hydrophobic RMB005 with a retention time of approximately 2.6 min using 5 mM ammonium acetate as aqueous phase and acetonitrile as organic phase. Compounds RMB059 and RMB060 ionized better in ammonium acetate containing acetic acid. Ideal retention was obtained for RMB060 on the Gemini column, but a Restek Raptor Biphenyl column delivered better retention of RMB059. The ideal elution range lies within the gradient or in the high organic phase of the gradient. Polar compounds will elute early and result in possible ion suppression. Elution beyond the high non-polar phase could also result in possible ion suppression, as lipids and other hydrophobic background molecules will elute late. Methods were adjusted until the final method produced an acceptable retention time within this window.

Table 8- 11: Summary of liquid chromatography analytical conditions.

Analyte	**Analytical column**	**Flow rate (uL/min)**	**Run time (min)**	**Matrix**
WHN012	Gemini NX-C18 (5 µm, 2.1 mm x 50 mm)	600	7	Plasma
AD01	Gemini NX-C18 (5 µm, 2.1 mm x 50 mm)	600	7	Whole blood
PhX6	Gemini NX-C18 (5 µm, 2.1 mm x 50 mm)	600	7	Whole blood
DpNEt	Gemini NX-C18 (5 µm, 2.1 mm x 50 mm)	600	5	Whole blood
RMB005	Gemini NX-C18 (5 µm, 2.1 mm x 50 mm)	600	5	Whole blood
RMB059	Restek Raptor Biphenyl (5 µm, 2.1 mm x 50 mm)	600	5	Whole blood
RMB060	Gemini NX-C18 (5 µm, 2.1 mm x 50 mm)	600	5	Whole blood
DQ	Gemini NX-C18 (5 µm, 2.1 mm x 50 mm)	600	6	Whole blood

Table 8-12: MRM transitions and final mass spectrometer conditions.

Analyte	Transition	Dwell Time (ms)	Declustering potential (V)	Entrance Potential (V)	Collision Energy (V)	Cell Exit Potential (V)
WHN012	490 → 224	100	46	9	17	4
	490 → 163	100	46	9	27	6
PhX6	395 → 351	150	131	9	31	6
	395 → 78.2	150	131	9	77	6
AD01	341 → 297	150	61	11	47	6
	341 → 253	150	61	11	71	12
DpNEt	286 → 241	150	46	5	15	6
	286 → 183	150	46	5	12	6
RMB005	475 → 334	150	-110	-10	-34	-4
	475 → 277	150	-110	-10	-58	-4
RMB059	531 → 114	150	111	9.5	41	2
	531 → 71.2	150	111	9.5	69	2
RMB060	608 → 204	150	121	12	85	4
	608 → 372	150	121	12	36	4
DQ	418 → 372	150	56	11	29	6
	418 → 203	150	56	11	57	4

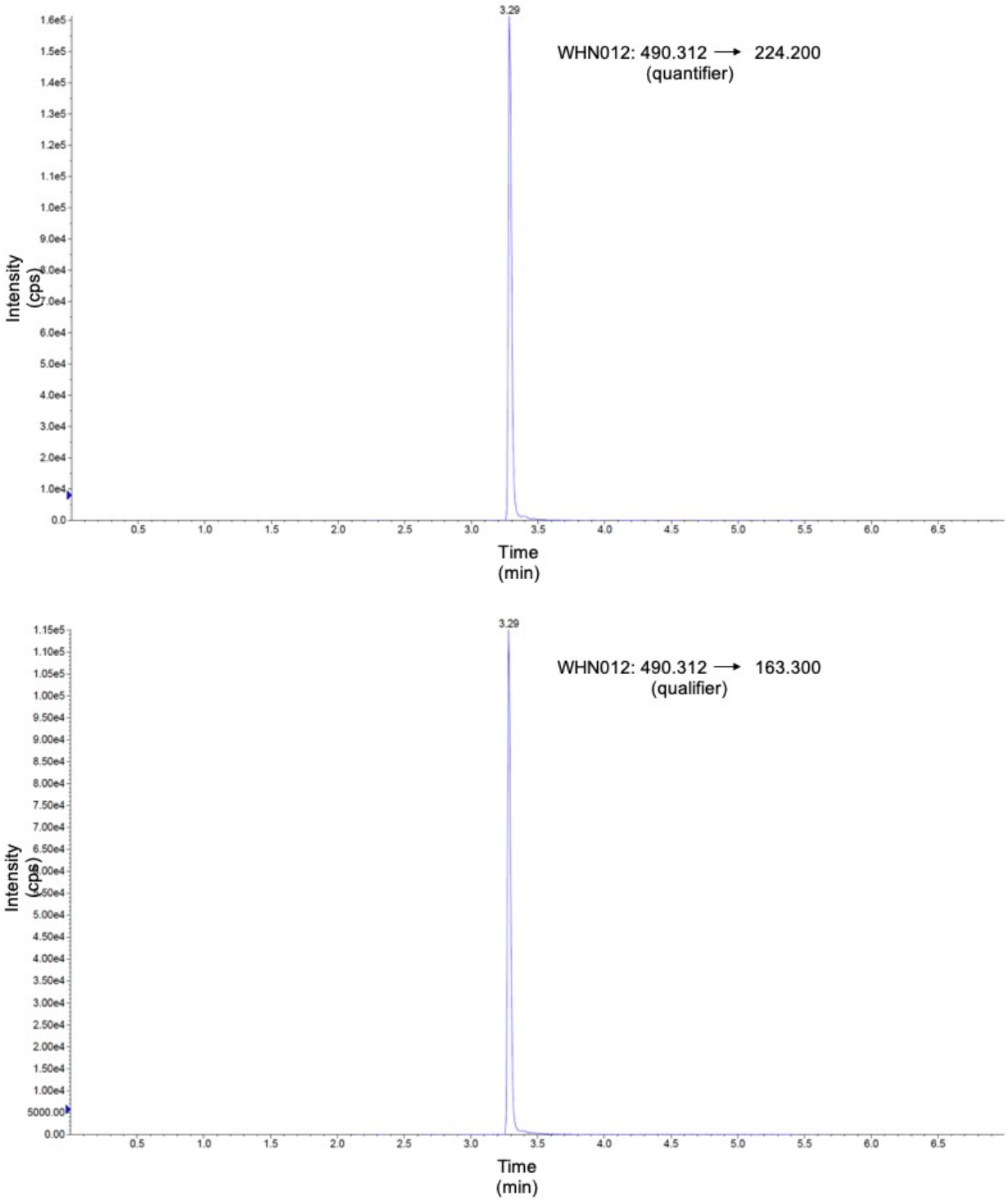

Figure 8-10: Representative MRM chromatograms of WHN012.

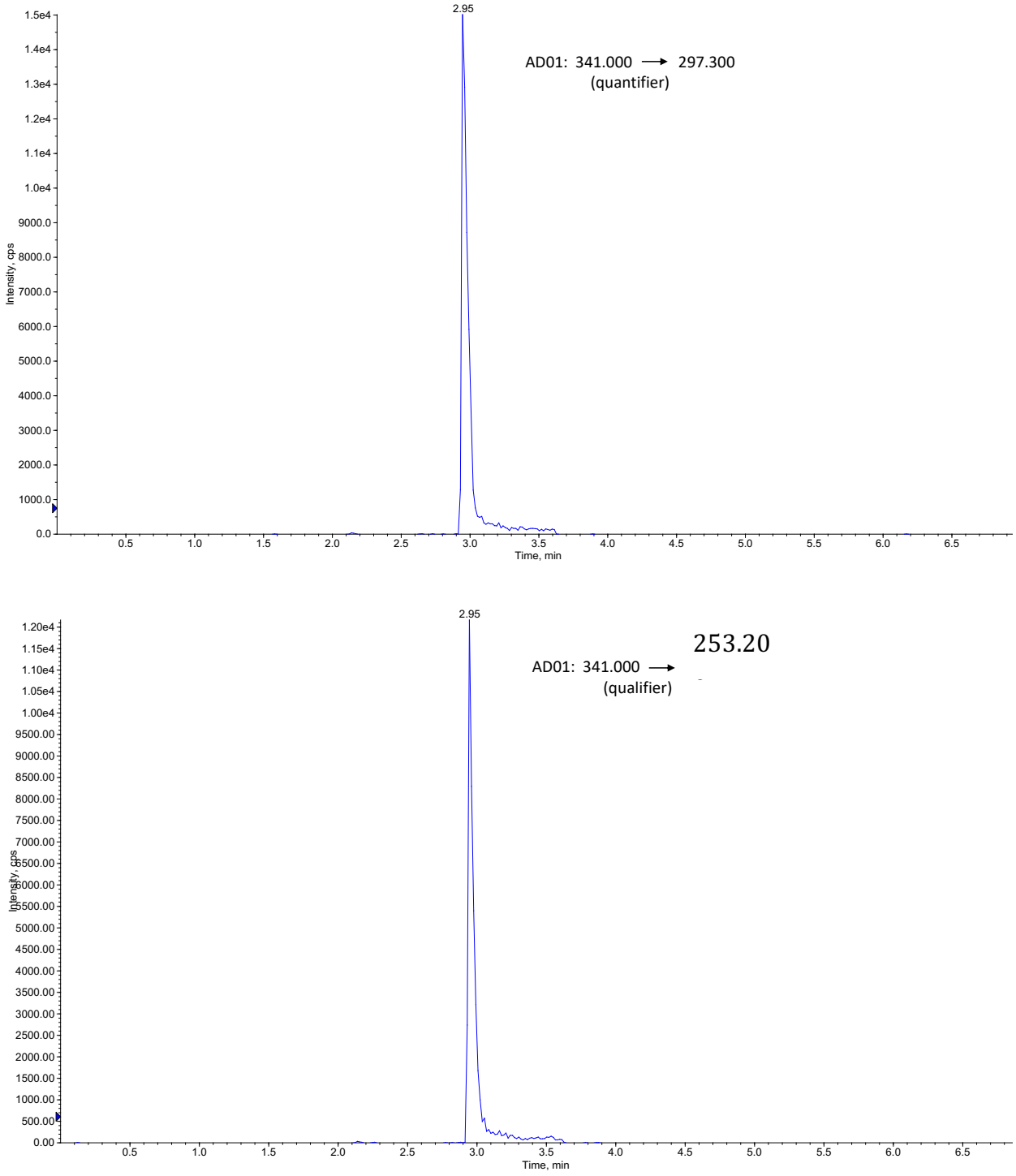

Figure 8-11: Representative MRM chromatograms of AD01.

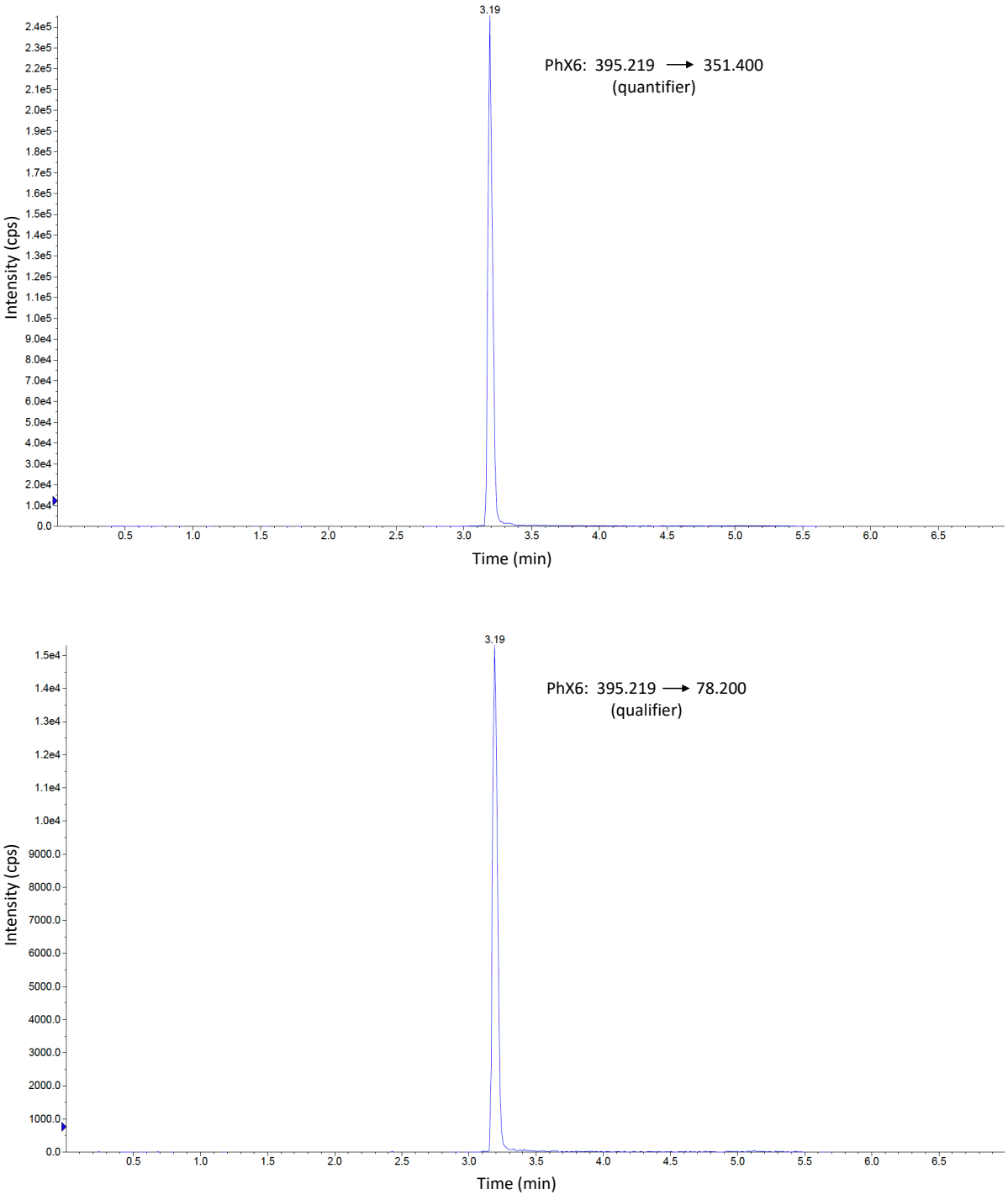

Figure 8-12: Representative MRM chromatograms of PhX6.

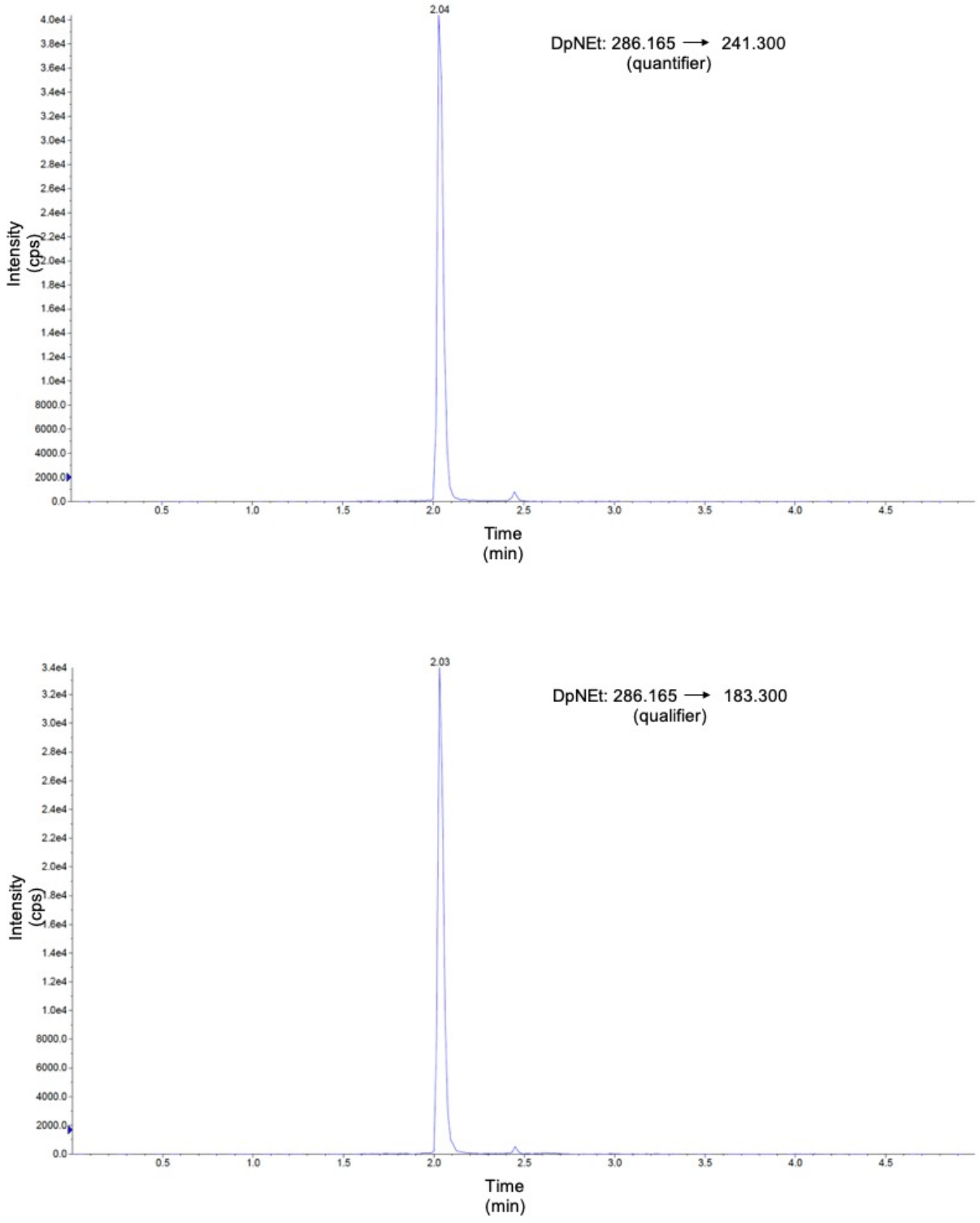

Figure 8-13: Representative MRM chromatograms of DpNEt.

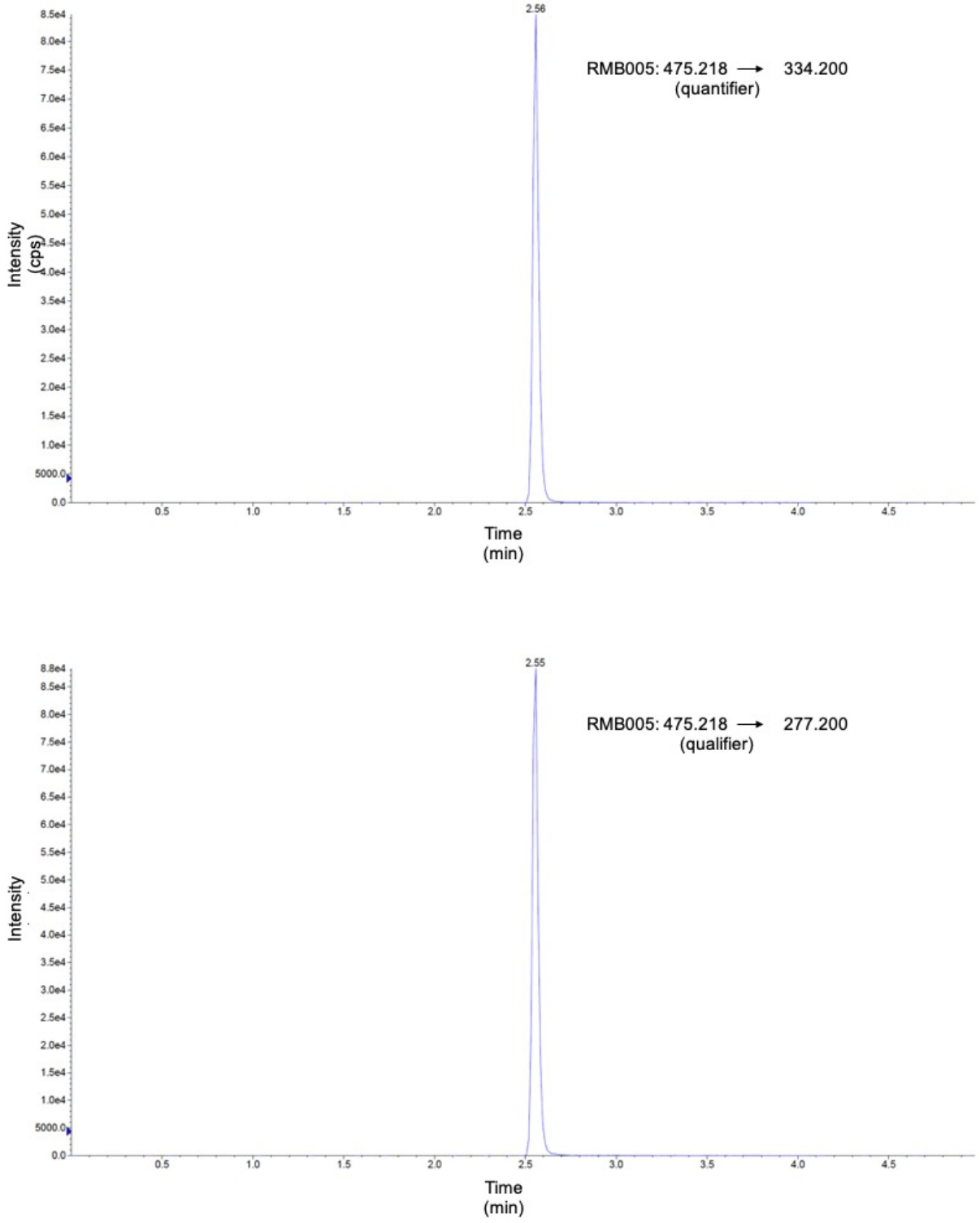

Figure 8-14: Representative MRM chromatograms of RMB005.

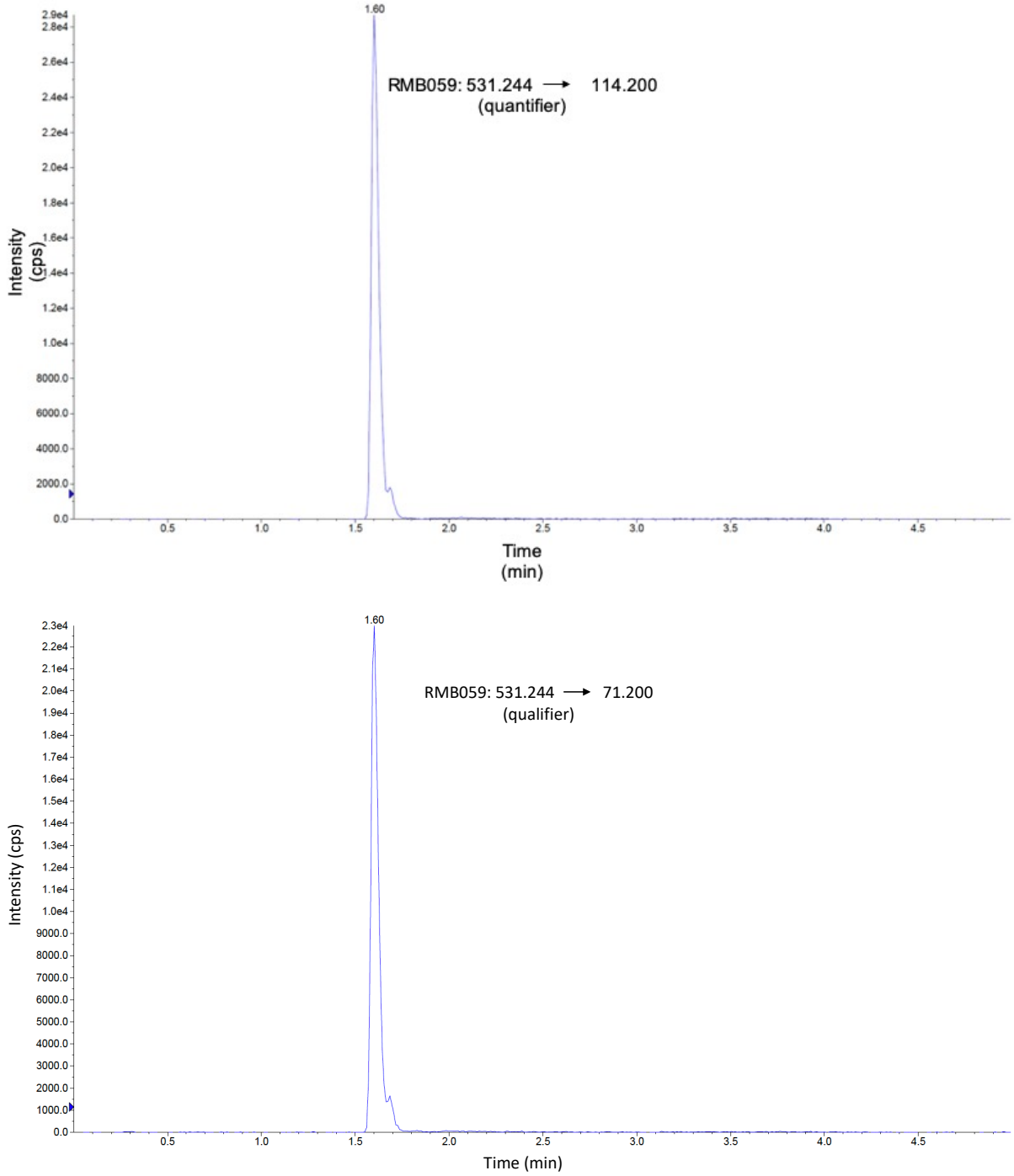

Figure 8-15: Representative MRM chromatograms of RMB059.

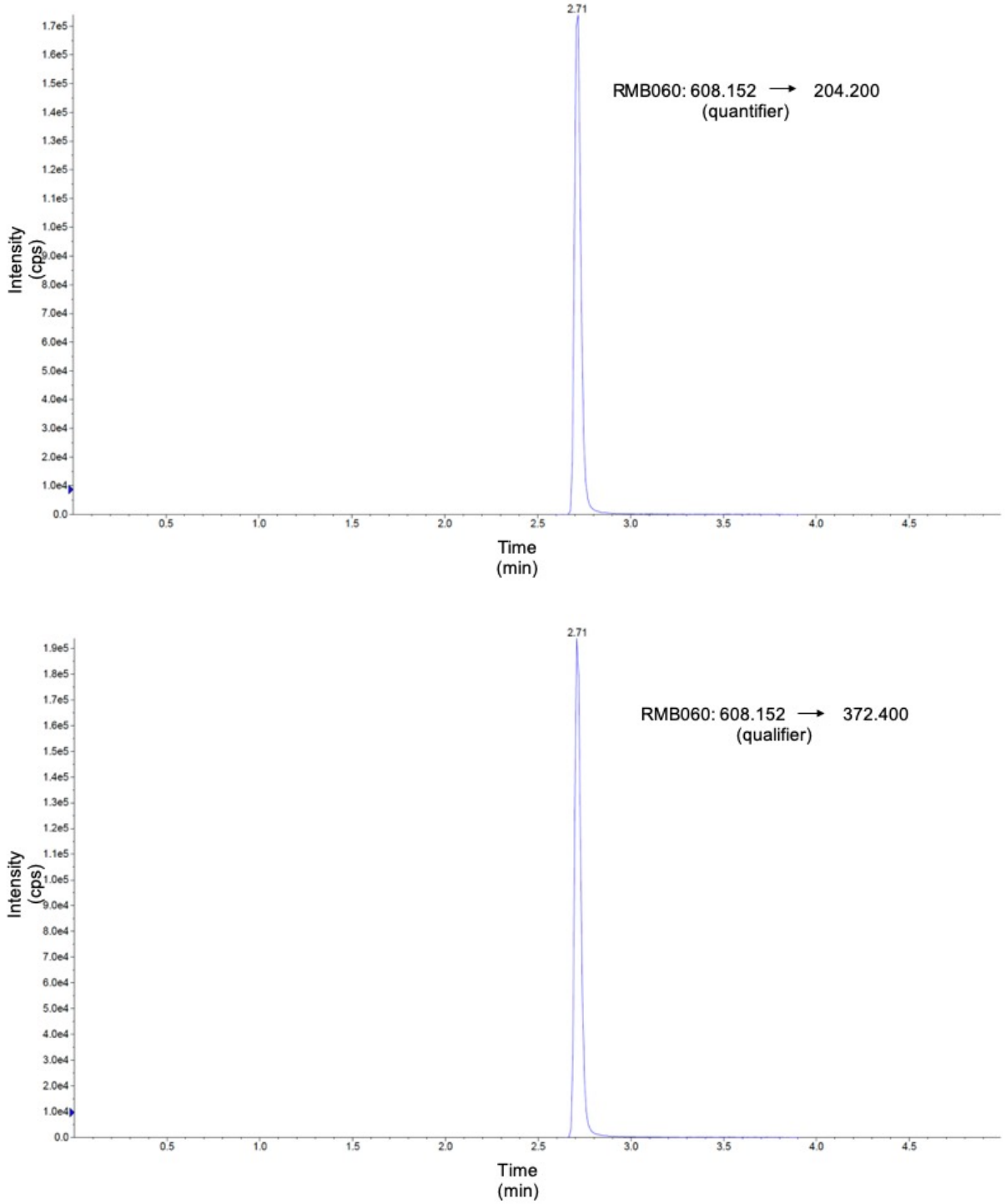

Figure 8-16: Representative MRM chromatograms of RMB060.

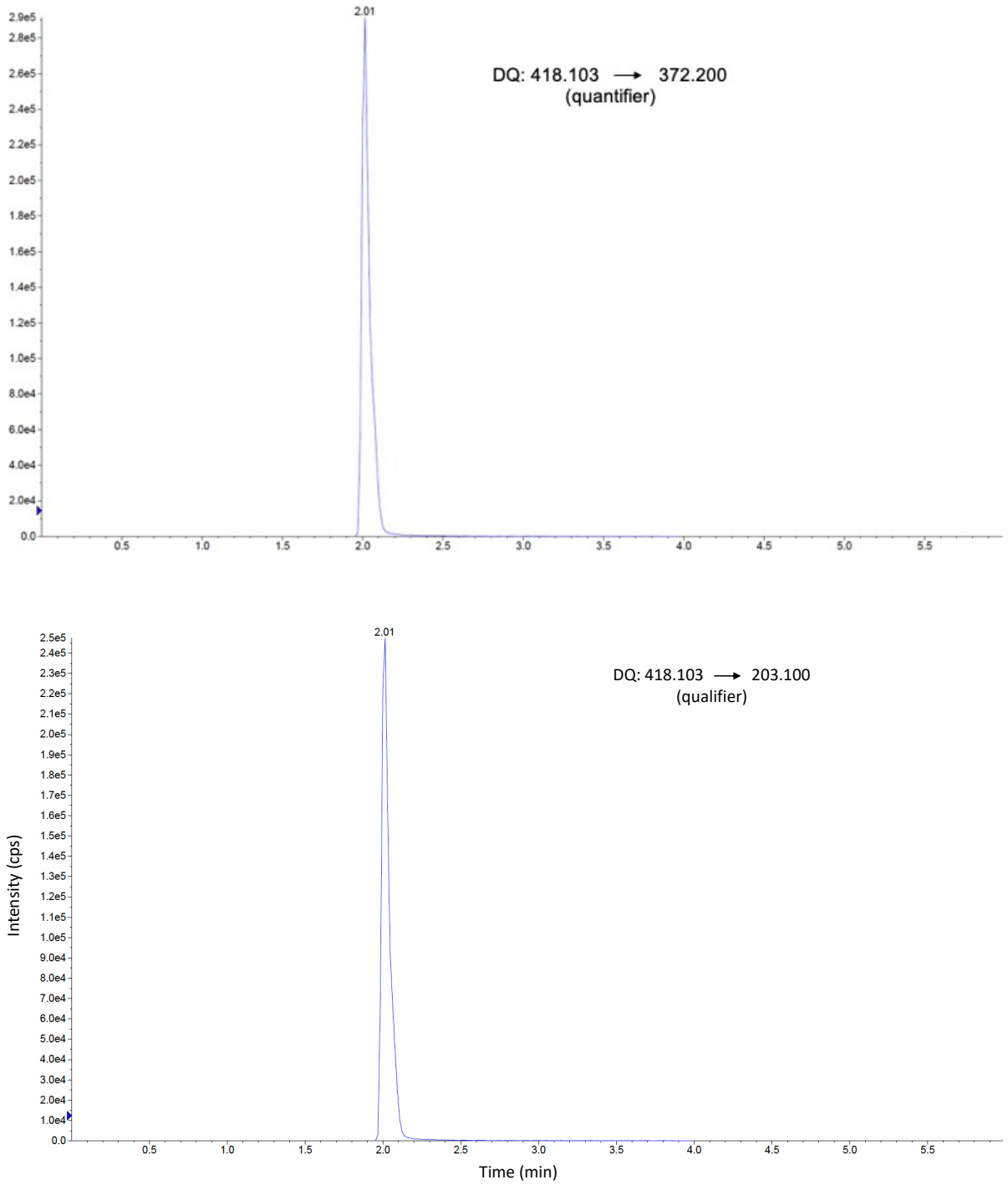

Figure 8-17: Representative MRM chromatograms of DQ.

Appendix D

Appendix D represents the outcomes of the partial validation as per the FDA and EMA under the FFP recommendations, which were associated with bioanalytical methods used in Chapter 3 and Chapter 4.[258,259] To adequately assess possible variabilities or interferences with accurate measurement of analytes, certain parameters have been tested in order to ensure reproducibility and accuracy of the data generated in this project. These parameters included linearity, accuracy, precision, stability, carryover, matrix effects, and extraction efficiency.

Linearity

In order to determine the systemic concentrations during mouse pharmacokinetic evaluation, standard curves were spiked in blank matrix (Table 4-2, Chapter 4, pg. 102) consisting of at least six concentration points (Table 4-1, Chapter 4, pg. 101) and analysed together with experimental samples via LC-MS/MS. The concentration of experimental samples was then extrapolated from the standard curve. A quadratic regression equation was fitted to the calibration curves and the 1/concentration (1/x) weighting factor was applied.

QC samples should be spiked at 80% concentration of the highest calibration standard (upper limit of quantitation), at mid-point and three times the lower limit of quantitation, to demonstrate accuracy and precision of samples with known concentrations. It is important to acknowledge that 75% of calibration standard samples and 67% of QC samples should be included in the analysis in order for the curve to be validated. Variation in back-calculated standard curve samples should not exceed 15%, excluding the LLOQ which should not exceed 20%.

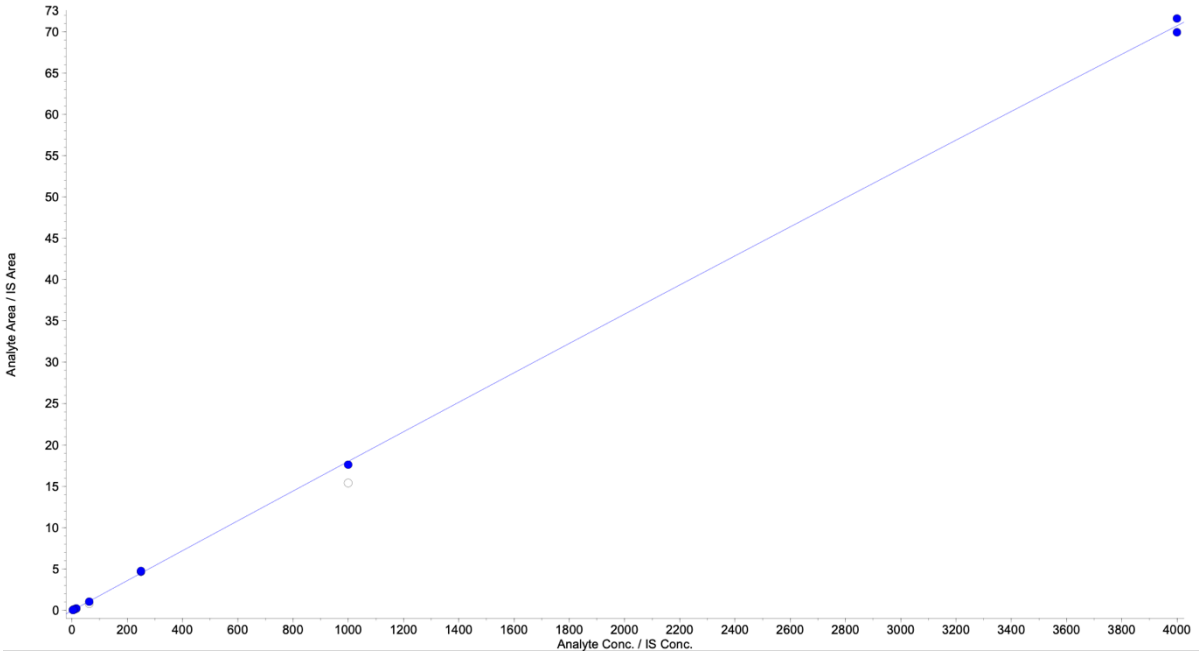

Figure 8-18: Calibration curve of WHN012 (r = 0.9998).

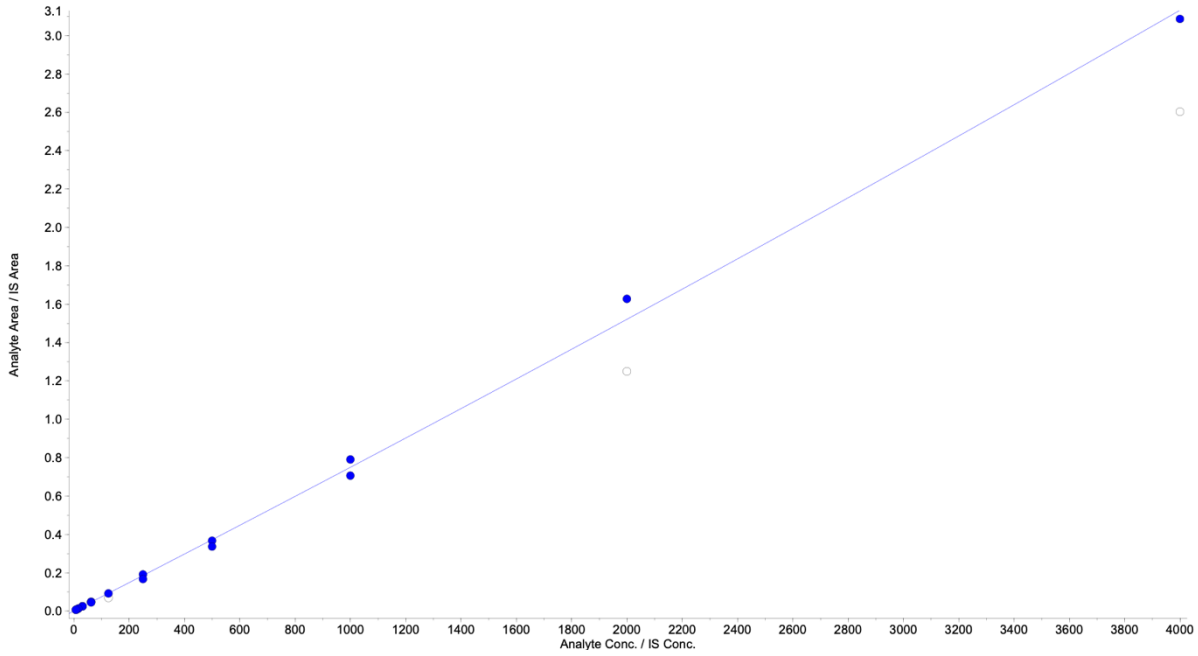

Figure 8-19: Calibration curve of AD01 (r = 0.9987).

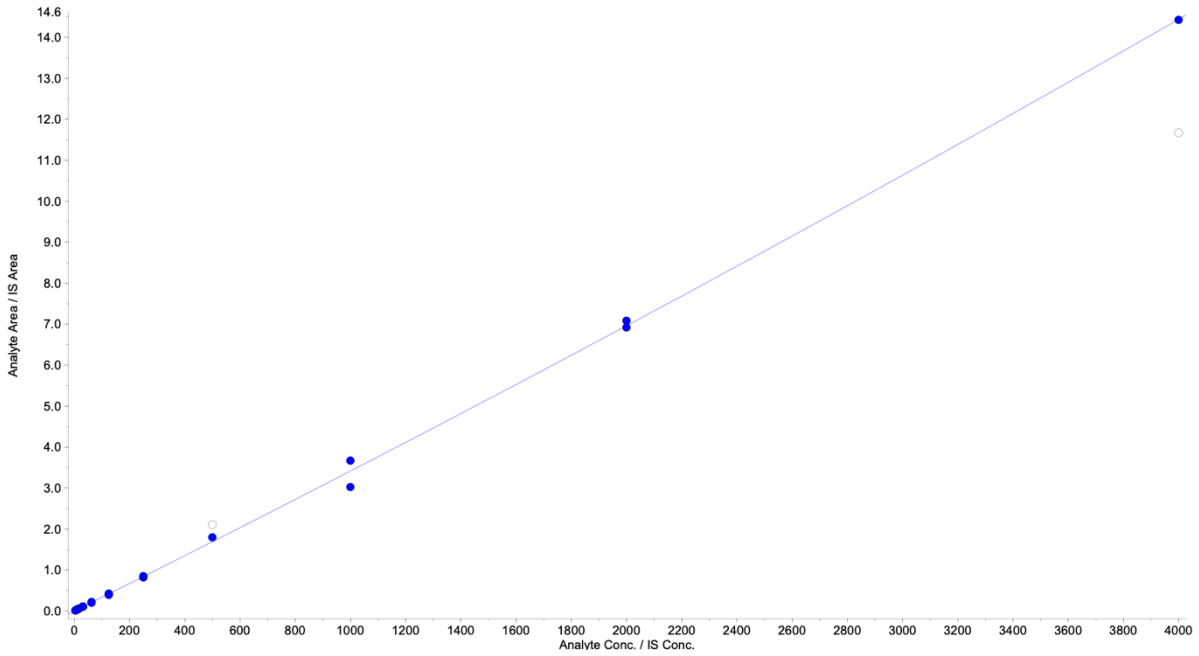

Figure 8-20: Calibration curve of PhX6 (r = 0.9990).

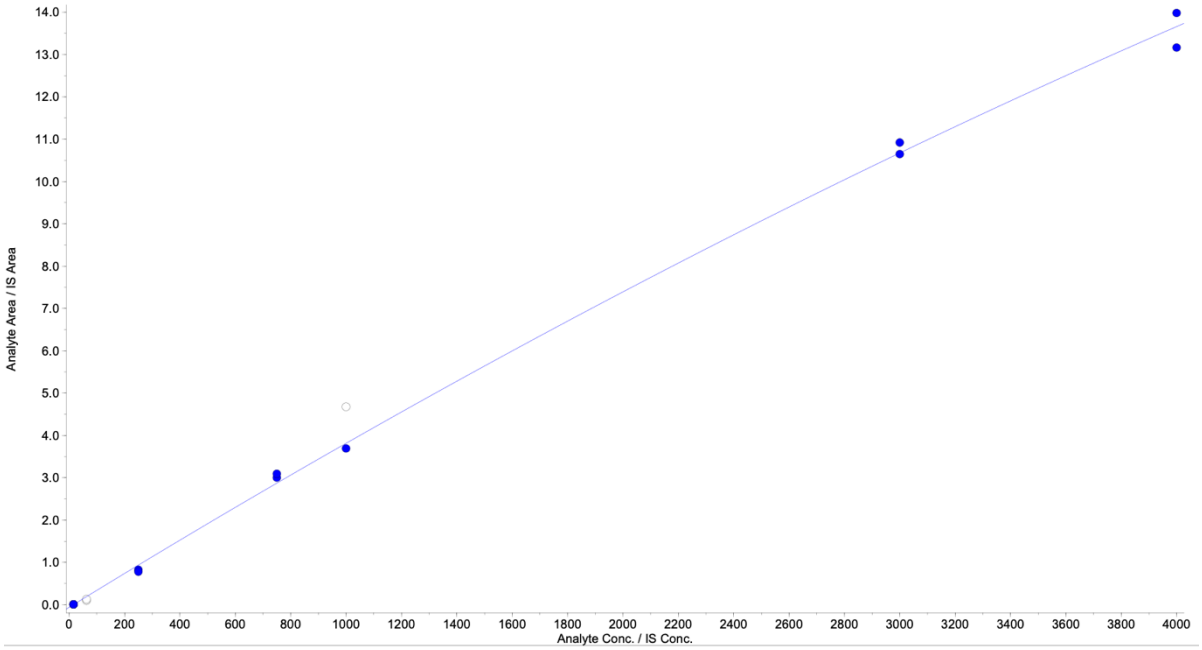

Figure 8-21: Calibration curve of DpNEt (r = 0.9991).

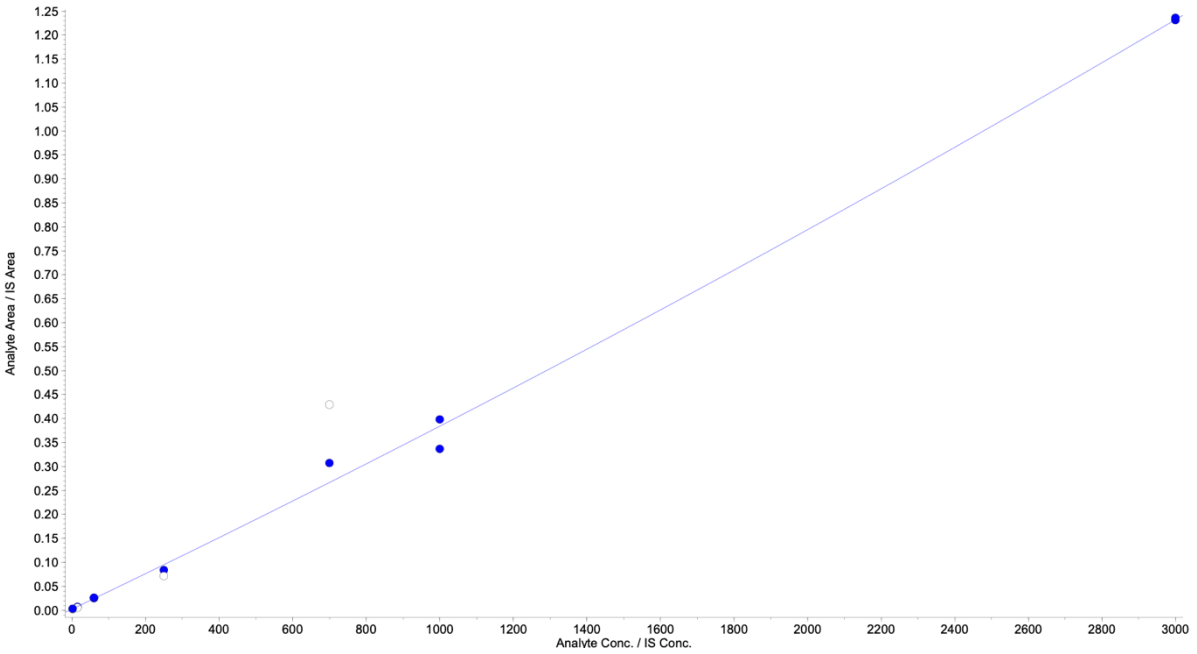

Figure 8- 22: Calibration curve of RMB005 (r = 0.9981).

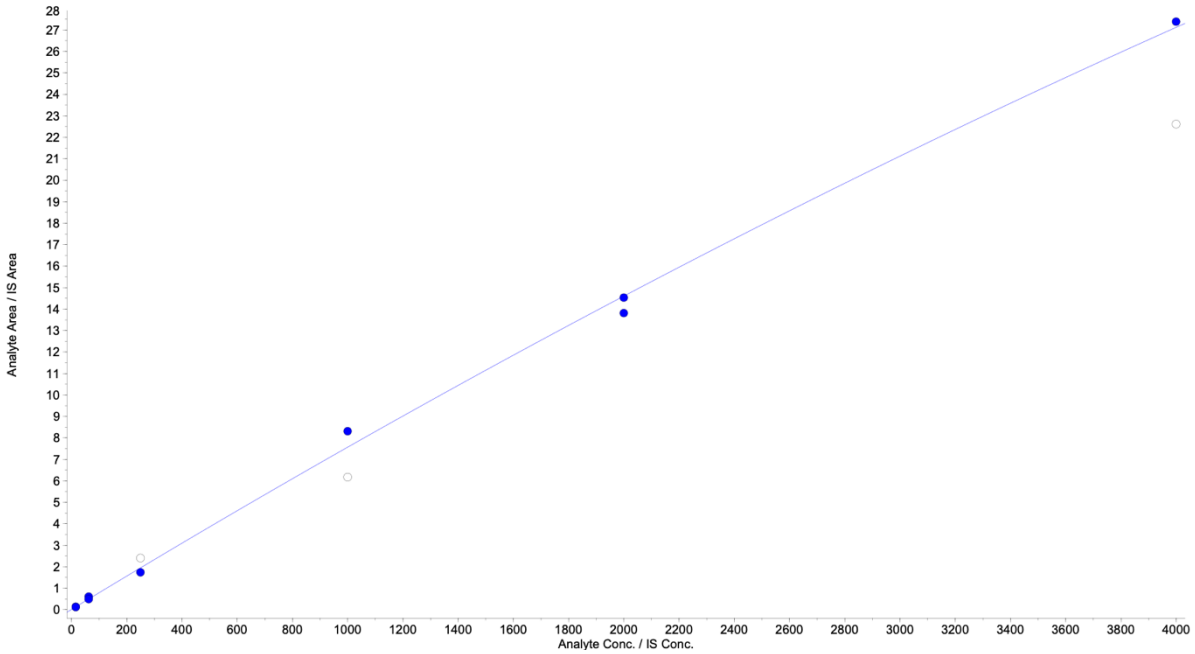

Figure 8-23: Calibration curve of DQ (r = 0.9986).

Accuracy and precision

Final transitions of the compounds were analysed on a 3200 QTRAP mass spectrometer and used for the quantification of peak areas. For data to be deemed reliable, one should know if the experimentally measured concentration is within an acceptable range of the nominal, true concentration value (accuracy) and if the degree of variation between replicates (precision) is within an acceptable range.

Quantification accuracy and precision were measured for the calibration range of the standard curve, as well as high, medium, and low concentration QCs of all analytes. Variability of calculated concentrations between standards should not be >15% at all concentration levels, except the lower limit of quantitation that should not be >20%. The quantification statistics of each compound with the range of accuracy (%) and highest percentage coefficient of variation (precision, CV) of all parent and metabolite compounds are shown in Table 8-13 and Table 8-14 respectively.

Table 8-13: Accuracy and precision from standard curves tested over calibration range.

Compound	Transition	Accuracy (%)	CV (%)
WHN012	490.312 → 224.200	91.4 – 109.2	5.68
AD01	341.000 → 297.300	91.2 – 104.7	17.8
PhX6	395.219 → 351.400	96.3 – 106.2	10.4
DpNEt	286.165 → 241.300	86.3 – 106.1	5.11
RMB005	475.218 → 334.200	83.9 – 114.8	11.5
DQ	418.103 → 372.200	88.9 – 109.8	15.5

Table 8-14: Accuracy and precision from quality control samples prepared at high, medium and low concentration.

Compound	Transition	Accuracy (%)	CV (%)
WHN012	490.312 → 224.200	89.2 – 102.9	14.8
AD01	341.000 → 297.300	87.4 – 109.8	12.2
PhX6	395.219 → 351.400	99.1 – 110.1	10.2
DpNEt	286.165 → 241.300	85.1 – 106.5	11.7
RMB005	475.218 → 334.200	94.5 – 106.5	12.4
DQ	418.103 → 372.200	81.3 – 96.2	4.2

Stability

Loss of compound sensitivity was determined for compounds during storage, extraction and analysis conditions. These parameters included:

i) stock solution
ii) spiking solution stability,
iii) stability of the compounds on instrument by assessment of autosampler stability
iv) on bench and freeze/thaw stability in whole-blood samples
v) stability of the compounds in oral and intravenous formulations.

Under the FFP recommendations of the FDA, it was determined that sample degradation should not exceed 20%. The stability values are reported as percentage stability values which reflected the stability of the compound in relation to a fresh sample prepared just before analysis. Compound stability was assessed at both a high (1000 ng/mL) and low (25 ng/mL) concentrations for mouse whole-blood or mouse plasma (freeze-thaw and on ice) and samples assessed for on-instrument stability. Only high concentrations for the oral and IV formulation stability samples were tested as these compounds were dosed at a single high concentration.

i) Stock solution, spiking solution and autosampler stability

The short-term stability of the compounds was investigated in DMSO stock solution. During preparation of samples for *in vitro* efficacy studies, preparation of test samples or calibration standards, samples are at room temperature (~22°C) on bench for as long as 2 hours. Freshly prepared stock solutions were compared to solutions left on bench at room temperature for 2 hours. Reference and test samples were diluted to 250 ng/mL in injection solution containing the ISTD and analysed with LC/MS-MS. The stability was reported as percentage stability (which reflects the stability of the compound in comparison to the reference prepared just before analysis) and shown in Table 8-15.

All the investigated compounds, apart from RMB060, had acceptable stability in organic solution. Room temperature stock solution samples of RMB060 had a degradation >20% and indicated that caution should be taken with regards to the time spent on bench. It was therefore not possible to complete solubility studies during ADME analysis, as the compound would not provide accurate data under the experimental conditions.

Table 8-15: Stability testing of compounds in organic solutions.[a]

Compound	**Stock solution (room temp, 2h)[b]**	**Spiking solution (room temp, 2h)[b]**	**Autosampler stability (24 h)[b]**	
			High[c]	Low[c]
WHN012	92.6	98.1	96.6	91.4
PhX6	96.1	86.8	84.6	83.9
AD01	85.2	94.4	95.4	99.7
DpNEt	96.5	88.4	91.9	93.7
RMB005	95.9	99.6	89.9	81.6
RMB059	106.0	88.5	98.3	97.4
RMB060	73.8	94.4	92.1	92.6
DQ	85.1	97.2	99.1	87.1

[a]values represented as percentages compared to that obtained from freshly prepared reference sample; [b]values reported had a %CV less than 15%; [c]high, 1000 ng/mL; low, 25 ng/mL. Samples were analysed in triplicate.

ii) Matrix stability

Compounds are exposed to the matrix for some time during preparation of standards and QCs for calibration curves and during the extraction of study samples and are susceptible to enzymes present in the blood and plasma.[243] Awareness of stability of the analytes during these processes is crucial for the reliability and reproducibility of data. Blank matrix (mouse plasma or whole blood) spiked with analytes at high and low concentrations were left on ice for 2 hours and compared to freshly spiked reference samples. The matrix stability data is presented in Table 8-16.

Table 8-16: Matrix stability on bench and after a freeze-thaw cycles.

Compound	**Matrix on ice, 2h[b]**		**Matrix stability (-80°C freeze-thaw)[b]**	
	High[c]	Low[c]	High[c]	Low[c]
WHN012	111.0	101.0	111.6	103.0
PhX6	92.4	86.2	88.8	88.7
AD01	92.6	85.1	87.1	93.3
DpNEt	96.5	90.1	91.4	88.1
RMB005	92.1	83.1	81.6	84.3
RMB059	37.8	25.9	nd	nd
RMB060	46.3	49.8	nd	nd
DQ	104.7	104.8	97.8	99.1

[a]values presented as percentages compared to that obtained from freshly prepared reference sample; [b]values reported had a %CV less than 15%; [c]high, 1000 ng/mL; low, 25 ng/mL. Samples were analysed in triplicate

All the investigated compounds had acceptable stability in their respective matrices (mouse whole blood or plasma), except for RMB059 and RMB060. This was also reflected in the plasma stability assay during ADME analysis. This suggested that they were substrates for hydrolytic enzymes, converting them to their parent compound DQ and this contributed majorly to the compounds' instability in blood. It was determined, from these experiments, that the metabolite DQ be analysed during *in vivo* experiments of these two RMB compounds.

iii) Formulation stability

The stability of compounds in their respective solutions used for both oral and intravenous administration to animals was tested over the course of 30 minutes, as compounds were administered within 30 minutes of preparation. Compounds were prepared as per Section 4.3.2 in Chapter 4, diluted in injection solution and analysed by LC-MS/MS. The results of the formulation stability are presented in Table 8-17.

Table 8-17: Stability of compounds in oral and intravenous dosing solution.

Compound	**Formulation stability[a]**	
	Oral	Intravenous
WHN012	82.8	101.5
PhX6	82.4	82.4
AD01	101.7	101.7
DpNEt	79.7	126.9
RMB005	113.5	108.9
RMB059	71.7	106.6
RMB060	78.8	103.6

[a]values presented as percentages compared to that obtained from freshly prepared reference sample, CV values were below 15% for all values. Samples were analysed in triplicate

WHN012, PhX6, AD01 and RMB005 presented acceptable stability (i.e. < 20% degradation) in both the oral and intravenous formulations. Oral formulations of DpNEt, RMB059 and RMB060, however, had slightly higher degradation than what was acceptable. Compound administration was therefore completed with the least possible time between compound preparation and administration.

Carry over

Carry-over was monitored throughout all analytical runs. This was done by injecting a blank sample containing only ISTD immediately after the highest calibration standard sample. Following this, a double blank sample containing no analyte or ISTD was injected to assess if additional carry-over effects by the ISTD was potentially contaminating the analyte. Chromatograms of blank and double blank samples are shown in Figure 8-24 to 35. Contamination of the blank or double blank samples would lead to high variability between samples, inaccurate calculation of peak areas and subsequent interpretation of the concentration profile of the compounds. No contamination of test compound or internal standard was observed between the highest standard, blank or double blank samples, as indicated by the comparison of chromatograms.

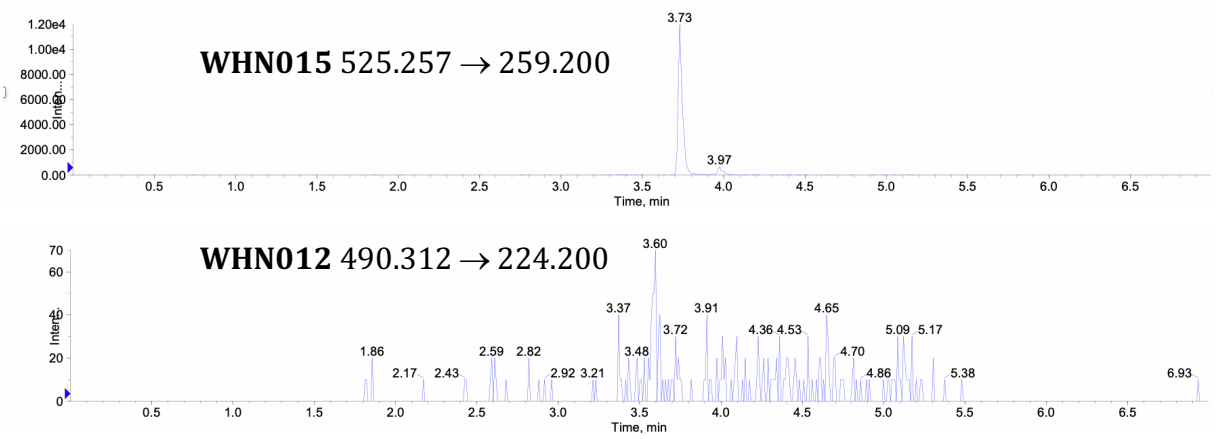

Figure 8-24: Chromatogram of a blank mouse plasma sample. MRM transitions of the ISTD (top) and quantifying ion for WHN012 (bottom) are shown.

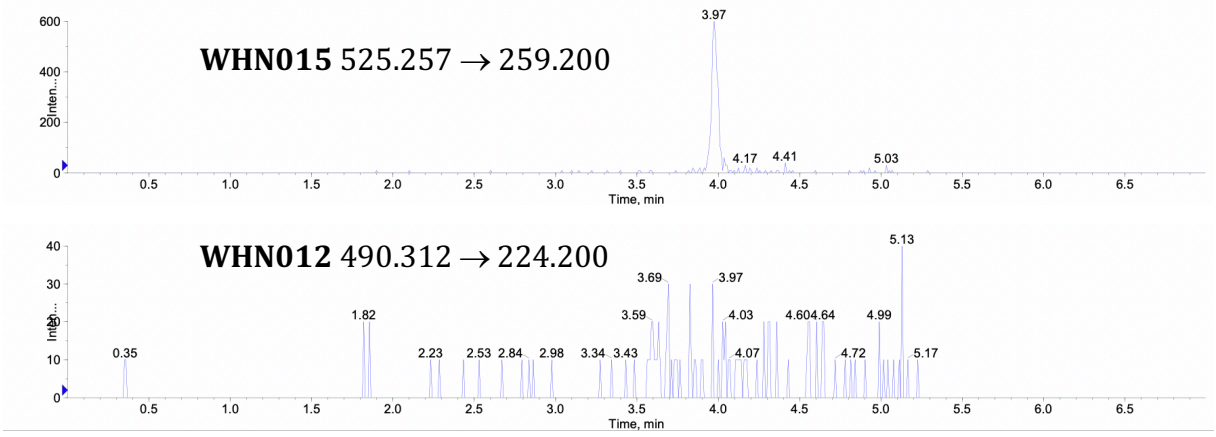

Figure 8-25: Chromatogram of a double blank mouse plasma sample. MRM transitions of the ISTD (top) and quantifying ion for WHN012 (bottom) are shown.

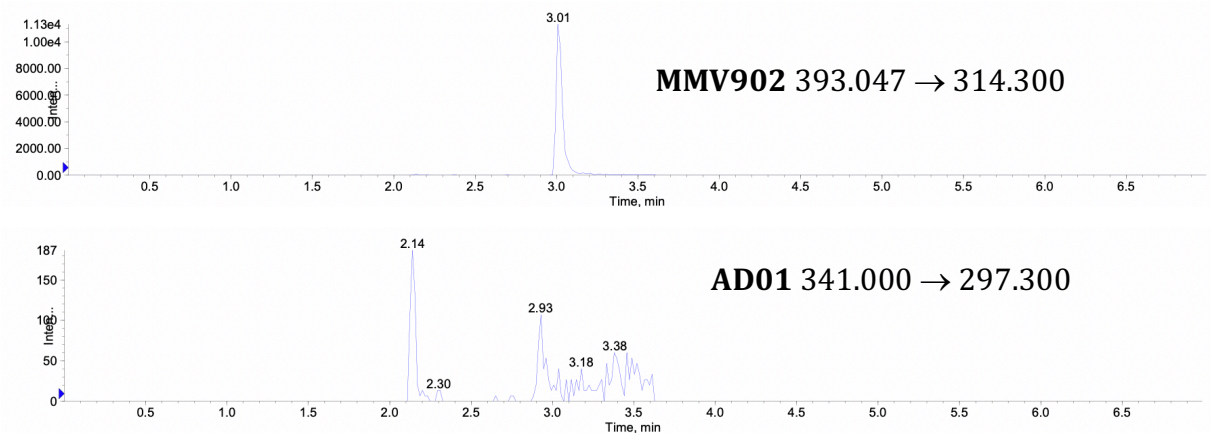

Figure 8-26: Chromatogram of a blank mouse whole blood sample. MRM transitions of the ISTD (top) and quantifying ion for AD01 (bottom) are shown.

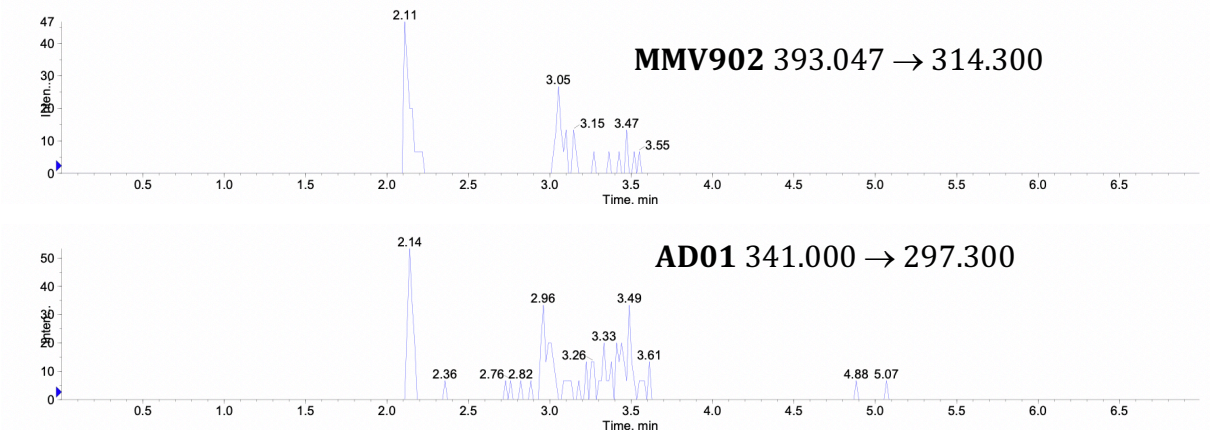

Figure 8-27: Chromatogram of a double blank mouse whole blood sample. MRM transitions of the ISTD (top) and quantifying ion for AD01 (bottom) are shown.

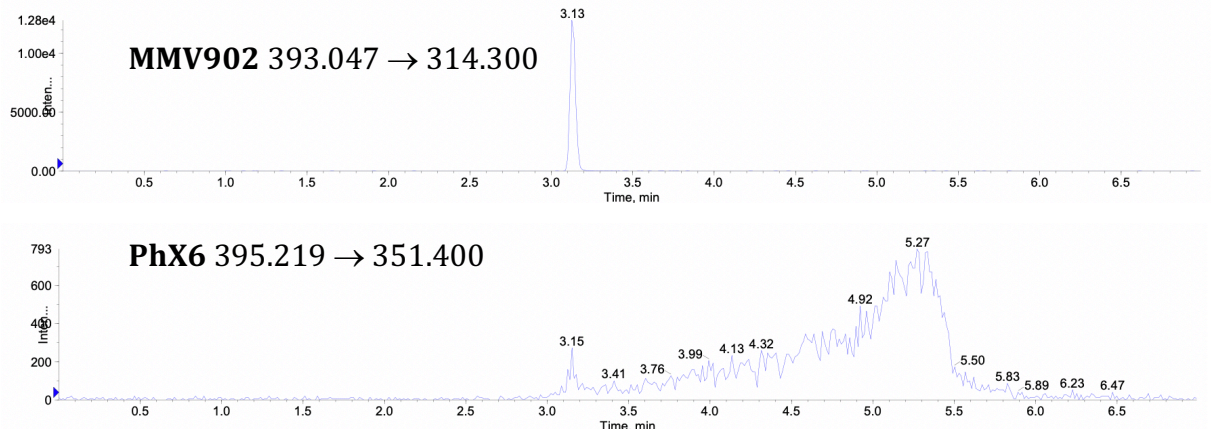

Figure 8-28: Chromatogram of a blank mouse whole blood sample. MRM transitions of the ISTD (top) and quantifying ion for PhX6 (bottom) are shown.

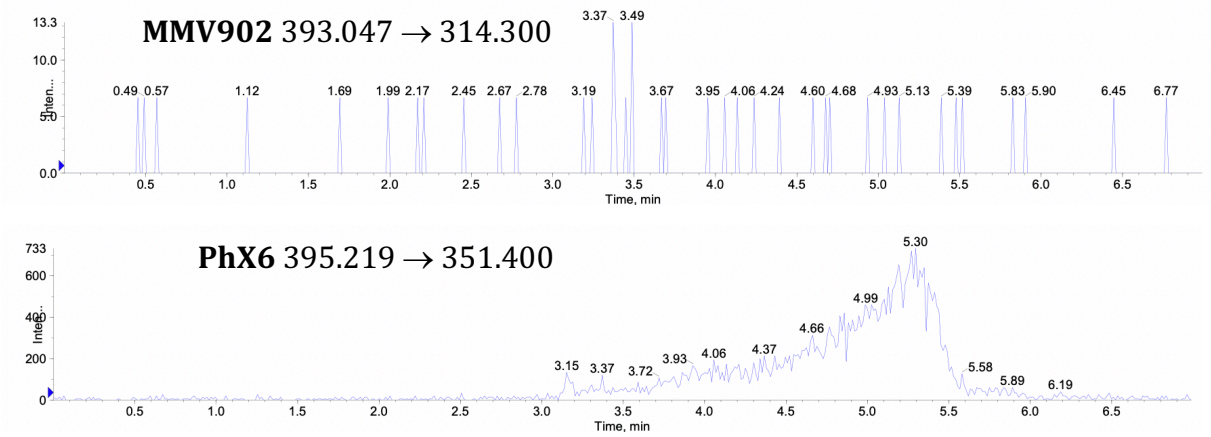

Figure 8-29: Chromatogram of a double blank mouse whole blood sample. MRM transitions of the ISTD (top) and quantifying ion for PhX6 (bottom) are shown.

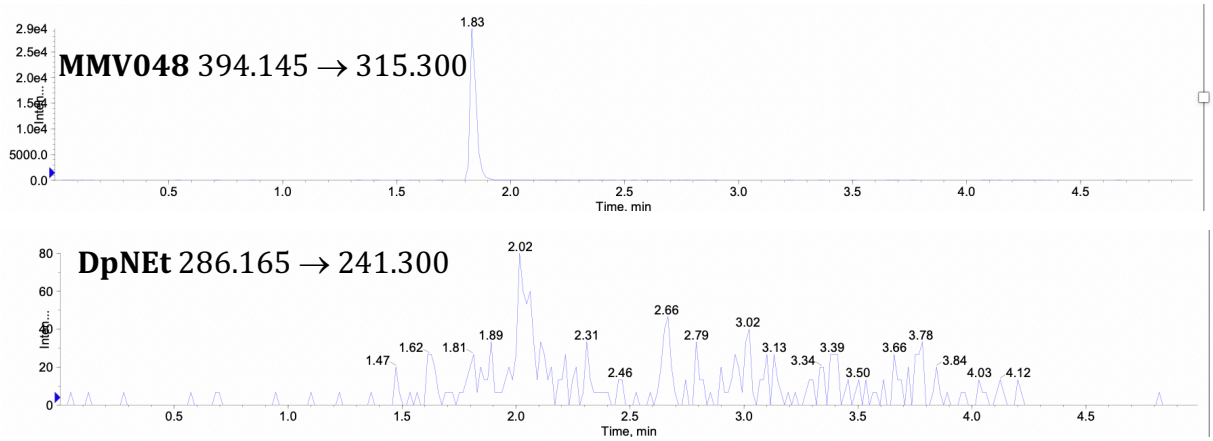

Figure 8-30: Chromatogram of a blank mouse whole blood sample. MRM transitions of the ISTD (top) and quantifying ion for DpNEt (bottom) are shown.

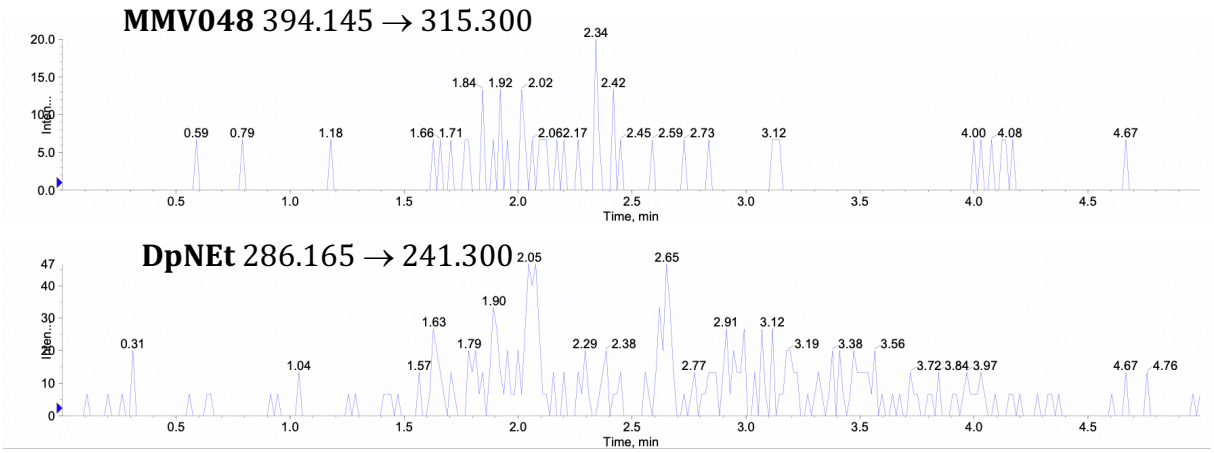

Figure 8-31: Chromatogram of a double blank mouse whole blood sample. MRM transitions of the ISTD (top) and quantifying ion for DpNEt (bottom) are shown.

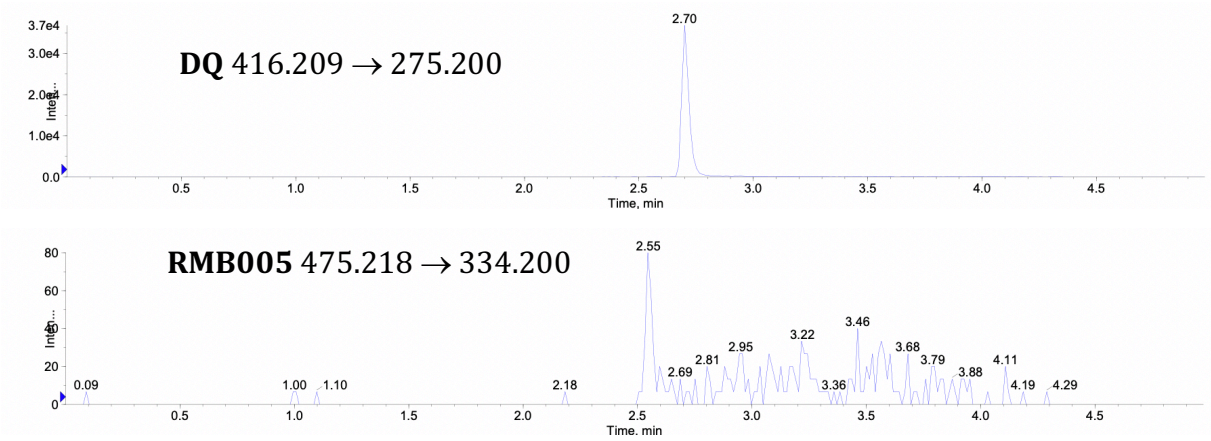

Figure 8-32: Chromatogram of a blank mouse whole blood sample. MRM transitions of the ISTD (top) and quantifying ion for RMB005 (bottom) are shown.

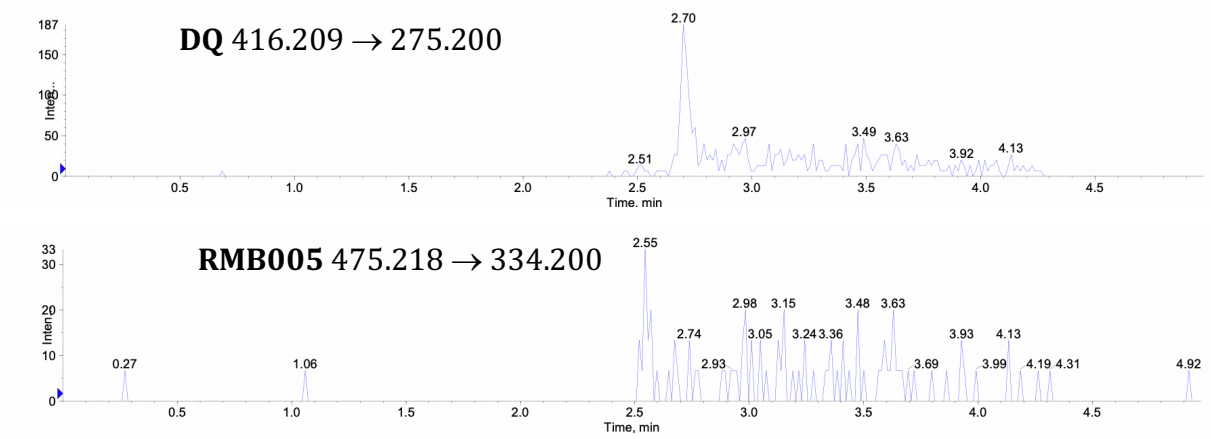

Figure 8-33: Chromatogram of a double blank mouse whole blood sample. MRM transitions of the ISTD (top) and quantifying ion for RMB005 (bottom) are shown.

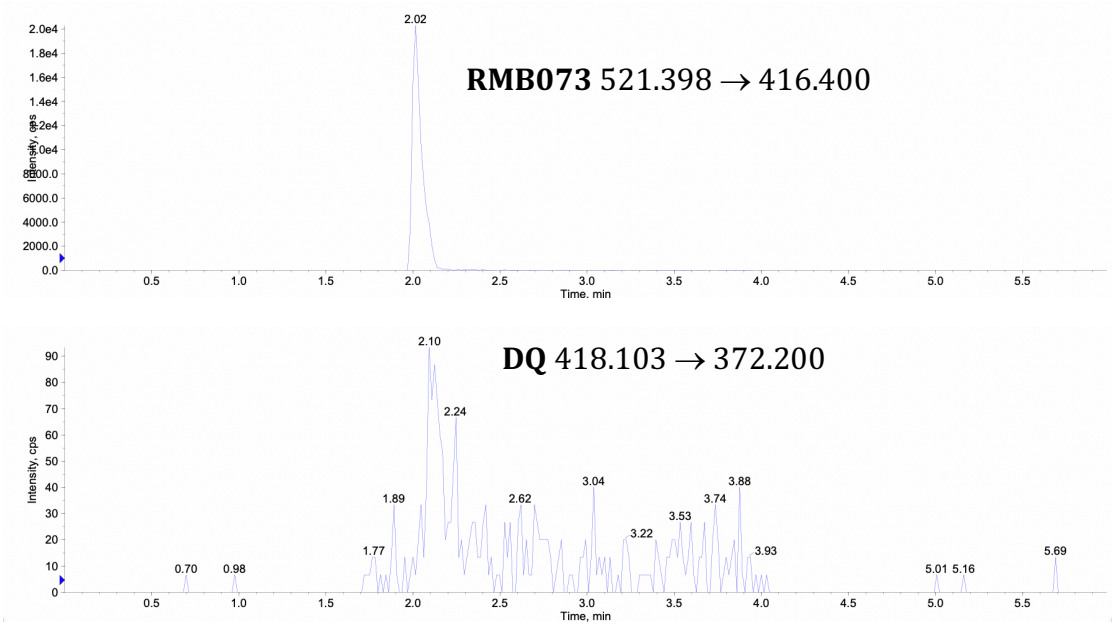

Figure 8-34: Chromatogram of a blank mouse whole blood sample. MRM transitions of the ISTD (top) and quantifying ion for DQ (bottom) are shown.

Figure 8-35: Chromatogram of a double blank mouse whole blood sample. MRM transitions of the ISTD (top) and quantifying ion for DQ (bottom) are shown.

Matrix effects and extraction efficiency

Potential ion enhancement or suppression effects of components within the matrix were assessed using the Matuszewski method. The method utilizes a calibration range to quantify the effect on ionization, as a calculation of variability. The compounds were spiked into the matrix (mouse plasma or whole blood) at a high and low concentration and analysed in order to determine possible matrix effects. Peak area ratios were used to generate regression curves for each replicate and determine the variability (%CV). It is suggested that this precision value should not exceed 3–4%, to be considered reliable and free from the relative matrix effect liability.[359,360] These results are presented in Table 8-18, together with the evaluation of compound recoveries obtained through the extraction methods described in Section 4.3.7. No matrix effects were observed for any of the compounds, indicating that their methods were highly robust and reproducible. Compound recovery was sufficient for all the compounds from their respective matrices and reproducible as indicated by a CV of <15%.

Table 8-18: Matrix effects and recovery of compounds spiked in matrix.

Compound	**Matrix Effect as % CV**	**% Recovery**		
		Low QC (25 ng/mL)	High QC (1000 ng/mL)	Average recovery (%CV)
WHN012	3.5	82	96	89 (11.3)
PhX6	3.9	94	97	95 (2.30)
AD01	3.2	113	99	106 (8.60)
DpNEt	3.3	109	115	112 (3.90)
RMB005	1.9	62	62	62 (0.10)
DQ	1.4	65	55	60 (11.1)

Samples were analysed in triplicate.